On the Solution of First Excursion Problems by Simulation with Applications to Probabilistic Seismic Performance Assessment

Thesis by

Siu-Kui Au

In Partial Fulfillment of the Requirements

for the Degree of

Doctor of Philosophy

California Institute of Technology

Pasadena, California

2001

(Defended May 9, 2001)

Acknowledgements

It has been a 'long and winding road,' and it is my pleasure to thank all who have helped me get to this stage.

I would like to express my sincere gratitude to my advisor, Prof. James L. Beck, for his enthusiastic guidance and encouragement throughout my doctoral study. I benefit a lot from his philosophical perspectives and visions, which make this work an exciting endeavor. Our many evening conversations are most enjoyable, which also constitute a valuable form of education for me in other aspects outside research.

I would like to thank the members of my thesis committee, Prof. Joel P. Conte (University of California, Los Angeles), Prof. John F. Hall, Prof. Wilfred D. Iwan, Prof. Hiroo Kanamori and Prof. Lambros S. Katafygiotis (Hong Kong University of Science and Technology), for spending their precious time reading my thesis and making valuable suggestions. Special thanks are due to Prof. Costas Papadimitriou (University of Thessaly) and Prof. Asparsia Zerva (Drexel University) for their encouragement throughout my graduate study.

The financial support from the Li Ming Foundation, Harold Hellwig Foundation, and the Pacific Earthquake Engineering Center are gratefully acknowledged.

My thanks also go to my buddies at Caltech, including fellow students at Thomas Building, members of HKSA, and among others, the founding members of NGF, Kelvin Yuen and Lawrence Chung.

Last but not the least, my deepest gratitude goes to the two most important women in my life: my mother, Shuk Hing Siu and my fiancée, Janice Yu, to whom this thesis is dedicated, for their love and patience in the pursuit of my long and winding educational goals.

Abstract

In a probabilistic assessment of the performance of structures subjected to uncertain environmental loads such as earthquakes, an important problem is to determine the probability that the structural response exceeds some specified limits within a given duration of interest. This problem is known as the first excursion problem, and it has been a challenging problem in the theory of stochastic dynamics and reliability analysis. In spite of the enormous amount of attention the problem has received, there is no procedure available for its general solution, especially for engineering problems of interest where the complexity of the system is large and the failure probability is small.

The application of simulation methods to solving the first excursion problem is investigated in this dissertation, with the objective of assessing the probabilistic performance of structures subjected to uncertain earthquake excitations modeled by stochastic processes. From a simulation perspective, the major difficulty in the first excursion problem comes from the large number of uncertain parameters often encountered in the stochastic description of the excitation. Existing simulation tools are examined, with special regard to their applicability in problems with a large number of uncertain parameters. Two efficient simulation methods are developed to solve the first excursion problem. The first method is developed specifically for linear dynamical systems, and it is found to be extremely efficient compared to existing techniques. The second method is more robust to the type of problem, and it is applicable to general dynamical systems. It is efficient for estimating small failure probabilities because the computational effort grows at a much slower rate with decreasing failure probability than standard Monte Carlo simulation. The simulation methods are applied to assess the probabilistic performance of structures subjected to uncertain earthquake excitation. Failure analysis is also carried out using the samples generated during simulation, which provide insight into the probable scenarios that will occur given that a structure fails.

Contents

List of Figures

List of Tables

Chapter 1 Introduction

The proper assessment of the performance of engineering structures is an important component in a modern performance-based engineering framework (SEAOC 1995 2000; Wen 2000; Cornell 1996). This includes realistic modeling of material constitutive behavior, structural components, loading conditions, mechanism of deterioration, etc., that are anticipated during the working life of a structure. Due to incomplete information, uncertainty always exists in the loading conditions as well as the structural behavior. Uncertainty in structural behavior arises because no mathematical model is a perfect description of a physical structure, and even so, the parametric properties that should be used in the mathematical model representing the physical structure may not be known precisely. The uncertainty in loading arises because structures are expected to function in a variety of loading conditions in their daily operation and the actual loading conditions are not precisely known.

Whenever feasible, uncertainties may be reduced by means of quality control or system identification (Mottershead and Friswell 1993; Aktan et al. 1997; Beck and Katafygiotis 1998), for example. In many cases, it is more cost-effective to accept and deal with uncertainties rather than trying to eliminate them (Freudenthal 1947; Housner and Jennings 1982). In any case, it is not possible in many situations to gain the information necessary to remove the uncertainties. This calls for a rational and scientific approach for quantifying uncertainties and modeling the mechanism by which plausible reasoning is made in decision making. Probability theory is well-known to provide a rational and consistent framework for treating uncertainties and plausible reasoning (Cox 1961; Papoulis 1965; Jaynes 1983; Jaynes 1978). A probabilistic approach allows scientific and engineering predictions to be made with different degrees of confidence reflecting one's incomplete information. A sound application of probability theory to engineering problems requires a proper choice of probability models to reflect one's uncertainty on the mathematical model for making predictions about the physical system, in addition to those efforts needed for modeling a physical phenomenon.

Application of probability concepts to structural safety was initiated in the mid 40's, due to the work of Freudenthal and his co-workers (Freudenthal 1947; Freudenthal 1956; Freudenthal et al. 1966). Structural reliability is concerned with the probability that a structure will not reach some specified state of failure. For structures subjected to dynamic loading such as due to earthquake, wind or ocean waves, the exceedence of some output response magnitude beyond some threshold limit within the response duration is of paramount importance. This leads to the 'first excursion problem,' the focus of this dissertation, which is to determine the 'first excursion probability' that any one of the output response states of interest exceeds in magnitude some specified threshold level

within a given time duration.

The first excursion problem is one of the most challenging problems in structural reliability and stochastic dynamics (Lin 1967; Soong and Grigoriu 1993; Schuëller et al. 1993; Lutes and Sarkani 1997). In spite of the enormous amount of attention the problem has received, there is no procedure available for its *general* solution, especially for engineering problems of interest where the number of output states is large and the failure probability is small. Most existing work focuses on the 'classical' case where the uncertainty comes only from the excitation which is modeled by a given stochastic process. Pioneered by Rice, early work on the first excursion problem was focused on out-crossing theory to give an analytical approximation (Rice 1944; Rice 1945; Crandall et al. 1966; Yang and Shinozuka 1971; Vanmarcke 1975; Mason and Iwan 1983; Langley 1988; Naess 1990). While the analytical solutions from out-crossing theory offer important insights into the problem, they are nevertheless approximate and applicable only for a single output state. A class of numerical solution methods involves solving the backward Kolmogorov equation for the reliability function (Roberts 1976; Bergman and Heinrich 1981; Spencer and Bergman 1993). These numerical solutions are limited in application to systems of small size since their complexity increases at least exponentially with the state-space dimension of the system (Lin and Cai 1995; Schuëller et al. 1993).

Monte Carlo simulation methods (Hammersley and Handscomb 1964; Rubinstein 1981; Fishman 1996) offer a feasible alternative for the numerical solution of first excursion problems and, in general, any structural reliability problem, regardless of the complexity of the problem. In this approach, random realizations, or samples, of the uncertain parameters in the problem are generated according to their probability distributions specified in the problem. The failure probability is then estimated as the fraction of the number of samples that leads to failure. Checking whether the structure has failed for each sample often requires a structural analysis. As is well known, Monte Carlo simulation is not computationally efficient for estimating small failure probabilities, since the number of samples required to achieve a given accuracy is inversely proportional to the failure probability when the failure probability is small. Essentially, estimating small probabilities requires information from rare samples which lead to failure, and on average it requires many samples before one such failure sample occurs. In view of this, the importance sampling method (Rubinstein 1981; Schuëller and Stix 1987) has been introduced, which basically chooses an importance sampling distribution to generate samples that lead to failure more frequently so as to gain more information about failure for better failure probability estimation. The efficiency of the method relies on a proper choice of the importance sampling distribution, which inevitably requires some knowledge about failure. Importance sampling has been successfully applied to time-invariant or static reliability problems where the number of uncertain parameters in the problem is not too large (Schuëller and Stix 1987; Melchers 1989; Papadimitriou et al. 1997; Der Kiureghian and Dakessian 1998; Au et al. 1999; Bucher 1988; Karamchandani et al. 1989; Ang et al. 1992; Au and Beck 1999). For the first

excursion problem, which is characterized by a large number of uncertain parameters with complexity arising from its dynamic nature, the application of importance sampling is much more difficult. One class of simulation techniques that shows promise for solving the classical first excursion problem is called Controlled Monte Carlo simulation (Pradlwarter et al. 1994; Pradlwarter and Schuëller 1997a; Pradlwarter and Schuëller 1997b; Pradlwarter and Schuëller 1999), in which the basic idea is to generate samples to populate uniformly both the large and low failure probability regions, which provide information for improving the accuracy of the failure probability estimate. Generally speaking, efficient and robust simulation methods for solving the first excursion problem are still at their early exploration stage.

1.1 Outline of this work

This dissertation is motivated by the need to assess the failure probability of structures with respect to first excursion failures in an uncertain seismic environment, which plays an important role in a performance-based earthquake engineering design framework. In this work, the development and use of simulation methods for solving the first excursion problem will be investigated. The next section gives a definition of the problem which is the focus of this dissertation. A brief review of standard Monte Carlo simulation then follows, which provides a baseline procedure for every simulation method to compare in terms of efficiency and robustness.

Chapter 2 investigates the application of importance sampling to solving reliability problems, with particular attention to the case when the number of uncertain parameters is large, which is a characteristic of first excursion problems. Conditions for applicability in high dimensions using some common choices of importance sampling densities will be provided and proved. Chapter 3 discusses a powerful technique called Markov chain Monte Carlo simulation for simulating samples according to the conditional distribution of uncertain parameters given that failure occurs. This technique has great potential for application to reliability problems. Applicability issues in high dimensions with the original algorithms are investigated. The study shows that the original algorithms are inapplicable in problems with a large number of uncertain parameters. A modified algorithm is proposed which is applicable to high dimensional simulation problems.

Two efficient simulation methods are developed in Chapters 4 and 5 to solve the first excursion problem. Chapter 4 focuses on the first excursion problem for deterministic linear dynamical systems subjected to Gaussian white noise excitation. The characteristics of the failure region are investigated first. Using the information from this study, an importance sampling distribution is proposed, which results in a very efficient importance sampling procedure for estimating the first excursion failure probability. In Chapter 5, a method called subset simulation is developed to solve the first excursion problem in general, with no assumption on the structure and the modeling of excitation. The method

is based on expressing small failure probabilities as a product of larger conditional probabilities, where the latter are estimated using the modified Markov chain Monte Carlo simulation method proposed in Chapter 3.

In Chapter 6, the subset simulation methodology developed in Chapter 5 is applied to probabilistic performance assessment of structures subjected to uncertain earthquake excitation modeled by a stochastic process with uncertain stochastic model parameters. The application is focused on efficient estimation of failure probabilities as well as failure analysis using the samples generated during subset simulation. These samples provide insight into the probable scenarios that will occur when the structure fails. This dissertation is concluded in Chapter 7.

1.2 Problem definition

The first excursion problem to be solved by simulation is posed in general as a reliability problem. Parametric uncertainties, such as uncertain parameters in the structural model, are modeled by random variables. Uncertain-valued functions, such as time-varying excitations, are modeled by stochastic processes, which are specified by some stochastic excitation model parameters. For digital simulation purposes, a discrete-representation for a stochastic process is used, if necessary, in terms of a sequence of 'additive' excitation parameters (Lin 1967). In this setting, all uncertainties in the problem are parametric, referred to as the uncertain parameters and denoted by $\boldsymbol{\theta} = [\theta_1, \ldots, \theta_n]$, where n is their number. The symbol $\mathcal{P}(n)$ is used to denote a set of n-dimensional joint probability density functions (PDF). With little loss of generality, it is assumed that all uncertain parameters are continuous-valued, with joint PDF denoted by $q \in \mathcal{P}(n)$. The PDF q will be called the 'parameter PDF' for the uncertain parameters $\boldsymbol{\theta}$. It is assumed that the parameter PDF q is specified from standard class of probability distributions (Ross 1972) for which efficient methods for evaluating the value of $q(\boldsymbol{\theta})$ at a given $\boldsymbol{\theta}$, as well as for generating independent random samples according to $\boldsymbol{\theta}$, are available. This distinguishes the reliability problems considered in this dissertation from the Bayeisan reliability updating problems (Beck and Katafygiotis 1991; Katafygiotis and Beck 1998; Beck and Au 2000; Papadimitriou et al. 2001), where the probability distributions of the uncertain parameters given some measurement data can only be evaluated up to a normalizing constant and the generation of random samples of the uncertain parameters according to the updated probability distributions given the measurement data is a highly non-trivial problem.

The statement that defines a failure criterion describes a failure event when true, and is denoted by F. For example, $F = \{X > b\}$ is a failure event, where X is an uncertain response and b is a given value. It is assumed that the failure statement can be determined as either true or false by knowing the value of $\boldsymbol{\theta}$; that is, the failure state is completely specified by the uncertain parameters. The same symbol is used to denote the 'failure region' corresponding to the failure event F, which is

defined as the region in the n-dimensional uncertain parameter space such that all states in the region correspond to a failure event. For example, in the previous example, $F = \{\boldsymbol{\theta} \in \mathbb{R}^n : X(\boldsymbol{\theta}) > b\} \subset \mathbb{R}^n$ is the failure region.

In terms of the probability density function $q(\boldsymbol{\theta})$ and the failure region F, the failure probability can be written in a generic way as

$$P_F = \int \mathbb{I}_F(\boldsymbol{\theta})\, q(\boldsymbol{\theta})\, d\boldsymbol{\theta} \tag{1.1}$$

where $\mathbb{I}_F(\cdot) : \mathbb{R}^n \mapsto \{0, 1\}$ is called the indicator function, which is equal to 1 when $\boldsymbol{\theta} \in F$ and zero otherwise. Unless otherwise mentioned, all integrals are to be interpreted as the integral over the whole parameter space of the parameter to be integrated.

The symbol $P(\cdot)$ is reserved for the probability of a statement or probability content of a region given in the argument. The symbol $p(\cdot)$ is reserved for the probability density evaluated at its argument. For convenience, we use the same symbol to denote an uncertain quantity (random variable or vector) as well as a value that the uncertain quantity may assume, where the uncertain nature of the quantity will be mentioned in the former. For example, in '$P(\boldsymbol{\theta} \in F)$,' $\boldsymbol{\theta}$ denotes a random vector, while in '$q(\boldsymbol{\theta})$,' $\boldsymbol{\theta}$ denotes a vector value at which q is evaluated. The notation $\mathsf{E}_f[\cdot]$ denotes the mathematical expectation of the uncertain quantity in the argument, whose probability distribution is specified in the subscript f. For example, if X is a function of $\boldsymbol{\theta}$, then $\mathsf{E}_f[X(\boldsymbol{\theta})] = \int X(\boldsymbol{\theta})\, f(\boldsymbol{\theta})\, d\boldsymbol{\theta}$. When the distribution is clearly implied in the discussion, the subscript for the distribution will be dropped.

1.3 Standard Monte Carlo simulation

The standard Monte Carlo simulation method (MCS) for estimating failure probabilities is briefly reviewed here, since it is the most basic method in simulation. In standard MCS, the failure probability for a given failure event F is estimated as the average of the indicator function $\mathbb{I}_F(\cdot)$ over samples $\{\boldsymbol{\theta}_1, \ldots, \boldsymbol{\theta}_N\}$ simulated independently and identically (i.i.d.) according to the parameter PDF q:

$$P_F \approx \tilde{P}_F = \frac{1}{N} \sum_{k=1}^{N} \mathbb{I}_F(\boldsymbol{\theta}_k) \tag{1.2}$$

The estimator $\tilde{P}_F$ converges to the failure probability P_F with probability 1 (Strong Law of Large Numbers), and is asymptotically Normally distributed as the number of samples $N \to \infty$ (Central Limit Theorem). It is unbiased, i.e., $\mathsf{E}[\tilde{P}_F] = P_F$. The efficiency of the MCS procedure, and in general the efficiency of a simulation-based reliability method, can be measured by the coefficient of variation (c.o.v.) of the estimator, which is defined as the ratio of its standard deviation to its expectation. Since $\{\boldsymbol{\theta}_k : k = 1, \ldots, N\}$ are i.i.d., $\mathsf{Var}[\tilde{P}_F] = \mathsf{Var}[\mathbb{I}_F(\boldsymbol{\theta})]/N$. On the other hand, $\mathbb{I}_F(\boldsymbol{\theta})$ is a Bernoulli random variable equal to 1 and 0 with probabilities P_F and $1 - P_F$, respectively, so $\mathsf{Var}[\mathbb{I}_F(\boldsymbol{\theta})] = P_F(1 - P_F)$. Using these results yields the coefficient of variation δ as:

$$\delta^2 \triangleq \frac{\mathsf{Var}[\tilde{P}_F]}{\mathsf{E}[\tilde{P}_F]^2} = \frac{1 - P_F}{P_F N} \tag{1.3}$$

Note that the expression for the c.o.v. depends only on the failure probability and the number of samples N. The c.o.v. δ can thus be estimated in a simulation run using the above equation with P_F replaced by its estimate $\tilde{P}_F$.

Implicit in the MCS procedure is that an efficient method is available for simulating samples according to the parameter PDF. This is often feasible in common applications when the parameter PDF q is chosen based on prior information and from some standard family of distributions (e.g., Normal, Lognormal, Exponential) for which simulation methods for generating samples are well established. Other than this requirement, the MCS procedure is quite robust to the type of application. As far as the problem of structural reliability is concerned, MCS is applicable for all types of structures, types of excitation models, types of parameter PDFs, number of uncertain parameters, etc. Apart from the simulation of samples, these specifications of the problem enter the MCS procedure through only the indicator function $\mathbb{I}_F$, whose value is determined by a system analysis.

Not only the applicability, but also the efficiency of MCS, is independent of the specification of the problem for a given failure probability. The expression for c.o.v. in (1.3) is applicable irrespective of the specifications of the problem. The only drawback of MCS, as is well-known, is that MCS is not efficient for dealing with *rare events*, defined as those events that occur with *small probability*.

In terms of the number of samples N_δ required to achieve a given c.o.v. of δ, from (1.3),

$$N_\delta = \frac{1 - P_F}{P_F \delta^2} \sim \frac{1}{P_F \delta^2} \quad \text{when } P_F \text{ is small} \tag{1.4}$$

which is inversely proportional to the probability of failure P_F when P_F is small. For example, to compute a failure probability of $P_F = 10^{-3}$ with a c.o.v. of 30%, it requires 11,100 samples. As a rule of thumb, to achieve a target failure probability of P_F with a c.o.v. of 30%, it requires on average $10/P_F$ samples, or 10 *failed* samples.

In our context, standard Monte Carlo simulation presents the most robust method for failure probability estimation. Any simulation method other than standard Monte Carlo simulation is expected to be less robust to the type of applications. The efficiency of standard Monte Carlo simulation provides a baseline for comparison. Judging on efficiency and robustness, any simulation method that requires more computational effort to compute a given failure probability is not worth-pursuing.

Chapter 2 Importance Sampling Simulation

In view of the small fraction of simulated samples lying in the failure region in standard Monte Carlo simulation when the failure probability is small, a natural attempt is to develop a method that generates more samples in the failure region. This will utilize more information there to possibly yield a better estimate. This is the essential idea of importance sampling simulation (Hammersley and Handscomb 1964; Rubinstein 1981; Schuëller and Stix 1987; Engelund and Rackwitz 1993; Hohenbichler and Rackwitz 1988). In importance sampling simulation, an importance sampling density (ISD) $f(\boldsymbol{\theta}) \in \mathcal{P}$ is first chosen. Samples are then generated from this importance sampling density rather than from the parameter PDF q. The estimator based on these samples is different from the one used in standard Monte Carlo simulation, to account for the fact that the samples are not simulated from the parameter PDF q. It can be derived as follows. First note that

$$P_F = \int \frac{\mathbb{I}_F(\boldsymbol{\theta}) q(\boldsymbol{\theta})}{f(\boldsymbol{\theta})} f(\boldsymbol{\theta}) d\boldsymbol{\theta} = \mathsf{E}_f[\mathbb{I}_F(\boldsymbol{\theta}) R(\boldsymbol{\theta})] \tag{2.1}$$

where

$$R(\boldsymbol{\theta}) = \frac{q(\boldsymbol{\theta})}{f(\boldsymbol{\theta})} \tag{2.2}$$

is called the importance sampling quotient. Since the theoretical mean in (2.1) can be estimated by a sample mean, the failure probability P_F is estimated by:

$$P_F \approx \tilde{P}_F = \frac{1}{N} \sum_{k=1}^{N} \mathbb{I}_F(\boldsymbol{\theta}_k) R(\boldsymbol{\theta}_k) \tag{2.3}$$

where $\{\boldsymbol{\theta}_k : k = 1, \ldots, N\}$ are i.i.d. samples simulated according to f instead of from q.

The variability of the failure probability estimate is measured by its c.o.v., δ_{IS}, given by

$$\delta_{IS} = \frac{\Delta_{IS}}{\sqrt{N}} \tag{2.4}$$

where Δ_{IS} is called the 'unit c.o.v.' of the importance sampling estimator, defined as the c.o.v. of the importance sampling estimator with $N = 1$ on the R.H.S. of (2.3):

$$\begin{aligned} \Delta_{IS}^2 &= \frac{\mathsf{Var}_f[\mathbb{I}_F(\boldsymbol{\theta}) R(\boldsymbol{\theta})]}{\mathsf{E}_f[\mathbb{I}_F(\boldsymbol{\theta}) R(\boldsymbol{\theta})]^2} \\ &= \frac{\mathsf{Var}_f[\mathbb{I}_F(\boldsymbol{\theta}) R(\boldsymbol{\theta})]}{P_F^2} \end{aligned} \tag{2.5}$$

and it has been assumed in the above expression that the importance sampling estimator is unbiased, so that $\mathsf{E}_f[\mathbb{I}_F(\boldsymbol{\theta})R(\boldsymbol{\theta})] = P_F$.

For suitable choice of the ISD f, the importance sampling estimator converges with probability 1 (Strong Law of Large Numbers) to P_F and is Normally distributed asymptotically as $N \to \infty$ (Central Limit Theorem). Essentially, the chosen ISD has to have a support region $S_f = \{\boldsymbol{\theta} \in \mathbb{R}^n : f(\boldsymbol{\theta}) > 0\}$ which covers the failure region, i.e., $F \subset S_f$. It should also have a tail which decays at a slower rate than the parameter PDF q, so that the c.o.v. of $\tilde{P}_F$ is finite. These conditions ensure that the contributions from all parts of the failure region in the uncertain parameter space can be accounted for, provided one uses a sufficiently large number of samples, so that the resulting estimate is not biased. Although these conditions are sometimes difficult to check either analytically or numerically in practical applications, careful investigation often suffices to make sure that the convergence problem is not severe. Throughout this chapter, the first property, that is, $F \subset S_f$, will be assumed, so that the integral of any quantity multiplied with the indicator function over the support S_f of f is equal to the integral over $\mathbb{R}^n$.

Under the approach of importance sampling, the main problem in applications is how to choose the ISD that results in small variability in the failure probability estimate (δ_{IS} in (2.4)) and hence leads to an efficient simulation procedure. Many schemes for constructing the ISD have appeared in the engineering reliability literature. Most schemes involve first finding the important parts of the failure region which give significant contribution to the failure probability, and then constructing an ISD based on information about such important failure regions. For example, a popular strategy is to construct the ISD as a mixture distribution among one or more design point(s) $\boldsymbol{\theta}_i^*$ $(i = 1, \ldots, m)$ that have the highest probability density, at least locally, among all other points in their neighborhood within the failure region (Harbitz 1986; Schuëller and Stix 1987; Papadimitriou et al. 1997; Liu and Der Kiureghian 1991; Melchers 1989; Der Kiureghian and Dakessian 1998; Au et al. 1999). Another popular strategy, called adaptive importance sampling, is to construct the ISD as a mixture distribution among some 'pre-samples' which are generated in the failure region by some pre-designed stochastic algorithm (Bucher 1988; Karamchandani et al. 1989; Melchers 1990; Ang et al. 1992; Au and Beck 1999). Generally speaking, importance sampling has been successfully applied to static problems of small to medium sized structures. Applications to large scale structures or to dynamic problems where the stochastic excitation is explicitly represented are still at the early stage of exploration (Schuëller et al. 1993). The general difficulty encountered is due to the large number of uncertain parameters involved in the problem, where the construction of a good ISD seems to require a huge amount of information that cannot be gained numerically in an efficient way.

In this chapter, some aspects of importance sampling are investigated analytically, with the aim of providing a quantitative understanding of how the efficiency of an importance sampling procedure is influenced by the choice of the ISD. Particular attention is given to application of importance

sampling to problems with a large number of uncertain parameters, which is motivated by the need to compute failure probabilities of large scale dynamical systems. The main theme is to relate the c.o.v. of the importance sampling estimator to the relative entropy of the chosen ISD to the optimal ISD. This provides new results and the basic insights for the applicability of importance sampling in problems with a large number of uncertain parameters, for which it appears that no formal account has been reported in the literature.

2.1 Optimal ISD and its implications

In terms of the variance of the importance sampling estimator, the optimal ISD can be defined as the PDF among the class of PDFs $\mathcal{P}$ for which the variance is minimized. That is,

$$f_{\text{opt}}(\boldsymbol{\theta}) = \arg \inf_{f \in \mathcal{P}} \text{Var}_f[\frac{\mathbb{I}_F(\boldsymbol{\theta}) q(\boldsymbol{\theta})}{f(\boldsymbol{\theta})}] \tag{2.6}$$

According to this criterion, the optimal ISD is simply the conditional PDF given failure occurs:

$$f_{\text{opt}}(\boldsymbol{\theta}) = q(\boldsymbol{\theta}|F) = \frac{\mathbb{I}_F(\boldsymbol{\theta})\, q(\boldsymbol{\theta})}{P_F} \tag{2.7}$$

which is basically the parameter PDF $q(\boldsymbol{\theta})$ confined to the failure region F, normalized by the failure probability P_F. The optimality of f_{opt} can be easily verified by noting that it leads to zero variance in the importance sampling estimator when substituted into (2.5). Although the optimal ISD can be written in a simple way, its use is not feasible, due to two basic reasons. The first is that its evaluation involves knowledge of the failure probability P_F, which is the quantity to be computed in the reliability problem. The second reason is that an efficient method for simulating samples according to f_{opt} is often not available. This may not be obvious from first glance, since f_{opt} is just proportional to the parameter PDF q for which an efficient method is assumed to be available for generating samples. The difficulty comes from the indicator function $\mathbb{I}_F$, which gives a conditioning on the original distribution q that causes the samples distributed according to f_{opt} to be very different from q, especially when P_F is small. To understand this, consider one simple, but not efficient, way of generating samples according to f_{opt} as follows: generate a sample $\boldsymbol{\theta}$ according to q, then accept it if $\boldsymbol{\theta} \in F$ (i.e., $\mathbb{I}_F(\boldsymbol{\theta}) = 1$); otherwise, generate another sample until the condition is met. The reason why this 'acceptance-rejection' method works is obvious (Rubinstein 1981). It is not efficient, however, since to generate one sample according to f_{opt}, on average it requires $1/P_F$ samples simulated according to q as well as $1/P_F$ checks on the indicator function. The problem comes from the evaluation of the indicator function, since each evaluation involves one analysis of the system to determine if failure occurs. Thus, when P_F is small, the conditioning induced by failure is so significant that the conditional samples are very different in distribution from the original

samples. Philosophically, efficient simulation of samples according to the conditional distribution is the main challenge in a simulation-based reliability method.

2.2 Basic trade-off

Since an optimal choice of the ISD is not feasible, it is important to understand how the variability of the failure probability estimate is affected by the choice of a sub-optimal ISD. A form for the variance of the unit c.o.v. of the IS estimator is derived here, which formalizes the basic trade-off involved in the choice of ISD as commonly exercised in applications.

Proposition 2.1. *The unit coefficient of variation of the importance sampling estimator can be expressed as*

$$\Delta_{IS}^2 \triangleq \frac{\mathsf{Var}[\mathbb{I}_F(\boldsymbol{\theta})R(\boldsymbol{\theta})]}{P_F^2} = (\frac{1}{Q_F} - 1) + \frac{\Delta_{R|F}^2}{Q_F} \tag{2.8}$$

where

$$Q_F = \int \mathbb{I}_F(\boldsymbol{\theta})\, f(\boldsymbol{\theta})\, d\boldsymbol{\theta} \tag{2.9}$$

is the probability that a sample simulated according to the ISD f lies in the failure region F, and

$$\Delta_{R|F} = \sqrt{\frac{\mathsf{Var}_f[R(\boldsymbol{\theta})|F]}{\mathsf{E}_f[R(\boldsymbol{\theta})|F]^2}} \tag{2.10}$$

is the coefficient of variation of the importance sampling quotient $R(\boldsymbol{\theta}) = q(\boldsymbol{\theta})/f(\boldsymbol{\theta})$ given that $\boldsymbol{\theta}$ distributed according to the ISD f lies in F.

Proof. For convenience, we will drop the dependence of $\boldsymbol{\theta}$ in $\mathbb{I}_F(\boldsymbol{\theta})$ and $R(\boldsymbol{\theta})$. First note that,

$$\begin{aligned} \mathsf{Var}_f[\mathbb{I}_F R] &= \mathsf{E}_f[\mathbb{I}_F^2 R^2] - \mathsf{E}_f[\mathbb{I}_F R]^2 \\ &= \mathsf{E}_f[\mathbb{I}_F R^2] - P_F^2 \end{aligned} \tag{2.11}$$

Now

$$\begin{aligned} \mathsf{E}_f[\mathbb{I}_F R^2] &= \int \mathbb{I}_F(\boldsymbol{\theta}) R(\boldsymbol{\theta})^2 f(\boldsymbol{\theta}) d\boldsymbol{\theta} \\ &= Q_F \int R(\boldsymbol{\theta})^2 \frac{\mathbb{I}_F(\boldsymbol{\theta}) f(\boldsymbol{\theta})}{Q_F} d\boldsymbol{\theta} \\ &= Q_F \int R(\boldsymbol{\theta})^2 f(\boldsymbol{\theta}|F) d\boldsymbol{\theta} \\ &= Q_F \mathsf{E}_f[R^2|F] \end{aligned} \tag{2.12}$$

Further,

$$\mathsf{E}_f[R^2|F] = \mathsf{Var}_f[R|F] + \mathsf{E}_f[R|F]^2 = \mathsf{Var}_f[R|F] + \frac{P_F^2}{Q_F^2} \tag{2.13}$$

since

$$\mathsf{E}_f[R|F] = \int \frac{q(\boldsymbol{\theta})}{f(\boldsymbol{\theta})} \frac{f(\boldsymbol{\theta})\,\mathbb{I}_F(\boldsymbol{\theta})}{Q_F}\, d\boldsymbol{\theta} = \frac{1}{Q_F} \int q(\boldsymbol{\theta})\,\mathbb{I}_F(\boldsymbol{\theta})\, d\boldsymbol{\theta} = \frac{P_F}{Q_F} \tag{2.14}$$

Substituting (2.13) into (2.12) gives

$$\mathsf{E}_f[\mathbb{I}_F R^2] = \mathsf{Var}_f[R|F]\, Q_F + \frac{P_F^2}{Q_F} \tag{2.15}$$

Substituting (2.15) into (2.11) yields

$$\mathsf{Var}_f[\mathbb{I}_F R] = P_F^2(\frac{1}{Q_F} - 1) + \mathsf{Var}_f[R|F]Q_F \tag{2.16}$$

which gives (2.8) when divided by P_F^2 and using (2.14). □

Equation (2.8) says that the unit c.o.v. of the importance sampling estimator comes from two sources. The first source, in the first term, comes from the fact that not all samples generated according to the ISD f lies in the failure region F, but only with probability Q_F. When all samples lie in F, $Q_F = 1$ and the first term vanishes. The second source comes from the variability of the importance sampling quotient given that $\boldsymbol{\theta}$ generated from f lies in the failure region F. It arises as a result of the difference in the variation between the chosen ISD f and the parameter PDF q in the failure region. In terms of efficiency of the importance sampling estimator, there are thus two challenges in choosing a suitable ISD, namely, to choose the ISD so that the samples generated from f lie frequently in the failure region and so that the ratio of the parameter PDF to the ISD has small variability in the failure region. These two requirements may often be conflicting, since the first says that the ISD should be focused on the failure region, and often times choosing the ISD with different variation from the parameter PDF is inevitable, which conflicts with the second requirement that the ISD and the parameter PDF be similar. Note that the effect of having an ISD that results in a large value of Q_F is quite significant compared to one with a small value of Q_F, since Δ_{IS} is dominated by $1/Q_F$ when Q_F is small. That is, a significant improvement over standard MCS can be readily achieved by shifting the ISD towards the failure region. Most of the work in the literature has thus focused on the first requirement, e.g., by shifting the ISD towards design points. The second requirement seems to have been overlooked because there is little problem associated with it when the number of uncertain parameters is not large. It could become a severe problem when the number of uncertain parameters is large, however, although no formal account has

been given in the literature. This issue has an important impact on the applicability of importance sampling to solving the first excursion problem for dynamical systems or static reliability problems of systems with a large number of uncertain parameters. This aspect of importance sampling will be expounded in a later section when we investigate the applicability of importance sampling in problems with a large number of uncertain parameters.

2.3 Variance of importance sampling estimator and relative entropy

We first derive two forms for the unit c.o.v. of the importance sampling estimator which will be used frequently for analysis in later sections.

$$\begin{aligned}\Delta_{IS}^2 &= \frac{\mathsf{E}_f[R(\boldsymbol{\theta})^2 \mathbb{I}_F(\boldsymbol{\theta})^2]}{P_F^2} - 1 \\ &= \frac{1}{P_F^2} \int \frac{q(\boldsymbol{\theta})^2 \mathbb{I}_F(\boldsymbol{\theta})^2}{f(\boldsymbol{\theta})^2} f(\boldsymbol{\theta})\, d\boldsymbol{\theta} - 1 \\ &= \frac{1}{P_F^2} \int \frac{q(\boldsymbol{\theta})}{f(\boldsymbol{\theta})} \mathbb{I}_F(\boldsymbol{\theta})\, q(\boldsymbol{\theta})\, d\boldsymbol{\theta} - 1 \\ &= \frac{1}{P_F^2} \mathsf{E}_q[R(\boldsymbol{\theta})\, \mathbb{I}_F(\boldsymbol{\theta})] - 1 \end{aligned} \tag{2.17}$$

where $R(\boldsymbol{\theta}) = q(\boldsymbol{\theta})/f(\boldsymbol{\theta})$ is the importance sampling quotient. Also, from the second line in (2.17),

$$\begin{aligned}\Delta_{IS}^2 &= \int \frac{q(\boldsymbol{\theta}) \mathbb{I}_F(\boldsymbol{\theta})/P_F}{f(\boldsymbol{\theta})} \frac{q(\boldsymbol{\theta}) \mathbb{I}_F(\boldsymbol{\theta})}{P_F}\, d\boldsymbol{\theta} - 1 \\ &= \int \frac{q(\boldsymbol{\theta}|F)}{f(\boldsymbol{\theta})} q(\boldsymbol{\theta}|F)\, d\boldsymbol{\theta} - 1 \\ &= \mathsf{E}_{q|F}[\frac{q(\boldsymbol{\theta}|F)}{f(\boldsymbol{\theta})}] - 1 \end{aligned} \tag{2.18}$$

The concept of 'relative entropy' is introduced in the following:

Definition 2.1. *The relative entropy of a PDF p_2 (relative) to a PDF p_1 is defined as:*

$$H(p_1, p_2) = \int p_1(\boldsymbol{\theta}) \log \frac{p_1(\boldsymbol{\theta})}{p_2(\boldsymbol{\theta})}\, d\boldsymbol{\theta} \tag{2.19}$$

The relative entropy $H(p_1, p_2)$ is a useful measure for the difference between two PDFs (Kullback 1959; Renyi 1970; Jumarie 1990). It is always non-negative, and is equal to zero if and only if $p_1 \equiv p_2$. To see the non-negativity, first note that $\log(x) \leq x - 1$ for any positive number x (equality holds

if and only if $x = 1$), and so with $x = p_2(\theta)/p_1(\theta)$,

$$\log \frac{p_2(\theta)}{p_1(\theta)} \leq \frac{p_2(\theta)}{p_1(\theta)} - 1 \tag{2.20}$$

Multiplying both sides by $p_1(\theta)$ and integrate with respect to θ,

$$\int p_1(\theta) \log \frac{p_2(\theta)}{p_1(\theta)} \, d\theta \leq \int p_1(\theta) \frac{p_2(\theta)}{p_1(\theta)} \, d\theta - \int p_1(\theta) \, d\theta = 0 \tag{2.21}$$

and hence the non-negativity follows by noting that the L.H.S. of (2.21) is just $-H(p_1, p_2)$.

Applying the concept of relative entropy to the choice of ISD, one can expect that if the relative entropy of the ISD $f(\theta)$ to $q(\theta|F)$ (the optimal ISD) is small, then the unit c.o.v. Δ_{IS} will also be small, and vice versa. In particular, the relative entropy is zero if and only if Δ_{IS} is zero, since both statements require $f(\theta) = q(\theta|F)$. These statements are indeed true and quite intuitive. It should be noted that relative entropy is not a proper metric, however. In particular, it is not symmetric with respect to its arguments, i.e., $H(p_1, p_2) \neq H(p_2, p_1)$ in general.

The following proposition relates the variance of the importance sampling estimator to the relative entropy of the ISD $f(\theta)$ to the conditional density $q(\theta|F)$.

Proposition 2.2.

$$\Delta_{IS}^2 \geq \exp[H(q(\cdot|F), f)] - 1 \tag{2.22}$$

where

$$H(q(\cdot|F), f) = \mathsf{E}_{q|F}[\log \frac{q(\theta|F)}{f(\theta)}] = \int q(\theta|F) \log \frac{q(\theta|F)}{f(\theta)} \, d\theta \geq 0 \tag{2.23}$$

is the relative entropy of the ISD $f(\theta)$ to the conditional density $q(\theta|F)$.

Proof. The proposition follows immediately from application of Jensen's inequality (Rudin 1974) to (2.18), by noting the convexity of the exponential function:

$$\begin{aligned} \Delta_{IS}^2 &= \mathsf{E}_{q|F}[\frac{q(\theta|F)}{f(\theta)}] - 1 \\ &= \mathsf{E}_{q|F} \exp[\log \frac{q(\theta|F)}{f(\theta)}] - 1 \\ &\geq \exp[\mathsf{E}_{q|F} \log \frac{q(\theta|F)}{f(\theta)}] - 1 \\ &= \exp[H(q(\cdot|F), f)] - 1 \end{aligned} \tag{2.24}$$

□

2.4 Importance sampling in high dimensions

The applicability of importance sampling in high dimensional problems for reliability analysis is examined in this section. For importance sampling to be efficient, one requires the c.o.v. of the importance sampling estimator to be small, which, according to (2.8), depends on two factors. The first factor is whether the ISD can generate samples that lie frequently in the failure region, thus making the first term in (2.8) small. The second factor is whether the ISD is chosen such that the variability of the importance sampling quotient $R(\boldsymbol{\theta}) = q(\boldsymbol{\theta})/f(\boldsymbol{\theta})$ is small, when $\boldsymbol{\theta}$ is distributed as $f(\boldsymbol{\theta}|F)$. When the dimension n is not large, one often concentrates on the first factor, and as a result a common strategy is to construct the ISD as a distribution centered among design point(s). Reported cases in the literature reveal that the variability in $R(\boldsymbol{\theta})$ in this case is not very large, and so the second factor is often ignored in the construction of ISD. When the dimension n is large, however, there is a question of whether the variability of $R(\boldsymbol{\theta})\mathbb{I}_F(\boldsymbol{\theta})$ will increase in a somewhat systematic way as the number of uncertain parameters n increases, rendering importance sampling inapplicable. From Proposition 2.2, we note that:

Proposition 2.3. *A necessary condition for importance sampling to be applicable in problems with a large number of uncertain parameters is*

$$H(q(\cdot|F), f) < \infty \quad as\ n \to \infty \tag{2.25}$$

This proposition is evident from Proposition 2.2, and roughly says that the ISD f should be reasonably close to the parameter PDF q.

The basic problems of concern that may occur when n is large arise from the probabilistic property of the importance sampling quotient, which can be readily illustrated in terms of relative entropy. Consider the i.i.d. case when $q(\boldsymbol{\theta}|F) = q(\boldsymbol{\theta}) = \prod_{i=1}^n q_1(\theta_i)$ and $f(\boldsymbol{\theta}) = \prod_{i=1}^n f_1(\theta_i)$, where q_1 and f_1 are the one-dimensional PDF for each component θ_i of $\boldsymbol{\theta} = [\theta_1, \ldots, \theta_n]$ distributed according to $q(\boldsymbol{\theta})$ and $f(\boldsymbol{\theta})$, respectively. Note that

$$\log \frac{q(\boldsymbol{\theta})}{f(\boldsymbol{\theta})} = \sum_{i=1}^n \log \frac{q_1(\theta_i)}{f_1(\theta_i)} \tag{2.26}$$

and so

$$H(q, f) = \mathsf{E}_q[\log \frac{q(\boldsymbol{\theta})}{f(\boldsymbol{\theta})}] = n\, \mathsf{E}_{q_1}[\log \frac{q_1(\theta_i)}{f_1(\theta_i)}] = n\, H(q_1, f_1) \tag{2.27}$$

where $H(q_1, f_1)$ is the relative entropy of f_1 to q_1. This means that, unless $H(q_1, f_1)$ is at most of the order of $1/n$, $H(q, f)$ will grow with n. Consequently, according to (2.22), the unit c.o.v. Δ_{IS} will grow exponentially with n, and importance sampling is not applicable. In fact, if $f_1 \neq q_1$ and

the choice of f_1 does not depend on n, then when θ is distributed as $f(\theta) = \prod_{i=1}^{n} f_1(\theta_i)$, by the Strong Law of Large Numbers,

$$\frac{1}{n}\log\frac{q(\theta)}{f(\theta)} = \frac{1}{n}\sum_{i=1}^{n}\log\frac{q_1(\theta_i)}{f_1(\theta_i)} \to \mathsf{E}_{f_1}[\log\frac{q_1(\theta_i)}{f_1(\theta_i)}] = -H(f_1, q_1) \quad \text{as } n \to \infty \tag{2.28}$$

with probability 1, since $\{\log[q_1(\theta_i)/f_1(\theta_i)] : i = 1, \ldots, n\}$ are i.i.d.. Consequently, with probability 1,

$$\frac{q(\theta)}{f(\theta)} \to \exp[-n\,H(f_1, q_1)] \quad \text{as } n \to \infty \tag{2.29}$$

and hence the importance sampling quotient is exponentially small as $n \to \infty$. By noting that, theoretically,

$$\mathsf{E}_f[\frac{q(\theta)}{f(\theta)}] = \int_{S_f}\frac{q(\theta)}{f(\theta)}f(\theta)\,d\theta = \int_{S_f} q(\theta)\,d\theta \tag{2.30}$$

and hence is $O(1)$, one can perceive that when n is large, the importance sampling quotient is exponentially small for most of the time, but on some rare occasions, it assumes extremely large values, so that its theoretical mean is maintained. This phenomenon stems from the difference between the one-dimensional PDFs q_1 and f_1, which is amplified exponentially in the unit c.o.v. Δ_{IS} as the dimension n increases. When this phenomenon occurs, it is unlikely that importance sampling will be successful, since the importance sampling estimate is likely to be biased in practice as well as having large variability.

The question now is whether it is feasible in practice to choose an ISD that remains close to the parameter PDF, in the sense that $H(q, f)$ remains bounded or $H(q_1, f_1) = O(1/n)$ for this example, as $n \to \infty$. Specifically, suppose $q(\theta) = \prod_{i=1}^{n}\phi(\theta_i)$ is the standard Normal PDF with independent components, where

$$\phi(\theta) = \frac{1}{\sqrt{2\pi}}\exp(-\frac{\theta^2}{2}) \tag{2.31}$$

is the (one-dimensional) standard Normal PDF. Let the ISD be a Normal PDF with independent components centered at a single design point $\theta^* = [\theta_1^*, \ldots, \theta_n^*]$, that is, $f(\theta) = \prod_{i=1}^{n}\phi(\theta_i - \theta_i^*)$. Then $q_1(\theta_i) = \phi(\theta_i)$, $f_1(\theta_i) = \phi(\theta_i - \theta_i^*)$ and

$$\log\frac{q_1(\theta_i)}{f_1(\theta_i)} = \log\frac{\phi(\theta_i)}{\phi(\theta_i - \theta_i^*)} = -\theta_i\theta_i^* + \frac{1}{2}\theta_i^{*2} \tag{2.32}$$

and so in the i-th component, the relative entropy is

$$H_i(q_1, f_1) = \mathsf{E}_{q_1}[\log \frac{q_1(\theta_i)}{f_1(\theta_i)}] = \frac{1}{2}\theta_i^{*2} \tag{2.33}$$

since $\mathsf{E}_{q_1}[\theta_i] = 0$. To determine if $H_i(f_1, q_1)$ is $O(1/n)$, we note that $||\boldsymbol{\theta}^*||$, the Euclidean norm of $\boldsymbol{\theta}^*$, is intimately related to the failure probability. For example, if F is a half-space defined by a hyperplane with the design point $\boldsymbol{\theta}^*$, then the failure probability is $P_F = \Phi(-||\boldsymbol{\theta}^*||)$, where

$$\Phi(x) = \int_{-\infty}^{x} \phi(z)\, dz \tag{2.34}$$

is the standard Normal cumulative distribution function. Assuming that we are investigating similar problems, then when the number of uncertain parameters n increases, the failure probability P_F should remain nonzero and hence $||\boldsymbol{\theta}^*||$ should remain finite as $n \to \infty$. Since $||\boldsymbol{\theta}^*||^2 = \sum_{i=1}^{n} \theta_i^{*2} = O(1)$, this implies $\theta_i^{*2} = O(1/n)$, and from (2.33), $H_i(f_1, q_1) = O(1/n)$. As a result,

$$H(q, f) = \mathsf{E}_q[\log \frac{q(\boldsymbol{\theta})}{f(\boldsymbol{\theta})}] = \sum_{i=1}^{n} H_i(f_1, q_1) = \frac{1}{2}\sum_{i=1}^{n} \theta_i^{*2} = \frac{1}{2}||\boldsymbol{\theta}^*||^2 \tag{2.35}$$

is bounded as $n \to \infty$. Importance sampling is thus applicable in high dimensions in this case.

This example suggests that importance sampling using design points may still be applicable in high dimensions, as the design point automatically adjusts itself so that the ISD f remains close to the parameter PDF q as the dimension n increases. In general, however, this comes with some conditions and may not be taken for granted. One counter example for this is the case when f_1 in the last example has fixed standard deviation $s \neq 1$, that is, $f_1(\theta_i) = \exp(-(\theta_i - \theta_i^*)^2/2s^2)/\sqrt{2\pi}s$. One can easily show that in this case,

$$H_i(q_1, f_1) = \frac{1}{2}(\frac{1}{s^2} + \log s^2 - 1) + \frac{1}{2}\theta_i^{*2} \tag{2.36}$$

The first term in (2.36) comes from the fact that a standard deviation $s \neq 1$ is used in the ISD, while the second term is due to the shift of ISD from the origin to the design point $\boldsymbol{\theta}^*$. Note that the first term is equal to the relative entropy of f_1 to q_1 if $\theta_i^* = 0$, which can be easily verified by setting $\theta_i^* = 0$ in (2.36). It is non-negative and is equal to zero if and only if $s = 1$. Obviously, for fixed $s \neq 1$, the first term is $O(1)$. The second term is $O(1/n)$ as in the last example. This means $H_i(q_1, f_1) = O(1)$ and

$$H(q, f) = \frac{n}{2}(\frac{1}{s^2} + \log s^2 - 1) + \frac{1}{2}||\boldsymbol{\theta}^*||^2 \tag{2.37}$$

grows in a linear fashion with n, that is, importance sampling is not applicable as long as s is fixed and

not equal to unity. Thus, although the shift of ISD to the design point does not render importance sampling inapplicable in high dimensions, the use of standard deviation s different from that of the original PDF (equal to unity) does. Intuitively, one may expect that importance sampling is not applicable when $s < 1$ even when n is not large, since then the ISD decays faster than the parameter PDF at its 'tail' where the importance sampling quotient $R(\boldsymbol{\theta}) = q(\boldsymbol{\theta})/f(\boldsymbol{\theta})$ grows without bound. Also, in this case the spread of the ISD is not large enough to cover the support of the parameter PDF that can cause potential bias in the failure probability estimate. The surprising observation from this example is that, although importance sampling with $s > 1$ is applicable when n is not large, the same is not true in high dimensions.

2.4.1 Definition of applicability in high dimensions

To address formally the issue of whether importance sampling is applicable in high dimensional problems, we need to define what we mean by 'applicable in high dimensions'. For the question of applicability to be meaningful, assume that we have a generic reliability problem with n uncertain parameters, $n \in \mathbb{Z}^+$, from which a sequence of similar problems of increasing number of uncertain parameters can be induced by increasing n by some admissible increments. For example, consider computing the failure probability of a deterministic SDOF oscillator subjected to Gaussian white noise discretized in the time domain by n i.i.d. standard Gaussian random variables. Then a legitimate sequence of problems with increasing dimension n can be generated by refining the discretization in the time-domain. In particular, if each refinement corresponds to subdividing each existing time interval by half, then an admissible increment of dimension n may be taken as n (assuming the first point of the time horizon is not represented). Starting with n_1 discrete time instants (and hence uncertain parameters), the sequence of dimensions associated with this sequence of reliability problems will be $\mathcal{N} = \{n_k : k = 1, 2, \dots\} = \{n_1, 2n_1, 4n_1, \dots\}$. For example, when $n_1 = 1000$, then $\mathcal{N} = \{1000, 2000, 4000, \dots\}$.

Let a reliability problem with n uncertain parameters be defined by the ordered pair $\mathcal{R}(q_n, F_n)$, where q_n is the joint PDF for the uncertain parameters and $F_n \subset \mathbb{R}^n$ is the failure region. For a given sequence of admissible dimensions $\mathcal{N} = \{n_k : k = 1, 2, \dots\}$, consider a sequence of reliability problems $\{\mathcal{R}(q_{n_k}, F_{n_k}) : k = 1, 2, \dots\}$. For the k-th problem in the sequence, let $f_{n_k}(\boldsymbol{\theta}) \in \mathcal{P}_{\mathcal{IS}}(n_k)$ be the ISD chosen for computing the failure probability by importance sampling:

$$P(F_{n_k}) \approx \tilde{P}(F_{n_k}) = \frac{1}{N} \sum_{r=1}^{N} \frac{q_{n_k}(\boldsymbol{\theta}_r)}{f_{n_k}(\boldsymbol{\theta}_r)} \mathbb{I}_{F_{n_k}}(\boldsymbol{\theta}_r) \tag{2.38}$$

where $\{\boldsymbol{\theta}_r : r = 1, \dots, N\}$ are i.i.d. samples simulated according to the ISD f_{n_k}. Let Δ_{n_k} be the

unit c.o.v. of the importance sampling estimator $\tilde{P}(F_{n_k})$, that is, according to (2.17),

$$\Delta_{n_k}^2 = \frac{1}{P(F_{n_k})^2} \mathsf{E}_{q_{n_k}}[R_{n_k}(\boldsymbol{\theta})\, \mathbb{I}_{F_{n_k}}(\boldsymbol{\theta})] - 1 \tag{2.39}$$

where $R_{n_k} = q_{n_k}(\boldsymbol{\theta})/f_{n_k}(\boldsymbol{\theta})$ is the importance sampling quotient in the k-th problem of the sequence. Then we will say that

Definition 2.2. *Importance sampling is applicable in high dimensions with ISD chosen from the class of PDFs $\mathcal{P}_{\mathcal{IS}}(n)$ for the reliability problem $\mathcal{R}(q_n, F_n)$, if*

$$\Delta_{n_k} < \infty \quad \text{as } k \to \infty \tag{2.40}$$

for any increasing sequence $\mathcal{N} = \{n_k \in \mathbb{Z}^+ : k = 1, 2, \dots\}$ of admissible dimensions with $n_k \to \infty$.

In our context, 'applicability' does not imply 'efficiency,' that is, if according to Definition 2.2, importance sampling is found to be applicable in high dimensions, it is not necessary that the importance sampling procedure will be efficient. This is because the unit c.o.v. of the failure probability estimate may be large even if it remains bounded as the dimension increases. Also, the study of applicability does not offer an explicit answer as to whether the importance sampling estimate is biased or not. Rather, it is assumed that the estimate is unbiased in the analysis. The issue of bias is related to whether the ISD has accounted for the parts in the failure region which give the major contribution to the failure probability. It depends on which particular member from the class of ISDs $\mathcal{P}_{\mathcal{IS}}(n)$ is chosen, rather than on what general properties $\mathcal{P}_{\mathcal{IS}}(n)$ should possess. In short, the concern with 'applicability' is whether it is possible to apply importance sampling at all, leaving aside the issues of how to gain information about the failure region to avoid bias or whether the resulting ISD will lead to an efficient estimate. Applicability is the first concern when one applies importance sampling to high dimensional problems, however, since if the chosen class of ISDs already implies that the variability of the failure probability estimate will generally increase without bound as n increases, the effort spent on searching for a suitable ISD from $\mathcal{P}_{\mathcal{IS}}(n)$ will be in vain.

In what follows, we will investigate the conditions under which importance sampling is applicable in high dimensions. For convenience in analysis, we assume that the reliability problem $\mathcal{R}(q_n, F_n)$ is defined for every $n \in \mathbb{Z}^+$, so that we take the sequence of admissible dimensions as $\mathcal{N} = \{n_k : k = 1, 2, \dots\} = \{1, 2, \dots\}$. Since the subscript k now becomes redundant, it will be dropped in our analysis. We will also drop the dependence of quantities on the dimension n, with the implicit understanding that all quantities under consideration are specific to a simulation problem with n uncertain parameters. For example, $f_n(\boldsymbol{\theta})$ will be abbreviated to $f(\boldsymbol{\theta})$, and F_n to F.

It will be assumed that for every $n \in \mathbb{Z}^+$, $P(F_n) > \varepsilon$ for some fixed $\varepsilon > 0$ independent of n.

This implies that $P(F_n)$ does not vanish as $n \to \infty$, and essentially reflects that we are studying problems of non-vanishing failure probabilities.

Ideally, the question of applicability can be answered if we know either analytically or numerically how Δ_{IS} behaves with increasing n. The analysis of Δ_{IS}, given by either (2.17) or (2.18) or otherwise, is difficult in general, due to the fact that the expression of the importance sampling quotient could be complicated depending on the form of ISD used. Also, the failure region is not known in advance or it has complicated structure. The evaluation of Δ_{IS} by simulation is not computationally favorable, since it involves evaluating the indicator function $\mathbb{I}_F(\boldsymbol{\theta})$ during the averaging process which requires system analyses. Realizing that the applicability problem basically arises due to the variability of the importance sampling quotient $R(\boldsymbol{\theta}) = q(\boldsymbol{\theta})/f(\boldsymbol{\theta})$, one is interested to see whether the behavior of Δ_{IS} can be inferred from that of Δ_R. If the answer is positive, then the applicability problem may be solved at least numerically in an efficient manner, since then one can estimate $\Delta_R = \mathsf{E}_q[R] - 1$ by simulation, which involves evaluation of $R(\boldsymbol{\theta})$ and so does not require any system analysis, and then deduce the behavior of Δ_{IS} from that of Δ_R. The following proposition says that half of the answer to the above question is positive.

Proposition 2.4. *As $n \to \infty$, if $\Delta_R < \infty$, then $\Delta_{IS} < \infty$ also.*

Proof. First note that, using (2.17) with $F = \mathbb{R}^n$,

$$\Delta_R^2 = \mathsf{E}_q[R(\boldsymbol{\theta})] - 1 \tag{2.41}$$

From (2.17),

$$\begin{aligned}
\Delta_{IS}^2 &= \frac{\mathsf{E}_q[R(\boldsymbol{\theta})\mathbb{I}_F(\boldsymbol{\theta})]}{P_F^2} - 1 \\
&\leq \frac{\mathsf{E}_q[R(\boldsymbol{\theta})]}{P_F^2} - 1 \\
&= \frac{\Delta_R^2 + 1}{P_F^2} - 1 \\
&= \frac{\Delta_R^2}{P_F^2} + \frac{1}{P_F^2} - 1
\end{aligned} \tag{2.42}$$

Since P_F does not vanish as $n \to \infty$, the boundedness of Δ_R implies that of Δ_{IS}. □

The proposition says that $\Delta_R < \infty$ provides a sufficient condition for Δ_{IS} as $n \to \infty$. Thus, if we know for certain problems and under certain conditions on the ISD that Δ_R will remain bounded as n increases, then we can conclude that Δ_{IS} will also be bounded, and hence importance sampling is applicable in high dimensions in the given situation. However, it is also important to examine the other half of the question, that is, whether $\Delta_R < \infty$ is a necessary condition for $\Delta_{IS} < \infty$, since the sufficient condition could be so restrictive that it excludes a large class of ISDs which are applicable.

This is what motivates the logic throughout the analysis to follow, where an attempt will be made to investigate the relationship between Δ_{IS} and Δ_R, or equivalently, between $\mathsf{E}_q[R\mathbb{I}_F]$ and $\mathsf{E}_q[R]$.

The focus will be placed on the case where the uncertain parameters are i.i.d. standard Normal, that is, for a given $n \in \mathbb{Z}^+$,

$$q(\boldsymbol{\theta}) = \phi(\boldsymbol{\theta}) = (2\pi)^{-n/2} \exp(-\frac{1}{2}\boldsymbol{\theta}^T\boldsymbol{\theta}) \tag{2.43}$$

which is a common PDF used in applications. The independent assumption does not introduce any loss of generality, since dependent random variables can be generated by a suitable transformation of independent ones; in fact, this seems to be the only way when numerical simulation of dependent variables is done.

2.4.2 ISD with a single point

The applicability aspects of ISDs chosen from the class of Normal PDFs centered at a single point $\tilde{\boldsymbol{\theta}}$ and with a positive definite covariance matrix $\mathbf{C}$ is investigated first. That is,

$$\mathcal{P}_{\mathcal{IS}}(n) = \{\phi_n(\cdot; \tilde{\boldsymbol{\theta}}, \mathbf{C}) : \tilde{\boldsymbol{\theta}} \in \mathbb{R}^n; \mathbf{C} \in \mathbb{R}^{n\times n}, \mathbf{C} > 0\} \tag{2.44}$$

where $\phi_n(\cdot; \tilde{\boldsymbol{\theta}}, \mathbf{C})$ denotes the n-dimensional joint Normal PDF with independent components, whose mean and covariance matrix is given by $\tilde{\boldsymbol{\theta}}$ and $\mathbf{C}$, respectively. The notation '$\mathbf{C} > 0$' denotes that $\mathbf{C}$ is positive definite, that is, $\mathbf{x}^T\mathbf{C}\mathbf{x} > 0$ for all $\mathbf{x} \in \mathbb{R}^n \backslash \{0\}$. An ISD $f(\boldsymbol{\theta})$ chosen from the class $\mathcal{P}_{\mathcal{IS}}(n)$ will then be given by:

$$f(\boldsymbol{\theta}) = (2\pi)^{-n/2}\sqrt{|\mathbf{C}^{-1}|}\exp[-\frac{1}{2}(\boldsymbol{\theta} - \tilde{\boldsymbol{\theta}})^T\mathbf{C}^{-1}(\boldsymbol{\theta} - \tilde{\boldsymbol{\theta}})] \tag{2.45}$$

For the purpose of analysis, some properties of the positive definite covariance matrix $\mathbf{C}$ are recalled. First, the eigenvalues of $\mathbf{C}$, denoted by $\{s_j^2 : j = 1, \ldots, n\}$, are all positive. The inverse of the covariance matrix, $\mathbf{C}^{-1}$, is also positive-definite, with corresponding eigenvalues $\{1/s_j^2 : j = 1, \ldots, n\}$. There exists an orthonormal basis of eigenvectors $\{\boldsymbol{\psi}_j \in \mathbb{R}^n : j = 1, \ldots, n\}$ of $\mathbf{C}$ and $\mathbf{C}^{-1}$, which satisfies the orthogonality conditions:

$$\boldsymbol{\psi}_j^T\mathbf{C}^{-1}\boldsymbol{\psi}_k = \frac{\delta_{jk}}{s_j^2} \quad \text{and} \quad \boldsymbol{\psi}_j^T\boldsymbol{\psi}_k = \delta_{jk} \tag{2.46}$$

where δ_{jk} is the Kronecker delta function: $\delta_{jk} = 1$ if $j = k$ and $\delta_{jk} = 0$ otherwise. The eigenmatrix of $\mathbf{C}$ and $\mathbf{C}^{-1}$ will be denoted by $\boldsymbol{\Psi} = [\boldsymbol{\psi}_1, \ldots, \boldsymbol{\psi}_n] \in \mathbb{R}^{n\times n}$. Note that $\boldsymbol{\Psi}^{-1} = \boldsymbol{\Psi}^T$.

We will analyze Δ_{IS} based on (2.17), which necessitates the study of $R(\boldsymbol{\theta})\mathbb{I}_F(\boldsymbol{\theta})$ when $\boldsymbol{\theta}$ is distributed as $q(\boldsymbol{\theta})$. For this purpose, we start with an expression for the importance sampling

quotient $R(\boldsymbol{\theta})$ that facilitates analysis later.

Proposition 2.5. *Let the parameter PDF q be a standard Normal PDF given by* (2.43) *and the ISD f be a Normal PDF centered at $\tilde{\boldsymbol{\theta}}$ with covariance matrix $\mathbf{C}$, as given by* (2.45).

If $\boldsymbol{\theta}$ is distributed as q, then the importance sampling quotient $R = q(\boldsymbol{\theta})/f(\boldsymbol{\theta})$ can be represented as

$$R(\boldsymbol{\theta}) = R(\boldsymbol{\Psi}\boldsymbol{\xi}) = (\prod_{i=1}^{n} s_i)\, \exp(\frac{1}{2}\sum_{i=1}^{n}\frac{\tilde{\xi}_i^2}{s_i^2})\, \exp\{\sum_{i=1}^{n}[\frac{1}{2}(\frac{1}{s_i^2}-1)\xi_i^2 - (\frac{\tilde{\xi}_i}{s_i^2})\xi_i]\} \tag{2.47}$$

where $\{s_i^2 : i = 1,\ldots,n\}$ are the eigenvalues of $\mathbf{C}$, $\tilde{\boldsymbol{\xi}} = [\tilde{\xi}_1,\ldots,\tilde{\xi}_n]^T = \boldsymbol{\Psi}^T\tilde{\boldsymbol{\theta}}$, and $\boldsymbol{\xi} = [\xi_1,\ldots,\xi_n]^T = \boldsymbol{\Psi}^T\boldsymbol{\theta}$ is a standard Normal vector.

Proof. From (2.43) and (2.45),

$$\begin{aligned} R(\boldsymbol{\theta}) = \frac{q(\boldsymbol{\theta})}{f(\boldsymbol{\theta})} &= \frac{(2\pi)^{-n/2}\exp(-\frac{1}{2}\boldsymbol{\theta}^T\boldsymbol{\theta})}{(2\pi)^{-n/2}\sqrt{|\mathbf{C}^{-1}|}\exp[-\frac{1}{2}(\boldsymbol{\theta}-\tilde{\boldsymbol{\theta}})^T\mathbf{C}^{-1}(\boldsymbol{\theta}-\tilde{\boldsymbol{\theta}})]} \\ &= (\prod_{i=1}^{n} s_i)\exp(-\frac{1}{2}\boldsymbol{\theta}^T\boldsymbol{\theta} + \frac{1}{2}\boldsymbol{\theta}^T\mathbf{C}^{-1}\boldsymbol{\theta} - \tilde{\boldsymbol{\theta}}^T\mathbf{C}^{-1}\boldsymbol{\theta} + \frac{1}{2}\tilde{\boldsymbol{\theta}}^T\mathbf{C}^{-1}\tilde{\boldsymbol{\theta}}) \end{aligned} \tag{2.48}$$

since $|\mathbf{C}^{-1}| = 1/\prod_{i=1}^{n} s_i^2$ (the determinant of a matrix is equal to the product of its eigenvalues). By rotational symmetry of standard Normal vectors, $\boldsymbol{\theta}$ distributed as $q(\boldsymbol{\theta}) = \phi(\boldsymbol{\theta})$ has the following representation with respect to the orthonormal basis $\{\boldsymbol{\psi}_i : i = 1,\ldots,n\}$ for $\mathbf{C}^{-1}$:

$$\boldsymbol{\theta} = \sum_{i=1}^{n}\boldsymbol{\psi}_i\,\xi_i \tag{2.49}$$

where $\boldsymbol{\xi} = [\xi_1,\ldots,\xi_n]^T = \boldsymbol{\Psi}^{-1}\boldsymbol{\theta} = \boldsymbol{\Psi}^T\boldsymbol{\theta}$ is a standard Normal vector. Using this representation and the orthonormal conditions in (2.46),

$$\boldsymbol{\theta}^T\mathbf{C}^{-1}\boldsymbol{\theta} = \sum_{i=1}^{n}\sum_{j=1}^{n}(\boldsymbol{\psi}_i^T\mathbf{C}^{-1}\boldsymbol{\psi}_j)\,\xi_j\xi_j = \sum_{i=1}^{n}\frac{\xi_i^2}{s_i^2} \tag{2.50}$$

and

$$\boldsymbol{\theta}^T\boldsymbol{\theta} = \sum_{i=1}^{n}\sum_{j=1}^{n}(\boldsymbol{\psi}_i^T\boldsymbol{\psi}_j)\,\xi_i\xi_j = \sum_{i=1}^{n}\xi_i^2 \tag{2.51}$$

Similarly, using the following representation for $\tilde{\boldsymbol{\theta}}$:

$$\tilde{\boldsymbol{\theta}} = \sum_{i=1}^{n}\boldsymbol{\psi}_i\,\tilde{\xi}_i \tag{2.52}$$

we have

$$\tilde{\theta}^T \mathbf{C}^{-1} \theta = \sum_{i=1}^{n} \frac{\tilde{\xi}_i \xi_i}{s_i^2} \tag{2.53}$$

and

$$\tilde{\theta}^T \mathbf{C}^{-1} \tilde{\theta} = \sum_{i=1}^{n} \frac{\tilde{\xi}_i^2}{s_i^2} \tag{2.54}$$

Substituting (2.50), (2.51), (2.53) and (2.54) into (2.48) and simplifying gives the required proposition. □

Proposition 2.6. *Let the parameter PDF q be a standard Normal PDF given by* (2.43) *and the ISD f be a Normal PDF centered at $\tilde{\theta}$ with covariance matrix $\mathbf{C}$, as given by* (2.45). *Let $\{s_i^2 : i = 1, \ldots, n\}$ be the eigenvalues of $\mathbf{C}$ and $R(\theta) = q(\theta)/f(\theta)$ be the importance sampling quotient.*

Then, if $s_i > 1/\sqrt{2}$ for all $i = 1, \ldots, n$,

$$\mathsf{E}_q[R(\theta)\, \mathbb{I}_F(\theta)] = Q(\tilde{\theta}, \mathbf{C}, F) \left(\prod_{i=1}^{n} \frac{s_i^2}{\sqrt{2s_i^2 - 1}} \right) \exp\left[\sum_{i=1}^{n} \frac{\tilde{\xi}_i^2}{2s_i^2 - 1} \right] \tag{2.55}$$

where

$$Q(\tilde{\theta}, \mathbf{C}, F) = \int \phi(z)\, \mathbb{I}_F(\Psi(\Lambda_{\hat{s}} z + \hat{\xi}))\, dz \tag{2.56}$$

is the probability that the vector $\Psi(\Lambda_{\hat{s}} Z - \hat{\xi})$ lies in the failure region F, where Z is an n-dimensional standard Normal vector; Ψ is the eigenmatrix of $\mathbf{C}$; $\hat{\xi} = [\hat{\xi}_1, \ldots, \hat{\xi}_n]^T$, where

$$\hat{\xi}_i = -\frac{\tilde{\xi}_i}{2s_i^2 - 1} \tag{2.57}$$

and $\Lambda_{\hat{s}} \in \mathbb{R}^{n \times n}$ is a diagonal matrix with the i-th diagonal element equal to $\hat{s}_i$ given by

$$\hat{s}_i = \frac{s_i}{\sqrt{2s_i^2 - 1}} \tag{2.58}$$

Proof. Using (2.47),

$$\begin{aligned} \mathsf{E}_q[R(\theta)\, \mathbb{I}_F(\theta)] &= \mathsf{E}_\phi[R(\Psi\xi)\, \mathbb{I}_F(\Psi\xi)] \\ &= \left(\prod_{i=1}^{n} s_i\right) \exp\left(\frac{1}{2} \sum_{i=1}^{n} \frac{\tilde{\xi}_i^2}{s_i^2}\right) \mathsf{E}_\phi\left[\exp\left\{\sum_{i=1}^{n} \left[\frac{1}{2}\left(\frac{1}{s_i^2} - 1\right)\xi_i^2 - \left(\frac{\tilde{\xi}_i}{s_i^2}\right)\xi_i\right]\right\}\right] \mathbb{I}_F(\Psi\xi) \end{aligned} \tag{2.59}$$

where the subscript ϕ in $\mathsf{E}_\phi[\cdot]$ denotes that the expectation is taken with ξ distributed as ϕ, that is,

with $\xi_1, \ldots, \xi_n$ being i.i.d. standard Normal. It remains to evaluate the expectation $\mathsf{E}_\phi[\cdot]$ in (2.59).

$$\begin{aligned}
&\mathsf{E}_\phi[\exp\{\sum_{i=1}^n [\frac{1}{2}(\frac{1}{s_i^2}-1)\xi_i^2 - (\frac{\tilde{\xi}_i}{s_i^2})\xi_i]\}\, \mathbb{I}_F(\Psi\boldsymbol{\xi})] \\
&= \int \exp\{\sum_{i=1}^n [\frac{1}{2}(\frac{1}{s_i^2}-1)\xi_i^2 - (\frac{\tilde{\xi}_i}{s_i^2})\xi_i]\}\, \mathbb{I}_F(\Psi\boldsymbol{\xi}) \times (2\pi)^{-n/2} \exp(-\frac{1}{2}\sum_{i=1}^n \xi_i^2)\, d\boldsymbol{\xi} \\
&= (2\pi)^{-n/2} \int \exp\{-\frac{1}{2}\sum_{i=1}^n \left[(\frac{2s_i^2-1}{s_i^2})\xi_i^2 + 2(\frac{\tilde{\xi}_i}{s_i^2})\xi_i\right]\}\, \mathbb{I}_F(\Psi\boldsymbol{\xi})\, d\boldsymbol{\xi} \qquad (2.60)
\end{aligned}$$

By completing the square in the exponent inside the integral and bring the constant terms outside the integral, we have

$$\begin{aligned}
&\mathsf{E}_\phi[\exp\{\sum_{i=1}^n [\frac{1}{2}(\frac{1}{s_i^2}-1)\xi_i^2 - (\frac{\tilde{\xi}_i}{s_i^2})\xi_i]\}\, \mathbb{I}_F(\Psi\boldsymbol{\xi})] \\
&= (2\pi)^{-n/2} \prod_{i=1}^n \frac{\sqrt{2s_i^2-1}}{s_i} \int \exp\left[-\frac{1}{2}\sum_{i=1}^n \left(\frac{2s_i^2-1}{s_i^2}\right)\left(\xi_i + \frac{\tilde{\xi}_i}{2s_i^2-1}\right)^2\right] \mathbb{I}_F(\Psi\boldsymbol{\xi})\, d\boldsymbol{\xi} \\
&\quad \times \prod_{i=1}^n \frac{s_i}{\sqrt{2s_i^2-1}} \exp\left[\sum_{i=1}^n \frac{\tilde{\xi}_i^2}{2s_i^2(2s_i^2-1)}\right] \\
&= \int (2\pi)^{-n/2} (\prod_{i=1}^n \hat{s}_i)^{-1} \exp\left[-\frac{1}{2}\sum_{i=1}^n \left(\frac{\xi_i - \hat{\xi}_i}{\hat{s}_i}\right)^2\right] \mathbb{I}_F(\Psi\boldsymbol{\xi})\, d\boldsymbol{\xi} \\
&\quad \times \prod_{i=1}^n \frac{s_i}{\sqrt{2s_i^2-1}} \exp\left[\sum_{i=1}^n \frac{\tilde{\xi}_i^2}{2s_i^2(2s_i^2-1)}\right] \qquad (2.61)
\end{aligned}$$

where $\hat{\xi}_i = -\tilde{\xi}_i/(2s_i^2-1)$ and $\hat{s}_i = s_i/\sqrt{2s_i^2-1}$. By a change of integration variable $z_i = (\xi_i - \hat{\xi}_i)/\hat{s}_i$, $i = 1, \ldots, n$, the first integral in (2.61) is just equal to $Q(\tilde{\boldsymbol{\theta}}, \mathbf{C}, F)$ given by (2.56). Replacing the first integral in (2.61) by $Q(\tilde{\boldsymbol{\theta}}, \mathbf{C}, F)$ and substituting the resulting expression into (2.59), one obtains (2.55) after simplifications. □

The situation is less determinate if $s_j \le 1/\sqrt{2}$ for some $j \in \{1, \ldots, n\}$. In this case, $\mathsf{E}_q[R\mathbb{I}_F]$ may not be bounded, depending on the structure of the failure region F. In the special case when $F = \mathbb{R}^n$, $\mathsf{E}_q[R\mathbb{I}_F] = \mathsf{E}_q[R]$ is always unbounded when there exists $s_j \le 1/\sqrt{2}$ for some $j \in \{1, \ldots, n\}$. In general, the situation depends on the structure of F in the direction of $\boldsymbol{\psi}_j$, that is, the j-th eigen-direction of $\mathbf{C}$ for which $s_j \le 1/\sqrt{2}$, although it can be argued that $\mathsf{E}_q[R\mathbb{I}_F]$ is generally unbounded except for some special F. This information about F is usually not available when importance sampling is applied, and therefore choosing some $s_j \le 1/\sqrt{2}$ may render $\mathsf{E}_q[R\mathbb{I}_F]$ and hence Δ_{IS} unbounded, even for finite n. This case is thus of little practical interest, and we will focus on the case when $s_i > 1/\sqrt{2}$ for all $i = 1, \ldots, n$.

Corollary 2.1. *In the context of Proposition 2.6, if $s_i > 1/\sqrt{2}$ for all $i = 1, \ldots, n$, then*

$$\mathsf{E}_q[R(\theta)] = \left(\prod_{i=1}^{n} \frac{s_i^2}{\sqrt{2s_i^2 - 1}} \right) \exp\left(\sum_{i=1}^{n} \frac{\tilde{\xi}_i^2}{2s_i^2 - 1} \right) \tag{2.62}$$

Otherwise, $\mathsf{E}_q[R]$ is unbounded for every $n \in \mathbb{Z}^+$.

Proof. If $s_i > 1/\sqrt{2}$ for all $i = 1, \ldots, n$, then the corollary follows from Proposition 2.6 with $F = \mathbb{R}^n$ where $Q(\tilde{\theta}, \mathbf{C}, F) = 1$. Otherwise, if $s_j \leq 1/\sqrt{2}$ for some $j \in \{1, \ldots, n\}$, the integrand in (2.60) grows exponentially large at either $+\infty$ or $-\infty$ in the eigen-direction where $s_j \leq 1/\sqrt{2}$, and hence $\mathsf{E}_q[R] = \mathsf{E}_q[R\,\mathbb{I}_F]$ (for $F = \mathbb{R}^n$) is unbounded for every n. □

Corollary 2.2. *In the context of Proposition 2.6, if $s_i > 1/\sqrt{2}$ for all $i = 1, \ldots, n$, then*

$$\mathsf{E}_q[R(\theta)\,\mathbb{I}_F(\theta)] = Q(\tilde{\theta}, \mathbf{C}, F)\,\mathsf{E}_q[R(\theta)] \tag{2.63}$$

Proposition 2.7. *Let the parameter PDF q be a standard Normal PDF given by* (2.43) *and the ISD f be a Normal PDF centered at $\tilde{\theta}$ with covariance matrix $\mathbf{C}$, as given by* (2.45). *Let $\{s_i^2 : i = 1, \ldots, n\}$ be the eigenvalues of $\mathbf{C}$.*

Assume $s_i > 1/\sqrt{2}$ for all $i = 1, \ldots, n$. Then for $\Delta_{IS} < \infty$ as $n \to \infty$, it is necessary and sufficient that

$$\mathsf{E}_q[R] < \infty \quad \text{as } n \to \infty \tag{2.64}$$

or, equivalently,

$$\sum_{i=1}^{n} \left[\frac{\tilde{\xi}_i^2}{2s_i^2 - 1} + \log \frac{s_i^2}{\sqrt{2s_i^2 - 1}} \right] < \infty \quad \text{as } n \to \infty \tag{2.65}$$

Proof. According to (2.17)

$$\Delta_{IS}^2 = \frac{\mathsf{E}_q[R(\theta)\,\mathbb{I}_F(\theta)]}{P_F^2} - 1 \tag{2.66}$$

and so $\Delta_{IS}^2 < \infty$ if and only if $\mathsf{E}_q[R(\theta)\,\mathbb{I}_F(\theta)] < \infty$, since P_F does not vanish as $n \to \infty$. If $s_i > 1/\sqrt{2}$ for all $i = 1, \ldots, n$, then Corollary 2.2 follows, and so $\mathsf{E}_q[R\,\mathbb{I}_F] < \infty$ if and only if $\mathsf{E}_q[R] < \infty$ since $Q(\tilde{\theta}, \mathbf{C}, F)$ does not vanish as $n \to \infty$. The L.H.S. of (2.65) is just the logarithm of $\mathsf{E}_q[R]$, and hence is equivalent to (2.64). □

Proposition 2.8. *Let the parameter PDF q be a standard Normal PDF given by* (2.43) *and the ISD f be a Normal PDF centered at $\tilde{\theta}$ with covariance matrix $\mathbf{C}$, as given by* (2.45). *Let $\{s_i^2 : i = 1, \ldots, n\}$ be the eigenvalues of $\mathbf{C}$.*

Assume $s_i > 1/\sqrt{2}$ for all $i = 1,\ldots,n$, and the choice of s_i is independent of n. Then for $\mathsf{E}_q[R] < \infty$ as $n \to \infty$, it is necessary and sufficient that

1. *$s_i \neq 1$ for at most a finite number of indexes $i \in \mathbb{Z}^+$ and*

2. *$||\tilde{\theta}|| < \infty$.*

Proof. We first prove the backward part of the statement, which is straightforward. By hypothesis, conditions (1) and (2) hold. Let $I_2(n) = \{i : s_i \neq 1, 1 \leq i \leq n\}$ be the set of indexes for which $s_i \neq 1$. By noting that for $s_i > 1/\sqrt{2}$, $s_i^2/\sqrt{2s_i^2 - 1} = 1$ if and only if $s_i = 1$, and writing

$$\sum_{i=1}^{n} \frac{\tilde{\xi}_i^2}{2s_i^2 - 1} = \sum_{i=1}^{n} \tilde{\xi}_i^2 - \sum_{i \in I_2(n)} \tilde{\xi}_i^2 \frac{s_i^2 - 1}{s_i^2 - 1/2} \tag{2.67}$$

equation (2.62) gives

$$\mathsf{E}_q[R] = \left(\prod_{i \in I_2} \frac{s_i^2}{\sqrt{2s_i^2 - 1}} \right) \exp\left[\sum_{i=1}^{n} \tilde{\xi}_i^2 - \sum_{i \in I_2(n)} \tilde{\xi}_i^2 \frac{s_i^2 - 1}{s_i^2 - 1/2} \right] \tag{2.68}$$

which is bounded since the number of indexes in $I_2(n)$ is finite by condition (1) and $\sum_{i=1}^{n} \tilde{\xi}_i^2 = ||\tilde{\theta}||^2 < \infty$ by condition (2).

For the forward part, assume $\mathsf{E}_q[R] < \infty$ as $n \to \infty$. We will prove condition (1) holds by showing that if it does not, $\mathsf{E}_q[R]$ will be unbounded as $n \to \infty$, leading to a contradiction. Thus, assume condition (1) is not true, that is, there is an infinite number of indexes $i \in \mathbb{Z}^+$ for which $s_i \neq 1$. Let $I_1(n) = \{i : s_i = 1, 1 \leq i \leq n\}$ and $I_2(n) = \{i : s_i \neq 1, 1 \leq i \leq n\}$. For $s_i > 1/\sqrt{2}$,

$$\frac{s_i^2}{\sqrt{2s_i^2 - 1}} = \sqrt{1 + \frac{(s_i^2 - 1)^2}{2(s_i^2 - 1/2)}} \geq 1 \tag{2.69}$$

with equality holds if and only if $s_i = 1$. Thus, the first term of the product in (2.62) for $\mathsf{E}_q[R]$ becomes

$$\prod_{i=1}^{n} \frac{s_i^2}{\sqrt{2s_i^2 - 1}} = \prod_{i \in I_2(n)} \frac{s_i^2}{\sqrt{2s_i^2 - 1}} \tag{2.70}$$

which is unbounded as $n \to \infty$ since the product has infinitely many terms and each term is greater than unity. On the other hand, the second term of the product in (2.62) is always greater than unity, since the sum in the exponent of the term is always positive for $s_i > 1/\sqrt{2}$ for all $i \in \{1,\ldots,n\}$. As a result, $\mathsf{E}_q[R]$ is unbounded as $n \to \infty$, leading to a contradiction. This shows that condition (1) must hold when $\Delta_{IS} < \infty$.

To show condition (2) holds, note that when $s_i > 1/\sqrt{2}$ for all $i = 1,\ldots,n$, the first term in the product of (2.62) is always greater than unity and hence does not vanish as $n \to \infty$. When $\Delta_R < \infty$,

the second term in the product of (2.62) must then be bounded, and is given by the exponential term in (2.68). Since condition (1) holds as we have just shown, the second sum in the exponent of (2.68) consists of only a finite number of terms and is thus finite. Consequently, $||\tilde{\theta}||^2 = \sum_{i=1}^{n} \tilde{\xi}_i^2$ must be bounded, which completes the proof. □

Proposition 2.9. *Let the parameter PDF q be a standard Normal PDF given by* (2.43) *and the ISD f be a Normal PDF centered at $\tilde{\theta}$ with covariance matrix $\mathbf{C}$, as given by* (2.45). *Let $\{s_i^2 : i = 1, \ldots, n\}$ be the eigenvalues of $\mathbf{C}$.*

Assume $s_i > 1/\sqrt{2}$ for all $i = 1, \ldots, n$. Then the following statements are equivalent.

1. $\Delta_{IS} < \infty$
2. $\mathsf{E}_q[R\mathbb{I}_F] < \infty$
3. $\mathsf{E}_q[R] < \infty$
4. $\Delta_R < \infty$

In addition, if the choice of s_i does not depend on n, then each of the above statements is equivalent to

5. *$s_i \neq 1$ for at most a finite number of $i \in \mathbb{Z}^+$, and $||\tilde{\theta}|| < \infty$ as $n \to \infty$*

Proof. Statement (1) is equivalent to (2) by (2.17). Statement (2) is equivalent to (3) by Corollary 2.2. Statement (3) is equivalent to (4) since $\Delta_R = \mathsf{E}_q[R] - 1$. Thus, statements (1) to (4) are equivalent.

If the choice of s_i does not depend on n, then Proposition 2.8 applies, which completes the proof. □

Corollary 2.3. *Importance sampling with ISD chosen from the class*

$$\mathcal{P}_{IS}(n) = \{\phi_n(\cdot; \tilde{\theta}, \mathbf{C}) : \tilde{\theta} \in \mathbb{R}^n; \mathbf{C} \in \mathbb{R}^{n \times n}, \mathbf{C} > 0, \text{ with fixed eigenvalues} > 1/2\} \tag{2.71}$$

for the reliability problem $\mathcal{R}(\phi_n, F_n)$ is applicable in high dimensions if and only if

1. *there is at most a finite number of eigenvalues of $\mathbf{C}$ not equal to unity as $n \to \infty$*
2. *$||\tilde{\theta}|| < \infty$ as $n \to \infty$*

Practically, this corollary says that, to implement importance sampling with ISD constructed with a single point, one can only choose a very small number of the principal standard deviations $s_i \neq 1$. Note that when $\tilde{\theta}$ is a design point, $||\tilde{\theta}||$ is equal to the reliability index associated with the design point, and so condition (2) holds. The exponent in (2.62) for $\mathsf{E}_q[R]$ is then bounded, and the

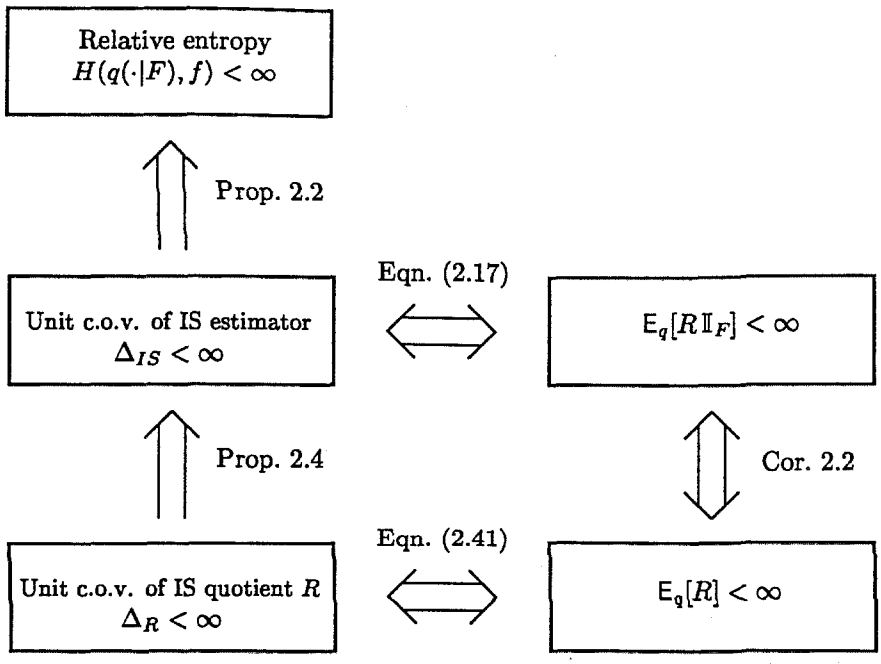

Figure 2.1: Summary of propositions for the case of a single design point

behavior of the c.o.v. Δ_R is governed by the first term in the product, which grows exponentially with the number of indexes where $s_i \neq 1$. The detrimental effect of using principal standard deviation different from unity in some principal directions thus grows exponentially fast with the number of these directions. This effect remains regardless of dimension and will not become vanishingly small even when $n \to \infty$. Indeed, we note in the proof of Proposition 2.8 that $\mathsf{E}_q[R]$ is not bounded even if the number of indexes for which $s_i \neq 1$ is $o(n)$ but still infinite, because the product in (2.70) will grow without bound as long as the number of indexes in I_2 is infinite, no matter of what small order compared to n.

The propositions for the applicability of importance sampling in high dimensions are summarized in Figure 2.1 for $s_i > 1/\sqrt{2}$ for all $i = 1, \ldots, n$.

2.4.3 ISD with multiple points

The study is next extended to the case of ISDs constructed with multiple points. Due to the mathematical difficulties in analyzing Δ_{IS}, most of the results here are sufficient conditions that guarantee applicability in high dimensions. This means that it is possible for importance sampling with multiple points to be applicable in high dimensions under more general conditions than the derived sufficient conditions, although necessary and sufficient conditions are not yet known. Here, the number of points from which the ISD is constructed, m_n, can possibly depend on the dimension n, which is the case frequently encountered in high dimensional simulation problems.

Proposition 2.10. *Let $H(q(\cdot|F), f_i)$ be the relative entropy of the ISD f_i to the conditional PDF $q(\cdot|F)$, $i = 1, \ldots, m_n$; and $H(q(\cdot|F), f)$ be the relative entropy of the mixture distribution $f = \sum_{i=1}^{m_n} w_i f_i$ to $q(\cdot|F)$, where each $w_i \geq 0$ and $\sum_{i=1}^{m_n} w_i = 1$. Then*

$$H(q(\cdot|F), f) \leq \sum_{i=1}^{m_n} w_i H(q(\cdot|F), f_i) \tag{2.72}$$

Proof. By viewing the weights $\{w_i : i = 1, \ldots, m_n\}$ as discrete probabilities and noting that the function $\log(1/\cdot)$ is convex, Jensen's inequality gives

$$\log \frac{q(\theta|F)}{f(\theta)} = \log \frac{q(\theta|F)}{\sum_{i=1}^{m_n} w_i f_i(\theta)} \leq \sum_{i=1}^{m_n} w_i \log \frac{q(\theta|F)}{f_i(\theta)} \tag{2.73}$$

The proposition follows after taking expectation $\mathsf{E}_{q|F}[\cdot]$ on both sides of the inequality. □

The following proposition shows a similar relationship for the unit c.o.v. Δ_{IS}

Proposition 2.11. *Let Δ_i be the unit c.o.v. of importance sampling estimator when the ISD f_i is used, $i = 1, \ldots, m_n$; and Δ_{IS} be the unit c.o.v. of importance sampling estimator when the mixture distribution $f = \sum_{i=1}^{m_n} w_i f_i$ is used as the ISD. Then*

$$\Delta_{IS}^2 \leq \sum_{i=1}^{m_n} w_i \Delta_i^2 \tag{2.74}$$

Proof. By viewing the weights $\{w_i : i = 1, \ldots, m_n\}$ as discrete probabilities and noting that the function $1/\cdot$ is convex, Jensen's inequality gives

$$\frac{q(\theta|F)}{f(\theta)} = \frac{q(\theta|F)}{\sum_{i=1}^{m_n} w_i f_i(\theta)} \leq \sum_{i=1}^{m_n} w_i \frac{q(\theta|F)}{f_i(\theta)} \tag{2.75}$$

The proposition follows after taking expectation $\mathsf{E}_{q|F}[\cdot]$ on both sides of the inequality and noting from (2.18) that $\Delta_i^2 = \mathsf{E}_{q|F}[q(\theta|F)/f_i(\theta)] - 1$ and $\Delta_{IS}^2 = \mathsf{E}_{q|F}[q(\theta|F)/f(\theta)] - 1$. □

Corollary 2.4. *Let Δ_{R_i} be the unit c.o.v. of the importance sampling quotient $R_i(\theta) = q(\theta)/f_i(\theta)$ when the ISD f_i is used, $i = 1, \ldots, m_n$; and Δ_R be the unit c.o.v. of importance sampling quotient $R(\theta) = q(\theta)/f(\theta)$ when the mixture distribution $f = \sum_{i=1}^{m_n} w_i f_i$ is used as the ISD. Then*

$$\Delta_R^2 \leq \sum_{i=1}^{m_n} w_i \Delta_{R_i}^2 \tag{2.76}$$

Proof. Take $F = \mathbb{R}^n$ in Proposition 2.11. □

Proposition 2.11 and Corollary 2.4 says that importance sampling is applicable in high dimensions if the R.H.S. of either (2.74) or (2.76) is bounded as $n \to \infty$. From a practical point of view, the

latter is easier to check than the former, since the unit c.o.v. of the importance sampling quotient can be readily estimated by simulation, but the same is not true for the importance sampling estimator. When $m_n = m$ does not depend on n, it is sufficient to have $\Delta_{R_i} < \infty$ as $n \to \infty$ for every $i = 1, \ldots, m$ in order that importance sampling be applicable in high dimensions.

We next focus on the case when the ISD is constructed as a mixture distribution with Normal kernels using the points $\tilde{\theta}_1, \ldots, \tilde{\theta}_{m_n}$, where the covariance matrix associated with each Normal kernel is taken as the identity matrix, that is,

$$\begin{aligned} f(\theta) &= \sum_{i=1}^{m_n} w_i \, \phi(\theta; \tilde{\theta}_i, \mathrm{I}) \\ &= \sum_{i=1}^{m_n} w_i \, (2\pi)^{-n/2} \exp[-\frac{1}{2}(\theta - \tilde{\theta}_i)^T(\theta - \tilde{\theta}_i)] \end{aligned} \tag{2.77}$$

In this case, using Proposition 2.4 and equation (2.62), we note that a sufficient condition for importance sampling to be applicable in high dimensions is:

$$\sum_{i=1}^{m_n} w_i \exp(||\tilde{\theta}_i||^2) < \infty \quad \text{as } n \to \infty \tag{2.78}$$

Note that for (2.78) to hold, it is not sufficient to have $||\tilde{\theta}_i|| < \infty$ for every $i = 1, \ldots, m_n$, unless m_n does not depend on n. In fact, (2.78) imposes a restriction on the choice of the weights $\{w_i : i = 1, \ldots, m_n\}$. For example, suppose $m_n = n$ and $||\tilde{\theta}_n||$ is non-vanishing as n increases. Then (2.78) says that the weights have to decrease for large n in order that the L.H.S. of (2.78) be bounded. We next derive a less restrictive sufficient condition on the weights.

Proposition 2.12. *Let the parameter PDF q be a standard Normal PDF given by* (2.43) *and the ISD f be a mixture distribution with Normal kernels using the points $\tilde{\theta}_1, \ldots, \tilde{\theta}_{m_n}$, $m_n \geq 1$ with unit covariance matrix, given by* (2.77).

Then

$$\mathsf{E}_q[R(\theta)] \leq \exp(\sum_{i=1}^{m_n} w_i \, ||\tilde{\theta}_i||^2) \tag{2.79}$$

Proof. First note that,

$$R(\theta) = \frac{q(\theta)}{\sum_{i=1}^{m_n} w_i \, \phi(\theta; \tilde{\theta}_i, \mathrm{I})} \leq \frac{q(\theta)}{\prod_{i=1}^{m_n} \phi(\theta; \tilde{\theta}_i, \mathrm{I})^{w_i}} = \prod_{i=1}^{m_n} [\frac{q(\theta)}{\phi(\theta; \tilde{\theta}_i, \mathrm{I})}]^{w_i} \tag{2.80}$$

since the arithematic mean of a set of positive numbers is greater than or equal to the geometric

mean. Substituting $q(\boldsymbol{\theta}) = \phi(\boldsymbol{\theta})$ into (2.80) and simplifying, we have, for every $i = 1, \ldots, m_n$,

$$\frac{q(\boldsymbol{\theta})}{\phi(\boldsymbol{\theta}; \tilde{\boldsymbol{\theta}}_i, \mathbf{I})} = \exp(\frac{1}{2}||\tilde{\boldsymbol{\theta}}_i||^2) \exp(-\langle \tilde{\boldsymbol{\theta}}_i, \boldsymbol{\theta} \rangle) \tag{2.81}$$

and so (2.80) becomes

$$R(\boldsymbol{\theta}) \leq \exp(\frac{1}{2} \sum_{i=1}^{m_n} w_i \, ||\tilde{\boldsymbol{\theta}}_i||^2) \exp(-\langle \sum_{i=1}^{m_n} w_i \, \tilde{\boldsymbol{\theta}}_i, \boldsymbol{\theta} \rangle) \tag{2.82}$$

When $\boldsymbol{\theta}$ is distributed as $q(\boldsymbol{\theta}) = \phi(\boldsymbol{\theta})$, i.e., a standard Normal vector, the second term in (2.82) is Lognormally distributed with mean given by

$$\mathsf{E}_q[\exp(-\langle \sum_{i=1}^{m_n} w_i \, \tilde{\boldsymbol{\theta}}_i, \boldsymbol{\theta} \rangle)] = \exp(\frac{1}{2}|| \sum_{i=1}^{m_n} w_i \, \tilde{\boldsymbol{\theta}}_i||^2) \tag{2.83}$$

Thus, taking expectation $\mathsf{E}_q[\cdot]$ on both sides of (2.82) gives

$$\begin{aligned} \mathsf{E}_q[R(\boldsymbol{\theta})] &\leq \exp(\frac{1}{2} \sum_{i=1}^{m_n} w_i \, ||\tilde{\boldsymbol{\theta}}_i||^2) \, \mathsf{E}_q[\exp(-\langle \sum_{i=1}^{m_n} w_i \, \tilde{\boldsymbol{\theta}}_i, \boldsymbol{\theta} \rangle)] \\ &= \exp(\frac{1}{2} \sum_{i=1}^{m_n} w_i \, ||\tilde{\boldsymbol{\theta}}_i||^2) \exp(\frac{1}{2}|| \sum_{i=1}^{m_n} w_i \, \tilde{\boldsymbol{\theta}}_i||^2) \end{aligned} \tag{2.84}$$

Now

$$\begin{aligned} || \sum_{i=1}^{m_n} w_i \, \tilde{\boldsymbol{\theta}}_i||^2 &= \langle \sum_{i=1}^{m_n} w_i \, \tilde{\boldsymbol{\theta}}_i, \sum_{j=1}^{m_n} w_j \, \tilde{\boldsymbol{\theta}}_j \rangle \\ &= \sum_{i=1}^{m_n} \sum_{j=1}^{m_n} w_i \, w_j \, \langle \tilde{\boldsymbol{\theta}}_i, \tilde{\boldsymbol{\theta}}_j \rangle \\ &\leq \sum_{i=1}^{m_n} \sum_{j=1}^{m_n} w_i \, w_j \, ||\tilde{\boldsymbol{\theta}}_i|| \, ||\tilde{\boldsymbol{\theta}}_j|| \\ &= (\sum_{i=1}^{m_n} w_i \, ||\tilde{\boldsymbol{\theta}}_i||)^2 \\ &\leq \sum_{i=1}^{m_n} w_i \, ||\tilde{\boldsymbol{\theta}}_i||^2 \end{aligned} \tag{2.85}$$

by Jensen's inequality, since $(\cdot)^2$ is convex. Combining (2.84) and (2.85) gives (2.79)

□

Corollary 2.5. *In the context of Proposition 2.12,* $\Delta_{IS} < \infty$ *as* $n \to \infty$ *if*

$$\sum_{i=1}^{m_n} w_i \, ||\tilde{\boldsymbol{\theta}}_i||^2 < \infty \quad \text{as } n \to \infty \tag{2.86}$$

Proof. Under the hypothesis, $\Delta_R^2 = \mathsf{E}_q[R] - 1 < \infty$ as $n \to \infty$ by Proposition 2.12, which implies $\Delta_{IS} < \infty$ by Proposition 2.4. □

Note that, by Jensen's inequality,

$$\sum_{i=1}^{m_n} \exp(w_i \, ||\tilde{\theta}_i||^2) \leq \sum_{i=1}^{m_n} w_i \, \exp(||\tilde{\theta}_i||^2) \tag{2.87}$$

and hence (2.86) holds whenever (2.78) holds, showing that the condition in the former is less restrictive than the latter.

Proposition 2.13. *Importance sampling with ISD chosen from the class*

$$\mathcal{P}_{IS}(n) = \{\sum_{i=1}^{m_n} w_i \, \phi_n(\cdot; \tilde{\theta}_i, \mathbf{I}) : \tilde{\theta}_i \in \mathbb{R}^n; w_i \geq 0, \sum_{i=1}^{m_n} w_i = 1\} \tag{2.88}$$

for the reliability problem $\mathcal{R}(\phi_n, F_n)$ is applicable in high dimensions if (2.86) *holds.*

ISD with random pre-samples

When the ISD is constructed using design points, it is often true that $||\tilde{\theta}_i|| < \infty$ for every $i = 1, \ldots, m_n$ and n, although it is possible that $||\tilde{\theta}_{m_n}||$ becomes unbounded as $n \to \infty$. In this case, the condition in (2.86) can often be achieved by properly choosing the weights, for example, to decay with i such that the L.H.S. of (2.86) remains bounded as $n \to \infty$. However, the same may not be true for ISDs constructed using pre-samples simulated by some prescribed procedure intended to populate the important parts of the failure region, that is,

$$\begin{aligned} f(\theta) &= \sum_{i=1}^{m_n} w_i \, \phi(\theta; \hat{\theta}_i, \mathbf{C}_i) \\ &= \sum_{i=1}^{m_n} w_i \, (2\pi)^{-n/2} \sqrt{|\mathbf{C}_i^{-1}|} \exp[-\frac{1}{2} (\theta - \hat{\theta}_i)^T \mathbf{C}_i^{-1} (\theta - \hat{\theta}_i)] \end{aligned} \tag{2.89}$$

where $\{\hat{\theta}_i : i = 1, \ldots, m_n\}$ are the random pre-samples. The reason is that in this case the Euclidean norm of the pre-samples may grow with the dimension n, even if the design point of the failure region remains bounded. For example, in the case where the failure region is a half-space defined by a hyperplane with the design point θ^*, a random vector $\hat{\theta}$ distributed according to the conditional distribution $q(\theta|F)$ can be represented as (see (4.19) in Chapter 4)

$$\hat{\theta} = Z + (\alpha - \langle Z, \mathbf{u}^* \rangle) \mathbf{u}^* \tag{2.90}$$

where $\mathbf{u}^* = \theta^*/||\theta^*||$ is a unit vector in the direction of the design point θ^*, Z is a standard Normal vector and α is standard Normally distributed conditional on $\alpha > \beta = ||\theta^*||$. Consider the expected

value of $||\hat{\theta}||^2$,

$$\mathsf{E}[||\hat{\theta}||^2] = \mathsf{E}[||\boldsymbol{Z}||^2] + 2\mathsf{E}(\alpha - \langle \boldsymbol{Z}, \mathbf{u}^* \rangle)\langle \boldsymbol{Z}, \mathbf{u}^* \rangle + \mathsf{E}(\alpha - \langle \boldsymbol{Z}, \mathbf{u}^* \rangle)^2 ||\mathbf{u}^*||^2 \tag{2.91}$$

To simplify, first note that $||\mathbf{u}^*|| = 1$ and $\mathsf{E}||\boldsymbol{Z}||^2 = \sum_{i=1}^n \mathsf{E}Z_i^2 = n$. Also, $\langle \boldsymbol{Z}, \mathbf{u}^* \rangle = \sum_{i=1}^n Z_i u_i^*$ is a sum of Normal random variables, and hence is also Normally distributed. Since $\mathsf{E}\langle \boldsymbol{Z}, \mathbf{u}^* \rangle = \sum_{i=1}^n (\mathsf{E}Z_i) u_i^* = 0$ and $\mathsf{E}\langle \boldsymbol{Z}, \mathbf{u}^* \rangle^2 = \sum_{i,j}^n u_i^* u_j^* \mathsf{E}Z_i Z_j = \sum_{i=1}^n u_i^{*2} = 1$, $\langle \boldsymbol{Z}, \mathbf{u}^* \rangle$ is standard Normally distributed, and is independent of α. Thus

$$\begin{aligned} \mathsf{E}(\alpha - \langle \boldsymbol{Z}, \mathbf{u}^* \rangle)\langle \boldsymbol{Z}, \mathbf{u}^* \rangle &= \mathsf{E}\alpha \langle \boldsymbol{Z}, \mathbf{u}^* \rangle - \mathsf{E}\langle \boldsymbol{Z}, \mathbf{u}^* \rangle^2 \\ &= \mathsf{E}\alpha \, \mathsf{E}\langle \boldsymbol{Z}, \mathbf{u}^* \rangle - \mathsf{E}\langle \boldsymbol{Z}, \mathbf{u}^* \rangle^2 \\ &= -1 \end{aligned} \tag{2.92}$$

and

$$\begin{aligned} \mathsf{E}(\alpha - \langle \boldsymbol{Z}, \mathbf{u}^* \rangle)^2 &= \mathsf{E}\alpha^2 + \mathsf{E}\langle \boldsymbol{Z}, \mathbf{u}^* \rangle^2 - 2\mathsf{E}\alpha \, \mathsf{E}\langle \boldsymbol{Z}, \mathbf{u}^* \rangle \\ &= \mathsf{E}\alpha^2 + 1 \end{aligned} \tag{2.93}$$

Substituting (2.92) and (2.93) into (2.91), we have

$$\mathsf{E}||\hat{\theta}||^2 = n - 1 + \mathsf{E}\alpha^2 \tag{2.94}$$

It can thus be expected that $||\hat{\theta}|| = O(\sqrt{n})$ probabilistically, which is unbounded as $n \to \infty$. Condition (2) of Proposition 2.8 is then violated when the ISD given in (2.89) with only one pre-sample ($m_n = 1$) is used. The implication of this is that importance sampling using only one pre-sample simulated according to the conditional distribution $q(\boldsymbol{\theta}|F)$, which was supposed to be the optimal way of generating pre-samples (Ang et al. 1992; Au and Beck 1999), will not be applicable in high dimensions. The remaining question is whether importance sampling is applicable in high dimensions when the ISD is constructed using more than one pre-sample, which is the usual case of interest. Note that violation of Condition (2) does not immediately imply importance sampling using ISD constructed with multiple pre-samples ($m_n \geq 1$) will not be applicable in high dimensions, since Conditions (1) and (2) are only sufficient conditions in the case of ISD with multiple points. The unknown factor here is whether the 'interaction' arising from the pre-samples can help prevent Δ_{IS} from growing without bound as n increases. To answer this question, one needs to study Δ_{IS} and hence the variability of $R(\boldsymbol{\theta})\mathbb{I}_F(\boldsymbol{\theta})$ when $\boldsymbol{\theta}$ is distributed as $f = \sum_{i=1}^{m_n} w_i f_i$. Due to the structure of the ISD, such an analytical study has not been possible. Rather, the variability of the reciprocal of $R(\boldsymbol{\theta})$, i.e., $L(\boldsymbol{\theta}) = 1/R(\boldsymbol{\theta})$, will be studied. This could give insight on the variability of R, assuming

that if $R(\theta)$ has finite variance, then so does its reciprocal $L(\theta) = 1/R(\theta)$. The next proposition shows that the variability of $L(\theta)$ increases exponentially with the order of the Euclidean norm of the pre-samples, which suggests that importance sampling using ISD constructed from random pre-samples is not applicable in high dimensions.

Proposition 2.14. *Let the parameter PDF q be a standard Normal PDF given by* (2.43) *and the ISD f be a mixture distribution with Normal kernels using the points $\tilde{\theta}_1, \ldots, \tilde{\theta}_{m_n}$, $m_n \geq 1$ with unit covariance matrix:*

$$\begin{aligned} f(\theta) &= \sum_{i=1}^{m_n} w_i \, \phi(\theta; \tilde{\theta}_i, \mathrm{I}) \\ &= \sum_{i=1}^{m_n} w_i \, (2\pi)^{-n/2} \exp[-\frac{1}{2}(\theta - \tilde{\theta}_i)^T(\theta - \tilde{\theta}_i)] \end{aligned} \tag{2.95}$$

Let $L(\theta) = f(\theta)/q(\theta)$ be the reciprocal of the importance sampling quotient.

Then the unit c.o.v. Δ_L of $L(\theta)$ when θ is distributed as f is $O(\exp(\rho^2/2))$, where ρ is some representative scale among $||\tilde{\theta}_i||$, $i = 1, \ldots, m_n$.

Proof.

$$L(\theta) = \sum_{i=1}^{m_n} w_i \frac{\phi(\theta - \tilde{\theta}_i)}{\phi(\theta)} \tag{2.96}$$

Since θ is distributed as f, it can be be represented as $\theta = Z + \tilde{\theta}_I$, where $Z = [Z_1, \ldots, Z_n]$ is a standard Normal vector and I is a random index independent of Z and discretely distributed on $\{1, \ldots, m_n\}$ with corresponding probabilities $\{w_1, \ldots, w_{m_n}\}$. Let $L_i = \phi(\theta - \tilde{\theta}_i)/\phi(\theta)$. Then

$$\begin{aligned} L_i &= \frac{\phi(Z + \tilde{\theta}_I - \tilde{\theta}_i)}{\phi(Z + \tilde{\theta}_I)} \\ &= \exp\{-\frac{1}{2}\sum_{j=1}^{n}[Z_j + \tilde{\theta}_I(j) - \tilde{\theta}_i(j)]^2 - [Z_j + \tilde{\theta}_I(j)]^2\} \\ &= \exp\{-\frac{1}{2}\sum_{j=1}^{n}[-\tilde{\theta}_i(j)][2Z_j + 2\tilde{\theta}_I(j) - \tilde{\theta}_i(j)]\} \\ &= \exp[\sum_{j=1}^{n}\tilde{\theta}_i(j)\, Z_j + \sum_{j=1}^{n}\tilde{\theta}_i(j)\,\tilde{\theta}_I(j) - \frac{1}{2}\sum_{j=1}^{n}\tilde{\theta}_i(j)^2] \\ &= \exp(-\frac{||\tilde{\theta}_i||^2}{2})\exp(\langle\tilde{\theta}_i, Z\rangle)\exp(\langle\tilde{\theta}_i, \tilde{\theta}_I\rangle) \end{aligned} \tag{2.97}$$

In the above expression, the first term is a fixed quantity. The second term is Lognormally distributed with mean $\exp(||\tilde{\theta}_i||^2/2)$ and variance $\exp(||\tilde{\theta}_i||^2)[\exp(||\tilde{\theta}_i||^2) - 1]$. The third term is a discrete random variable with mean $\sum_{j=1}^{n} w_j \exp(\langle\tilde{\theta}_i, \tilde{\theta}_j\rangle)$ and second moment $\sum_{j=1}^{n} w_j \exp(2\langle\tilde{\theta}_i, \tilde{\theta}_j\rangle)$. Since the three terms are independent, the expectation of L_i is just the product of the expectation of the

individual terms:

$$\mathsf{E}_f[L_i] = \exp(-\frac{||\tilde{\theta}_i||^2}{2})\mathsf{E}\exp(\langle\tilde{\theta}_i, Z\rangle)\mathsf{E}\exp(\langle\tilde{\theta}_i, \tilde{\theta}_I\rangle) \tag{2.98}$$

Substituting the expression for the individual expectations and simplifying the resulting expression gives

$$\mathsf{E}_f[L_i] = \sum_{j=1}^{n} w_j \exp(\langle\tilde{\theta}_i, \tilde{\theta}_j\rangle) \tag{2.99}$$

The expectation of $L = \sum_{i=1}^{n} w_i L_i$ is thus given by

$$\mathsf{E}_f[L] = \sum_{i,j=1}^{n} w_i w_j \exp(\langle\tilde{\theta}_i, \tilde{\theta}_j\rangle) \tag{2.100}$$

To compute the second moment of L, first note from (2.97) that

$$L_i L_j = \exp[-\frac{1}{2}(||\tilde{\theta}_i||^2 + ||\tilde{\theta}_j||^2)] \exp(\langle\tilde{\theta}_i + \tilde{\theta}_j, Z\rangle) \exp(\langle\tilde{\theta}_i + \tilde{\theta}_j, \tilde{\theta}_I\rangle) \tag{2.101}$$

The first term is a fixed quantity. The second term is Lognormally distributed with mean $\exp(||\tilde{\theta}_i||^2/2 + ||\tilde{\theta}_j||^2/2 + \langle\tilde{\theta}_i, \tilde{\theta}_j\rangle)$. The third term is a discrete random variable with mean

$$\begin{aligned}\mathsf{E}_f[\exp(\langle\tilde{\theta}_i + \tilde{\theta}_j, \tilde{\theta}_I\rangle)] &= \sum_{k=1}^{n} w_i \exp(\langle\tilde{\theta}_i + \tilde{\theta}_j, \tilde{\theta}_k\rangle) \\ &= \sum_{k=1}^{n} w_k \exp(\langle\tilde{\theta}_i, \tilde{\theta}_k\rangle + \langle\tilde{\theta}_j, \tilde{\theta}_k\rangle)\end{aligned} \tag{2.102}$$

Using these results and simplifying the resulting expression for $\mathsf{E}_f[L_i L_j]$,

$$\mathsf{E}[L_i L_j] = \sum_{k=1}^{n} w_k \exp(\langle\tilde{\theta}_i, \tilde{\theta}_j\rangle + \langle\tilde{\theta}_j, \tilde{\theta}_k\rangle + \langle\tilde{\theta}_i, \tilde{\theta}_k\rangle) \tag{2.103}$$

So

$$\begin{aligned}\mathsf{E}_f[L^2] &= \sum_{i,j=1}^{n} w_i w_j \mathsf{E}[L_i L_j] \\ &= \sum_{i,j,k=1}^{n} w_i w_j w_k \exp(\langle\tilde{\theta}_i, \tilde{\theta}_j\rangle + \langle\tilde{\theta}_j, \tilde{\theta}_k\rangle + \langle\tilde{\theta}_i, \tilde{\theta}_k\rangle)\end{aligned} \tag{2.104}$$

To assess the order of magnitude of the first and second moment of L and hence its c.o.v., first note that the sets of numbers $\{w_i w_j : i, j = 1, \ldots, n\}$ and $\{w_i w_j w_k : i, j, k = 1, \ldots, n\}$ are both non-negative and sum up to unity, and hence they can be viewed as a discrete set of probabilities.

Thus $\mathsf{E}[L]$ can be viewed as the expectation of $\exp(\langle\tilde{\theta}_I, \tilde{\theta}_J\rangle)$ over random index pairs (I, J) with corresponding discrete probabilities $\{w_i w_j : i, j = 1, \ldots, n\}$. Similarly, $\mathsf{E}[L^2]$ can be viewed as as the expectation of $\exp(\langle\tilde{\theta}_I, \tilde{\theta}_J\rangle + \langle\tilde{\theta}_J, \tilde{\theta}_K\rangle + \langle\tilde{\theta}_I, \tilde{\theta}_K\rangle)$ over random index triples (I, J, K) with corresponding probabilities $\{w_i w_j w_j : i, j, k = 1, \ldots, n\}$. Note that $|\langle\tilde{\theta}_i, \tilde{\theta}_j\rangle| \leq ||\tilde{\theta}_i|| ||\tilde{\theta}_j||$ with equality holding for $i = j$, so $|\langle\tilde{\theta}_i, \tilde{\theta}_j\rangle| = O(\rho^2)$ where ρ is some representative scale among $||\tilde{\theta}_i||$, $i = 1, \ldots, m_n$. Thus, $\mathsf{E}[L] = O(\exp(\rho^2))$ and $\mathsf{E}[L^2] = O(\exp(3\rho^2))$. Consequently, for the unit c.o.v. of L,

$$\begin{aligned} \Delta_L^2 &= \frac{\mathsf{E}_f[L^2]}{\mathsf{E}_f[L]^2} - 1 \\ &\sim O\left(\frac{\exp(3\rho^2)}{\exp(\rho)^2}\right) \\ &= O\left(\exp(\rho^2)\right) \end{aligned} \tag{2.105}$$

and hence $\Delta_L = O(\exp(\rho^2/2))$. □

2.4.4 Assessment of c.o.v. of importance sampling estimator

Using the expression for $\mathsf{E}_q[R\mathbb{I}_F]$ given by (2.63), we can assess Δ_{IS} and hence the performance of importance sampling based on a single design point. As a first order approximation, assume the failure region is a half space defined by a hyperplane with the design point $\boldsymbol{\theta}^*$. First, we note that $P_F = \Phi(-\beta)$, where $\beta = ||\boldsymbol{\theta}^*||$ is the reliability index. To evaluate $Q(\boldsymbol{\theta}^*, \mathbf{C}, F)$, note that, according to (2.56), it is the probability that a standard Normal vector $\boldsymbol{Z}$ lies in the region $F' = \{\Psi(\Lambda_{\hat{s}}\boldsymbol{Z} + \hat{\boldsymbol{\xi}}^*) \in F\}$, where $\hat{\boldsymbol{\xi}}^* = [\hat{\xi}_1^*, \ldots, \hat{\xi}_n^*]^T$ with $\hat{\xi}_i^* = -\xi_i^*/(2s_i^2 - 1)$ and $\boldsymbol{\xi}^* = [\xi_1^*, \ldots, \xi_n^*]^T = \Psi^T\boldsymbol{\theta}^*$. Since the transformation between $\boldsymbol{\theta}$ and $\boldsymbol{Z}$ is linear and invertible, the region F' is still a half-space defined by a hyperplane in the standard Normal space of $\boldsymbol{Z}$. To find the design point associated with F', note that the design point associated with F is given by $\boldsymbol{\theta}^*$, and so the design point $\boldsymbol{z}^*$ associated with F' will satisfy $\Psi(\Lambda_{\hat{s}}\boldsymbol{z}^* + \hat{\boldsymbol{\xi}}^*) = \boldsymbol{\theta}^*$, which gives

$$\boldsymbol{z}^* = \Lambda_{\hat{s}^{-1}}(\Psi^T\boldsymbol{\theta}^* - \hat{\boldsymbol{\xi}}^*) = \Lambda_{\hat{s}^{-1}}(\boldsymbol{\xi}^* - \hat{\boldsymbol{\xi}}^*) \tag{2.106}$$

since $\boldsymbol{\theta}^* = \Psi\boldsymbol{\xi}^*$. In terms of the components of $\boldsymbol{z}^*$,

$$z_i^* = \frac{1}{\hat{s}_i}(\xi_i^* - \hat{\xi}_i^*) \tag{2.107}$$

and so

$$\begin{aligned}\|z^*\|^2 &= \sum_{i=1}^{n} \frac{1}{\hat{s}_i^2}(\xi_i^* - \hat{\xi}_i^*)^2 \\ &= \sum_{i=1}^{n} \frac{1}{\hat{s}_i^2}(\xi_i^* + \frac{\xi_i^*}{2s_i^2 - 1})^2 \\ &= \sum_{i=1}^{n} (\frac{4s_i^2}{2s_i^2 - 1})\xi_i^{*2}\end{aligned} \tag{2.108}$$

since $\hat{s}_i = s_i/\sqrt{2s_i^2 - 1}$ by (2.58). Thus, $Q(\boldsymbol{\theta}^*, \mathbf{C}, F)$ can be evaluated using standard results for the failure probability for a half-space in the standard Normal space:

$$Q(\boldsymbol{\theta}^*, \mathbf{C}, F) = \Phi(-\|z^*\|) = \Phi(-\sqrt{\sum_{i=1}^{n} (\frac{4s_i^2}{2s_i^2 - 1})\xi_i^{*2}}) \tag{2.109}$$

When $s_i = 1$ for all $i = 1, \ldots, n$, we have $\|z^*\| = 2\|\boldsymbol{\theta}^*\| = 2\beta$, where β is the reliability index, so

$$Q(\boldsymbol{\theta}^*, \mathbf{C}, F) = \Phi(-2\beta) \tag{2.110}$$

Also, using (2.62),

$$\mathrm{E}_q[R] = \exp(\beta^2) \tag{2.111}$$

Substituting (2.110) and (2.111) into (2.63), and using (2.17), we have

$$\Delta_{IS} = \frac{\Phi(-2\beta)\exp(\beta^2)}{\Phi(-\beta)^2} - 1 \tag{2.112}$$

For large β (e.g., $\beta > 3$), $\Phi(-\beta) \sim \phi(\beta)/\beta$ and $\Phi(-2\beta) \sim \phi(2\beta)/2\beta$. Applying these asymptotic relationships to (2.112) gives

$$\Delta_{IS} \sim \frac{\beta}{2} - 1 \quad \text{as } \beta \to \infty \tag{2.113}$$

and so the computational effort required by importance sampling grows linearly with increasing β, or roughly in a logarithmic fashion with decreasing failure probability P_F. This, of course, excludes the computational effort for the search of the design point and is meaningful only when the failure region can be well characterized by a design point such that the importance sampling estimate is unbiased. Finally, assuming a target c.o.v. δ of 30%, the computational effort required for importance sampling in this case (excluding that needed for the search of design point) is $N_\delta = \Delta_{IS}^2/\delta^2 \sim 6\beta$, which is indeed quite small. Extrapolating this conclusion to the general case, it may explain why the

computational effort in the sampling part of importance sampling is often negligible compared to that needed for searching the design point(s).

2.4.5 Diagnosis for applicability in high dimensions

The foregoing analysis focuses on the case of Normal PDF $q(\boldsymbol{\theta})$ and ISD constructed from Normal PDFs. It provides guidelines for how the ISD should be chosen in the cases considered. In general, it is desirable in a particular application to check whether importance sampling using an ISD from a chosen class of ISDs is applicable or not, before the actual simulation is started. Theoretically, one can estimate Δ_{IS} for the sequence of reliability problems in increasing dimensions and check if it grows without bound with the dimension n. However, this is not computationally favorable, since the estimation of Δ_{IS} involves estimating the variability of $R\mathbb{I}_F$ and hence the evaluation of the indicator function $\mathbb{I}_F$, which requires system analyses. A better strategy is to estimate Δ_R, which only involves estimating the variability of the importance sampling quotient and not the indicator function. Then, if Δ_R remains bounded as n increases, it can be guaranteed by Proposition 2.4 that Δ_{IS} is bounded too, and hence importance sampling is applicable in high dimensions for the particular problem. On the other hand, if Δ_R is unbounded as n increases, then it is likely that Δ_{IS} is unbounded too, although the answer is not definite. In this case, one may try to implement importance sampling in high dimensions, and stop the process if Δ_{IS} estimated during the simulation process is large. In the latter case, however, one is cautioned that the importance sampling quotient is likely to be exponentially small. The resulting failure probability estimate may be practically biased, whose large variability may not be detected when the sample size is not sufficiently large. The advice here is that one should pay extra caution when it is found that Δ_R is unbounded as n increases.

Regarding the estimation of Δ_R, it is noted that it is better to use $\Delta_R = \mathsf{E}_q[R] - 1$ in (2.62) by estimating $\mathsf{E}_q[R]$ with samples $\{\boldsymbol{\theta}_1, \ldots, \boldsymbol{\theta}_N\}$ simulated according to q, that is,

$$\mathsf{E}_q[R] = \frac{1}{N}\sum_{k=1}^{N} R(\boldsymbol{\theta}_k) \tag{2.114}$$

rather than to use $\Delta_R = \mathsf{E}_f[R^2] - 1$ by estimating $\mathsf{E}_f[R^2]$ with samples simulated according to f, although the latter is often adopted. It is because when R has large variability, the variance of the estimate for $\mathsf{E}_q[R]$ and hence Δ_R^2 is given by

$$\frac{\mathsf{E}_q[R^2] - \mathsf{E}_q[R]^2}{N} = O(\mathsf{E}_q[R^2]) \tag{2.115}$$

Table 2.1: Four cases of covariance matrix $\mathbf{C}$

Case	Covariance matrix $\mathbf{C}$
1	$s_i = 1, i = 1, \ldots, n$
2	$s_i = 0.9, i = 1, \ldots, n$
3	$s_i = 1.1, i = 1, \ldots, n$
4	$s_i = 0.9, i = 1, \ldots, [n/2];$ $s_i = 1.1, i = [n/2]+1, \ldots, n$

while in the latter case, the variance is

$$\frac{\mathsf{E}_f[R^4] - \mathsf{E}_q[R]^2}{N} = \frac{\mathsf{E}_q[R^3] - \mathsf{E}_q[R]^2}{N} = O(\mathsf{E}_q[R^3]) \tag{2.116}$$

This means that the variance in the latter could be an order of magnitude greater than the former. The intuitive reason for this reduction of estimation error when Δ_R is obtained by estimating $\mathsf{E}_q[R]$ is that in this case the samples are simulated from q, and populate in the region where $R = q/f$ assumes large values that give the major contribution to $\mathsf{E}_q[R]$. In contrast, when $\mathsf{E}_f[R^2]$ is estimated, the samples are simulated from f which are concentrated in the region where R is small. In fact, when the variability of R is really large, this could give a practically biased estimate for its variance.

2.4.6 Example 1

This example demonstrates the preceding propositions for the case of an ISD constructed with a single point. The parameter PDF $q(\boldsymbol{\theta})$ is standard Normal, and the failure region F is a half space defined by a design point $\boldsymbol{\theta}^*$:

$$F = \{\langle \boldsymbol{\theta}, \boldsymbol{\theta}^* \rangle \geq \beta^2\} \tag{2.117}$$

where the design point $\boldsymbol{\theta}^*$ is given by

$$\boldsymbol{\theta}^* = \frac{\beta}{\sqrt{n}}[1, \ldots, 1] \tag{2.118}$$

The exact failure probability is $P_F = \Phi(-\beta)$, regardless of the number of uncertain parameters n. The ISD is a Normal PDF centered at the design point with covariance matrix $\mathbf{C}$, given by (2.45). The covariance matrix is assumed to be diagonal with diagonal elements $\{s_i^2 : i = 1, \ldots, n\}$ which are also its eigenvalues. Four cases, corresponding to different choice of $\mathbf{C}$ are considered, and are shown in Table 2.1.

The formulae for Δ_R and Δ_{IS} are first verified using simulation results. The theoretical value of Δ_R is computed using (2.62). For Δ_{IS}, (2.63) is used, where $Q(\boldsymbol{\theta}^*, \mathbf{C}, F)$ is obtained from (2.109).

On the other hand, using simulation, the estimate for Δ_R is obtained by estimating $\mathsf{E}_q[R]$ based on (2.114) using 10,000 samples simulated according to q. To obtain Δ_{IS} by simulation, we note that it is possible in the current example to generate conditional samples according to $q(\boldsymbol{\theta}|F)$, using (2.90). Thus, we estimate $\mathsf{E}_{q|F}[R]$ with 10,000 samples simulated according to $q(\boldsymbol{\theta}|F)$ and then obtain an estimate for Δ_{IS} using (2.18).

Figures 2.2 to 2.5 show the results for Δ_R for Cases 1 to 4. The corresponding results for Δ_{IS} are shown in Figures 2.6 to 2.9. These figures show that the trends of the estimates for Δ_R and Δ_{IS} agree with the theoretical results given by (2.62) and (2.63). Also, the boundedness of Δ_R can be consistently checked based on (2.114).

Next, the variation of Δ_R and Δ_{IS} with the dimension n is compared for different cases, as shown in Figures 2.10 to 2.13, where only the theoretical values are plotted. Except for Case 1, both Δ_R and Δ_{IS} increase exponentially with n, indicating that importance sampling is not applicable in high dimensions in these cases. This conclusion is precisely what is predicted by Proposition 2.8. On the other hand, for given n, although Δ_R increases exponentially with β, the same is not true for Δ_{IS}. The plots of Δ_{IS} for different values of β are very close to each other. In fact, according to Section 2.8, Δ_{IS} increases only linear with β. In general, the values of Δ_R are seen to be orders of magnitude greater than those of Δ_{IS}, which indicates that the magnitude of Δ_{IS} cannot be inferred from that of Δ_R. Nevertheless, the trend of Δ_{IS} and Δ_R with n are similar; Δ_{IS} remains bounded as n increases whenever Δ_R does (Case 1), and Δ_{IS} grows exponentially with n whenever Δ_R does (Cases 2 to 4). This shows that the behavior of Δ_R with n can be used for concluding the behavior of Δ_{IS}, and hence for diagnosing applicability in high dimensions.

2.4.7 Example 2

This example investigates the applicability in high dimensions of importance sampling with an ISD constructed from multiple design points. The failure region in this case is the union of three half-space regions:

$$F = \cup_{i=1}^{3} \{\langle \boldsymbol{\theta}, \boldsymbol{\theta}_i^* \rangle > \beta^2\} \tag{2.119}$$

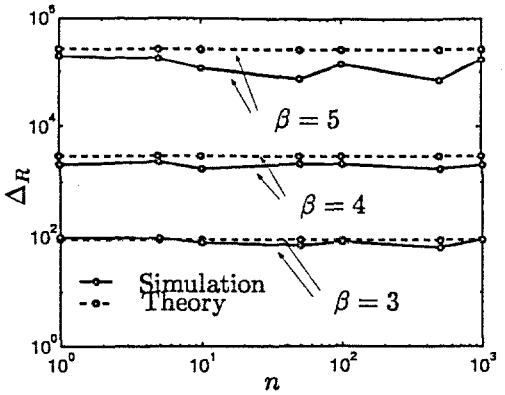

Figure 2.2: Variation of Δ_R with n for Case 1 of Example 1 ($s_i = 1, i = 1, \ldots, n$)

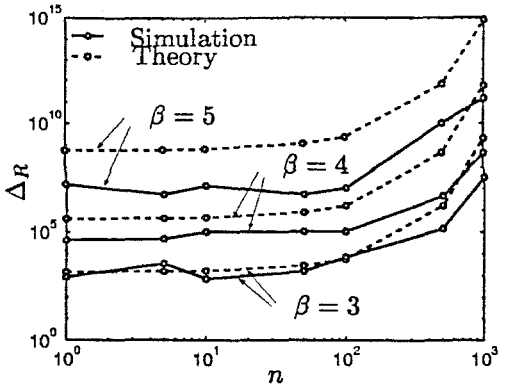

Figure 2.3: Variation of Δ_R with n for Case 2 of Example 1 ($s_i = 0.9, i = 1, \ldots, n$)

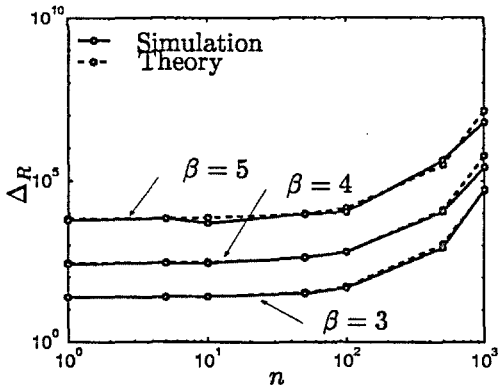

Figure 2.4: Variation of Δ_R with n for Case 3 of Example 1 ($s_i = 1.1, i = 1, \ldots, n$)

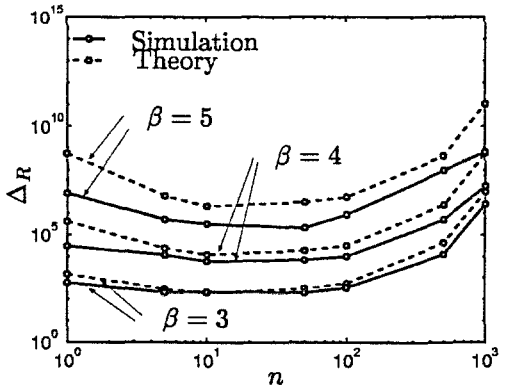

Figure 2.5: Variation of Δ_R with n for Case 4 of Example 1 ($s_i = 0.9, i = 1, \ldots, [n/2]; s_i = 1.1, i = [n/2] + 1, \ldots, n$)

where

$$\boldsymbol{\theta}_1^* = \frac{\beta}{\sqrt{n}}[1, \ldots, 1]$$

$$\boldsymbol{\theta}_2^*(i) = \begin{cases} \beta\sqrt{\frac{2}{n}} & k = 1, \ldots, n/2 \\ 0 & k = n/2 + 1, \ldots, n \end{cases}$$

$$\boldsymbol{\theta}_3^*(i) = \begin{cases} 0 & k = 1, \ldots, n/2 \\ \beta\sqrt{\frac{2}{n}} & k = n/2 + 1, \ldots, n \end{cases} \tag{2.120}$$

are the design points corresponding to the failure boundaries. Note that $||\boldsymbol{\theta}_i^*|| = \beta$, and so the three failure regions have the same probability content, given by $\Phi(-\beta)$. However, the probability content of F, i.e., $P_F = P(F)$, is not equal to the sum of the probability contents of the three failure

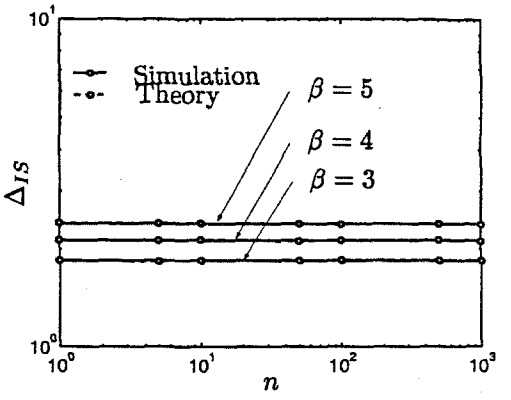

Figure 2.6: Variation of Δ_{IS} with n for Case 1 of Example 1 ($s_i = 1, i = 1, \ldots, n$)

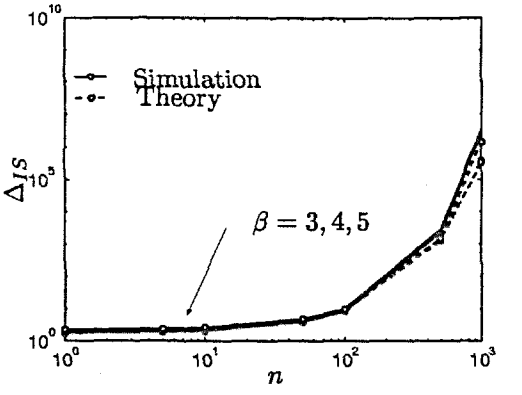

Figure 2.7: Variation of Δ_{IS} with n for Case 2 of Example 1 ($s_i = 0.9, i = 1, \ldots, n$)

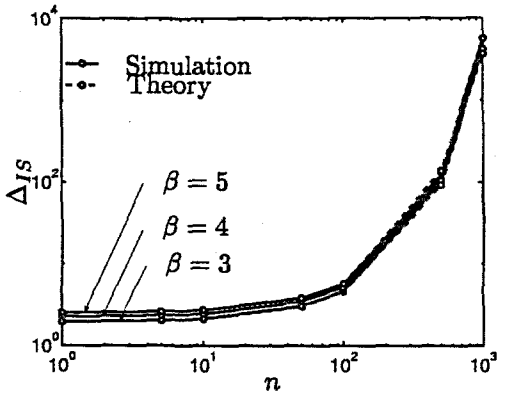

Figure 2.8: Variation of Δ_{IS} with n for Case 3 of Example 1 ($s_i = 1.1, i = 1, \ldots, n$)

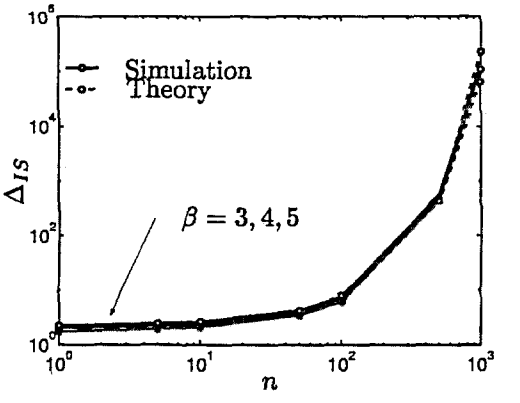

Figure 2.9: Variation of Δ_{IS} with n for Case 4 of Example 1 ($s_i = 0.9, i = 1, \ldots, [n/2]; s_i = 1.1, i = [n/2] + 1, \ldots, n$)

regions because of the intersections among these failure regions. The ISD is constructed as a mixture distribution with Normal kernels centered among the three design points and with covariance matrix $\mathbf{C}$, with the same weighting for all the design points, equal to $1/3$:

$$f(\boldsymbol{\theta}) = \sum_{i=1}^{3} \frac{1}{3} \phi(\boldsymbol{\theta}; \boldsymbol{\theta}_i^*, \mathbf{C}) \tag{2.121}$$

The four cases corresponding to different choice of $\mathbf{C}$ as in the last example are considered (see Table 2.1). In this example, Δ_R is estimated based on (2.114) using $10,000$ samples simulated from q, as in the last example. As is common in most applications, it is not possible in this example to generate efficiently conditional samples according to $q(\boldsymbol{\theta}|F)$, and so Δ_{IS} is estimated using $10,000$ samples generated from the ISD.

Figures 2.14 to 2.17 show the estimates for Δ_R and Δ_{IS} for increasing dimensions n. Except

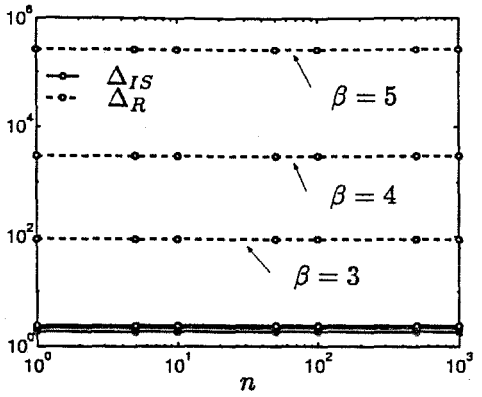

Figure 2.10: Variation of Δ_R and Δ_{IS} with n for Case 1 of Example 1 ($s_i = 1, i = 1, \ldots, n$)

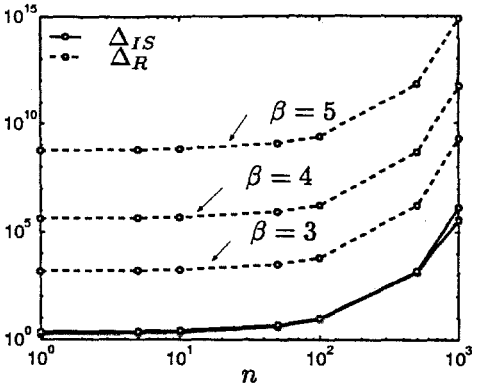

Figure 2.11: Variation of Δ_R and Δ_{IS} with n for Case 2 of Example 1 ($s_i = 0.9, i = 1, \ldots, n$)

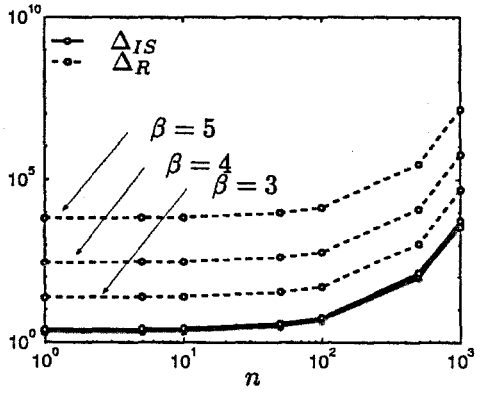

Figure 2.12: Variation of Δ_R and Δ_{IS} with n for Case 3 of Example 1 ($s_i = 1.1, i = 1, \ldots, n$)

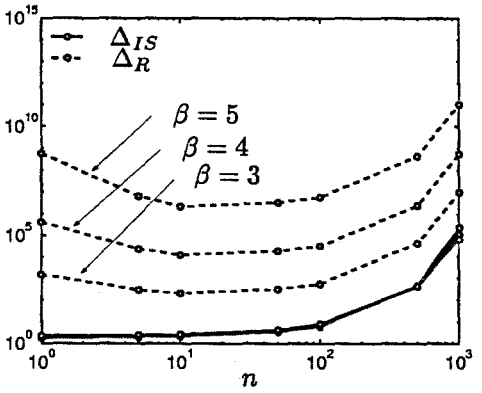

Figure 2.13: Variation of Δ_R and Δ_{IS} with n for Case 4 of Example 1 ($s_i = 0.9, i = 1, \ldots, [n/2]; s_i = 1.1, i = [n/2] + 1, \ldots, n$)

for Case 1, both Δ_R and Δ_{IS} grow exponentially with n, indicating importance sampling is not applicable in Cases 2 to 4. Also, the variation of Δ_{IS} with n is similar to the variation of Δ_R; Δ_{IS} remains bounded as n increases whenever Δ_R does (Case 1), and Δ_{IS} grows exponentially with n whenever Δ_R does (Cases 2 to 4). This suggests that, in this example, the boundedness of Δ_R as $n \to \infty$ could be a necessary and sufficient condition for the boundedness of Δ_{IS}, although only the sufficiency part has been proven in Section 2.4.3.

2.5 Summary of this chapter

The variability of importance sampling estimators has been analyzed from different perspectives to gain insight into the factors governing the choice of an importance sampling density. The lower-bound for the unit coefficient of variation of importance sampling estimators in terms of relative

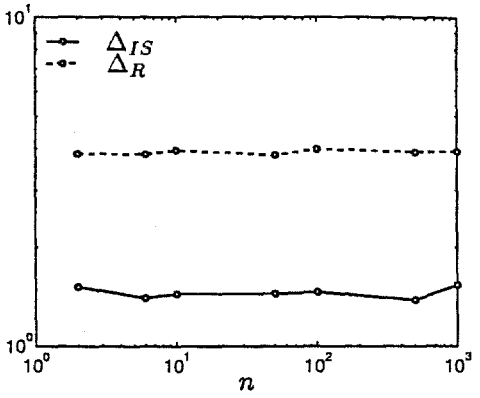

Figure 2.14: Variation of Δ_R and Δ_{IS} with n for Case 1 of Example 2 ($s_i = 1, i = 1, \ldots, n$)

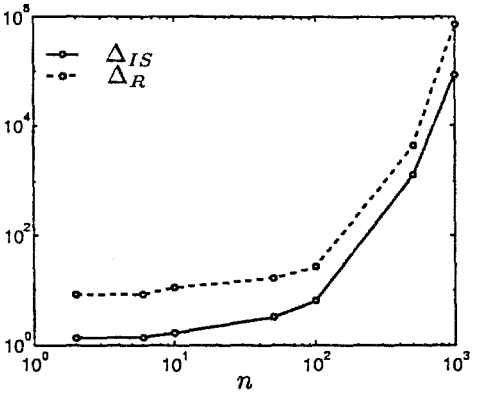

Figure 2.15: Variation of Δ_R and Δ_{IS} with n for Case 2 of Example 2 ($s_i = 0.9, i = 1, \ldots, n$)

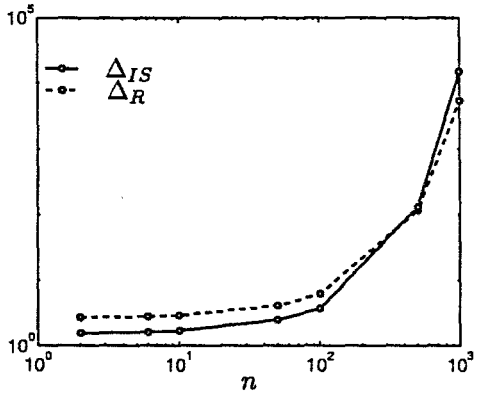

Figure 2.16: Variation of Δ_R and Δ_{IS} with n for Case 3 of Example 2 ($s_i = 1.1, i = 1, \ldots, n$)

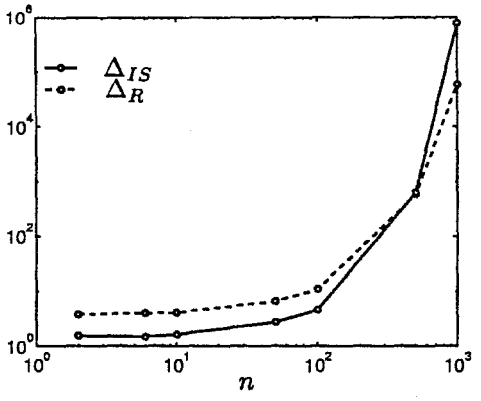

Figure 2.17: Variation of Δ_R and Δ_{IS} with n for Case 4 of Example 2 ($s_i = 0.9, i = 1, \ldots, [n/2]; s_i = 1.1, i = [n/2] + 1, \ldots, n$)

entropy provides the basic insight into the factors that render importance sampling inapplicable in problems with a large number of uncertain parameters. The new results on the applicability of importance sampling in high dimensions should provide important guidelines for applications to simulation problems involving a large number of uncertain parameters, such as first excursion problems where a stochastic process is used for modeling the excitation, or reliability problems with uncertain structures having a large number of uncertain model parameters.

Chapter 3 Markov Chain Monte Carlo Simulation

Markov Chain Monte Carlo Simulation (MCMC) is a class of powerful simulation techniques for generating samples according to any given probability distribution, at least in the asymptotic sense as the number of samples increases. It originates from the Metropolis method developed by Metropolis and his co-workers for applications in statistical physics (Metropolis et al. 1953; Wood and Parker 1957; Alder and Wainwright 1959; Abraham 1986; Duane et al. 1987). The Metropolis method was later applied to solving global optimization problems, resulting in a well-known technique called 'simulated annealing' (Kirkpatrick et al. 1983; Hajek 1988; Bertsimas and Tsitsiklis 1993). A major generalization of the Metropolis method was due to Hastings for applications in Bayesian statistics (Hastings 1970; Bhanot 1988; Besag and Green 1993; Tierney 1994). Other applications of MCMC include image processing (Geman and Geman 1984) and econometrics (Chib and Greenberg 1994; Chib et al. 1998). See Fishman (1996) for a comprehensive discussion of MCMC. Applications to reliability calculations and Bayesian system identification in civil engineering include Au and Beck (1999) and Beck and Au (2000).

In MCMC, successive samples are generated from a specially designed Markov chain whose limiting stationary distribution tends to the target PDF $\pi(\boldsymbol{\theta})$ as the length of the Markov chain increases. Let $\{\boldsymbol{\theta}_1, \boldsymbol{\theta}_2, \dots\}$ be the Markov chain samples, then if the initial sample $\boldsymbol{\theta}_1$ is distributed exactly as $\pi(\boldsymbol{\theta})$, the subsequent samples $\{\boldsymbol{\theta}_2, \boldsymbol{\theta}_3, \dots\}$ are distributed as $\pi(\boldsymbol{\theta})$. If the initial sample is not distributed as $\pi(\boldsymbol{\theta})$, under mild regularity conditions, the distribution of the subsequent samples tends to $\pi(\boldsymbol{\theta})$, that is, $p(\boldsymbol{\theta}_N) \to \pi(\boldsymbol{\theta}_N)$ as $N \to \infty$. Since the samples are generated from a Markov chain, they are dependent, and in general when the initial sample is not distributed as the target PDF, they are not identically distributed. In spite of the fact that the Markov chain samples are not i.i.d., they can still be used for statistical averaging as if they were i.i.d., to yield estimates of the expectation of quantities of interest, by virtue of the laws of large numbers.

The significance of MCMC to solving reliability problems is that it provides a versatile way for generating samples according to the conditional PDF $q(\boldsymbol{\theta}|F)$ given failure occurs, which has been the main challenge in a simulation-based reliability method. The Markov chain samples explore and gain information about the failure region as the Markov chain develops. Proper utilization of these samples can lead to better estimates for the failure probability. Moreover, in a MCMC procedure, only the ratio of the target PDF at different states is evaluated, which means that the target PDF need only be known up to a scaling constant. It is thus possible to generate samples according to the conditional PDF $q(\boldsymbol{\theta}|F) = q(\boldsymbol{\theta})\mathbb{I}_F(\boldsymbol{\theta})/P_F$ even when the scaling factor P_F is unknown. These features make MCMC a favorable tool for generating samples conditional on the failure region for

reliability analysis.

The classical scheme of MCMC, i.e., the Metropolis-Hastings algorithm, will be presented first, followed by a comparison of MCMC with importance sampling. We will then discuss the potential problems that will be encountered when the scheme is applied to problems with a large number of uncertain parameters. A modified MCMC scheme will then be developed, which will form a major component in the subset simulation method developed in Chapter 5 for solving the first excursion problem for general nonlinear systems.

3.1 Metropolis-Hastings algorithm

The Metropolis-Hastings algorithm for generating Markov chain samples $\{\boldsymbol{\theta}_1, \boldsymbol{\theta}_2, \dots\}$ with limiting stationary distribution equal to the target PDF $\pi(\boldsymbol{\theta})$ is described as follows. Let $p^*(\boldsymbol{\xi}|\boldsymbol{\theta})$, called the 'proposal PDF,' be a chosen n-dimensional joint PDF for $\boldsymbol{\xi}$ that depends on $\boldsymbol{\theta}$. In general, let the current Markov chain sample be $\boldsymbol{\theta}_k$ $(k = 1, 2, ...)$. To generate the next Markov chain sample $\boldsymbol{\theta}_{k+1}$, first generate $\boldsymbol{\xi}_k$ according to the proposal PDF $p^*(\cdot|\boldsymbol{\theta}_k)$. Compute the ratio $r_k = \pi(\boldsymbol{\xi}_k)p^*(\boldsymbol{\theta}_k|\boldsymbol{\xi}_k)/\pi(\boldsymbol{\theta}_k)p^*(\boldsymbol{\xi}_k|\boldsymbol{\theta}_k)$. Set $\boldsymbol{\theta}_{k+1} = \boldsymbol{\xi}_k$ with probability $\min\{1, r_k\}$ and set $\boldsymbol{\theta}_{k+1} = \boldsymbol{\theta}_k$ with the remaining probability $1 - \min\{1, r_k\}$.

For our purpose, the Metropolis-Hastings algorithm is presented in the following when the target PDF is equal to the conditional PDF, that is, $\pi(\boldsymbol{\theta}) = q(\boldsymbol{\theta}|F) = q(\boldsymbol{\theta})\mathbb{I}_F(\boldsymbol{\theta})/P_F$. Here, the first Markov chain sample $\boldsymbol{\theta}_1$ is assumed to lie in the failure region F, but it need not be distributed as $q(\boldsymbol{\theta}|F)$.

Metropolis-Hastings algorithm

Repeat for $k = 1, 2, \dots$:

1. *Generate a 'candidate state' $\tilde{\boldsymbol{\theta}}_{k+1}$:*

   (a) Simulate a 'pre-candidate state' $\boldsymbol{\xi}_{k+1}$ according to $p^*(\boldsymbol{\xi}_{k+1}|\boldsymbol{\theta}_k)$.

   (b) Compute the acceptance ratio:

   $$r_{k+1} = \frac{\pi(\boldsymbol{\xi}_{k+1})\, p^*(\boldsymbol{\theta}_k|\boldsymbol{\xi}_{k+1})}{\pi(\boldsymbol{\theta}_k)\, p^*(\boldsymbol{\xi}_{k+1}|\boldsymbol{\theta}_k)} \tag{3.1}$$

   (c) Set $\tilde{\boldsymbol{\theta}}_{k+1} = \boldsymbol{\xi}_{k+1}$ with probability $\min\{1, r_{k+1}\}$ and set $\tilde{\boldsymbol{\theta}}_{k+1} = \boldsymbol{\theta}_k$ with the remaining probability $1 - \min\{1, r_{k+1}\}$

2. *Accept/reject $\tilde{\boldsymbol{\theta}}_{k+1}$ according to F:*

   If $\tilde{\boldsymbol{\theta}}_{k+1} = \boldsymbol{\theta}_k$, increment k by 1 and go to Step 1. Otherwise, check the location of $\tilde{\boldsymbol{\theta}}_{k+1}$. If

$\tilde{\boldsymbol{\theta}}_{k+1} \in F$, accept it as the next sample, i.e., $\boldsymbol{\theta}_{k+1} = \tilde{\boldsymbol{\theta}}_{k+1}$; otherwise reject it and take the current sample as the next sample, i.e., $\boldsymbol{\theta}_{k+1} = \boldsymbol{\theta}_k$, then increment k by 1 and go to Step 1.

Note that Step 2 could have been omitted if the acceptance ratio in Step 1 is multiplied with the term $\mathbb{I}_F(\boldsymbol{\xi}_{k+1})$. The algorithm is presented in two steps for discussion purposes. In the first step, a candidate state $\tilde{\boldsymbol{\theta}}_{k+1}$ is generated, whose distribution is related to the proposal distribution $p^*(\cdot|\boldsymbol{\theta}_k)$. The second step ensures that the next sample lies in the failure region F. In other words, to generate the next Markov chain sample from the current one, we first generate a candidate state, and then take either the candidate state or the current sample as the next sample according to whether the candidate state lies in the failure region or not. Note that the Markov chain samples $\{\boldsymbol{\theta}_1, \boldsymbol{\theta}_2, \dots\}$ are not all distinct, since it is possible that some of them are 'repeated.' This occurs when the candidate state is equal to the current state due to rejection of the pre-candidate state in Step 1, or when the candidate state does not lie in the failure region and hence is rejected in Step 2. As we will see later, this 'repeating' aspect of the Metropolis-Hastings algorithm is the key mechanism that maintains the distribution of the next sample to be equal to that of the current state when the current sample is distributed as the target PDF.

Proof of stationarity

We now show that the next Markov chain sample is distributed as the target PDF when the current one is, and hence the target PDF is the stationary distribution of the Markov chain. Although the proof can be done for general target PDF $\pi(\boldsymbol{\theta})$, we focus on the case of conditional PDF, i.e., $\pi(\boldsymbol{\theta}) = q(\boldsymbol{\theta}|F)$, since the latter provides more insight into the algorithm with respect to the conditioning aspect of the failure region F in the reliability problem. The proof and the techniques involved for the general case are very similar to this special case, which are quite standard and can be readily found in the MCMC literature (see, e.g., Fishman 1996).

The goal is to show that $p(\boldsymbol{\theta}_{k+1}) = q(\boldsymbol{\theta}|F)$ when $p(\boldsymbol{\theta}_k) = q(\boldsymbol{\theta}|F)$. Note that all the Markov chain samples lie in the failure region F, as enforced by Step 2. It is thus sufficient to consider the transition between the states in F, which is governed by Step 1.

First, consider the case of distinct states, i.e., $\boldsymbol{\theta}_{k+1} \neq \boldsymbol{\theta}_k$. According to Step 1, the transition PDF to the next state given the current state $\boldsymbol{\theta}_k$ is given by

$$p(\boldsymbol{\theta}_{k+1}|\boldsymbol{\theta}_k) = p^*(\boldsymbol{\theta}_{k+1}|\boldsymbol{\theta}_k) \min\{1, \frac{p^*(\boldsymbol{\theta}_k|\boldsymbol{\theta}_{k+1})\, q(\boldsymbol{\theta}_{k+1})}{p^*(\boldsymbol{\theta}_{k+1}|\boldsymbol{\theta}_k)\, q(\boldsymbol{\theta}_k)}\} \tag{3.2}$$

Since $\boldsymbol{\theta}_k$ and $\boldsymbol{\theta}_{k+1}$ lie in F and $q(\boldsymbol{\theta})$ differs from $q(\boldsymbol{\theta}|F)$ by a multiplicative constant, the above is equivalent to

$$p(\boldsymbol{\theta}_{k+1}|\boldsymbol{\theta}_k) = p^*(\boldsymbol{\theta}_{k+1}|\boldsymbol{\theta}_k) \min\{1, \frac{p^*(\boldsymbol{\theta}_k|\boldsymbol{\theta}_{k+1})\, q(\boldsymbol{\theta}_{k+1}|F)}{p^*(\boldsymbol{\theta}_{k+1}|\boldsymbol{\theta}_k)\, q(\boldsymbol{\theta}_k|F)}\} \tag{3.3}$$

and so

$$p(\boldsymbol{\theta}_{k+1}|\boldsymbol{\theta}_k)\, q(\boldsymbol{\theta}_k|F) = \min\{1, \frac{p^*(\boldsymbol{\theta}_k|\boldsymbol{\theta}_{k+1})\, q(\boldsymbol{\theta}_{k+1}|F)}{p^*(\boldsymbol{\theta}_{k+1}|\boldsymbol{\theta}_k)\, q(\boldsymbol{\theta}_k|F)}\}\, p^*(\boldsymbol{\theta}_{k+1}|\boldsymbol{\theta}_k)\, q(\boldsymbol{\theta}_k|F) \tag{3.4}$$

Using the following identity for positive real numbers a, b:

$$\min\{1, \frac{a}{b}\}\, b \equiv \min\{1, \frac{b}{a}\}\, a \tag{3.5}$$

equation (3.4) becomes

$$p(\boldsymbol{\theta}_{k+1}|\boldsymbol{\theta}_k)\, q(\boldsymbol{\theta}_k|F) = \min\{1, \frac{p^*(\boldsymbol{\theta}_{k+1}|\boldsymbol{\theta}_k)\, q(\boldsymbol{\theta}_k|F)}{p^*(\boldsymbol{\theta}_k|\boldsymbol{\theta}_{k+1})\, q(\boldsymbol{\theta}_{k+1}|F)}\}\, p^*(\boldsymbol{\theta}_k|\boldsymbol{\theta}_{k+1})\, q(\boldsymbol{\theta}_{k+1}|F) \tag{3.6}$$

and so

$$p(\boldsymbol{\theta}_{k+1}|\boldsymbol{\theta}_k)\, q(\boldsymbol{\theta}_k|F) = p(\boldsymbol{\theta}_k|\boldsymbol{\theta}_{k+1})\, q(\boldsymbol{\theta}_{k+1}|F) \tag{3.7}$$

The above equation is commonly known as the 'reversibility condition' or 'detailed balance' in the theory of Markov chains. Essentially, it says that the 'transition rate' from $\boldsymbol{\theta}_k$ to $\boldsymbol{\theta}_{k+1}$ is equal to the transition rate from $\boldsymbol{\theta}_{k+1}$ to $\boldsymbol{\theta}_k$. Note that the reversibility condition holds trivially when $\boldsymbol{\theta}_{k+1} = \boldsymbol{\theta}_k$, and hence it holds for all cases of $\boldsymbol{\theta}_k$ and $\boldsymbol{\theta}_{k+1}$. The reversibility condition forms the skeleton of the proof, since then:

$$\begin{aligned}
p(\boldsymbol{\theta}_{k+1}) &= \int p(\boldsymbol{\theta}_{k+1}|\boldsymbol{\theta}_k)\, p(\boldsymbol{\theta}_k)\, d\boldsymbol{\theta}_k \\
&= \int p(\boldsymbol{\theta}_{k+1}|\boldsymbol{\theta}_k)\, q(\boldsymbol{\theta}_k|F)\, d\boldsymbol{\theta}_k \\
&= \int p(\boldsymbol{\theta}_k|\boldsymbol{\theta}_{k+1})\, q(\boldsymbol{\theta}_{k+1}|F)\, d\boldsymbol{\theta}_k \quad \text{by (3.7)} \\
&= q(\boldsymbol{\theta}_{k+1}|F) \int p(\boldsymbol{\theta}_k|\boldsymbol{\theta}_{k+1})\, d\boldsymbol{\theta}_k \\
&= q(\boldsymbol{\theta}_{k+1}|F)
\end{aligned} \tag{3.8}$$

since $\int p(\boldsymbol{\theta}_k|\boldsymbol{\theta}_{k+1})\, d\boldsymbol{\theta}_k = 1$. Thus, when the current sample $\boldsymbol{\theta}_k$ is distributed as the target PDF, $q(\boldsymbol{\theta}|F)$, the next sample $\boldsymbol{\theta}_{k+1}$, and hence all subsequent samples $\{\boldsymbol{\theta}_{k+2}, \boldsymbol{\theta}_{k+3}, \ldots\}$ will also be distributed as $q(\boldsymbol{\theta}|F)$.

In the general case when the initial sample $\boldsymbol{\theta}_1$ is not distributed as the target PDF, it can be shown that the distribution of the subsequent samples will still tend to the target PDF, under some mild regularity conditions. The conditions for convergence essentially ensure that the resulting Markov chain is 'ergodic,' which roughly means that the Markov chain samples can visit any state in the support of the target PDF, or equivalently, the failure region F, when the length of the Markov

chain is sufficiently large. With a finite number of Markov chain samples, the issue of ergodicity in practice is whether the generated Markov chain samples can visit sufficiently well the failure region. This determines whether the estimate for the expectation of the quantity of interest obtained by averaging over the Markov chain samples is unbiased.

Conditioning mechanism

The conditioning by the failure region F on the Markov chain samples does not play a significant role in the proof of the stationarity of the Markov chain samples, as it has been assumed that all the Markov chain samples lie in the failure region. The acceptance procedure in Step 1 of the M-H algorithm, which generates the candidate state $\tilde{\boldsymbol{\theta}}_{k+1}$ by acceptance/rejection of the pre-candidate state $\boldsymbol{\xi}_{k+1}$ generated from the proposal PDF p^*, is thus responsible for ensuring that the distribution of the Markov chain samples is equal, or converges, to the parameter PDF $q(\boldsymbol{\theta})$. This can be verified by taking $F = \mathbb{R}^n$ in Step 2 and then noting that $p(\boldsymbol{\theta}_{k+1}) = q(\boldsymbol{\theta}_{k+1})$ in (3.8). Step 2 is very similar to the standard (inefficient) Monte Carlo simulation (MCS) procedure to simulate samples conditional on F, and hence according to $q(\boldsymbol{\theta}|F)$ by the acceptance/rejection method (Rubinstein 1981): simulate a sample $\boldsymbol{\xi}$ from the parameter PDF $q(\boldsymbol{\theta})$, if $\boldsymbol{\xi}$ lies in F, then take $\boldsymbol{\xi}$ as the sample; otherwise repeat the process until acceptance. However, in the standard MCS procedure, one may need to iterate many times before one sample lying in F can be obtained, especially when the probability of failure is small. On average, it requires $1/P_F$ iterations to obtain one sample lying in F. Since determining whether the sample lies in F requires a system analysis, it means that the standard MCS procedure for obtaining conditional samples will be computationally expensive. On the contrary, the 'acceptance rate' of the Markov chain samples generated according to the M-H algorithm can be expected to be significantly higher than the MCS samples, since the candidate state can be generated in the neighborhood of the current sample (which already lies in F), achieved by a suitable choice of the proposal PDF to be discussed later. Of course, this is achieved at the expense of introducing dependence among the samples, and consequently the information provided by the samples is less than if they were independent.

3.2 MCMC estimator

Using the Markov chain samples $\{\boldsymbol{\theta}_1, \ldots, \boldsymbol{\theta}_N\}$ generated by the M-H algorithm with target PDF equal to $\pi(\boldsymbol{\theta})$, the expectation of some quantity of interest, $h(\boldsymbol{\theta})$, say, when $\boldsymbol{\theta}$ is distributed as $\pi(\boldsymbol{\theta})$ can be estimated by simulation as

$$I_\pi = \mathsf{E}_\pi[h(\boldsymbol{\theta})] = \int h(\boldsymbol{\theta})\, \pi(\boldsymbol{\theta})\, d\boldsymbol{\theta} \approx \tilde{I}_\pi = \frac{1}{N} \sum_{k=1}^{N} h(\boldsymbol{\theta}_k) \tag{3.9}$$

When $\pi(\boldsymbol{\theta}) = q(\boldsymbol{\theta}|F)$, then I_π is the conditional expectation of $h(\boldsymbol{\theta})$ given that failure occurs. For example, if h is the repair cost of the structure for a given $\boldsymbol{\theta}$ and F is the event that the peak interstory drift exceeds some specified serviceability limit, then I_π will be the expected repair cost given that the serviceability limit is exceeded. This indicates a straightforward application of MCMC to failure analysis using the Markov chain samples. In contrast, the application of MCMC for estimating the failure probability is not as trivial, which will be discussed in Chapter 5.

If the Markov chain is started with the initial sample distributed as the target PDF, the Markov chain is stationary and all the Markov chain samples are exactly distributed as the target PDF. In this case, $\tilde{I}_\pi$ is unbiased, as is obvious by taking expectation on $\tilde{I}_\pi$ in (3.9). In the general case when the initial sample is not distributed as the target PDF, the Markov chain is not stationary, and $\tilde{I}_\pi$ is biased for every N, although it is asymptotically unbiased as $N \to \infty$.

In spite of the dependence among the Markov chain samples, the MCMC estimator $\tilde{I}_\pi$ still have the usual convergence properties of estimators using independent samples (Fishman 1996). For example, $\tilde{I}_\pi$ converges almost surely to I_π (Strong Law of Large Numbers), and, under similar conditions for MCS estimators, it is Normally distributed as $N \to \infty$ (Central Limit Theorem).

Assuming that the Markov chain is stationary, it can be shown that the coefficient of variation of $\tilde{I}_\pi$ is given by

$$\delta^2_{\tilde{I}_\pi} = \frac{\Delta_h^2}{N}(1+\gamma) \tag{3.10}$$

where Δ_h is the c.o.v. of $h(\boldsymbol{\theta})$ when $\boldsymbol{\theta}$ is distributed as the target distribution $\pi(\boldsymbol{\theta})$,

$$\gamma = 2\sum_{k=1}^{N-1}(1-\frac{k}{N})\rho(k) \tag{3.11}$$

is a correlation factor and $\rho(k)$ is the correlation coefficient between the values of h evaluated at Markov chain samples at lag k apart:

$$\rho(k) = \frac{1}{\Delta_h^2}\mathrm{E}_\pi[h(\boldsymbol{\theta}_1) - I_\pi]\,[h(\boldsymbol{\theta}_{1+k}) - I_\pi] \tag{3.12}$$

Note that the term Δ_h^2/N in (3.10) is the c.o.v. for $\tilde{I}_\pi$ if the Markov chain samples were independent. The c.o.v. for MCMC estimators still decays with $1/\sqrt{N}$ as in the case of MCS estimators. The term $(1+\gamma)$ arises from the correlation among the Markov chain samples. In the usual case when $\gamma > 0$, the efficiency of the estimator using dependent samples of a Markov chain is reduced compared to the case when the samples are independent ($\gamma = 0$). Thus, smaller values of γ imply higher efficiency. The efficiency of the MCMC procedure for estimating I_π, measured in terms of $\delta_{\tilde{I}_\pi}$, is thus governed by the correlation among Markov chain samples. The correlation among the Markov chain samples is strongly affected by the proposal PDF, which will be discussed

next.

3.3 Proposal PDF

Successful applications of MCMC rely on a proper choice of the proposal PDF, which affects the distribution of the candidate state given the current state, and consequently the convergence rate of the MCMC estimator. Two major types of the proposal PDF are discussed here, which reveals the mechanism by which the MCMC procedure works.

Chain-adaptive symmetric (Metropolis) proposal PDF

One common type for the proposal PDF is a symmetric distribution centered at the current sample, that is, $p^*(\xi|\theta) = p^*(\theta|\xi)$. Using this type of proposal PDF, the Metropolis-Hastings algorithm reduces to the original Metropolis algorithm (Metropolis et al. 1953). Since the distribution of the candidate state depends on the current Markov chain sample, the proposal PDF is in this sense 'chain-adaptive'. Experience shows that in this case the form of the proposal PDF is not important in affecting the convergence rate of the estimator, and so those PDFs that are easy to operate are often chosen. For example, the n-dimensional uniform distribution centered at the current sample θ_k with maximum step lengths $\{l_j : j = 1, \ldots, n\}$, say, is a common choice. The maximum step lengths $\{l_j : j = 1, \ldots, n\}$ govern the maximum allowable distance that the next sample can depart from the current one, and consequently affect the size of the region that can be covered by the Markov chain samples within a given number of steps. In general, the larger the maximum step lengths, the larger the region covered by the Markov chain samples. Small values of maximum step lengths tend to increase the correlation among the Markov chain samples, slowing down the convergence of the MCMC estimator. On the other hand, excessively large values of l_j will increase the number of repeated samples and thus slow down the convergence of the MCMC estimator. The reason is that when the maximum step lengths are large, the candidate state will often be generated far away from the current sample, and so the candidate state may not have a high probability of lying in F, and hence be rejected frequently. Thus, the choice of the maximum step lengths, or in general the 'spread' of the proposal PDF, is a trade off between correlation effects arising from proximity and repeated samples from rejection.

Non-adaptive proposal PDF

At the other extreme, the proposal PDF can be 'non-adaptive,' which does not depend on the current sample, that is, $p^*(\xi; \theta) = f(\xi)$. The construction of the proposal PDF in this case is often based on prior knowledge about the target PDF. Under this choice, the proposal PDF should be chosen as close to the conditional PDF $q(\theta|F)$ as possible. To see this, consider the case when

$p^*(\xi) = q(\xi|F)$. In Step 1, the acceptance ratio is given by $r = q(\xi)q(\theta|F)/q(\theta)q(\xi|F) = 1$, since $q(\cdot)$ and $q(\cdot|F)$ differ only by a multiplicative factor. The pre-candidate state ξ will then be taken as the candidate state $\tilde{\theta}$ with probability $\min\{1, r\} = 1$. In Step 2, since $\tilde{\theta} = \xi \in F$ as ξ is simulated from $q(\xi|F)$, the candidate state $\tilde{\theta}$ will always be accepted as the next state. In this case, all the Markov chain samples will be distinct, independent and identically distributed as the target PDF, equal to $q(\theta|F)$. The MCMC procedure then reduces to a standard Monte Carlo procedure. Of course, this choice of proposal PDF is not feasible in practice, for the same reason that the optimal choice of importance sampling density is not possible in importance sampling. Nevertheless, this observation shows that in general the non-adaptive proposal PDF should be chosen as close as possible to the target PDF. The proposal PDF here plays a similar role as the importance sampling density $f(\theta)$ in an importance sampling procedure. The next section establishes the connection between importance sampling and MCMC with a non-adaptive proposal PDF. The choice of proposal PDF will be further explored in Chapter 5 with specific regard to solving the first excursion problem.

3.4 MCMC and importance sampling

Let f be the ISD used in an importance sampling procedure and $R(\theta) = q(\theta)/f(\theta)$ be the importance sampling quotient. Then the importance sampling estimator for failure probability can be written as the average of the importance sampling quotient $R(\theta)$ and the indicator function $\mathbb{I}_F(\theta)$ over i.i.d. samples $\{\xi_1, \ldots, \xi_N\}$ simulated according to the ISD f:

$$P_F = \mathsf{E}_f[\mathbb{I}_F(\theta)R(\theta)] \approx \frac{1}{N}\sum_{k=1}^{N}\mathbb{I}_F(\xi_k)R(\xi_k) \tag{3.13}$$

On the other hand, a MCMC procedure with a non-adaptive proposal PDF equal to f, i.e., $p^*(\xi|\theta) = f(\xi)$ can be considered as first generating a pre-candidate state ξ_k from f and then accepting it as the next Markov chain sample with probability

$$P_A = \min\{1, \frac{\mathbb{I}_F(\xi_k)R(\xi_k)}{\mathbb{I}_F(\theta_k)R(\theta_k)}\} \tag{3.14}$$

By comparing (3.13) and (3.14), it can be seen that importance sampling involves averaging $\mathbb{I}_F(\theta)R(\theta)$ over samples generated by f, while MCMC involves comparing $\mathbb{I}_F(\theta)R(\theta)$ over samples generated by f. In importance sampling, the samples used in the failure probability estimator are distributed as f, while in MCMC, although the pre-candidate states are all i.i.d. according to f, the Markov chain samples $\{\theta_1, \ldots, \theta_N\}$ are at least asymptotically distributed according to the target conditional PDF $q(\theta|F)$. Note that averaging using directly the Markov chain samples yields the conditional expectation of the quantity of interest given F. The efficiency of importance sampling and MCMC depends on the variability of $\mathbb{I}_F(\theta)R(\theta)$, which depends on whether the samples generated according

to f lie frequently in the failure region or not, as well as the variability of $R(\theta)$ given that θ lies in F. It can be expected that, whenever the importance sampling procedure with ISD f is efficient (due to small variability of $\mathbb{I}_F(\theta)R(\theta)$), the MCMC procedure with a non-adaptive proposal PDF $p^* = f$ for generating Markov chain samples with target PDF $q(\theta|F)$ will also be efficient, and vice versa. One should notice, however, when a chain-adaptive proposal PDF (e.g., the Metropolis proposal PDF) is used in the MCMC procedure, it could happen that the MCMC procedure is efficient, but a good ISD is not available. Since the Markov chain using an adaptive proposal PDF can still adapt as the chain develops even if a good ISD is not available, MCMC is a more robust procedure than importance sampling.

Whenever one performs importance sampling to compute the failure probability based on (3.13), one can always obtain Markov chain samples which are at least asymptotically distributed as $q(\theta|F)$. Basically, to generate the k-th Markov chain sample ($k = 2, \ldots, N$), use the k-th sample ξ_k generated from f, and take it as the k-th Markov chain sample with probability

$$\min\{1, \frac{\mathbb{I}_F(\xi_k)R(\xi_k)}{\mathbb{I}_F(\theta_{k-1})R(\theta_{k-1})}\}$$

where θ_{k-1} is the $(k-1)$-th Markov chain sample, with $\theta_1 = \xi_1$ assumed to lie in F. It can be readily seen that this procedure is just a MCMC procedure with a non-adaptive proposal PDF equal to f and with target PDF equal to $q(\theta|F)$.

In the general case when $\mathbb{I}_F(\theta)$ is replaced by some quantity of interest $h(\theta)$, then the quantity computed by importance sampling will give an estimate for $\mathsf{E}_f[h(\theta)\,R(\theta)] = \mathsf{E}_q[h(\theta)]$. Correspondingly, the Markov chain samples generated will be at least asymptotically distributed as $\pi(\theta) = c\,h(\theta)q(\theta)$ for some normalizing constant c. Note that when $h(\theta) = P(F|\theta)$, i.e., the conditional failure probability given θ, then the target PDF is still the conditional failure probability, since then $\pi(\theta) = c\,P(F|\theta)q(\theta) = q(\theta|F)$ by Bayes' Theorem.

3.5 High dimensional aspects of MCMC

The efficiency of a MCMC procedure depends on the correlation among the MCMC samples, according to (3.10). Given that the spread of the proposal PDF is not too small, the correlation is often governed by how frequent the pre-candidate state ξ is rejected. If the pre-candidate state is rejected frequently, the Markov chain will consist of many repeated samples, and the correlation among the Markov chain samples will be large. According to the Metropolis-Hastings algorithm, assuming the Markov chain is stationary, the 'rejection probability' P_R, i.e., the probability that the

pre-candidate state will be rejected in a Markov step, is given by

$$P_R = 1 - \int \min\{1, \frac{p^*(\theta|\xi)q(\xi|F)}{p^*(\xi|\theta)q(\theta|F)}\} p^*(\xi|\theta)q(\theta|F)\, d\xi\, d\theta \tag{3.15}$$

The rejection probability P_R is intimately related to the statistical properties of the acceptance ratio:

$$r = \frac{p^*(\theta|\xi)q(\xi|F)}{p^*(\xi|\theta)q(\theta|F)} = \frac{p^*(\theta|\xi)q(\xi)}{p^*(\xi|\theta)q(\theta)} \tag{3.16}$$

when ξ and θ are jointly distributed as $p^*(\xi|\theta)q(\theta|F)$. In general, if r is probabilistically small, P_R will be close to 1, and the correlation among the MCMC samples will be high. The concern that arises when MCMC is applied to simulating samples of high dimensions is whether the rejection probability will become close to 1 in a systematic manner as $n \to \infty$. This concern is similar to the one considered in the applicability of importance sampling in high dimensions (Chapter 2).

An example is given next which indicates that the rejection probability in the Metropolis algorithm will tend to 1 as $n \to \infty$, and hence the algorithm may not be applicable in high dimensions. It will be seen that the mechanism by which the Metropolis algorithm becomes inapplicable in high dimensions is in some respect similar to that by which importance sampling is not applicable in high dimensions, namely, that the quotient of PDFs evaluated at random arguments becomes exponentially small as the dimension n increases.

Metropolis algorithm

Assume $F = \mathbb{R}^n$ and consider the i.i.d. case where $q(\theta) = \prod_{j=1}^n q_1(\theta_j)$, and $q_1(\theta_j)$ is the one-dimensional parameter PDF for the component θ_j $(j = 1, \ldots, n)$. As a common choice, assume that $p^*(\xi|\theta) = \prod_{j=1}^n p_1^*(\xi_j|\theta_j)$, where $p_1^*(\xi_j|\theta_j)$ denotes the one-dimensional PDF for ξ_j centered at θ_j with the symmetric property $p_1^*(\xi_j|\theta_j) = p_1^*(\theta_j|\xi_j)$, then $r = \prod_{j=1}^n q_1(\xi_j)/q_1(\theta_j)$. Let u be uniformly distributed on [0,1], independent of everything else. According to the Metropolis algorithm, the event $\{r < 1\}$ and an independent failed Bernoulli trial with probability $(1 - r)$ imply that the pre-candidate state ξ will be rejected and hence the next state will be equal to the current state. Thus,

$$\begin{aligned} P_R &\geq P(r < 1, u > r) \\ &= P(u > r | r < 1) P(r < 1) \\ &= \mathsf{E}[1 - r | r < 1] P(r < 1) \\ &= \{1 - \mathsf{E}[r | r < 1]\} P(r < 1) \end{aligned} \tag{3.17}$$

To assess the quantities appearing in (3.17), first note that, since $\{(\xi_j, \theta_j) : j = 1, \ldots, n\}$ are independently and identically distributed as $p_1^*(\xi_j|\theta_j)q_1(\theta_j)$, we have, with probability 1,

$$\frac{\log(r)}{n} = \frac{1}{n}\sum_{j=1}^{n} \log \frac{q_1(\xi_j)}{q_1(\theta_j)} \to \mathsf{E}[\log \frac{q_1(\xi)}{q_1(\theta)}] \quad \text{as } n \to \infty \tag{3.18}$$

by the Strong Law of Large Numbers, where ξ and θ in (3.18) are jointly distributed as $p_1^*(\xi|\theta)q_1(\theta)$. Now

$$\begin{aligned} \mathsf{E}[\log \frac{q_1(\xi)}{q_1(\theta)}] &= \int p_1^*(\xi|\theta)q_1(\theta) \log \frac{q_1(\xi)}{q_1(\theta)} \, d\xi \, d\theta \\ &= \int p_1^*(\xi|\theta)q_1(\theta) \log \frac{p_1^*(\theta|\xi)q_1(\xi)}{p_1^*(\xi|\theta)q_1(\theta)} \, d\xi \, d\theta \quad \text{since } p_1^*(\xi|\theta) = p_1^*(\theta|\xi) \\ &= -H_* \end{aligned} \tag{3.19}$$

where

$$H_* = \int p_1^*(\xi|\theta)q_1(\theta) \log \frac{p_1^*(\xi|\theta)q_1(\theta)}{p_1^*(\theta|\xi)q_1(\xi)} \, d\xi \, d\theta > 0 \tag{3.20}$$

is the relative entropy of the joint density $p_1^*(\theta|\xi)q_1(\xi)$ to the joint density $p_1^*(\xi|\theta)q_1(\theta)$. Note that H_* is strictly positive, since if $H_* = 0$, then $p_1^*(\xi|\theta)\, q_1(\theta) = p_1^*(\theta|\xi)\, q_1(\xi)$, i.e., $q_1(\theta) = q_1(\xi)$ for all ξ and θ, which is impossible. Combining (3.19) with (3.18) implies, with probability 1,

$$r \to \exp(-n\, H_*) \quad \text{as } n \to \infty \tag{3.21}$$

and hence r is exponentially small when the dimension n of the uncertain parameter space is large. It can be expected that $\mathsf{E}[r|r < 1] \to 0$, $P(r < 1) \to 1$ and so $P_R \to 1$ as $n \to \infty$. Thus, it is unlikely that the Metropolis chain will transit to any other new distinct state when the dimension n is large, in which case nearly all the Markov chain samples will be equal. We call this a 'zero-acceptance' phenomenon.

Although it has not been demonstrated analytically, numerical simulations show that zero-acceptance phenomenon occurs in more general situations, for example, when $F \subset \mathbb{R}^n$ or when the components θ_j are not all identically distributed.

Metropolis-Hastings algorithm

In the case of Metropolis-Hastings algorithm with a non-adaptive proposal PDF, let $p^*(\xi) = f(\xi)$. Note that Step 2 of the algorithm can be absorbed into Step 1 by having an acceptance ratio r that

includes the indicator function, that is,

$$r = \frac{q(\xi)}{f(\xi)} \times \frac{f(\theta)}{q(\theta)} \mathbb{I}_F(\xi) \tag{3.22}$$

Since $q(\cdot|F) = q(\cdot)\mathbb{I}_F(\cdot)/P_F$, and the current Markov chain sample θ lies in F, r can be written as

$$r = \frac{q(\xi|F)}{f(\xi)} \times \frac{f(\theta)}{q(\theta|F)} \tag{3.23}$$

Taking logarithm on both sides yields

$$\log r = \log \frac{q(\xi|F)}{f(\xi)} - \log \frac{q(\theta|F)}{f(\theta)} \tag{3.24}$$

where θ and ξ are distributed according to $q(\theta|F)$ and $f(\xi)$, respectively. Unlike the case of adaptive proposal PDF, θ and ξ are independent. The expectation of $\log r$ is given by

$$\mathsf{E}[\log r] = \mathsf{E}_f[\log \frac{q(\xi|F)}{f(\xi)}] - \mathsf{E}_{q|F}[\frac{q(\theta|F)}{f(\theta)}] = -[H(f, q(\cdot|F)) + H(q(\cdot|F), f)] \tag{3.25}$$

and so if either $H(f, q(\cdot|F))$ or $H(q(\cdot|F), f)$ are large, the acceptance ratio r may assume small values probabilistically and hence the rejection probability is large.

Focus now on the case studied for the Metropolis algorithm, where $F = \mathbb{R}^n$ and $q(\theta) = \prod_{i=1}^n q_1(\theta_i)$. Assume $f(\theta) = \prod_{i=1}^n f_1(\theta_i)$. Using a similar procedure as before, we can conclude that if f_1 does not depend on n, then with probability 1,

$$r \to \exp\left[-n\left(H(f_1, p_1) + H(p_1, f_1)\right)\right] \quad \text{as } n \to \infty \tag{3.26}$$

where $H(p_1, f_1)$ and $H(f_1, p_1)$ are the relative entropy of f_1 to p_1 and of p_1 to f_1, respectively. In this case, it may be possible to choose the non-adaptive proposal PDF so that $H(p_1, f_1)$ and $H(f_1, p_1)$ are both at most $O(1/n)$, so that the rejection probability may not tend to 1. Otherwise, by a similar argument as before, the acceptance probability in the Metropolis-Hastings algorithm will tend to zero as the dimension increases, and hence the zero-acceptance phenomenon occurs.

3.6 Modified MCMC

The last section shows that the original Metropolis scheme is not applicable in high dimensions. Similar problems may occur for the Metropolis-Hastings scheme, depending on the choice of the proposal PDFs. The breakdown of the Metropolis algorithm in simulating random vectors of independent components is basically due to the zero-acceptance phenomenon, where the acceptance ratio becomes exponentially small as the dimension n increases. A modified MCMC scheme is developed

in this work which is applicable in high dimensions. The basic idea is to suppress the zero-acceptance phenomenon by generating the candidate state component by component, so that the associated acceptance ratios of the individual components of the pre-candidate state remain non-vanishing as the dimension increases. The modified MCMC scheme for generating samples with limiting stationary PDF equal to $q(\theta|F)$ is presented as follows.

Let $I = \{I_1, \ldots, I_{n_G}\}$, where n_G is the number of groups, be some grouping (or partition) of the indexes $\{1, \ldots, n\}$ corresponding to the uncertain parameters $\{\theta_1, \ldots, \theta_n\}$. Without loss of generality, assume that the ordering of the indexes is not affected by grouping. For example, a valid grouping of $\{1, \ldots, 6\}$ is $\{\{1,2\}, \{3\}, \{4,5,6\}\}$, for which $I_1 = \{1,2\}$, $I_2 = \{3\}$, $I_3 = \{4,5,6\}$ and $n_G = 3$. Let n_j be the number of members in the j-th group ($j = 1, \ldots, n_G$). The whole set of uncertain parameters $\boldsymbol{\theta}$ consists of members from all the groups, that is, $\boldsymbol{\theta} = [\boldsymbol{\theta}^{(1)}, \ldots, \boldsymbol{\theta}^{(n_G)}] \in \mathbb{R}^n$. The n_j-dimensional vector of uncertain paremeters for the j-th group will be denoted by $\boldsymbol{\theta}^{(j)} = \{\theta_s : s \in I_j\}$. For each group j, let $p_j^*(\boldsymbol{\xi}^{(j)}|\boldsymbol{\theta}^{(j)}) : \mathbb{R}^{n_j} \times \mathbb{R}^{n_j} \mapsto [0, \infty)$ be a chosen proposal PDF for generating a random 'pre-candidate component' $\boldsymbol{\xi}^{(j)} \in \mathbb{R}^{n_j}$ based on the vector $\boldsymbol{\theta}^{(j)} \in \mathbb{R}^{n_j}$. To generate the next Markov chain sample $\boldsymbol{\theta}_{k+1} = [\boldsymbol{\theta}_{k+1}^{(1)}, \ldots, \boldsymbol{\theta}_{k+1}^{(n_G)}]$ from the current sample $\boldsymbol{\theta}_k = [\boldsymbol{\theta}_k^{(1)}, \ldots, \boldsymbol{\theta}_k^{(n_G)}]$:

Modified Metropolis-Hastings algorithm

1. *Generate a candidate state* $\tilde{\boldsymbol{\theta}}_{k+1} = [\tilde{\boldsymbol{\theta}}_{k+1}^{(1)}, \ldots, \tilde{\boldsymbol{\theta}}_{k+1}^{(n_G)}]$:
   For each group $j = 1, \ldots, n_G$,

   (a) Generate a pre-candidate component $\boldsymbol{\xi}_{k+1}^{(j)}$ from $p_j^*(\cdot|\boldsymbol{\theta}_k^{(j)})$

   (b) Compute the acceptance ratio:

$$r_{k+1}^{(j)} = \frac{q_j(\boldsymbol{\xi}_{k+1}^{(j)})\, p_j^*(\boldsymbol{\theta}_k^{(j)}|\boldsymbol{\xi}_{k+1}^{(j)})}{q_j(\boldsymbol{\theta}_k^{(j)})\, p_j^*(\boldsymbol{\xi}_{k+1}^{(j)}|\boldsymbol{\theta}_k^{(j)})} \tag{3.27}$$

   (c) Set the j-th component of $\tilde{\boldsymbol{\theta}}_{k+1}$ according to

$$\tilde{\boldsymbol{\theta}}_{k+1}^{(j)} = \begin{cases} \boldsymbol{\xi}_{k+1}^{(j)} & \text{with probability } \min(1, r_{k+1}^{(j)}) \\ \boldsymbol{\theta}_k^{(j)} & \text{with probability } 1 - \min(1, r_{k+1}^{(j)}) \end{cases} \tag{3.28}$$

2. *Accept/reject* $\tilde{\boldsymbol{\theta}}$:
   If $\tilde{\boldsymbol{\theta}}_{k+1} = \boldsymbol{\theta}_k$, set $\boldsymbol{\theta}_{k+1} = \boldsymbol{\theta}_k$. Otherwise, check the location of $\tilde{\boldsymbol{\theta}}_{k+1}$. If $\tilde{\boldsymbol{\theta}}_{k+1} \in F$, accept it as the next state, i.e., set $\boldsymbol{\theta}_{k+1} = \tilde{\boldsymbol{\theta}}_{k+1}$; otherwise reject it and take the current state as the next one, i.e., set $\boldsymbol{\theta}_{k+1} = \boldsymbol{\theta}_k$.

Proof of stationarity

Note from the algorithm that the distribution of the next sample $\boldsymbol{\theta}_{k+1}$ depends only on the current sample $\boldsymbol{\theta}_k$, and hence the samples $\{\boldsymbol{\theta}_1, \boldsymbol{\theta}_2, \dots\}$ form a Markov chain. We next show that if $\boldsymbol{\theta}_k$ is distributed as the target PDF $q(\boldsymbol{\theta}|F)$, then so is $\boldsymbol{\theta}_{k+1}$, and hence $q(\boldsymbol{\theta}|F)$ is the limiting stationary distribution of the Markov chain, based on ergodicity assumptions. Since all the Markov chain samples lie in F as enforced by Step 2, it suffices to consider the transition between the states in F, which is governed by Step 1. First, consider the transition between distinct states in F, i.e., $\boldsymbol{\theta}_k \neq \boldsymbol{\theta}_{k+1}$ and $\boldsymbol{\theta}_k, \boldsymbol{\theta}_{k+1} \in F$. According to Step 1, the transition of the individual groups are independent, so the transition PDF of the Markov chain between any two states in F can be expressed as a product of the group transition PDFs:

$$p(\boldsymbol{\theta}_{k+1}|\boldsymbol{\theta}_k) = \prod_{j=1}^{n_G} p_j(\boldsymbol{\theta}_{k+1}^{(j)}|\boldsymbol{\theta}_k^{(j)}) \tag{3.29}$$

where p_j is the transition PDF for the j-th component $\boldsymbol{\theta}_k^{(j)}$ of $\boldsymbol{\theta}_k$, given by

$$p_j(\boldsymbol{\theta}_{k+1}^{(j)}|\boldsymbol{\theta}_k^{(j)}) = p_j^*(\boldsymbol{\theta}_{k+1}^{(j)}|\boldsymbol{\theta}_k^{(j)}) \min\{1, r_{k+1}^{(j)}\} \tag{3.30}$$

Using (3.27) and (3.30), together with the identity $\min\{1, a/b\}\, b = \min\{1, b/a\}\, a$ for any positive numbers a and b, it is straightforward to show that p_j satisfies the following 'reversibility condition' with respect to q_j for every group $j = 1, \dots, n_G$:

$$p_j(\boldsymbol{\theta}_{k+1}^{(j)}|\boldsymbol{\theta}_k^{(j)})\, q(\boldsymbol{\theta}_k^{(j)}|F) = p_j(\boldsymbol{\theta}_k^{(j)}|\boldsymbol{\theta}_{k+1}^{(j)})\, q(\boldsymbol{\theta}_{k+1}^{(j)}|F) \tag{3.31}$$

Note that the equality in (3.31) is trivial when $\boldsymbol{\theta}_{k+1}^{(j)} = \boldsymbol{\theta}_k^{(j)}$. Combining (3.29) and (3.31), and the fact that all states lie in F, the transition PDF for the whole state $\boldsymbol{\theta}_k$ also satisfies the following reversibility condition with respect to $q(\cdot|F)$:

$$p(\boldsymbol{\theta}_{k+1}|\boldsymbol{\theta}_k)\, q(\boldsymbol{\theta}_k|F) = p(\boldsymbol{\theta}_k|\boldsymbol{\theta}_{k+1})\, q(\boldsymbol{\theta}_{k+1}|F) \tag{3.32}$$

Thus, if the current sample $\boldsymbol{\theta}_k$ is distributed as $q(\cdot|F)$, then

$$\begin{aligned} p(\boldsymbol{\theta}_{k+1}) &= \int p(\boldsymbol{\theta}_{k+1}|\boldsymbol{\theta}_k)\, q(\boldsymbol{\theta}_k|F)\, d\boldsymbol{\theta}_k \\ &= \int p(\boldsymbol{\theta}_k|\boldsymbol{\theta}_{k+1})\, q(\boldsymbol{\theta}_{k+1}|F)\, d\boldsymbol{\theta}_k \quad \text{by (3.32)} \\ &= q(\boldsymbol{\theta}_{k+1}|F) \int p(\boldsymbol{\theta}_k|\boldsymbol{\theta}_{k+1})\, d\boldsymbol{\theta}_k \\ &= q(\boldsymbol{\theta}_{k+1}|F) \end{aligned} \tag{3.33}$$

since $\int p(\theta_k|\theta_{k+1})d\theta_k = 1$. This shows that the next Markov chain sample θ_{k+1} will also be distributed as $q(\cdot|F)$, and so the latter is indeed the stationary distribution for the generated Markov chain.

3.7 Comparison of the modified and original scheme

The basic difference between the modified and the original MCMC scheme lies in the way the candidate state is generated in Step 1 of the algorithm; Step 2 of the algorithm that involves the conditioning by the failure region F is the same in both the modified and the original scheme. In the original MCMC scheme, the pre-candidate state is generated from an n-dimensional proposal PDF and then accepted as the candidate state based on an acceptance ratio that is a quotient between two n-dimensional joint densities. In the modified MCMC scheme, although the candidate state can still be considered as being generated directly by the n-dimensional proposal PDF $\prod_{j=1}^{n} p_j^*(\cdot|\theta_k^{(j)})$, its components are independently accepted/rejected based on the acceptance ratio $r^{(j)}$ $(j = 1, \ldots, n_G)$ that is a quotient between two n_j-dimensional joint densities, where n_j is the number of members in the j-th group. The candidate state is finally generated by combining all the components that have passed through the acceptance/rejection process individually. This 'component-wise' updating feature of the MCMC algorithm is the key modification that suppresses the zero-acceptance phenomenon and makes the algorithm applicable in high dimensions, because the acceptance ratios $\{r^{(j)} : j = 1, \ldots, n_G\}$ involved in the individual groups are only a quotient of two n_j-dimensional joint densities which can be of much smaller dimension than n. In the particular case where each uncertain parameter is grouped as just one component so that there are n components, the acceptance ratios involved are quotients of two one-dimensional densities, and hence their probabilistic behavior will not be systematically affected by n. The applicability of the modified MCMC scheme in high dimensions is next illustrated in terms of the rejection probability of the algorithm.

Applicability of modified MCMC scheme in high dimensions

Let $r^{(j)}$ $(j = 1, \ldots, n_G)$ be the acceptance ratio given by (3.27), and let $\{u_j : j = 1, \ldots, n_G\}$ be independent and uniformly distributed on $[0, 1]$, independent of everything else. For the modified Metropolis-Hastings algorithm, the next state is equal to the current state either when all the pre-candidate components $\{\xi^{(j)} : j = 1, \ldots, n_G\}$ are rejected so that the candidate state $\tilde{\theta}$ is equal to the current state θ_k, or when the candidate state $\tilde{\theta}$ does not lie in F and hence is rejected in Step 2.

So, the rejection probability is given by

$$\begin{aligned} P_R &= P(\{\bigcap_{j=1}^{n_G} r^{(j)} < 1, u_j > r^{(j)}\} \cup \tilde{\theta} \notin F) \\ &\leq P(\bigcap_{j=1}^{n_G} r^{(j)} < 1, u_j > r^{(j)}) + P(\tilde{\theta} \notin F) \\ &= \prod_{j=1}^{n_G} P(r^{(j)} < 1, u_j > r^{(j)}) + P(\tilde{\theta} \notin F) \\ &= \prod_{j=1}^{n_G} P(u_j > r^{(j)} | r^{(j)} < 1) P(r^{(j)} < 1) + P(\tilde{\theta} \notin F) \\ &= \prod_{j=1}^{n_G} \{1 - \mathrm{E}[r^{(j)} | r^{(j)} < 1]\} P(r^{(j)} < 1) + P(\tilde{\theta} \notin F) \end{aligned} \tag{3.34}$$

Since the factors in the first product are always less than 1, the first term tends to vanish as n_G increases. In this case, combining (3.34) with the fact that $P_R \geq P(\tilde{\theta} \notin F)$, it can be argued that $P_R \to P(\tilde{\theta} \notin F)$ as $n_G \to \infty$. This result can be expected intuitively, since when n_G is large, it is unlikely that the candidate state is equal to the current state, as this requires all the n_G pre-candidate components $\{\xi^{(j)} : j = 1, \ldots, n_G\}$ be rejected in Step 1 of the modified algorithm. The event that the next state is equal to the current state then nearly corresponds to the event where the candidate state is rejected for not lying in F. Consequently, when the number of groups n_G and hence the dimension n is large, P_R can be expected not to increase systematically with n, and hence the modified Metropolis-Hastings algorithm is applicable even when the dimension is large.

Regarding the choice of the proposal PDFs, the rules that are used in the original MCMC scheme can be applied for the modified scheme, except that the choice in the latter should be done group by group, rather than for the whole state $\boldsymbol{\theta}$. The choice of the proposal PDF for applications to solving the first excursion problem will be discussed in Chapter 5.

3.8 Summary of this chapter

Markov chain Monte Carlo simulation is a versatile tool for simulating random samples according to an arbitrary target distribution, and provides great promise for applications in reliability analysis. The basic algorithms of Markov chain Monte Carlo simulation, namely, the Metropolis algorithm and the Metropolis-Hastings algorithm, have been discussed in this chapter. Applicability issues in high dimensions have also been examined, which shows that the zero-acceptance phenomenon is likely to occur for these algorithms, due to similar mechanisms that render importance sampling inapplicable in high dimensions. A modified algorithm has been proposed which suppresses the zero-acceptance phenomenon. It will form an important component in the method proposed in Chapter 5, called subset simulation, which is applicable for reliability analysis of general systems.

Chapter 4 Linear Systems and Importance Sampling using Elementary Events

In this chapter, the first excursion problem for linear dynamical systems subjected to additive Gaussian white noise excitation is investigated, which is an important problem due to the widespread use of linear dynamical systems for modeling physical phenomena. In this case, a lot of vital information about the failure characteristics can be obtained analytically based on linear system and random vibration theory. The random vibration aspects of linear dynamical systems have been studied extensively in the literature (Lin 1967; Soong and Grigoriu 1993; Lin and Cai 1995; Lutes and Sarkani 1997). In particular, for Gaussian excitations, the response at multiple time instants are jointly Gaussian, and their joint probability distribution can be described based on unit impulse response functions. In the context of simulation where a discrete approximation of the excitation is used, the failure region corresponding to the failure of a particular output response at a particular time instant is a half space defined by a hyperplane in the load space. This 'elementary failure region' is completely described by a local design point, which can be obtained from unit impulse response functions. This fact has been appreciated in some recent work (e.g., Der Kiureghian 2000; Vijalapura et al. 2000). Recognition of this fact, however, only offers the solution for the failure probability that a *particular* response at a *particular* time exceeds (in magnitude) a given threshold level. The information that is still missing for evaluating the first excursion probability, which is the probability that *any* one of the output responses of interest exceeds (in magnitude) the given threshold level at *any* time instant within the duration of study, is rooted in the interaction of the elementary failure regions corresponding to each of the output responses at each time instant within the time duration of interest.

We investigate analytically the failure region of the first excursion problem for linear systems under Gaussian white-noise excitation with a view to constructing an efficient ISD. Based on information from this study, we propose an ISD which is shown to be very efficient compared to conventional ISDs constructed using information numerically obtained from the integrand function. This ISD has captured the complexity in the dynamics of the first excursion problem, and results in a very efficient importance sampling procedure, showing that the analytical investigation of the failure region is highly rewarding.

4.1 Discrete-time linear systems

We first describe the linear systems considered in the first excursion problem. By linear systems we mean that the relationship between the input excitation and the output response quantity of interest is linear. For convenience in notation, we will use braced quantities to denote the set of quantities inside the brace generated by running the subscripted index (or indexes) of the brace from 1 to the superscripted index (or indexes). For example, $\{Z_j(k)\}_k^{n_t} = \{Z_j(1), \ldots, Z_j(n_t)\}$ and $\{Z_j(k)\}_{j,k}^{l,n_t} = \{Z_1(1), \ldots, Z_l(1), \ldots, Z_1(n_t), \ldots, Z_l(n_t)\}$.

Let $W_1(t), \ldots, W_l(t)$ and $Y_1(t), \ldots, Y_m(t)$ be respectively the l input (excitation) and m output (response) time histories of a continuous-time linear system. Without loss of generality, the outputs are assumed to start from zero initial conditions at time $t = 0$. The input-output relationship can be generally written as, for $i = 1, \ldots, m$,

$$Y_i(t) = \sum_{j=1}^{l} \int_0^t h_{ij}(t, \tau) W_j(\tau) d\tau \tag{4.1}$$

where $h_{ij}(t, \tau)$ is the unit impulse response function (or Green's function) for the i-th output at time t due to a unit impulse applied at the j-th input at time τ. As a result of linearity, the response is a sum of the contributions from the individual input W_j. Causality has been assumed for the impulse response functions, namely, $h_{ij}(t, \tau) \equiv 0$ for $t < \tau$, so that the integration limit is from 0 to t instead of 0 to ∞. The representation in (4.1) is applicable for any linear system, including time-varying systems.

In practical applications, the output response is often solved at discrete time steps by some numerical integration scheme (Dokainish and Subbaraj 1989; Subbaraj and Dokainish 1989) using the values of the input at the sampled time instants. Let the sampling be uniform at time spacing $\Delta t = T/(n_t - 1)$ where T is the duration of study and n_t is the number of time instants, so that the sampling times are $t_k = (k-1)\Delta t$, $k = 1, \ldots, n_t$. The excitation $\{W_j\}_j^l$ in discrete-time is assumed to be band-limited Gaussian white noise:

$$W_j(t_k) = \sqrt{\frac{2\pi S_j}{\Delta t}} Z_j(k) \tag{4.2}$$

where S_j is the spectral intensity and $\{Z_j(k)\}_{j,k}^{l,n_t}$ are i.i.d. Gaussian random variables. In the discrete-time system, $\{Z_j(k)\}_{j,k}^{l,n_t}$ are considered as the input random variables, from which a realization of the excitation can be generated for simulation purposes. The vector $Z = [Z_1(1), \ldots, Z_l(1), \ldots, Z_1(n_t), \ldots, Z_l(n_t)]$ collecting all the input random variables is thus an $n = n_t \times l$-

dimensional standard Gaussian vector with independent components and so has joint PDF

$$p(z) = \phi(z) \triangleq (2\pi)^{-n/2} \exp(-\frac{1}{2}\sum_{i=1}^{n} z_i^2) \tag{4.3}$$

where $z = [z_1, \ldots, z_n]$ is a state of the input random vector $\boldsymbol{Z}$. Although the excitation is assumed to be stationary white noise in (4.2), the formulation is applicable for more general excitation by redefining the system. For example, if the excitation is a filtered white noise modulated by an envelope function, then h_{ij} will be equal to the convolution of the impulse response function of the original system and the filter, multiplied by the envelope function.

Using the representation of the excitation in (4.2), the discrete-time analog of the input-output relationship in (4.1) can be written in terms of the input random variables $\{Z_j(s)\}_{j,s}^{l,k}$:

$$Y_i(k) = \sum_{j=1}^{l}\sum_{s=1}^{k} g_{ij}(k,s) Z_j(s) \sqrt{2\pi S_j \Delta t} \tag{4.4}$$

where $\{Y_i(k)\}_i^m$ are the outputs at time step k and $g_{ij}(k,s)$ is the discrete-time unit impulse response of the i-th output at time step k due to a unit impulse $Z_j(s) = 1$ applied at the j-th input at time step s. The relationship between g_{ij} and h_{ij} depends on the numerical integration scheme used. The discrete-time impulse response g_{ij} can often be obtained numerically from dynamic analysis using finite element programs, for example. In particular, for time-invariant systems, $h_{ij}(t,\tau) = h_{ij}(t-\tau)$ and $g_{ij}(k,s) = g_{ij}(k-s+1)$, so the set of impulse response functions $\{g_{ij}\}_i^m$ corresponding to the j-th input excitation can be obtained in one dynamic analysis. Consequently, it requires l dynamic analyses to obtain the whole set of impulse response functions $\{g_{ij}\}_{i,j}^{m,l}$ which completely describe the input-output relationship.

As a fact that will be used later, it is noted that the discrete impulse response will tend to its continuous-time counterpart as the sampling interval Δt tends to zero:

$$g_{ij}(k,s) \to h_{ij}(t_k, t_s) \quad \text{as } \Delta t \to 0 \tag{4.5}$$

provided that the numerical scheme used to compute the response is convergent (i.e., consistent and stable) (Hughes 1987). In practical applications where the numerical scheme is sufficiently accurate, it may be assumed that the discrete-time and continuous-time impulse responses are equal at the sampled time instants.

4.2 Analysis of the failure region

In terms of the discrete-time system, the failure event F of interest is defined as the exceedence of the absolute response of any one of the outputs beyond a given threshold level at any time step between 1 and n_t:

$$F = \bigcup_{i=1}^{m} \bigcup_{k=1}^{n_t} \{|Y_i(k)| > b_i(k)\} = \bigcup_{i=1}^{m} \bigcup_{k=1}^{n_t} F_{ik} \tag{4.6}$$

where $b_i(k)$ is the threshold level for the i-th output at time step k, and F_{ik} is the 'elementary failure event' that the absolute response of the i-th output at time step k exceeds $b_i(k)$, that is,

$$F_{ik} = \{|Y_i(k)| > b_i(k)\} \tag{4.7}$$

Since F is the union of the elementary failure events $\{F_{ik}\}_{i,k}^{m,n_t}$, a study of the latter may help understand the former. We will thus begin by studying the elementary failure event F_{ik} for given i and k.

4.2.1 Elementary failure region

The elementary failure event F_{ik} is the union of the up-crossing and down-crossing events, $F_{ik}^{+} = \{Y_i(k) > b_i(k)\}$ and $F_{ik}^{-} = \{Y_i(k) < -b_i(k)\}$, respectively, which are mutually exclusive. Since F_{ik}^{-} can be written as $\{-Y_i(k) > b_i(k)\}$, that is, the up-crossing event of $-Y_i$ at time step k, and the two processes Y_i and $-Y_i$ are probabilistically identical, it suffices to consider the up-crossing event F_{ik}^{+}. Using (4.4), F_{ik}^{+} is the semi-infinite region $\{z : \sum_{j=1}^{l} \sum_{s=1}^{k} g_{ij}(k,s) z_j(s) \sqrt{2\pi S_j \Delta t} > b_i(k)\}$ in the standard n-dimensional Gaussian space of the input variables z where $n = n_t\, l$. The failure boundary is given by $\partial F_{ik}^{+} = \{z : \sum_{j=1}^{n} \sum_{s=1}^{k} g_{ij}(k,s) z_j(s) \sqrt{2\pi S_j \Delta t} = b_i(k)\}$, which is a hyperplane in the n-dimensional space of z. Note that ∂F_{ik}^{+} imposes a constraint only on $z_j(s)$ for all $s \leq k$, as a result of causality.

Design point: The point in F_{ik}^{+} which has the highest probability density among other points in F_{ik}^{+}, called the design point for F_{ik}^{+} in reliability terminology, is of particular importance. As the PDF $\phi(z)$ for Z decays radially from the origin, the design point lies on the failure boundary ∂F_{ik}^{+}. The design point maximizes the joint PDF $\phi(z)$ under the linear constraint

$$\sum_{j=1}^{l} \sum_{s=1}^{k} g_{ij}(k,s) z_j(s) \sqrt{2\pi S_j \Delta t} = b_i(k)$$

Since $\phi(z)$ is a decreasing function of only the distance of z from the origin, which is equal to the Euclidean norm of z, the design point is just the point on ∂F_{ik}^{+} with the smallest Euclidean norm.

Let $z^*_{ik} = \{z^*_{ik,j}(s)\}_{j,s}^{l,n_t} \in \mathbb{R}^n$ be the design point of the elementary failure event F^+_{ik}, where $z^*_{ik,j}(s)$ is the value of the j-th input at time step s corresponding to the design point. Direct constraint minimization yields:

$$z^*_{ik,j}(s) = U(k-s)\sqrt{2\pi S_j \Delta t}\,\frac{g_{ij}(k,s)}{\sigma^2_{ik}} b_i(k) \tag{4.8}$$

where $U(\cdot)$ is the unit step function: $U(x) = 1$ if $x \geq 0$ and zero otherwise, and

$$\sigma^2_{ik} = \mathrm{Var}[Y_i(k)] = \sum_{j=1}^{l}[\sum_{s=1}^{k} g_{ij}(k,s)^2]2\pi S_j \Delta t \tag{4.9}$$

is the variance of $Y_i(k)$, which can be readily obtained by direct analysis of (4.4). As a consequence of causality, $z^*_{ik,j}(s) = 0$ for $s > k$. It is interesting to note that the variance σ^2_{ik} of the i-th output at time step k is equal to the sum of all the 'energy' of the corresponding impulse responses from all inputs accumulated up to time step k. By (4.5), $g_{ij}(k,s) \to h_{ij}(t_k, t_s)$ as $\Delta t \to 0$, so we have

$$\sigma^2_{ik} \to \sum_{j=1}^{l} 2\pi S_j \int_0^{t_k} h_{ij}(t_k,\tau)^2 d\tau \quad \text{as } \Delta t \to 0 \tag{4.10}$$

$$= \text{variance of output } i \text{ at time } t_k \text{ of continuous-time system}$$

and so σ^2_{ik} varies 'continuously' with k as the sampling is refined.

The excitation $W^*_{ik,j}$ at the j-th input that corresponds to the design point $z^*_{ik,j}$ is

$$W^*_{ik,j}(t_s) = \sqrt{\frac{2\pi S_j}{\Delta t}} z^*_{ik,j}(s) = U(k-s)\frac{g_{ij}(k,s)}{\sum_{r=1}^{l}\sum_{s=1}^{k} g_{ir}(k,s)^2 \Delta t} b_i(k) \tag{4.11}$$

and so

$$W^*_{ik,j}(t_s) \to\ U(t_k - t_s) b_i(k) \frac{h_{ij}(t_k,t_s)}{\sum_{r=1}^{l}\int_0^t h_{ir}(t_k,\tau)^2 d\tau} \quad \text{as } \Delta t \to 0 \tag{4.12}$$

Reliability index and probability content: The Euclidean norm β_{ik} of the design point z^*_{ik}, often called the 'reliability index,' is given by:

$$\beta_{ik} = ||z^*_{ik}|| = \frac{b_i(k)}{\sigma_{ik}} \tag{4.13}$$

Since the components of z are i.i.d. standard Gaussian, the probability content of F^+_{ik} is given by

$$P(F^+_{ik}) = \Phi(-||z^*_{ik}||) = \Phi(-\beta_{ik}) \tag{4.14}$$

where $\Phi(\cdot)$ is the cumulative distribution function of the standard Gaussian distribution. Equation (4.14) can be obtained directly by noting that the i-th output has Gaussian distribution with mean zero and standard deviation σ_{ik} for a linear system under zero mean Gaussian excitation. Note that in the present case where the failure boundary is a hyperplane, the probability content of the failure region F_{ik}^{+} is completely determined by the reliability index β_{ik}.

Conditional distribution of input random variables: The conditional distribution of the input random vector $\boldsymbol{Z}$ given that it lies in the elementary failure region F_{ik}^{+} is just the original PDF $\phi(z)$ confined to F_{ik}^{+} and normalized by the probability content of F_{ik}^{+}:

$$p(z|F_{ik}^{+}) = \frac{\phi(z)\mathbb{I}_{F_{ik}^{+}}(z)}{\Phi(-\beta_{ik})} \tag{4.15}$$

Since the failure boundary ∂F_{ik}^{+} is a hyperplane, by the rotational symmetry of standard Gaussian vectors with independent components, the conditional vector $\boldsymbol{Z}_{ik}^{+}$ distributed as $p(z|F_{ik}^{+})$ can be represented as

$$\boldsymbol{Z}_{ik}^{+} = \alpha \mathbf{u}_{ik}^{*} + \boldsymbol{Z}_{ik}^{\perp} \tag{4.16}$$

where

$$\mathbf{u}_{ik}^{*} = \boldsymbol{z}_{ik}^{*}/||\boldsymbol{z}_{ik}^{*}|| = \boldsymbol{z}_{ik}^{*}/\beta_{ik} \tag{4.17}$$

is a unit vector in the direction of the design point $\boldsymbol{z}_{ik}^{*}$ (perpendicular to the hyperplane ∂F_{ik}^{+}); α is a standard Gaussian random variable conditional on $\{\alpha > \beta_{ik}\}$, that is, $p(\alpha) = \phi(\alpha)U(\alpha - \beta_{ik})/\Phi(-\beta_{ik})$; $\boldsymbol{Z}_{ik}^{\perp}$ is a standard Gaussian vector orthogonal to $\mathbf{u}_{ik}^{*}$ (parallel to the hyperplane ∂F_{ik}^{+}). It can be easily verified that $\boldsymbol{Z}_{ik}^{\perp}$ can be represented in the following form which allows for efficient simulation:

$$\boldsymbol{Z}_{ik}^{\perp} = \boldsymbol{Z} - \langle \boldsymbol{Z}, \mathbf{u}_{ik}^{*} \rangle \mathbf{u}_{ik}^{*} \tag{4.18}$$

where $\boldsymbol{Z}$ is a n-dimensional standard Gaussian vector with independent components. Substituting (4.18) into (4.16), $\boldsymbol{Z}_{ik}^{+}$ can be represented as

$$\boldsymbol{Z}_{ik}^{+} = \boldsymbol{Z} + (\alpha - \langle \boldsymbol{Z}, \mathbf{u}_{ik}^{*} \rangle)\mathbf{u}_{ik}^{*} \tag{4.19}$$

The foregoing results are applicable to the down-crossing event F_{ik}^{-}, except that the design point for F_{ik}^{-} is the negative of the design point for F_{ik}^{+}. Also, a random vector $\boldsymbol{Z}_{ik}^{-}$ distributed as $p(z|F_{ik}^{-})$ is identically distributed as $-\boldsymbol{Z}_{ik}^{+}$.

For the out-crossing event $F_{ik} = F_{ik}^+ \cup F_{ik}^-$, since F_{ik}^+ and F_{ik}^- are disjoint, F_{ik} has two design points corresponding to those from F_{ik}^+ and F_{ik}^-. The probability content of F_{ik} is simply the sum of those of F_{ik}^+ and F_{ik}^-, so $P(F_{ik}) = 2\Phi(-\beta_{ik})$. The input random vector $\boldsymbol{Z}_{ik}$ distributed according to $p(\boldsymbol{z}|F_{ik})$ is distributed as $\boldsymbol{Z}_{ik}^+$ with probability 1/2 and as $\boldsymbol{Z}_{ik}^-$ with probability 1/2.

4.2.2 Interaction of elementary failure regions

The results in the last section indicate that the failure regions corresponding to the elementary failure events can be described in a simple way. Their probabilistic properties are completely determined by their design points, which are known and can be computed readily from deterministic dynamic analysis. The complexity of the first excursion problem, however, lies in the interaction of the elementary failure events F_{ik} in forming the first excursion failure event $F = \cup_{i=1}^{m} \cup_{k=1}^{n_t} F_{ik}$.

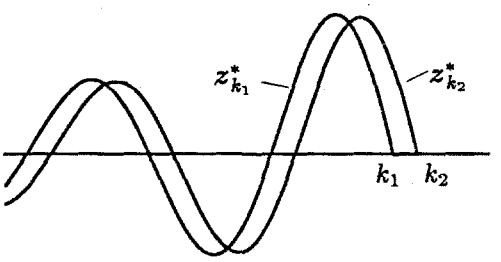

Figure 4.1: Neighboring design points

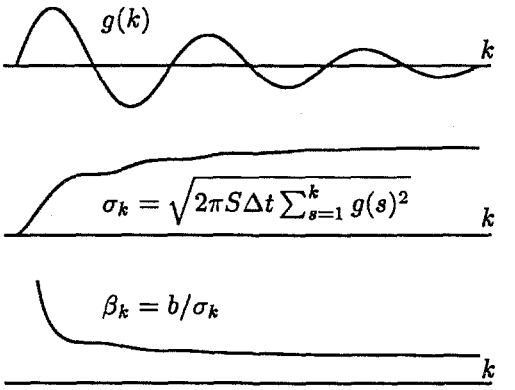

Figure 4.2: Variation with time of reliability index β_k, response standard deviation σ_k and impulse response $g(k)$

Two types of interaction between the elementary failure events can be distinguished. The first one involves interaction of the first excursion events $\{\cup_{k=1}^{n_t} F_{ik}\}_i^m$ among the different outputs $i = 1, \ldots, m$. The second type is the interaction of the elementary failure events at different failure time steps k for a given output i. The first type depends on the relationship between the outputs of the system, and would be different for different types of systems and definition of output states. This type of interaction should be studied for a particular type of system, and will not be pursued here. The second type of interaction between the failure events at different failure time steps k, however, can be studied in general, since it depends on the relationship of the response at different instants for a given output, and consequently it is governed by more general properties such as the continuity of the impulse response functions of the system. In this study, we will focus on the second type of interaction. For this purpose, we will examine the simple case of a single-input single-output time-invariant linear system with constant threshold level and excited by stationary white noise,

that is, $l = m = 1$ and $b_i(k) = b_1(k) = b$ is constant. The failure event will be $F = \cup_{k=1}^{n_t} F_k$, where $F_k = \{|Y(k)| > b\}$ and we have dropped the index on the output for simplicity in notation.

The set of elementary failure events $\{F_k : k = 1, \ldots, n_t\}$ corresponds to the failure of the output response at the consecutive time steps $t_1, \ldots, t_{n_t}$. These elementary failure events evolve approximately in a continuous fashion as k varies. Let $g(k,s) = g(k-s+1)$ and $h(t,\tau) = h(t-\tau)$ be respectively the impulse response for the discrete- and continuous-time systems. The design point of F_k is then given by $z_k^*(s) = U(k-s)\sqrt{2\pi S \Delta t}\, g(k-s+1) b/\sigma_k^2$. For small Δt, $g(k-s+1) \sim h(t_k - t_s)$, so $z_k^*(s) \sim U(t_k - t_s)\sqrt{2\pi S \Delta t}\, h(t_k - t_s) b/\sigma_k^2$ and correspondingly $w_k^*(t_s) = \sqrt{2\pi S/\Delta t}\, z_k^*(s)$ $\sim 2\pi S\, U(t_k - t_s) h(t_k - t_s) b/\sigma_k^2$, which evolves smoothly with k when h is continuous. This is illustrated in Figure 4.1, where design points $z_{k_1}^*$ and $z_{k_2}^*$ corresponding to two different failure times k_1 and k_2 are shown. The design points corresponding to two consecutive failure times will be very close, and their distance tends to zero as $\Delta t \to 0$. The distance of the design point from the origin, given by $\beta_k = b/\sigma_k$, decreases gradually with increasing k accordingly as σ_k increases with k, as shown in Figure 4.2. Due to causality, only the first k components of the design point z_k^* are nonzero, so as k increases by 1, the design point has one more nonzero component in a new dimension. Thus, as k increases, the set of design points $\{z_k^*\}_k^{n_t}$ 'spiral' towards the origin in the n_t-dimensional input variable space which form a continuous path as $\Delta t \to 0$. This path ends when k is largest, that is, $k = n_t$, at the 'global design point' $z^* = z_{n_t}^*$, defined as the design point with the smallest Euclidean norm, or equivalently, reliability index, among all other design points. Note that in the general case of multiple-input multiple-output systems, the failure time of the global design point is not necessarily equal to T, for example, when $b_i(k)$ is not constant or the excitation is modulated by an envelope function.

In the case of a continuous-time single-input-single-output time-invariant system considered for a duration of T, the excitation corresponding to the global design point is a continuous function of time, given by $w^*(t) = 2\pi S\, U(T-t) h(T-t) b/\sigma_T^2$, which has been obtained by Drenick as the 'critical excitation' for aseismic design (Drenick 1970). It was noted as the 'smallest energy' (in the sense of Euclidean norm) excitation which pushes the response at time T to the threshold level b. Since $w^*(t)$ is the excitation with the smallest energy which pushes the response at T to the threshold, and it requires more energy to fail at earlier times, it was concluded that if the structure is designed so that it will not fail when the excitation is $w^*(t)$, then it will not fail over time interval $[0,T]$ for any excitation with energy less than that of $w^*(t)$. Finally, the reader is referred to Appendix A for some additional observations on the failure region for SDOF causal time-invariant linear systems.

4.3 Development of importance sampling density

The analysis of the failure region F in the last section provides valuable information for constructing an efficient ISD to compute the first excursion probability. In particular, the elementary failure events are completely characterized by their design point which can be computed readily by deterministic dynamic analysis. It is thus natural to construct the ISD based on the design points to account for the contributions from the elementary failure regions. Since there are $n_t m$ design points, one is concerned with how many and which design points to use. Using more design points may potentially increase the computational effort, and it is often sufficient to use only those that are 'important'. The importance of an elementary failure event F_{ik} may be measured by the conditional probability $P(F_{ik}|F)$, as the latter gives the plausibility that the failure F is due to F_{ik}. Since the ratio of the conditional probabilities of two elementary failure events F_{ik} and F_{js} is

$$\frac{P(F_{ik}|F)}{P(F_{js}|F)} = \frac{P(F_{ik} \cap F)/P(F)}{P(F_{js} \cap F)/P(F)} = \frac{P(F_{ik})}{P(F_{js})} \tag{4.20}$$

and hence equal to the ratio of their unconditional probabilities, the relative importance of a given design point z^*_{ik} may be quantified based on the (unconditional) probability of the corresponding elementary failure event F_{ik}:

$$P_{ik} = P(F_{ik}) = 2\,\Phi(-\beta_{ik}) \tag{4.21}$$

The larger the P_{ik}, the more important the design point z^*_{ik}.

Since the global design point z^* is by definition the one with the smallest β_{ik} and hence largest P_{ik}, it is natural to center the ISD at it. However, as noted before, the design points that are neighbors of the global design point z^* are very close to z^* (see Figure 4.1). Their reliability index and hence the probability content of the corresponding elementary failure region are also very close to those of z^*. As illustrated in Figure 4.2, the reliability index drops dramatically for small k and then settles for moderate values of k when the impulse response function has decayed considerably. So it is only in the case when the duration T is sufficiently small that the global design point assumes significantly more importance than all other design points. In the usual case when the duration T is large compared to the time when the impulse response has decayed sufficiently, the design points in the neighborhood of the global design point are also important, and should therefore be included to construct the ISD. Since β_{ik} settles quickly with k, the number of design points per each output state i that should be included is of the order of the total number of time steps. Thus, as a result of the interaction between the elementary failure events for different failure times, a much larger number of design points in addition to the global design point are important and have to be included in constructing the ISD. For the sake of discussion here, we will assume that all the $n_t m$ design points

are used for constructing the ISD.

Regarding the choice of the functional form for the ISD, the fundamental criteria are as follows: (1) the value of the ISD can be evaluated readily; and (2) there exists a method to efficiently simulate samples distributed according to the ISD. These criteria are fundamental since the evaluation of the ISD and the simulation of its samples have to be carried out repeatedly during simulation. In constructing an ISD which should account for the contributions from the neighborhood of multiple design points, one important observation is that if one can simulate a sample according to the individual PDF $f_{ik}(z)$, which is designed to account for the contribution from the design point z^*_{ik}, then one can also simulate a sample according to a weighted sum of the f_{ik}s, that is, $f(z) = \sum_{i=1}^{m}\sum_{k=1}^{n_t} w_{ik} f_{ik}(z)$, where $w_{ik} \geq 0$ and $\sum_{i=1}^{m}\sum_{k=1}^{n_t} w_{ik} = 1$. This is because a sample distributed as f can be obtained by first drawing a random ordered pair (I, K) from $\{(i,k)\}_{i,k}^{m,n_t}$ with corresponding probabilities $\{w_{ik}\}_{i,k}^{m,n_t}$, and then drawing a sample from $f_{IK}(z)$. For this reason, a conventional choice for an ISD using the $n_t m$ design points is a weighted sum of Gaussian PDFs among the design points (Schuëller and Stix 1987; Melchers 1989; Au, Papadimitriou, and Beck 1999), that is,

$$f(z) = \sum_{i=1}^{m}\sum_{k=1}^{n_t} w_{ik}\phi(z - z^*_{ik}) \tag{4.22}$$

The failure probability will then be estimated by

$$P_F \approx \frac{1}{N}\sum_{r=1}^{N} \frac{\mathbb{I}_F(Z'_r)\phi(Z'_r)}{\sum_{i=1}^{m}\sum_{k=1}^{n_t} w_{ik}\phi(Z'_r - z^*_{ik})} \tag{4.23}$$

where $\{Z'_r\}_r^N$ are i.i.d. samples simulated from f. To investigate the feasibility of using this ISD, first note that the denominator in the sum of (4.23) should not be evaluated directly, since the individual terms

$$\phi(Z'_r - z^*_{ik}) = (2\pi)^{-n_t m/2}\exp(-\frac{1}{2}||Z'_r - z^*_{ik}||^2) \tag{4.24}$$

are too small to compute within computer precision when $n_t m$ is large. To seek a better form for computation, note that

$$\begin{aligned}\frac{\phi(Z'_r - z^*_{ik})}{\phi(Z'_r)} &= \exp(-\frac{1}{2}||Z'_r - z^*_{ik}||^2 + \frac{1}{2}||Z'_r||^2) \\ &= \exp(-\frac{1}{2}||z^*_{ik}||^2 + \langle Z'_r, z^*_{ik}\rangle) \\ &= \exp(-\frac{1}{2}\beta^2_{ik})\ \exp(\langle Z'_r, z^*_{ik}\rangle)\end{aligned} \tag{4.25}$$

Thus, a better strategy is to compute (4.23) via

$$P_F \approx \frac{1}{N}\sum_{r=1}^{N}\mathbb{I}_F(Z'_r)\left[\sum_{i=1}^{m}\sum_{k=1}^{n_t} w_{ik}\,\exp(-\frac{1}{2}\beta_{ik}^2)\,\exp(\langle Z'_r, z^*_{ik}\rangle)\right]^{-1} \tag{4.26}$$

so that the interim computation of small numbers is avoided, since it can be easily argued that the magnitude of $\langle Z'_r, z^*_{ik}\rangle$ does not grow systematically with $n_t m$. Given the form in (4.26) is employed for computation, the ISD in (4.22) should be applicable in high dimensions, which will be demonstrated in the examples. Nevertheless, evaluation of the sum in (4.26) requires $O(n_t^2 ml)$ operations of addition and multiplication and $n_t m$ numerical evaluations of exponential functions, which imposes a computational burden on the importance sampling procedure, since the number of time steps n_t is often large and the number of outputs m may be large even for medium size systems.

4.3.1 Proposed ISD

The drawback of the ISD in (4.22) stems from the fact that the variation of the original PDF $\phi(z)$ with respect to z is different from that of the individual PDFs $\phi(z - z^*_{ik})$, otherwise the variation will be canceled out in the importance sampling quotient $\phi(\cdot)/f(\cdot)$. This drawback may be avoided by choosing the ISD as a weighted sum of PDFs which follow the variation of $\phi(z)$ and whose samples can be simulated. At this point, it is noted that the conditional PDF of the elementary event F_{ik}, $p(z|F_{ik}) = \phi(z)\mathbb{I}_{F_{ik}}(z)/P(F_{ik})$, has this desirable property, since $\mathbb{I}_{F_{ik}}(z)$ is constant within F_{ik}. Also, using the representation for the conditional sample in (4.16), the samples distributed as $p(z|F_{ik})$ can be simulated. It is thus proposed to construct the ISD as a weighted sum of the conditional PDFs $p(z|F_{ik}) = \phi(z)\mathbb{I}_{F_{ik}}(z)/P(F_{ik})$, that is,

$$f(z) = \sum_{i=1}^{m}\sum_{k=1}^{n_t} w_{ik}\,p(z|F_{ik}) = \sum_{i=1}^{m}\sum_{k=1}^{n_t} w_{ik}\,\frac{\phi(z)\mathbb{I}_{F_{ik}}(z)}{P(F_{ik})} \tag{4.27}$$

where $\{w_{ik}\}_{i,k}^{m,n_t} \geq 0$ and $\sum_{i=1}^{m}\sum_{k=1}^{n_t} w_{ik} = 1$ are the chosen weights associated with the elementary failure event F_{ik}. The weight w_{ik} controls the relative frequency of samples simulated from $p(z|F_{ik})$, and may be chosen to reflect the relative importance of the elementary failure event in contributing to P_F. In this study, the weights are chosen to be proportional to the probability content of F_{ik}:

$$w_{ik} = \frac{P(F_{ik})}{\sum_{j=1}^{m}\sum_{s=1}^{n_t} P(F_{js})} = \frac{P_{ik}}{\sum_{j=1}^{m}\sum_{s=1}^{n_t} P_{js}} \tag{4.28}$$

Substituting (4.28) into (4.27), the proposed ISD f is then given by

$$f(z) = \frac{\phi(z)}{\sum_{i=1}^{m}\sum_{k=1}^{n_t} P_{ik}}\sum_{i=1}^{m}\sum_{k=1}^{n_t}\mathbb{I}_{F_{ik}}(z) \tag{4.29}$$

Using f in (4.29) as the importance sampling density, the first excursion probability P_F can be expressed as

$$\begin{aligned} P_F &= \int \frac{\phi(z)\mathbb{I}_F(z)}{f(z)} f(z)dz \\ &= (\sum_{i=1}^{m}\sum_{k=1}^{n_t} P_{ik}) \int \frac{\mathbb{I}_F(z)}{\sum_{i=1}^{m}\sum_{k=1}^{n_t}\mathbb{I}_{F_{ik}}(z)} f(z)dz \\ &= \hat{P}_F \times \mathsf{E}_f[\frac{1}{\sum_{i=1}^{m}\sum_{k=1}^{n_t}\mathbb{I}_{F_{ik}}(\boldsymbol{Z})}] \end{aligned} \tag{4.30}$$

where

$$\hat{P}_F = \sum_{i=1}^{m}\sum_{k=1}^{n_t} P_{ik} = 2\sum_{i=1}^{m}\sum_{k=1}^{n_t}\Phi(-\beta_{ik}) \tag{4.31}$$

and the subscript f on the expectation in (4.30) indicates that the expectation is taken with $\boldsymbol{Z}$ distributed according to f instead of ϕ. Also, the fact that $\mathbb{I}_F(\boldsymbol{Z}) = 1$ for every sample $\boldsymbol{Z}$ simulated according to f has been used in the third equality in (4.30). The first excursion probability P_F may therefore be estimated by simulation as

$$P_F \approx \tilde{P}_F = \hat{P}_F \times \frac{1}{N}\sum_{r=1}^{N} \frac{1}{\sum_{i=1}^{m}\sum_{k=1}^{n_t}\mathbb{I}_{F_{ik}}(\boldsymbol{Z}_r)} \tag{4.32}$$

where $\{\boldsymbol{Z}_r\}_r^N$ are i.i.d. samples simulated according to f.

4.3.2 Properties of proposed ISD and failure probability estimator

Support region of ISD

Except for the term involving the sum of indicator functions, the variation of the ISD $f(z)$ in (4.29) follows exactly that of the original density $\phi(z)$. Since the weight $w_{ik} = P_{ik}/\sum_{j=1}^{m}\sum_{s=1}^{n_t} P_{js}$ in (4.28) associated with the elementary failure region F_{ik} is nonzero if the latter has nonzero probability content P_{ik}, the support region of f, that is, the region in the space of z where $f(z) > 0$, is $\cup_{i=1}^{m}\cup_{k=1}^{n_t} F_{ik} = F$. Thus, all samples simulated according to f will lie in F, while at the same time the whole failure region F is covered by the support region of the ISD and hence the samples generated from it. The latter implies that the contribution from all parts of the failure region will be accounted for in the estimator. Thus, the estimator $\tilde{P}_F$ will be an unbiased estimator of the failure probability P_F. This can be seen directly by taking the expectation of $\tilde{P}_F$ defined in (4.32) and then using (4.30) to show that $\mathsf{E}_f[\tilde{P}_F] = P_F$.

Interpretation of importance sampling estimator

The estimator $\tilde{P}_F$ in (4.32) is a product of $\hat{P}_F$ and the average over N samples of the importance sampling quotient R, which is given by

$$R(\boldsymbol{Z}) = \frac{1}{\sum_{i=1}^{m}\sum_{k=1}^{n_t}\mathbb{I}_{F_{ik}}(\boldsymbol{Z})} \tag{4.33}$$

To compute $\tilde{P}_F$, only the average of $R(\boldsymbol{Z})$ needs to be computed by simulation. For each sample, the evaluation of $R(\boldsymbol{Z})$ does not involve the evaluation of probability densities, in contrast with the case when the ISD in (4.22) is used. Note that the denominator of R, $\sum_{i=1}^{m}\sum_{k=1}^{n_t}\mathbb{I}_{F_{ik}}(\boldsymbol{Z})$, is just the number of time steps with absolute response lying above the threshold level, and can be obtained easily from the simulated response by a simple counting procedure.

Bounds for importance sampling estimator

Since $1/n_t m \leq 1/\sum_{i=1}^{m}\sum_{k=1}^{n_t}\mathbb{I}_{F_{ik}} \leq 1$, we see that

$$\frac{\hat{P}_F}{n_t m} \leq \tilde{P}_F \leq \hat{P}_F \tag{4.34}$$

This result imposes bounds on the random quantity $\tilde{P}_F$, which depends on the simulated samples $\{\boldsymbol{Z}_r\}_r^N$, and is a stronger result than bounds on the expectation of $\tilde{P}_F$, that is, $\hat{P}_F/n_t m \leq P_F \leq \hat{P}_F$. The bounded property of the estimator $\tilde{P}_F$ is a desirable one, since it implies that $\tilde{P}_F$ will not jump to a significantly large value during simulation. This property is not shared by importance sampling estimators using a conventional choice of ISD, since it is often not possible to put explicit bounds on the importance sampling quotient R.

Optimality of ISD for mutually exclusive elementary failure events

When $\{F_{ik}\}_{i,k}^{m,n_t}$ are mutually exclusive, $\mathbb{I}_{F_{ik}}(\boldsymbol{Z}) = 1$ for one and only one (i,k), and $\mathbb{I}_{F_{js}}(\boldsymbol{Z}) = 0$ for $j \neq i$ or $s \neq k$. This is true for every sample $\boldsymbol{Z}$, and so $1/\sum_{i=1}^{m}\sum_{k=1}^{n_t}\mathbb{I}_{F_{ik}}(\boldsymbol{Z}) \equiv 1$. This means

$$P_F = \tilde{P}_F = \hat{P}_F \tag{4.35}$$

and hence the ISD f is equal to the optimal ISD that leads to zero variance in the failure probability estimator when the elementary failure events are mutually exclusive. It can be expected that when the failure events $\{F_{ik}\}_{i,k}^{m,n_t}$ are close to being mutually exclusive, the importance sampling quotient R will be close to unity, which leads to smaller variation in $\tilde{P}_F$ and hence faster convergence to P_F.

Failure probability and sojourne time

The use of the proposal PDF leads to an interesting relationship between the first excursion problem to the 'sojourne time', commonly defined as the duration over which the response spends above threshold level. From (4.30),

$$P_F = (\sum_{i=1}^{m}\sum_{k=1}^{n_t} P_{ik}\Delta t) \times \mathsf{E}[\frac{1}{\sum_{i=1}^{m}\sum_{k=1}^{n_t} \mathbb{I}_{F_{ik}}(Z)\Delta t}] = (\sum_{i=1}^{m}\sum_{k=1}^{n_t} P_{ik}\Delta t)\mathsf{E}_f[\frac{1}{T_b}] \tag{4.36}$$

where $T_b = \sum_{i=1}^{m}\sum_{k=1}^{n_t} \mathbb{I}_{F_{ik}}(Z)\Delta t$ is a discrete approximation to the sum of the sojourne times of all the output responses above the threshold. On the other hand,

$$\mathsf{E}_\phi[T_b] = \mathsf{E}_\phi[\sum_{i=1}^{m}\sum_{k=1}^{n_t} \mathbb{I}_{F_{ik}}(Z)\Delta t] = \sum_{i=1}^{m}\sum_{k=1}^{n_t} \mathsf{E}_\phi[\mathbb{I}_{F_{ik}}(Z)]\Delta t = \sum_{i=1}^{m}\sum_{k=1}^{n_t} P_{ik}\Delta t \tag{4.37}$$

and so

$$P_F = \mathsf{E}_\phi[T_b] \times \mathsf{E}_f[\frac{1}{T_b}] \tag{4.38}$$

which relates the failure probability P_F to the statistics of the sojourne time.

The c.o.v. of importance sampling estimator and sojourne time

The coefficient of variation (c.o.v.) δ of the failure probability estimator $\tilde{P}_F$, defined as the ratio of the standard deviation to the mean of $\tilde{P}_F$, is given by

$$\delta = \frac{\sqrt{\mathsf{Var}[\tilde{P}_F]}}{P_F} = \frac{\Delta}{\sqrt{N}} \tag{4.39}$$

where Δ is the unit c.o.v. of the importance sampling quotient:

$$\Delta = \frac{1}{P_F}\sqrt{\mathsf{Var}[\frac{\phi(Z)\mathbb{I}_F(Z)}{f(Z)}]} \tag{4.40}$$

Using (2.18),

$$\begin{aligned}
\Delta^2 &= \mathsf{E}_{\phi|F}[\frac{\phi(Z|F)}{f(Z)}] - 1 \\
&= \mathsf{E}_{\phi|F}[\frac{\phi(Z)\mathbb{I}_F(Z)/P_F}{\phi(Z)\sum_{i=1}^{m}\sum_{k=1}^{n_t} \mathbb{I}_{F_{ik}}(Z)/\hat{P}_F}] - 1 \\
&= \frac{\hat{P}_F\Delta t}{P_F} \times \mathsf{E}_{\phi|F}[\frac{1}{\sum_{i=1}^{m}\sum_{k=1}^{n_t} \mathbb{I}_{F_{ik}}(Z)\Delta t}] - 1 \\
&= \frac{\mathsf{E}_\phi[T_b]}{P_F} \times \mathsf{E}_{\phi|F}[\frac{1}{T_b}] - 1
\end{aligned} \tag{4.41}$$

which relates the unit c.o.v. of the importance sampling estimator to the statistics of the sojourne time T_b. Note that T_b is zero when failure does not occur, and so by the Theorem of Total Probability,

$$\begin{aligned} \mathsf{E}_\phi[T_b] &= \mathsf{E}_{\phi|F}[T_b]P_F + \mathsf{E}_{\phi|F}[T_b](1-P_F) \\ &= \mathsf{E}_{\phi|F}[T_b]P_F \end{aligned} \tag{4.42}$$

Thus, (4.41) becomes,

$$\Delta^2 = \mathsf{E}_{\phi|F}[T_b] \times \mathsf{E}_{\phi|F}[\frac{1}{T_b}] - 1 \tag{4.43}$$

which shows some similarity with (4.38).

4.4 Summary of proposed importance sampling procedure

1. Perform dynamic analysis to obtain impulse response functions $\{g_{ij}(k,s)\}_{i,j,k,s}^{m,l,n_t,n_t}$ which define the input-output relationship of the system. For time-invariant systems, $g_{ij}(k,s) = g_{ij}(k-s+1)$ and only l (the number of inputs) dynamic analyses are required.

2. Compute the output response standard deviations $\{\sigma_{ik}\}_{i,k}^{m,n_t}$ by (4.9), the elementary reliability indexes $\{\beta_{ik}\}_{i,k}^{m,n_t}$ by (4.13), the elementary failure probabilities $\{P_{ik}\}_{i,k}^{m,n_t}$ by (4.21), the upper bound $\hat{P}_F$ for failure probability by (4.31), and the weights $\{w_{ik}\}_{i,k}^{m,n_t}$ by (4.28).

3. Compute the failure probability estimate $\tilde{P}_F$ by (4.32), where $\{\boldsymbol{Z}_r : r = 1,\ldots,N\}$ are i.i.d. samples generated from the proposed ISD given by (4.29).

   To simulate a sample $\boldsymbol{Z}_r$ $(r = 1,\ldots,N)$ according to the proposed ISD given by (4.29):

   (a) Draw a random ordered pair (I,K) of indexes from the set $\{(i,k)\}_{i,k}^{m,n_t}$ with corresponding probabilities $\{w_{ik}\}_{i,k}^{m,n_t}$.

   (b) Simulate $\boldsymbol{Z}$ as a n-dimensional standard Gaussian vector with independent components, and U_1 and U_2 as uniform variables on $[0,1]$. Compute

$$\alpha = \Phi^{-1}[U_1 + (1-U_1)\Phi(\beta_{IK})] \tag{4.44}$$

   and set

$$\boldsymbol{Z}_r = \begin{cases} \boldsymbol{Z} + (\alpha - \langle \boldsymbol{Z}, \mathbf{u}_{IK}^* \rangle)\mathbf{u}_{IK}^* & \text{if } U_2 \le 1/2 \\ -\boldsymbol{Z} - (\alpha - \langle \boldsymbol{Z}, \mathbf{u}_{IK}^* \rangle)\mathbf{u}_{IK}^* & \text{otherwise} \end{cases} \tag{4.45}$$

   where $\mathbf{u}_{IK}^* = \boldsymbol{z}_{IK}^*/\beta_{IK}$ and $\boldsymbol{z}_{IK}^*$ is defined by (4.8).

It is worth noting that once the unit impulse response functions are computed in Step 1, the response of the structure can be computed by convoluting them with the excitation to evaluate each $\mathbb{I}_{F_{ik}}(Z_r)$ $(r = 1, \ldots, N)$. This can be done efficiently using the FFT algorithm and its inverse. This approach may save computational effort, since the setup of structural matrices in the finite element model, for example, can be avoided in the repeated computations of structural response for different excitations during simulation.

4.5 Generalization to non-causal systems

The foregoing discussions have focused on causal linear systems, for the sake of illustrating the dynamics behind the design points and their relationship with the unit impulse response functions of the system. Although non-causal systems are generally not physically realizable, there are cases where they have been used in stochastic modeling. One common example is the generation of stochastic ground motions compatible with a target response spectrum by modifying the spectrum of a modulated white noise sequence (Clough and Penzien 1975). In particular, the stochastic ground motion model considered in Chapter 6 is also non-causal. This motivates the generalization of the proposed method to the case of non-causal systems, which is quite straightforward. In this case, the upper limit in the Duhamel's integral representation of the input-output relationship in (4.1) theoretically tends to infinity:

$$Y_i(t) = \sum_{j=1}^{l} \int_0^{\infty} h_{ij}(t, \tau) W_j(\tau) d\tau \tag{4.46}$$

since now the excitation applied in the future also contributes to the current response. Note that the lower limit in the integral remains as zero, since it is assumed that the excitation starts from time zero. For computational purposes, it is useful to note that the upper limit can often be replaced by some duration T:

$$Y_i(t) = \sum_{j=1}^{l} \int_0^{T} h_{ij}(t, \tau) W_j(\tau) d\tau \tag{4.47}$$

where T is the time when the contribution from future excitation is sufficiently small to be neglected. For example, if the white noise excitation is modulated by an envelope function $e(t)$, then $h(t, \tau) = h_S(t, \tau)\, e(t)$ where h_S is the unit impulse response function of the structure; in this case, T can be taken as the time after which the envelope function $e(t)$ decays to a sufficiently small value (or zero).

The counterpart of (4.4) for non-causal systems is given by the discrete analogue of (4.47):

$$Y_i(k) = \sum_{j=1}^{l} \sum_{s=1}^{n_t} g_{ij}(k,s) Z_j(s) \sqrt{2\pi S_j \Delta t} \tag{4.48}$$

where $n_t = T/\Delta t + 1$. The only difference between (4.48) and (4.4) is that the sum in the former goes from 1 to the final time instant n_t instead of from 1 to the current time instant k. The resulting response variance has a similar modification:

$$\sigma_{ik}^2 = \mathrm{Var}[Y_i(k)] = \sum_{j=1}^{l} [\sum_{s=1}^{n_t} g_{ij}(k,s)^2] 2\pi S_j \Delta t \tag{4.49}$$

The expression for the design point z_{ik}^* corresponding to the failure at time t_k of the i-th output response is similar to (4.8) for causal systems, except that it does not involve the Unit step function and hence may assume non-zero value for $s > t$:

$$z_{ik,j}^*(s) = \sqrt{2\pi S_j \Delta t} \frac{g_{ij}(k,s)}{\sigma_{ik}^2} b_i(k) \tag{4.50}$$

In brief, the results for causal systems apply as well for non-causal systems, with a change in the upper limit of summation in the corresponding results. The proposed importance sampling procedure presented in the last section can thus be applied to non-causal systems, provided that (4.9) and (4.8) are replaced by (4.49) and (4.50), respectively.

4.6 Illustrative examples

4.6.1 Example 1: SDOF oscillator

Consider a single-degree-of-freedom (SDOF) oscillator with natural frequency $\omega = 2\pi$ rad/s (i.e., 1 Hz) and damping ratio $\zeta = 2\%$ subjected to white noise excitation:

$$\ddot{Y}(t) + 2\zeta\omega\dot{Y}(t) + \omega^2 Y(t) = W(t) \tag{4.51}$$

where $W(t)$ is a Gaussian white noise process with spectral intensity $S = 1$. The sampling interval is assumed to be $\Delta t = 0.05$ s and the duration of study is $T = 15$ s. The total number of time points, and hence the number of input random variables is thus $n_t = T/\Delta t + 1 = 15/0.05 + 1 = 301$. Failure is defined as the absolute displacement response exceeding a threshold level b, that is, $F = \cup_{k=1}^{n_t} \{|Y(t_k)| > b\}$ where $t_k = (k-1)\Delta t$, $k = 1, \ldots, n_t$. The impulse response function $h(t)$ of the

system is given by

$$h(t) = \frac{e^{-\zeta\omega t}}{w_d} \sin \omega_d \, t \tag{4.52}$$

where $w_d = w\sqrt{1-\zeta^2}$ is the damped natural frequency. Figure 4.3 shows the variation of $h(t)$ within the duration of study. The variance of $Y(t)$ is given by integrating the square of $h(\tau)$ up to time t:

$$\sigma^2(t) = 2\pi \int_0^t h(\tau)^2 \, d\tau \tag{4.53}$$

The standard deviation $\sigma(t)$ is shown in Figure 4.4. Note that $\sigma(t)$ is increasing with t and its wavy character is due to the oscillatory behavior of the impulse response function $h(t)$.

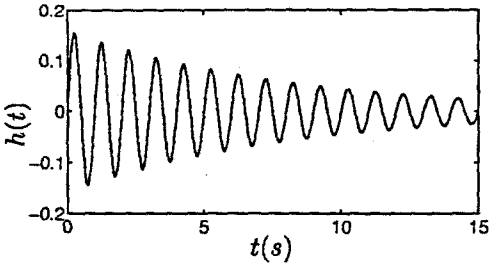

Figure 4.3: Impulse response function $h(t)$

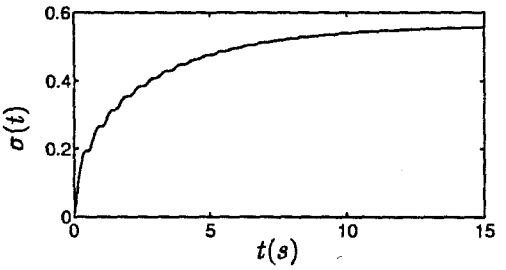

Figure 4.4: Standard deviation of response, $\sigma(t)$

The first excursion probability P_F for a given threshold level b is computed by importance sampling using the following three choices of ISD: (1) ISD centered at the global design point with unit covariance matrix; (2) ISD centered among all the n_t design points with unit covariance matrix, as given in (4.22); (3) the proposed ISD in (4.29). The weights used in (4.22) for Choice (2) are given by (4.28). Figure 4.5 shows the variation of the weights with time t for $b = 3, 4, 5 \times \sigma(T)$, where $\sigma(T)$ is the standard deviation of the response at time $T = 15$ s, being the largest within

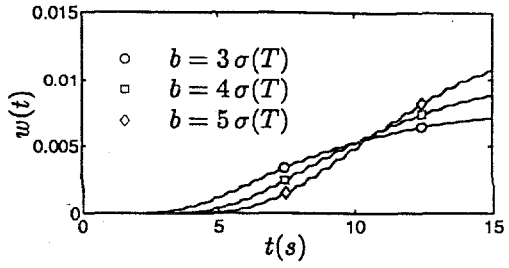

Figure 4.5: Weight $w(t)$

the duration of study. Note that, although Figures 4.3-4.5 plot the quantities $h(t)$, $\sigma(t)$ and $w(t)$ as a continuous function of time t, only the values at the discrete time instants $t_k = (k-1)\Delta t$, $k = 1, \ldots, n_t$, are evaluated and used in the actual computations.

The failure probability estimates for the three threshold levels are shown in Figure 4.6 for different sample sizes N. The results computed with ISD using Choices (1), (2) and (3) are shown with dotted, dashed and solid lines, respectively. For comparison, the results computed by standard Monte Carlo simulation (MCS) with 10^6 samples are shown as asterisks in the figure.

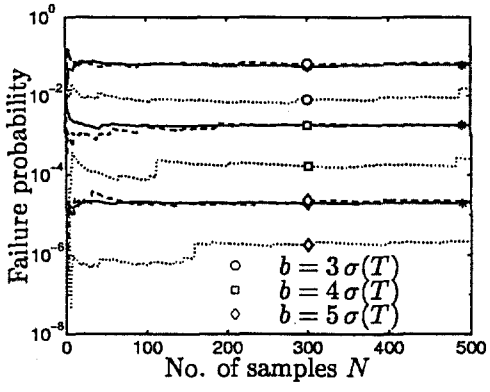

Figure 4.6: Failure probability estimates for different threshold levels b and number of samples N. Choice (1): dotted lines; Choice (2): dashed lines; Choice (3): solid lines; MCS with 10^6 samples: asterisks

From Figure 4.6, it can be seen that results computed by Choice (1) are practically biased within the number of samples considered, showing that it is not suitable for computing the first excursion probability. In particular, the failure probability estimates corresponding to Choice (1) are smaller than the exact failure probabilities by orders of magnitude. Note that this is not due to most of the samples generated by the ISD of Choice (1) lying in the safe region. In fact, the percentages of the 500 samples generated by the ISD of Choice (1) that lie in the failure region are 63%, 57% and 53%, showing that more than half of the samples lie in the failure region. Rather, the practical

Table 4.1: The unit c.o.v. Δ of importance sampling quotients for failure probability

$b/\sigma(T)$	P_F	Δ			
		Choice (1)	Choice (2)	Choice (3) (Proposed)	MCS
3	6.01×10^{-2}	28.9	1.80	1.24	3.95
4	1.79×10^{-3}	63.1	3.19	0.93	23.6
5	1.97×10^{-5}	69.3	4.36	0.80	226

bias observed in Choice (1) is due to the fact that the importance sampling quotient in Choice (1) takes on values which are orders of magnitude smaller than the probability of failure for most of the generated samples. The sudden 'jumps' in the simulation history of failure probability estimates of Choice (1) correspond to those rare occasions where the importance sampling quotient is much larger than the rest of the samples. At this point, it is worth noting that Corollary 2.3 in Chapter 2 deduces that Choice (1) is applicable in high dimensions. The large variability in the unit c.o.v. for Choice (1) arises from the small failure probability levels considered, but not from the large dimension n_t. This provides an example demonstrating that applicability in high dimensions does not imply the importance sampling estimate is practically unbiased, which has been noted in the definition of applicability in Section 2.4.1.

The results computed using Choices (2) and (3) have similar variability, although the latter has even smaller variability. The results for both Choices (2) and (3) converge to the target failure probability when N increases. To assess quantitatively the variability of the estimates and hence the efficiency of the importance sampling procedure using the different choices, the unit c.o.v. of the importance sampling estimators defined by (4.40) for the three choices are estimated from the 500 simulated samples. Note that the c.o.v. δ of the failure probability estimate using N samples is given by (4.39). For Choice (1), the values of Δ are estimated using 100,000 samples, since the estimates for failure probability and hence c.o.v. using 500 samples are biased. The results are shown in Table 4.1. Using the c.o.v. for the importance sampling quotient, the number of samples required to achieve a c.o.v. of δ in the failure probability estimate, given by $N_\delta = \Delta^2/\delta^2$, is also computed. For the results shown in Table 4.2, $\delta = 30\%$ has been used, which represents a moderate level of accuracy in the failure probability estimate.

Table 4.1 shows that the unit c.o.v.s Δ for Choice (1) are much larger than those of Choices (2) and (3). Also, for higher values of P_F, even standard MCS is more efficient than using Choice (1). The corresponding number of samples N_δ in Table 4.2 for Choice (1) are larger by orders of magnitude than those for Choices (2) and (3). The unit c.o.v.s for Choice (3) are smaller than those for Choice (2). As the failure probability decreases, the unit c.o.v. for Choice (2) increases steadily, while the unit c.o.v. for Choice (3) decreases. The number of samples for Choice (3) required to

Table 4.2: Number of samples N_δ to achieve a c.o.v. of $\delta = 30\%$ in $\tilde{P}_F$

$b/\sigma(T)$	P_F	N_δ ($\delta = 30\%$)			
		Choice (1)	Choice (2)	Choice (3) (Proposed)	MCS
3	6.01×10^{-2}	9302	37	18	174
4	1.79×10^{-3}	44,233	114	10	6206
5	1.97×10^{-5}	53,400	212	8	565,558

achieve a c.o.v. of $\delta = 30\%$ is remarkably small (< 20) compared with those commonly reported in the importance sampling literature, implying that the proposed ISD leads to a very efficient importance sampling strategy. This superior efficiency is made possible through the use of analytical results on the first excursion problem specifically for linear systems.

4.6.2 Example 2: Seismic response of moment-resisting steel frame

Consider a six-story moment-resisting steel frame as shown in Figure 4.7 with member sections given in Table 4.3. For each floor, the same section is used for all girders. The structure is modeled as a two-dimensional linear frame with beam elements connecting the joints of the frame. Masses are lumped at the nodes of the frame, which include the contributions from the dead load of the floors and the frame members. They are tabulated in Table 4.4. The natural frequencies of the first two modes are computed to be 0.552 Hz and 1.56 Hz, respectively. Rayleigh damping is assumed so that the first two modes have 5% of critical damping.

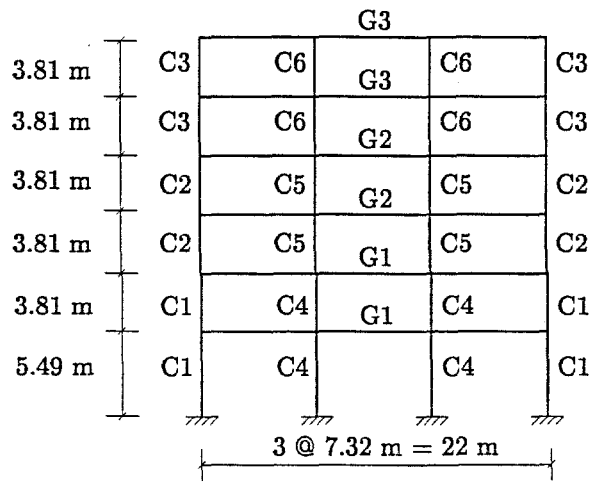

Figure 4.7: Moment-resisting frame structure

The structure is subjected to a stochastic ground acceleration $\ddot{a}(t)$ modeled by filtered white

noise with a Clough-Penzien spectrum and modulated by an envelope function $e(t)$:

$$\ddot{a}(t) + 2\zeta_{s2}\omega_{s2}\dot{a}(t) + \omega_{s2}^2 a(t) = 2\zeta_{s1}\omega_{s1}\dot{a}_1(t) + \omega_{s1}^2 a_1(t) \tag{4.54}$$

$$\ddot{a}_1(t) + 2\zeta_{s1}\omega_{s1}\dot{a}_1(t) + \omega_{s1}^2 a_1(t) = e(t)W(t) \tag{4.55}$$

where $\omega_{s1} = 15.7$ rad/s (2.5 Hz) and $\omega_{s2} = 1.57$ rad/s (0.25 Hz) are the dominant and lower-cutoff frequency of the spectrum; $\zeta_{s1} = 0.6$ and $\zeta_{s2} = 0.8$ are the damping parameters associated with the dominant and lower-cutoff frequency, respectively. The envelope function $e(t)$ is assumed to vary quadratically as $(t/4)^2$ for the first 4 seconds, then settle at unity for 10 seconds, and finally decay as $\exp[-(t-14)^2/2]$ starting from $t = 14$ s. In (4.55), $W(t)$ is the Gaussian white noise with spectral intensity $S = 1 \times 10^{-3} m^2/s^3$.

Table 4.3: Sections (AISC) for frame members

Story	Exterior Column	Interior Column	Girder
1, 2	C1: W14 × 159	C4: W27 × 161	G1: W24 × 94
3, 4	C2: W14 × 132	C5: W27 × 114	G2: W24 × 76
5, 6	C3: W14 × 99	C6: W24 × 84	G3: W24 × 55

Table 4.4: Point masses

Floor	Exterior Column ($\times 10^3$ kg)	Interior Column ($\times 10^3$ kg)
2	60.4	81.0
3	53.3	78.1
4	51.9	76.0
5	51.7	75.8
6	50.1	73.5
Roof	44.6	63.1

The input-output relationship between the input $W(t)$ and the output $Y_i(t)$ is

$$Y_i(t) = \int_0^t h_i(t-\tau)e(\tau)W(\tau)d\tau \tag{4.56}$$

where $h_i(\tau)$ is the impulse response of the augmented system which include the dynamics of the frame structure and the soil layers represented by the Clough-Penzien spectrum. The variance of $Y_i(t)$ is given by

$$\sigma_i^2(t) = 2\pi S \int_0^t h_i(t-\tau)^2 e(\tau)^2 d\tau \tag{4.57}$$

Table 4.5: The unit c.o.v. Δ of proposed importance sampling quotient for failure probability for peak interstory drift ratio

b (%)	P_F $(N = 200)$	Δ	N_δ $(\delta = 30\%)$
0.5	6.41×10^{-2}	1.34	20
0.75	2.79×10^{-4}	1.15	15
1	1.23×10^{-7}	1.09	13

Note that both the response $Y_i(t)$ and its variance $\sigma_i^2(t)$ can be obtained by convolution. A duration of $T = 30$ s and a time interval of $\Delta t = 0.02$ s are used in computing the response of the structure, leading to $n_t = T/\Delta t + 1 = 30/0.02 + 1 = 1501$ input random variables in the discrete approximation for $W(t)$.

Peak Interstory drift ratio

Consider the failure probability that the peak interstory drift ratio over all stories of the structure exceeds a threshold level b. The outputs $\{Y_i : i = 1, \ldots, m\}$ consist of the interstory drift ratio of all columns connecting two consecutive floors. There are thus $m = 24$ outputs, which can be expressed as a linear transformation of the state variables of the structure. The impulse response for the interstory drift ratios of the exterior columns at every floor are shown in the first column of Figure 4.8. These are obtained from one dynamic analysis of the structure. Although not shown in the figure, it is noted that the impulse response for the interior columns are close to those for the corresponding exterior columns.

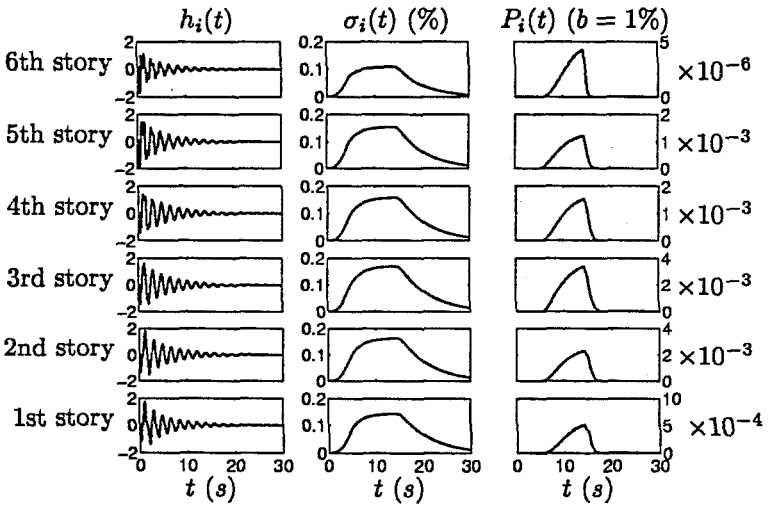

Figure 4.8: Impulse response $h_i(t)$, standard deviation $\sigma_i(t)$ and elementary failure probability $P_i(t)$ for interstory drift ratios

The standard deviations $\sigma_i(t)$ $(i = 1, \ldots, 6)$ computed based on (4.57) by numerical convolution

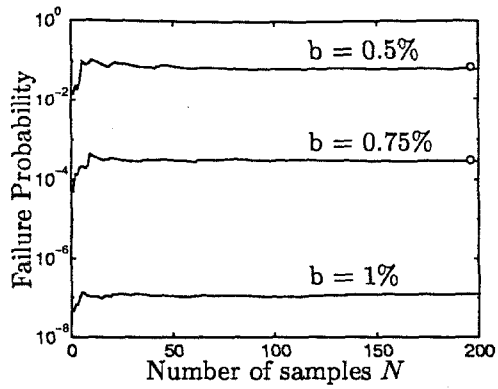

Figure 4.9: Failure probability estimates for peak interstory drift ratio for different threshold levels b and number of samples N. MCS estimates with 10,000 samples are shown with circles.

Table 4.6: Failure probability estimates for peak interstory drift ratio with $N = 20$ samples

b (%)	$\tilde{P}_F$ $(N = 200)$	Run	$\tilde{P}_F$ $(N = 20)$
0.5	6.41×10^{-2}	1	4.54×10^{-2}
		2	4.29×10^{-2}
		3	7.28×10^{-2}
0.75	2.79×10^{-4}	1	1.77×10^{-4}
		2	3.14×10^{-4}
		3	2.55×10^{-4}
1	1.23×10^{-7}	1	1.21×10^{-7}
		2	1.43×10^{-7}
		3	1.22×10^{-7}

are shown in the second column in Figure 4.8. The elementary failure probability for the i-th interstory drift ratio, $P_i(t) = P(|y_i(t)| > b) = 2\Phi(-b/\sigma_i(t))$, are also computed with $b = 1\%$ and shown in the third column in Figure 4.8. Although the quantities in Figure 4.8 are shown as a continuous function of t, only the values at the discrete time instants $t_k = (k-1)\Delta t$, $k = 1, \ldots, n_t$, are evaluated in the actual computations. It is seen in Figure 4.8 that the variation of the response standard deviation $\sigma_i(t)$ with t follows approximately that of the envelope function $e(t)$. In particular, the maximum standard deviation for each response over the duration of study occurs at $t = 14$ s, which coincides with the time when the envelope function starts to decay. The variation of the elementary failure probabilities with time is sharper than that of the corresponding response standard deviations. According to (4.37), the area under the curve of each $P_i(t)$ gives the expected time that the absolute response for the i-th story spends above the threshold level. The ratio of the area under the elementary failure probability $P_i(t)$ between different stories i gives an idea of the relative importance of the responses in contributing to the first excursion failure. Thus, from Figure 4.8, it can be expected that the second to fifth story should give the main contribution to

the failure probability.

The failure probability estimates $\tilde{P}_F$ for the threshold levels $b = 0.5\%, 0.75\%$ and 1% are shown in Figure 4.9 for different number of samples N. The estimates by standard Monte Carlo simulation with $10,000$ samples are also computed and shown with circles in the figure. Note that the Monte Carlo estimate for $b = 1\%$ is not shown in the figure, since the sample size is not large enough to provide a sufficiently accurate estimate for the failure probability corresponding to this threshold level. From Figure 4.9, it can be seen that the failure probability estimates computed using the proposed ISD converge quickly to the target probability of failure.

To investigate quantitatively the variability of the failure probability estimates, the unit c.o.v. Δ of the importance sampling quotient is computed using 200 samples and shown in Table 4.5. The number of samples required to achieve a c.o.v. of $\delta = 30\%$ in the failure probability estimate are shown in the last column of the table. In general, the unit c.o.v. Δ for the importance sampling quotient is quite small, and consequently only a small number of samples N_δ is required to achieve a c.o.v. of $\delta = 30\%$ in the failure probability estimates. The values of N_δ show that a sufficiently good failure probability estimate can be obtained with a small sample size of, say, $N = 20$. To demonstrate this, independent simulation runs are carried out with $N = 20$ samples to compute the failure probability estimates. The results are shown in Table 4.6, which demonstrate that the variability of the failure probability estimates among independent runs is indeed small.

Peak floor acceleration

Finally, consider the failure probability that the (absolute horizontal) peak floor acceleration over all stories of the structure exceeds (in magnitude) a threshold level b (in %g). As the horizontal displacement along the beam elements for the girders are linearly interpolated, this probability is equal to the failure probability that the horizontal absolute acceleration at any one of the nodes of the frame exceeds the threshold level b. There are thus $m = 24$ outputs, corresponding to the absolute horizontal acceleration at the 24 nodes of the frame. The results are shown in Figures 4.10 and 4.11 and Tables 4.7 and 4.8, in analogy with the results for the peak interstory drift in Figures 4.8 and 4.9 and Tables 4.5 and 4.6, respectively. Similar to the case of peak interstory drifts, these results show that fast convergence is achieved in the failure probability estimates. In particular, Table 4.7 shows that less than 20 samples are needed to achieve a c.o.v. of $\delta = 30\%$ in all the failure probability estimates, which is verified in Table 4.8.

4.7 Efficiency of proposed importance sampling method

The results from the two examples in the last section suggest that the proposed importance sampling method tends to be more efficient when applied to estimating small failure probabilities. A conjecture that explains this observation is the following: as the failure probability becomes

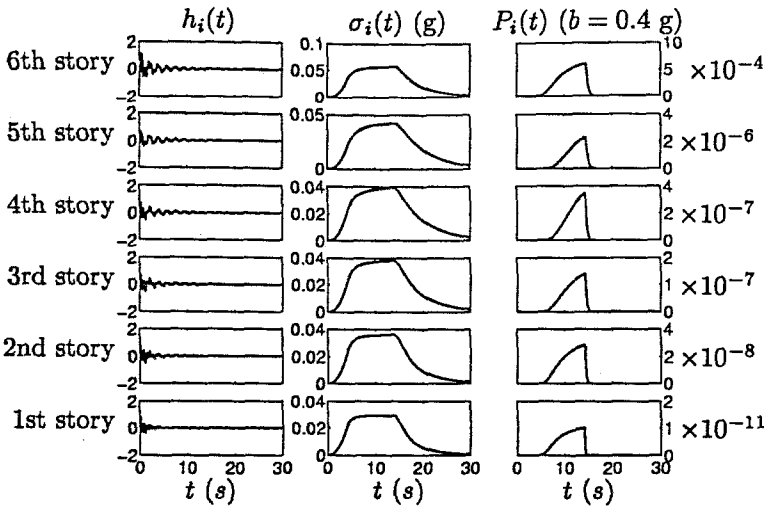

Figure 4.10: Impulse response $h_i(t)$, standard deviation $\sigma_i(t)$ and elementary failure probability $P_i(t)$ for floor accelerations

Table 4.7: The c.o.v. Δ of proposed importance sampling quotient for failure probability for peak floor acceleration

b (g)	$\tilde{P}_F$	Δ	N_δ ($\delta = 30\%$)
0.2	3.87×10^{-2}	1.05	12
0.3	2.24×10^{-5}	0.70	5
0.4	6.36×10^{-10}	0.83	8

smaller, the elementary failure events become more close to being mutually exclusive, and hence the proposed ISD is more close to being optimal, since it has been shown in Section 4.3.2 that the proposed ISD is the optimal choice (that leads to zero variance in the estimate) when the elementary failure events are mutually exclusive. In the spirit of this argument, it may also be conjectured that the proposed importance sampling method is more efficient as the damping of the system increases, because damping tends to reduce correlation among excursions. Further investigation of the SDOF system in Example 1 has been carried out to substantiate these claims. In particular, for several scenarios with different probability levels and damping ratios, the unit c.o.v. Δ of the importance sampling quotient $1/\sum_{k=1}^{n_t} \mathbb{I}_{F_k}(\boldsymbol{Z})$ is estimated using 500 samples, from which the number of samples N_δ required to achieve a c.o.v. δ of 30% can be calculated as $N_\delta = \Delta^2/\delta^2$. While other parameters remain the same as in Example 1, the scenarios correspond to threshold levels of $b = 3, 4, 5, 6 \times \sigma(T)$, and damping ratios of $\zeta = 1\%, 5\%, 10\%$ and 30%.

Tables 4.9, 4.10 and 4.11 show the probability levels, unit c.o.v. Δ and number of samples N_δ, respectively for different scenarios. Table 4.11 indicates that the number of samples to achieve a given c.o.v. of $\delta = 30\%$ in the importance sampling estimate decreases with decreasing probability

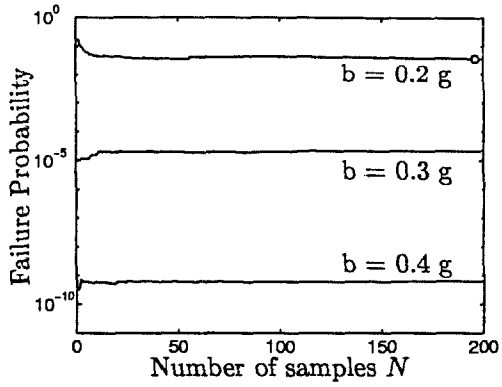

Figure 4.11: Failure probability estimates for peak floor acceleration for different threshold levels b and number of samples N. MCS estimates with 10,000 samples are shown with circles.

Table 4.8: Failure probability estimates for peak floor acceleration with $N = 20$ samples

b (g)	P_F $(N = 200)$	Run	P_F $(N = 20)$
0.2	3.87×10^{-2}	1	2.31×10^{-2}
		2	4.34×10^{-2}
		3	3.10×10^{-2}
0.3	2.24×10^{-5}	1	2.43×10^{-5}
		2	2.76×10^{-5}
		3	3.04×10^{-5}
0.4	6.36×10^{-10}	1	6.34×10^{-10}
		2	5.22×10^{-10}
		3	5.48×10^{-10}

level or increasing damping ratios, which shows that the conjectures are quite plausible.

4.8 Summary of this chapter

The complexity of the first excursion problem stems from the structure of the union of the elementary failure regions in the high-dimensional excitation space, although these regions are simple to describe. One important consequence of such structure is that, in addition to the global design point, a large number of neighboring design points are important in accounting for the failure probability, and hence have to be considered in constructing an ISD (importance sampling density). A new ISD is proposed which takes into account the contributions of all the elementary failure regions. It is built upon the following three important observations:

1. Appreciation of the fact that, for time linear invariant systems, the design points corresponding to failure at different time steps can be obtained simply from the unit impulse response function.

Table 4.9: Probability levels for different scenarios

$b/\sigma(T)$	ζ (%)			
	1	5	10	30
3	3×10^{-2}	1.37×10^{-1}	2.03×10^{-1}	2.71×10^{-1}
4	1.01×10^{-3}	4.81×10^{-3}	7.55×10^{-3}	9.25×10^{-3}
5	9.51×10^{-6}	5.83×10^{-5}	8.53×10^{-5}	1.00×10^{-4}
6	3.21×10^{-8}	2.39×10^{-7}	3.32×10^{-7}	3.89×10^{-7}

Table 4.10: The unit c.o.v. Δ of importance sampling quotient in Example 1

$b/\sigma(T)$	ζ (%)			
	1	5	10	30
3	1.32	1.04	0.85	0.69
4	1.09	0.80	0.61	0.53
5	0.90	0.60	0.48	0.47
6	0.75	0.48	0.41	0.40

Table 4.11: Number of samples N_δ required to achieve a c.o.v. of $\delta = 30\%$ in the failure probability estimate in Example 1

$b/\sigma(T)$	ζ (%)			
	1	5	10	30
3	20	13	9	6
4	14	8	5	4
5	10	5	3	3
6	7	3	2	2

2. Appreciation of the fact that, instead of only the global design point, a large number of design points are important in contributing to the failure probability.

3. The novel concept of constructing the ISD as a weighted sum of conditional PDFs rather than just Gaussian PDFs centered at the design points (as is commonly done) so that the original PDF is cancelled out in the importance sampling quotient. This makes the method extremely efficient, regardless of the size of the problem in terms of the number of time steps, the number of inputs and the number of outputs.

Whereas conventional choices for constructing the ISD using the design points are found to be inefficient, numerical examples show that the proposed ISD leads to very fast convergence in the first excursion failure probability estimates. Examples have shown that no more than 20 samples are required to achieve a c.o.v. of 30% in the failure probability estimates over a range of several orders of magnitude in the failure probabilities. This remarkable efficiency is achieved because vital information on the first excursion problem that is gained from an analytical study of the failure region for linear systems is utilized in constructing the proposed importance sampling density.

Chapter 5 General Systems and Subset Simulation Method

Analytical investigation of the dynamic aspects of the first excursion problem plays an important role in Chapter 4, where the focus was on linear systems. A similar exercise may not be feasible for general nonlinear systems, whose dynamic behavior is far more complex than linear systems. For example, analytical solution for the design point excitation, that is, the most probable excitation that leads to failure of a given output response at a given time, is not available for general nonlinear systems. On the other hand, the search for design point excitations by numerical optimization may not be feasible due to the high dimensionality of the problem. Also, there is a large number of design points to be searched for, which could mean that the computational effort invested in searching for the design points already exceeds the effort required in other techniques, e.g., standard Monte Carlo simulation. The presence of uncertainties in the structural model parameters as well as in the stochastic excitation model parameters worsen the situation. These considerations discourage the use of importance sampling for solving the first excursion problem in general.

This chapter presents a method for solving the first excursion problem for general systems with special regard to computing small failure probabilities and to applicability in high dimensions. The method is based on the observation that a small failure probability can be expressed as a product of larger conditional failure probabilities, which indicates the possibility of turning a rare failure event simulation problem (as in standard Monte Carlo) into several problems which only involve the conditional simulation of more frequent events. This idea is implemented using the Markov chain Monte Carlo simulation method discussed in Chapter 3 to efficiently generate samples conditional on failure events, which is otherwise a non-trivial task.

As we will see, subset simulation method is developed with no special regard to any characteristics of the system, which means that it is applicable to general reliability problems. It provides an efficient tool for solving general first excursion problems where the stochastic model parameters are possibly uncertain, in addition to uncertain additive excitation. Such an application will be discussed in Chapter 6.

5.1 Basic idea of subset simulation

Given a failure event F, let $F_1 \supset F_2 \supset \cdots \supset F_m = F$ be a decreasing sequence of failure events so that $F_k = \cap_{i=1}^{k} F_i$, $k = 1, \ldots, m$. For example, if failure of a system is defined as the exceedence

of an uncertain demand D over a given capacity C, that is, $F = \{D > C\}$, then a sequence of decreasing failure events can simply be defined as $F_i = \{D > C_i\}$, where $C_1 < C_2 < \cdots < C_m = C$. By definition of conditional probability, we have

$$\begin{aligned} P_F = P(F_m) &= P(\cap_{i=1}^{m} F_i) \\ &= P(F_m | \cap_{i=1}^{m-1} F_i) P(\cap_{i=1}^{m-1} F_i) \\ &= P(F_m|F_{m-1}) P(\cap_{i=1}^{m-1} F_i) = \dots \\ &= P(F_1) \prod_{i=1}^{m-1} P(F_{i+1}|F_i) \end{aligned} \tag{5.1}$$

Equation (5.1) expresses the failure probability as a product of a sequence of conditional probabilities $\{P(F_{i+1}|F_i) : i = 1, \dots, m-1\}$ and $P(F_1)$. The idea of subset simulation is to estimate the failure probability P_F by estimating these quantities. When the probability of failure is estimated by means of simulation, the difficulty often increases with decreasing failure probability. Basically, the smaller the P_F, the more rare the failure event is, and the more the number of samples required to realize failure events for estimating P_F. Observe that, although P_F is small, by choosing the intermediate failure events $\{F_i : i = 1, \dots, m-1\}$ appropriately, the conditional probabilities involved in (5.1) can be made sufficiently large so that they can be evaluated efficiently by simulation procedures. For example, suppose $P(F_1), P(F_{i+1}|F_i) \sim 0.1$, $i = 1, 2, 3$, then $P_F \sim 10^{-4}$ which is too small for efficient estimation by MCS. However, the conditional probabilities, which are of the order of 0.1, may be evaluated efficiently by simulation because the failure events are more frequent. The problem of simulating rare events in the original probability space is thus replaced by a sequence of simulations of more frequent events in the conditional probability spaces.

To compute P_F based on (5.1), one needs to compute the probabilities $P(F_1)$, $\{P(F_{i+1}|F_i) : i = 1, \dots, m-1\}$. $P(F_1)$ can be readily estimated by MCS. It is natural to compute the conditional failure probabilities based on an estimator similar to (5.2), which necessitates the simulation of samples according to the conditional distribution of $\boldsymbol{\theta}$ given that it lies in F_i, that is, $q(\boldsymbol{\theta}|F_i) = q(\boldsymbol{\theta})\mathbb{I}_{F_i}(\boldsymbol{\theta})/P(F_i)$. Although one can follow a 'direct' MCS approach and obtain such samples as those simulated from q which lie in the failure region F_i, it is not efficient to do so since on average it takes $1/P(F_i)$ samples before one such sample occurs. In general, the task of efficiently simulating conditional samples is not trivial. Nevertheless, it is noted that the use of the MCMC algorithm fits nicely into the problem of computing conditional failure probabilities by using Markov chain samples with limiting stationary distribution equal to $q(\cdot|F_i)$ $(i = 1, \dots, m-1)$. The whole procedure is summarized in the next section.

5.2 Subset simulation procedure

Utilizing the modified Metropolis-Hastings method developed in Chapter 3, subset simulation proceeds as follows. First, we simulate samples $\{\theta_1, \ldots, \theta_N\}$ by direct MCS to compute an estimate $\tilde{P}_1$ for $P(F_1)$ by

$$P(F_1) \approx \tilde{P}_1 = \frac{1}{N} \sum_{k=1}^{N} \mathbb{I}_{F_1}(\theta_k) \tag{5.2}$$

where $\{\theta_k : k = 1, \ldots, N\}$ are independent and identically distributed (i.i.d.) samples simulated according to PDF q. From these MCS samples, we can readily obtain some samples distributed as $q(\cdot|F_1)$, simply as those which lie in F_1. Starting from each of these samples, we can simulate Markov chain samples using the modified Metropolis method. These samples will also be distributed as $q(\cdot|F_1)$. They can be used to estimate $P(F_2|F_1)$ using an estimator $\tilde{P}_2$ similar to (5.2). Observe that the Markov chain samples which lie in F_2 are distributed as $q(\cdot|F_2)$ and thus they provide 'seeds' for simulating more samples according to $q(\cdot|F_2)$ to estimate $P(F_3|F_2)$. Repeating this process, we can compute the conditional probabilities of the higher conditional levels until the failure event of interest, F $(= F_m)$, has been reached. At the i-th conditional level, $1 \leq i \leq m-1$, let $\{\theta_k^{(i)} : k = 1, \ldots, N\}$ be the Markov chain samples with distribution $q(\cdot|F_i)$, possibly coming from different chains generated by different 'seeds'. Then

$$P(F_{i+1}|F_i) \approx \tilde{P}_{i+1} = \frac{1}{N} \sum_{k=1}^{N} \mathbb{I}_{F_{i+1}}(\theta_k^{(i)}) \tag{5.3}$$

Finally, combining (5.1), (5.2) and (5.3), the failure probability estimator is

$$\tilde{P}_F = \prod_{i=1}^{m} \tilde{P}_i \tag{5.4}$$

5.3 Choice of intermediate failure events

The choice of the intermediate failure events $\{F_i : i = 1, \ldots, m-1\}$ plays a key role in the subset simulation procedure. Two issues are basic to the choice of the intermediate failure events. The first is the parameterization of the target failure event F which allows the generation of intermediate failure events by varying the value of the defined parameter. The second is the choice of the specific sequence of values of the defined parameter, which affects the values of the conditional probabilities $\{P(F_{i+1}|F_i) : i = 1, \ldots, m-1\}$ and hence the efficiency of the subset simulation procedure.

Generic representation of failure event

Many failure events encountered in engineering applications can be defined using a combination of union and intersection of some component failure events. In particular, consider a failure event F of the following form:

$$F = \bigcup_{j=1}^{L} \bigcap_{k=1}^{L_j} \{D_{jk}(\boldsymbol{\theta}) > C_{jk}(\boldsymbol{\theta})\} \tag{5.5}$$

where $D_{jk}(\boldsymbol{\theta})$ and $C_{jk}(\boldsymbol{\theta})$ may be viewed as the demand and capacity variables of the (j,k) component of the system. The failure event F in (5.5) can be considered as the failure of a system with L sub-systems connected in series, where the j-th sub-system consists of L_j components connected in parallel.

In order to apply subset simulation to compute the failure probability P_F, it is desirable to parameterize F with a single parameter so that the sequence of intermediate failure events $\{F_i : i = 1,\ldots,m-1\}$ can be generated by varying the parameter. This can be accomplished as follows. For the failure event in (5.5), define the 'critical demand-to-capacity ratio' (CDCR) Y as

$$Y(\boldsymbol{\theta}) = \max_{j=1,\ldots,L} \min_{k=1,\ldots,L_j} \frac{D_{jk}(\boldsymbol{\theta})}{C_{jk}(\boldsymbol{\theta})} \tag{5.6}$$

Then it can be easily verified that

$$F = \{Y(\boldsymbol{\theta}) > 1\} \tag{5.7}$$

and so the sequence of intermediate failure events can be generated as

$$F_i = \{Y(\boldsymbol{\theta}) > y_i\} \tag{5.8}$$

where $0 < y_1 < \cdots < y_m = 1$ is a sequence of (normalized) intermediate threshold values.

Similarly, consider a failure event F of the form:

$$F = \bigcap_{j=1}^{L} \bigcup_{k=1}^{L_j} \{D_{jk}(\boldsymbol{\theta}) > C_{jk}(\boldsymbol{\theta})\} \tag{5.9}$$

which can be considered as the failure of a system with L sub-systems connected in parallel with the j-th sub-system consisting of L_j components connected in series. One can easily verify that the definition

$$Y(\boldsymbol{\theta}) = \min_{j=1,\ldots,L} \max_{k=1,\ldots,L_j} \frac{D_{jk}(\boldsymbol{\theta})}{C_{jk}(\boldsymbol{\theta})} \tag{5.10}$$

satisfies (5.7) and hence the sequence of failure events can again be generated based on (5.8).

The foregoing discussion can be generalized to failure events consisting of multiple stacks of union and intersection. Essentially, Y is defined using 'max' and 'min' in the same order corresponding to each occurrence of union ($\cup$) and intersection ($\cap$) in F, respectively. As another example, consider the first excursion failure of the interstory drift in any one story of a n_s-story building beyond a given threshold level b. Let the interstory drift response $\{X_j(t;\theta) : j = 1,\ldots,n_s\}$ be computed at the n_t time instants $t_1,\ldots,t_{n_t}$ within the duration of interest. Then

$$F = \bigcup_{j=1}^{n_s} \bigcup_{k=1}^{n_t} \{|X_j(t_k;\theta)| > b\} = \{Y(\theta) > 1\} \tag{5.11}$$

where

$$Y(\theta) = \max_{j=1,\ldots,n_s} \max_{k=1,\ldots,n_t} \frac{|X_j(t_k)|}{b} \tag{5.12}$$

Choice of intermediate threshold levels

The choice of the sequence of intermediate threshold values $\{y_1,\ldots,y_m\}$ appearing in the parameterization of intermediate failure events affects the values of the conditional probabilities and hence the efficiency of the subset simulation procedure. If the sequence increases slowly, then the conditional probabilities will be large, and so their estimation requires less samples N. A slow sequence, however, requires more simulation levels m to reach the target failure event, increasing the total number of samples $N_T = mN$ in the whole procedure. Conversely, if the sequence increases too rapidly that the conditional failure events become rare, it will require more samples N to obtain an accurate estimate of the conditional failure probabilities in each simulation level, which again increases the total number of samples. It can thus be seen that the choice of the intermediate threshold values is a trade-off between the number of samples required in each simulation level and the number of simulation levels required to reach the target failure event.

The choice of the intermediate threshold values $\{y_i : i = 1,\ldots,m-1\}$ deserves a detailed study which is left for future work. One strategy is to choose the y_i a priori, but then it is difficult to control values of the conditional probabilities $P(F_i|F_{i-1})$. In this work, the y_i are chosen 'adaptively' so that the estimated conditional probabilities are equal to a fixed value $p_0 \in (0,1)$. This is accomplished by choosing the intermediate threshold level y_i ($i = 1,\ldots,m-1$) as the $(1-p_0)N$-th largest value (i.e., an order statistic) among the CDCRs $\{Y(\theta_k^{(i-1)}) : k = 1,\ldots,N\}$ where the $\theta_k^{(i-1)}$ are the Markov chain samples generated at the $(i-1)$-th conditional level for $i = 2,\ldots,m-1$, and the $\theta_k^{(0)}$ are the samples from the initial Monte Carlo simulation. Here, p_0 is assumed to be chosen so that p_0N and hence $(1-p_0)N$ are positive integers, although this is not strictly necessary. This choice of the intermediate threshold levels implies that they are dependent on the conditional samples and will

vary in different simulation runs. For a target probability level of 10^{-3} to 10^{-6}, choosing $p_0 = 0.1$ is found to yield good efficiency.

Using this adaptive choice of the proposal PDF, the subset simulation procedure is illustrated in Figure 5.1 for simulation Levels 0 (Monte Carlo) and 1 (Markov Chain Monte Carlo).

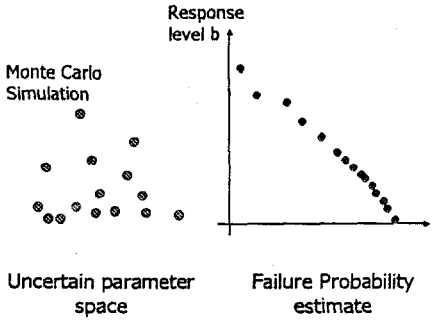

(a) Level 0 (initial phase): Monte Carlo simulation

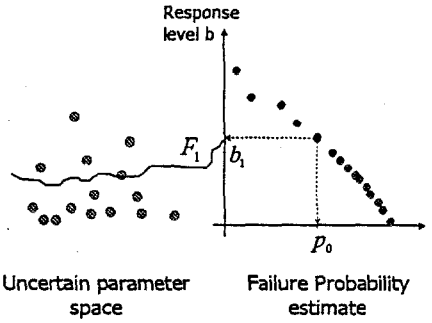

(b) Level 0: Adaptive selection of first intermediate threshold level

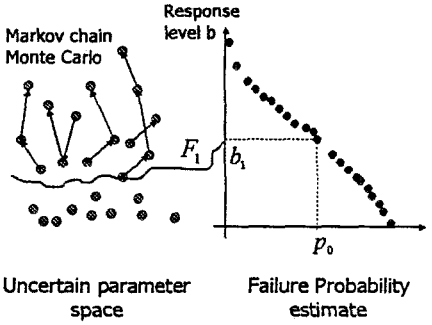

(c) Level 1: Markov chain Monte Carlo Simulation

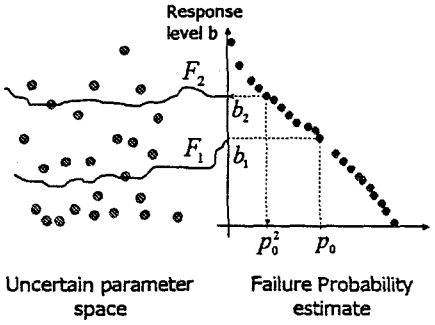

(d) Level 1: Adaptive selection of second intermediate threshold level

Figure 5.1: Illustration of subset simulation procedure

5.4 Choice of proposal PDF

The choice of the proposal PDF plays an important role in an MCMC procedure. It affects the distribution and the acceptance rate of the candidate state. These in turn affect the correlation among the Markov chain samples and consequently the efficiency of the subset simulation procedure. The choice of the proposal PDF is the major channel through which prior knowledge about a particular problem can be used to improve the efficiency of MCMC. A careful choice of the proposal PDF is thus worth examining. This section will discuss this choice with regard to solving the first excursion problem. In particular, we consider the choice of the proposal PDF p_j^* for each group j ($j = 1, \ldots, n_G$) to be used at the i-th simulation level ($i = 1, \ldots, m-1$).

Ideally, the proposal PDF should be chosen as a non-adaptive one equal to the conditional PDF $q(\boldsymbol{\theta}|F_i)$ (with all uncertain parameters collected in one group), in which case all states generated by the proposal PDF will be i.i.d. and accepted. Of course, this choice is not feasible, for the same reason as in importance sampling. The art of choosing the proposal PDF thus lies in how it can be chosen so that the candidate state has a distribution close to the conditional PDF in order that the simulation process is still efficient (with small correlation among Markov chain samples). Realizing that choosing an n-dimensional proposal PDF (i.e., with only one group of n uncertain parameters) will generally lead to zero acceptance rate when n is large, grouping of the uncertain parameters is inevitable.

For the modified MCMC scheme proposed in Chapter 3, the following two issues related to the choice of the proposal PDF are important: (1) how to group the uncertain parameters, and (2) what proposal PDF should be chosen for each group. To address the first issue, first note that the components of the candidate state corresponding to different groups are generated independently in Step 1. This is the key mechanism which suppresses zero-acceptance phenomenon in high dimensions, but at the expense of implicitly enforcing independence among the uncertain parameters of different groups in the generation of the candidate state. If some uncertain parameters belonging to different groups are strongly correlated when conditional on the failure region, the distribution of the candidate state will not be close to the conditional PDF, at least in terms of the correlation structure among the uncertain parameters. Consequently, the acceptance rate with respect to the conditioning by F_i for the candidate state will be small. Thus, uncertain parameters that are strongly correlated to each other when conditional on F_i should be grouped together. In any case, the number of uncertain parameters in a group should be kept small to avoid zero acceptance phenomenon.

Deciding what type of proposal PDF for a particular group depends on the role that the group of uncertain parameters has in affecting failure and on the information available for constructing the proposal PDF. Three types of groups are discussed in the following.

Insensitive parameters

If failure is insensitive to a particular group of uncertain parameters, then the proposal PDF should be chosen as the original parameter PDF, so that the pre-candidate component $\xi^{(j)}$ generated by the proposal PDF is always accepted into the candidate state in Step 1.

A small number of influential uncertain parameters

Consider the case where failure is sensitive to the uncertain parameters of a particular group. If there is some information about the failure region F_i so that a PDF can be constructed which is similar to the conditional PDF with respect to the uncertain parameters of this group, then such PDF may be used as the proposal PDF, assuming that an efficient method is available for evaluating its value and for generating random samples according to it. The proposal PDF in this case is non-adaptive, and its role is the same as the role of an importance sampling density with respect to the group of uncertain parameters. Similar methods to those for constructing ISDs can be used for constructing the proposal PDF. Regarding the information available for constructing the proposal PDF, it should be noted that the Markov chain samples from the last simulation level that lie in the failure region F_i are distributed as $q(\boldsymbol{\theta}|F_i)$, and hence provide information about the failure region F_i. In fact, these samples are used as the initial samples for starting individual Markov chains for the current simulation level. One way of utilizing these samples is to construct the proposal PDF as a Normal PDF with mean and covariance matrix estimated from the samples. Another strategy is to construct the proposal PDF as a kernel sampling density using the samples (Silverman 1986; Ang et al. 1992; Au and Beck 1999). Since the information from the last simulation level is utilized to construct the proposal PDF at the current level, this choice is 'level-adaptive,' although it is not chain-adaptive. It should be noted, however, that successful use of a level-adaptive proposal PDF is based on the premise that the conditional PDF with respect to the group of uncertain parameters can be approximated by the chosen type of PDF. Also, they should be used only when the number of uncertain parameters in the group is not large, for otherwise zero acceptance phenomenon may occur as the number of members n_j in the group increases.

A large number of i.i.d. uncertain parameters

When there is a large number of uncertain parameters which play a similar role in affecting failure, it often happens that these uncertain parameters as a whole affect failure significantly, but not individually. One common example is the set of i.i.d standard Normal parameters in the discrete-time representation of Gaussian white noise in the first excursion problem. In this case, each of these uncertain parameters should be grouped individually, to avoid the zero-acceptance phenomenon. For each uncertain parameter, one can choose a one-dimensional adaptive symmetric (Metropolis) proposal PDF. The advantage of this choice is that a reasonable acceptance rate of

Table 5.1: Different types of proposal PDFs

Type	Description	Advantage	Disadvantage	Suitable for
I	Parameter PDF, non-adaptive	100% acceptance in Step 1; pre-candidate component $\xi^{(j)}$ does not depend on current sample	Does not improve acceptance with respect to conditioning by F_i in Step 2	Insensitive parameters
II	1-D chain-adaptive symmetric (Metropolis)	Good acceptance rate of candidate state without prior information on F_i	Correlation between current sample and candidate state may be high	Uncertain parameters which are abundant and influential as a group
III	n_j-D Metropolis-Hastings, chain-non-adaptive, level-adaptive	High acceptance rate possible if uncertain parameters are influential, and conditional PDF well approximated by proposal PDF	Only for a small number of uncertain parameters	A small group of influential parameters

the candidate state can often be guaranteed when the spread of the proposal PDF is not too large, since then the corresponding components of the candidate state are generated in the neighborhood of those of the current sample. The correlation structure among the uncertain parameters with respect to the conditioning by F_i will be adapted in Step 2 of the modified Metropolis-Hastings algorithm. This choice of the proposal PDF will also cause the components of the candidate state to be positively correlated with those of current sample, thereby slowing convergence of the conditional failure probability estimate for the level, although this seems to be the best one can do in the absence of further prior knowledge about the failure region and to suppress the zero acceptance phenomenon in high dimensions. Table 5.1 gives a summary of the different types of proposal PDFs.

5.4.1 Choice of proposal PDF for first excursion problems

For applications to solving the first excursion problem, it is useful to group the uncertain parameters in the excitation model into two categories:

1. additive excitation parameters $\boldsymbol{\theta}_Z$
2. stochastic excitation model parameters $\boldsymbol{\theta}_E$

The first category includes the additive excitation parameters $\boldsymbol{\theta}_Z$ in the discrete representation of the stochastic excitation. The number of uncertain parameters in this category can be very large. For example, discretizing Gaussain white-noise excitation in the time-domain of duration $T_d = 30$ sec. and sampling time $\Delta t = 0.02$ sec. requires $T_d/\Delta t + 1 = 1501$ i.i.d. standard Normal random variables, assuming the time instants at time zero and 30 sec. are also represented. These uncertain parameters are often influential as a group, but they are insensitive individually, because the dynamic response is affected by the 'integral' (in continuous-time) or 'summation' (in discrete-time) effect of these parameters, and the effect of each individual uncertain parameter on the response is infinitesimally small (e.g., $O(\Delta t)$ in discrete-time). For this category of uncertain

Table 5.2: Recommended types of proposal PDFs for different parameters

Uncertain parameters in the problem	Type of proposal PDF for	
	$\boldsymbol{\theta}_Z$	$\boldsymbol{\theta}_E$
$\boldsymbol{\theta}_Z$	II	
$\boldsymbol{\theta}_Z, \boldsymbol{\theta}_E$	I/II	III/II

parameters, it is recommended that they be treated individually using Type I proposal PDF (1-D Metropolis).

The second category includes the stochastic excitation model parameters $\boldsymbol{\theta}_E$ involved in the characterization of the stochastic model for the excitation, which often have a multiplicative effect on the response. Examples are the spectral intensity of white-noise excitation or the moment magnitude and epicentral distance in a stochastic ground motion point-source model. Due to their multiplicative effect and their large assumed variability in applications, these uncertain parameters often have a dominant effect on the uncertain response, rendering other uncertain parameters, such as those in $\boldsymbol{\theta}_Z$, less sensitive. Since these uncertain parameters control failure, their conditional distribution $q(\boldsymbol{\theta}^{(j)}|F_i)$ is often significantly different from their original PDF $q(\boldsymbol{\theta}^{(j)})$. Capturing the conditional distribution of these uncertain parameters can lead to significant improvement in the efficiency of the simulation procedure, and hence a Type III proposal PDF is recommended, with the requirement that the number of uncertain parameters in the group should be kept small to suppress the zero acceptance phenomenon. Table 5.2 summarizes the types of proposal PDFs recommended for the uncertain parameters of different categories.

5.5 Statistical properties of the estimators

In this section, we present results on the statistical properties of the estimators $\tilde{P}_i$ and $\tilde{P}_F$. They are derived assuming that the Markov chain generated according to the modified Metropolis method is (theoretically) ergodic, that is, its stationary distribution is unique and independent of the initial state of the chain. A discussion on ergodicity will follow after this section. It is assumed in this section that the intermediate failure events are chosen a priori. In the case where the intermediate threshold levels are chosen dependent on the conditional samples and hence vary in different simulation runs, as is the case in the examples presented in this paper, the derived results should hold approximately, provided such variation is not significant. Nevertheless, this approximate analysis is justified since the objective is to have an assessment of the quality of the probability estimate based on information available in one simulation run.

5.5.1 MCS estimator $\tilde{P}_1$

As well-known, the MCS estimator $\tilde{P}_1$ in (5.2) computed using the i.i.d. samples $\{\boldsymbol{\theta}_1, \ldots, \boldsymbol{\theta}_N\}$ converges almost surely to P_1 (Strong Law of Large Numbers), is unbiased, consistent, and Normally distributed as $N \to \infty$ (Central Limit Theorem). The coefficient of variation (c.o.v.) of $\tilde{P}_1$, δ_1, defined as the ratio of the standard deviation to the mean of $\tilde{P}_1$, is given by

$$\delta_1 = \sqrt{\frac{1-P_1}{P_1 N}} \tag{5.13}$$

5.5.2 Conditional probability estimator $\tilde{P}_i$ $(2 \le i \le m)$

Since the Markov chains generated at each conditional level are started with samples (selected from the previous simulation level) distributed as the corresponding target conditional PDF, the Markov chain samples used for computing the conditional probability estimators based on (5.3) are identically distributed as the target conditional PDF. Using this result and taking expectation on both side of (5.3) shows that the conditional estimators $\tilde{P}_i$ $(i = 2, \ldots, m)$ are unbiased. On the other hand, the Markov chain samples are dependent. In spite of this dependence, all the estimators $\tilde{P}_i$ still have the usual convergence properties of estimators using independent samples (Doob 1953). For example, $\tilde{P}_i$ converges almost surely to $P(F_i|F_{i-1})$ (Strong Law of Large Numbers), is consistent, and Normally distributed as $N \to \infty$ (Central Limit Theorem).

An expression for the c.o.v. for $\tilde{P}_i$ is next derived. At the $(i-1)$-th conditional level, suppose that the number of Markov chains (each with a possibly different starting point) is N_c, and N/N_c samples have been simulated from each of these chains, so that the total number of Markov chain samples is N. Although the samples generated by different chains are in general dependent because the 'seeds' for each chain may be dependent, it is assumed for simplicity in analysis that they are uncorrelated through the indicator function $\mathbb{I}_{F_i}(\cdot)$, i.e., $E[\mathbb{I}_{F_i}(\boldsymbol{\theta})\mathbb{I}_{F_i}(\boldsymbol{\theta}')] - P(F_i|F_{i-1})^2 = 0$ if $\boldsymbol{\theta}$ and $\boldsymbol{\theta}'$ are from different chains. Let $\boldsymbol{\theta}_{jk}^{(i)}$ be the k-th sample in the j-th Markov chain at simulation level i. For simplicity in notation, let $I_{jk}^{(i)} = \mathbb{I}_{F_i}(\boldsymbol{\theta}_{jk}^{(i-1)})$ and $P_i = P(F_i|F_{i-1})$, $i = 2, \ldots, m$. Then

$$\begin{aligned} \mathsf{E}[\tilde{P}_i - P_i]^2 &= \mathsf{E}[\frac{1}{N}\sum_{j=1}^{N_c}\sum_{k=1}^{N/N_c}(I_{jk}^{(i)} - P_i)]^2 \\ &= \frac{1}{N^2}\sum_{j=1}^{N_c}\mathsf{E}[\sum_{k=1}^{N/N_c}(I_{jk}^{(i)} - P_i)]^2 \end{aligned} \tag{5.14}$$

For the j-th chain,

$$\mathsf{E}[\sum_{k=1}^{N/N_c}(I_{jk}^{(i)} - P_i)]^2 = \sum_{k,l=1}^{N/N_c} E(I_{jk}^{(i)} - P_i)(I_{jl}^{(i)} - P_i) = \sum_{k,l=1}^{N/N_c} R_i(k-l) \tag{5.15}$$

where

$$R_i(k) = E(I_{j1}^{(i)} - P_i)(I_{j,1+k}^{(i)} - P_i) = \mathsf{E}[I_{j1}^{(i)} I_{j,1+k}^{(i)}] - P_i^2 \tag{5.16}$$

is the covariance between $I_{jl}^{(i)}$ and $I_{j,l+k}^{(i)}$, for any $l = 1, ..., N/N_c$, and it is independent of l due to stationarity. It is also independent of the chain index j since all chains are probabilistically equivalent. Evaluating the sum in (5.15) with respect to $k - l$,

$$\begin{aligned}\mathsf{E}[\sum_{k=1}^{N/N_c}(I_{jk}^{(i)} - P_i)]^2 &= \frac{N}{N_c}R_i(0) + 2\sum_{k=1}^{N/N_c-1}(\frac{N}{N_c} - k)R_i(k) \\ &= \frac{N}{N_c}[R_i(0) + 2\sum_{k=1}^{N/N_c-1}(1 - \frac{kN_c}{N})R_i(k)]\end{aligned} \tag{5.17}$$

Substituting (5.17) into (5.14) yields

$$\begin{aligned}\mathsf{E}[\tilde{P}_i - P_i]^2 &= \frac{1}{N}[R_i(0) + 2\sum_{k=1}^{N/N_c-1}(1 - \frac{kN_c}{N})R_i(k)] \\ &= \frac{R_i(0)}{N}[1 + 2\sum_{k=1}^{N/N_c-1}(1 - \frac{kN_c}{N})\rho_i(k)]\end{aligned} \tag{5.18}$$

where

$$\rho_i(k) = R_i(k)/R_i(0) \tag{5.19}$$

is the correlation coefficient at lag k of the stationary sequence $\{\mathbb{I}_{jk}^{(i)} : k = 1, \ldots, N/N_c\}$. Finally, since $I_{jk}^{(i)}$ is a Bernouli random variable, $R_i(0) = \mathsf{Var}[I_{jk}^{(i)}] = P_i(1 - P_i)$, and so the variance of $\tilde{P}_i$ is given by

$$\sigma_i^2 = \mathsf{E}[\tilde{P}_i - P_i]^2 = \frac{P_i(1 - P_i)}{N}[1 + \gamma_i] \tag{5.20}$$

where

$$\gamma_i = 2\sum_{k=1}^{N/N_c-1}(1 - \frac{kN_c}{N})\rho_i(k) \tag{5.21}$$

The c.o.v. δ_i of $\tilde{P}_i$ is thus given by

$$\delta_i = \sqrt{\frac{1 - P_i}{P_i N}(1 + \gamma_i)} \tag{5.22}$$

The covariance sequence $\{R_i(k) : i = 0, \ldots, N/N_c - 1\}$ can be estimated using the Markov chain

samples $\{\boldsymbol{\theta}_{jk}^{(i-1)} : j = 1, \ldots, N_c; k = 1, \ldots, N/N_c\}$ at the $(i-1)$-th conditional level by:

$$R_i(k) \approx \tilde{R}(k) = \left(\frac{1}{N - kN_c} \sum_{j=1}^{N_c} \sum_{l=1}^{N/N_c - k} I_{jl}^{(i)} I_{j,l+k}^{(i)} \right) - \tilde{P}_i^2 \tag{5.23}$$

from which the correlation sequence $\{\rho_i(k) : k = 1, \ldots, N/N_c - 1\}$ and hence the correlation factor γ_i in (5.21) can also be estimated. Consequently, the c.o.v. δ_i for the conditional probability estimator $\tilde{P}_i$ can be estimated by (5.22), where P_i is approximated by $\tilde{P}_i$ using (5.3).

The factor $(1 - P_i)/P_i N$ in (5.22) is the familiar one for the square of the c.o.v. of the MCS estimators with N independent samples. The c.o.v. of $\tilde{P}_i$ can thus be considered as the one in MCS with an effective number of independent samples $N/(1 + \gamma_i)$. The efficiency of the estimator using dependent samples of a Markov chain ($\gamma_i > 0$) is therefore reduced compared to the case when the samples are independent ($\gamma_i = 0$), and smaller values of γ_i imply higher efficiency. The value of γ_i depends on the choice of the spread of the proposal PDFs.

5.5.3 Failure probability estimator $\tilde{P}_F$

Since $\tilde{P}_1 \to P(F_1)$ and $\tilde{P}_i \to P(F_i|F_{i-1})$ $(2 \leq i \leq m)$ almost surely as $N \to \infty$, $\tilde{P}_F \to P(F_1) \prod_{i=1}^{m-1} P(F_{i+1}|F_i) = P_F$ almost surely also. Due to the correlation between the conditional estimators $\{\tilde{P}_i\}$, $\tilde{P}_F$ is biased for every N, but it is asymptotically unbiased. This correlation is due to the fact that the samples used for computing $\tilde{P}_i$ which lie in F_i are used to start the Markov chains to compute $\tilde{P}_{i+1}$. The results concerning the mean and c.o.v. of the failure probability estimator $\tilde{P}_F$ are summarized in the following two propositions.

Proposition 5.1. *$\tilde{P}_F$ is biased for every N. The fractional bias is bounded above by*

$$|\mathsf{E}[\frac{\tilde{P}_F - P_F}{P_F}]| \leq \sum_{i>j} \delta_i \delta_j + o(1/N) = O(1/N) \tag{5.24}$$

$\tilde{P}_F$ is thus asymptotically unbiased and the bias is $O(1/N)$.

Proof. Define $Z_i = (\tilde{P}_i - P_i)/\sigma_i$, then it is clear that $\mathsf{E}[Z_i] = 0$ and $\mathsf{E}[Z_i^2] = 1$, and $\tilde{P}_i = P_i + \sigma_i Z_i$.

$$\begin{aligned} \frac{\tilde{P}_F - P_F}{P_F} &= \prod_{i=1}^{m} \tilde{P}_i / P_i - 1 \\ &= \prod_{i=1}^{m} (1 + \delta_i Z_i) - 1 \\ &= \sum_{i=1}^{m} \delta_i Z_i + \sum_{i>j} \delta_i \delta_j Z_i Z_j + \sum_{i>j>k} \delta_i \delta_j \delta_k Z_i Z_j Z_k + \cdots + \prod_{i=1}^{m} \delta_i Z_i \end{aligned} \tag{5.25}$$

Taking expectation and using $\mathsf{E}[Z_i] = 0$,

$$\mathsf{E}[\frac{\tilde{P}_F - P_F}{P_F}] = \sum_{i>j} \delta_i \delta_j \mathsf{E}[Z_i Z_j] + \sum_{i>j>k} \delta_i \delta_j \delta_k \mathsf{E}[Z_i Z_j Z_k] + \cdots + (\prod_{i=1}^{m} \delta_i)\mathsf{E}[\prod_{i=1}^{m} Z_i] \tag{5.26}$$

If $\{Z_i : i = 1, \ldots, m\}$ are uncorrelated, $\mathsf{E}[Z_i Z_j]$, $\mathsf{E}[Z_i Z_j Z_k]$, ..., are all zero, and hence $\tilde{P}_F$ will be unbiased. In general, however, $\{Z_i : i = 1, \ldots, m\}$ are correlated, so $\tilde{P}_F$ is biased for every N. On the other hand, since δ_i is $O(1/\sqrt{N})$ from (5.22), the first term in (5.26) is $O(1/N)$ while the remaining sums of higher products of the δ_i's are $o(1/N)$. Taking absolute value on both sides of (5.26), using Cauchy-Schwarz inequality to obtain $|\mathsf{E}[Z_i Z_j]| \leq \sqrt{\mathsf{E}[Z_i^2]\mathsf{E}[Z_j^2]} = 1$ and applying it to the R.H.S. of (5.26) proves the required proposition. □

Proposition 5.2. *The c.o.v. δ of $\tilde{P}_F$ is bounded above by*

$$\delta^2 = \mathsf{E}[\frac{\tilde{P}_F - P_F}{P_F}]^2 \leq \sum_{i,j=1}^{m} \delta_i \delta_j + o(1/N) = O(1/N) \tag{5.27}$$

$\tilde{P}_F$ is thus a consistent estimator and its c.o.v. δ is $O(1/\sqrt{N})$.

Proof. From (5.25),

$$\begin{aligned} \mathsf{E}[\frac{\tilde{P}_F - P_F}{P_F}]^2 &= \mathsf{E}[\sum_{i=1}^{m} \delta_i Z_i + \sum_{i>j} \delta_i \delta_j Z_i Z_j + \cdots + \prod_{i=1}^{m} \delta_i Z_i]^2 \\ &= \sum_{i,j=1}^{m} \delta_i \delta_j \mathsf{E}[Z_i Z_j] + o(1/N) \\ &\leq \sum_{i,j=1}^{m} \delta_i \delta_j + o(1/N) = O(1/N) \end{aligned} \tag{5.28}$$

since $\mathsf{E}[Z_i Z_j] \leq 1$ and $\delta_i = O(1/\sqrt{N})$. □

Note that the c.o.v. δ in (5.27) is defined through the expected deviation about the target failure probability P_F instead of $E[\tilde{P}_F]$ so that the effects of bias are accounted for. The upper bound corresponds to the case when the conditional probability estimators $\{\tilde{P}_i : i = 2, \ldots, m\}$ are fully correlated. The actual c.o.v. depends on the correlation between the $\tilde{P}_i$s. If all the $\tilde{P}_i$s were uncorrelated, then

$$\delta^2 = \sum_{i=1}^{m} \delta_i^2 \tag{5.29}$$

Although the $\tilde{P}_i$s are generally correlated, simulations show that δ^2 may be well approximated by (5.29). This will be illustrated in the examples.

To get an idea of the number of samples required to achieve a given accuracy in $\tilde{P}_F$, consider the case where $P(F_1) = P(F_{i+1}|F_i) = p_0$. Assume $\delta_i^2 = (1+\gamma)(1-p_0)/p_0 N$ to be the same for all levels. Using (5.22) and (5.28), and noting that the number of simulation levels to achieve the target failure probability is $m = \log P_F / \log p_0$, we conclude that to achieve a given c.o.v. of δ in the estimate $\tilde{P}_F$, the total number of samples required is roughly

$$N_T \approx mN = |\log P_F|^r \times \frac{(1+\gamma)(1-p_0)}{p_0 |\log p_0|^r \delta^2} \tag{5.30}$$

where $r \leq 3$ depends on the actual correlation of the $\tilde{P}_i$s. Thus, for a fixed p_0 and δ, $N_T \propto |\log P_F|^r$. Compared with MCS, where $N_T \propto 1/P_F$, this implies a substantial improvement in efficiency when estimating small probabilities.

5.6 Ergodicity of subset simulation procedure

The foregoing discussion assumes that the Markov chain generated according to the Metropolis method is ergodic, which guarantees that the conditional probability estimate based on the Markov chain samples from a single chain will tend to the corresponding theoretical conditional probability as $N \to \infty$. Theoretically, ergodicity can be always achieved by choosing a sufficiently large spread in the proposal PDFs. Practically, with a finite number of Markov chain samples, ergodicity often becomes an issue of whether the Markov chain samples used to estimate the conditional probabilities populate sufficiently well the important regions of the failure domain, where the main contributions to the failure probability come from. Intuitively, if there are some parts of the failure region of significant probability content that are not well visited by the Markov chain samples, the contribution of the probability mass from such regions will not be reflected in the estimator, and the conditional probability estimate will be significantly biased.

First of all, the use of a Type I proposal PDF will not cause any ergodicity problem, since then the pre-candidate state is generated from the parameter PDF. For a Type III proposal PDF, the problem of ergodicity is associated with whether the samples from the last level for constructing the level-adaptive proposal PDF have populated sufficiently well the parts in the failure region that give significant contribution to the failure probability. It is thus required that the number of samples for constructing the level-adaptive proposal PDF be sufficiently large to be representative of the whole failure region.

The case of using a Type I proposal PDF requires some consideration of the transitions between Markov chain samples. For a Markov chain started at a single point, ergodicity problems may arise due to the existence of disconnected failure regions that are separated by safe regions whose size is large compared to the spread of the proposal PDFs. To see this, recall that to go from the current

Markov state to the next, a candidate state is generated in the neighborhood of the current state according to the proposal PDFs. To transit from one failure region to another, the candidate state has to lie in the second failure region, but this is unlikely to happen if the spread of the proposal PDF is small compared to the safe region between the two failure regions. (Any candidate state that falls in the safe region is rejected by the Metropolis algorithm.) So, the safe region prohibits transition of the Markov chain between disconnected failure regions, resulting in ergodicity problems. The situation of disconnected failure regions may arise, for example, in failure problems for systems with components connected in series.

By using the samples from multiple Markov chains with different initial states obtained from previous conditional levels, as in the present methodology, ergodicity problems due to disconnected failure regions may be resolved. To see this, first note that the subset simulation procedure begins with MCS, which produces independent samples distributed in the whole parameter space. The MCS samples which lie in F_1 populate the different regions of F_1 according to the relative importance (probability content) of the regions. We can expect these samples to populate F_1 sufficiently well, since otherwise the c.o.v. of $\tilde{P}_1$ will be large and subsequently the c.o.v. of $\tilde{P}_F$ will not be acceptable as the errors accumulate through subsequent conditional simulation levels. For the next conditional level, we simulate multiple Markov chains, starting at the conditional MCS samples distributed among different regions in F_1. This allows us to have 'seeds' in the different regions of F_1, which could possibly be disconnected. The Markov chain initiated in each disconnected region will populate it at least locally, and so the combined Markov chains correctly account for the contributions from the regions to the conditional probability estimate. In this manner, the contribution from disconnected failure regions in higher conditional levels can also be accounted for as the Markov chain samples in these regions propagate through higher conditional levels. This argument holds, of course, as long as unimportant failure regions (i.e., those with negligible contribution) at lower conditional levels remain unimportant at higher conditional levels, since otherwise there may not be enough seeds (if any) at lower conditional levels to develop more Markov chain samples to account for their importance at higher levels. In conclusion, even though a Markov chain started from a single state may have ergodicity problems with disconnected failure regions, using Markov chain samples from multiple chains, as in the proposed method, can be expected to achieve practical ergodicity in spite of the existence of disconnected failure regions.

The foregoing argument suggests that the subset simulation procedure is likely to produce an ergodic estimator for failure probability; nevertheless it offers no guarantee for practical ergodicity. Whether ergodicity problems become an issue depends on the particular application and the choice of the proposal PDFs. It is worth noting that similar issues related to ergodicity are expected to arise in any simulation method which tries to conclude 'global' information from some known 'local' information, assuming implicitly that the known local information dominates the problem. For

example, importance sampling using design point(s) implicitly assumes that the main contribution of failure probability comes from the neighborhood of the known design points and there are no other design points of significant contribution. Thus, in situations such as when the failure region is highly concave or there are other unknown design points, the importance sampling estimator is biased and has an ergodicity problem. In view of this, one should appreciate the ergodic property of standard Monte Carlo simulation, since it is a totally global procedure in the sense that it does not accumulate information about the failure region developed from local states only.

5.7 Summary of this chapter

Subset simulation is based on (1) the representation of small failure probabilities as a product of larger conditional failure probabilities and (2) Markov chain Monte Carlo simulation to efficiently generate samples conditional on intermediate failure regions. During subset simulation, samples are gradually adapted to failure regions of small failure probabilities. Expressions for the variability of the failure probability estimates have been derived, which allow the assessment of the estimation error in a single simulation run. The applicability and efficiency of subset simulation method to probabilistic assessment of seismic performance will be investigated in Chapter 6.

Chapter 6 Applications to Probabilistic Assessment of Seismic Performance

The application of subset simulation to seismic risk analysis is illustrated in this chapter. The major goal is to demonstrate that subset simulation can be efficiently applied to compute the failure probability of a structure given an earthquake of uncertain magnitude and location occurs in a region of interest around the site where the structure is situated. This information can be used to assess the lifetime reliability, or equivalently, the lifetime failure probability of a structure in an uncertain seismic environment. Failure analysis is also carried out using the samples generated during subset simulation, which provide insight into the probable scenario that will happen when failure occurs.

6.1 Lifetime reliability

The lifetime failure probability of a structure is intimately related to the failure probability of a structure given an earthquake occurs. In particular, assuming that the occurrence of earthquakes follows a Poisson process and the failure event of the structure in different seismic events are independent with the same failure probability, then the lifetime failure probability $P(F_{\text{life}})$ is given by

$$P(F_{\text{life}}) = 1 - \exp[-\lambda T_{\text{life}} P(F|EQ)] \tag{6.1}$$

where λ is the mean number of earthquakes per annum and $P(F|EQ)$ is the failure probability given that an earthquake event of uncertain magnitude and location occurs in the region of interest. For small lifetime failure probability, $\exp(-\lambda T_{\text{life}} P(F|EQ)) \sim 1 - \lambda T_{\text{life}} P(F|EQ)$, and so

$$P(F_{\text{life}}) \sim \lambda T_{\text{life}} P(F|EQ) \tag{6.2}$$

which is equal to the mean number of earthquakes λT_{life} expected during the lifetime of the structure multiplied by the failure probability of the structure in a seismic event. Note that $P(F|EQ)$ is the channel through which structure-specific information is reflected in the seismic risk problem.

6.2 Stochastic ground motion model

The seismic risk problem is formulated using a stochastic ground motion model to describe the uncertainty associated with the ground motion at the site in a seismic event of given magnitude and earthquake source location. In this work, the stochastic ground motion model developed by Atkinson and Silva (2000) is adopted, which belongs to the class of point-source models characterized by the moment magnitude M and epicentral distance r (Brune 1971b; Brune 1971a; Hanks and McGuire 1981; Boore 1983). For easy reference, we will call this the A-S model. To generate a suite of time histories for the ground acceleration for given moment magnitude M and epicentral distance r, a discrete-time white noise sequence $\{W_j = \sqrt{2\pi/\Delta t}\, Z_j : j = 1, \ldots, n_t\}$, where $Z_1, \ldots, Z_{n_t}$ are i.i.d. standard Normally distributed, is first generated and then modulated by an envelope function $e(t; M, r)$ at the discrete time instants. A discrete Fourier transform is then applied to the modulated white noise sequence. The resulting spectrum is multiplied with the 'radiation spectrum' $A(f; M, r)$, after which the discrete inverse Fourier transform is applied to transform the sequence back to the time domain to yield a sample for the ground acceleration time history. The synthetic ground motion $a(t; \boldsymbol{Z}, M, r)$ generated from the A-S model is a function of the additive excitation parameters $\boldsymbol{Z} = [Z_1, \ldots, Z_{n_t}]$ and the stochastic excitation model parameters M and r. Note that, for given M and r, the transformation from $\boldsymbol{Z}$ to $a(t; \boldsymbol{Z}, M, r)$ is linear.

Radiation Spectrum

The A-S model is characterized by the radiation spectrum $A(f; M, r)$ and the envelope function $e(t; M, r)$. The radiation spectrum $A(f; M, r)$ consists of several factors which account for the spectral effects from the source as well as propagation through the earth crust. It is given by

$$A(f; M, r) = A_0(f)\, V(f)\, \frac{1}{R} \exp(-\gamma(f)\, R) \exp(-\pi\, f\, \kappa) \tag{6.3}$$

In (6.3), A_0 is the 'equivalent point-source spectrum' based on two corner frequencies, given by

$$A_0(f) = C\, M_o\, (2\pi\, f)^2 \left[\frac{1-\varepsilon}{1+(f/f_a)^2} + \frac{\varepsilon}{1+(f/f_b)^2}\right] \tag{6.4}$$

where M_o is the seismic moment (in dyn-cm) given by (Kanamori 1977; Hanks and Kanamori 1979)

$$M_o = 10^{1.5\,(M+10.7)} \tag{6.5}$$

and $C = C_R\, C_P\, C_{FS}/(4\pi\rho\beta^3)$; $C_R = 0.55$ is the average radiation pattern coefficient (over all azimuths) for shear waves; $C_P = 1/\sqrt{2}$ is a coefficient to account for the partition of waves into two horizontal components; $C_{FS} = 2$ is the free surface amplification; ρ and β are the density and shear-

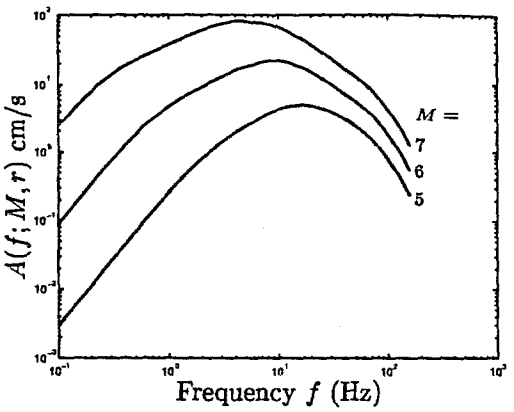

Figure 6.1: Radiation spectrum $A(f;M,r)$ for $r = 20$ km and $M = 5, 6, 7$

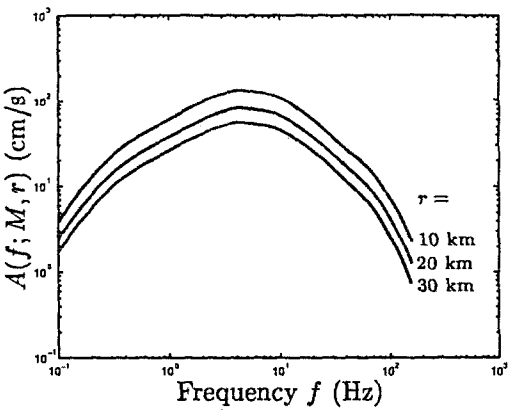

Figure 6.2: Radiation spectrum $A(f;M,r)$ for $M = 7$ and $r = 10, 20, 30$ km

wave velocity in the vicinity of the earthquake source, respectively, assumed to be 2.8 g/cm^3 and 3.5 km/s. In (6.4), f_a and f_b are the lower and upper corner frequencies (in Hz) for the equivalent point-source spectrum, respectively, given by

$$f_a = 10^{2.18-0.496\,M} \tag{6.6}$$

$$f_b = 10^{2.41-0.408\,M} \tag{6.7}$$

The parameter ε is a weighting parameter given by

$$\varepsilon = 10^{0.605-0.255\,M} \tag{6.8}$$

In (6.3), $V(f)$ describes the amplification through the crustal velocity gradient as well as soil layer. Without detailed specification of the soil properties at the site, it is assumed that $V(f) = 2$, which lies in the range of values for NEHRP class C (corresponding to a mix of rock and soil sites) for frequencies between 0.4 Hz and 4 Hz (Boore and Joyner 1997). The term $1/R$ is the geometric spreading factor, where $R = \sqrt{h^2 + r^2}$ is the radial distance from the earthquake source to the site, r is the epicentral distance (in km), and h is the nominal depth of fault (in km). It is assumed that $h = 10^{-0.05+0.15\,M}$, which ranges from about 5 km at $M = 5$ to 14 km at $M = 8$. The term $\exp(-\gamma(f)\,R)$ in (6.3) accounts for anelastic attenuation, where $\gamma(f) = \pi\, f/Q\,\beta$ and $Q = 180\, f^{0.45}$ is a regional quality factor. The term $\exp(-\pi\, f\, \kappa)$ accounts for the near surface attenuation of high frequency amplitudes, where κ is assumed to be 0.04.

Figure 6.1 illustrates the dependence of the radiation spectrum on the moment magnitude for a nominal epicentral distance of $r = 20$ km. Figure 6.2 illustrates the dependence of the radiation spectrum on the epicentral distance for a nominal moment magnitude of $M = 7$. From Figure 6.1, it

can be seen that as the moment magnitude increases, the spectral amplitude in general increases at all frequencies, with a shift of dominant frequency content towards the lower frequency regime. On the other hand, from Figure 6.2, the spectral amplitude decreases at all frequencies as the epicentral distance r increases, and there is no significant dependence of frequency content on r. It should be noted that, roughly speaking, both M and r has a multiplicative effect on the synthetic ground acceleration $a(t; \boldsymbol{Z}, M, r)$ and hence on the structural response.

Envelope function

The envelope function $e(t; M, r)$ is the major factor affecting the duration of simulated ground motions for given M and r. It is assumed to be (Boore 1983)

$$e(t; M, r) = c_3\, t^{c_1}\, \exp(-c_2\, t)\, U(t) \tag{6.9}$$

where $U(t)$ is the unit-step function,

$$c_1 = -\frac{\varepsilon_1 \log \varepsilon_2}{1 + \varepsilon_1\,(\log \varepsilon_1 - 1)} \tag{6.10}$$

$$c_2 = \frac{c_1}{\varepsilon_1\, T_w} \tag{6.11}$$

and c_3 is a normalizing factor, chosen to be

$$c_3 = \sqrt{\frac{(2c_2)^{2c_1+1}}{\Gamma(2c_1+1)}} \tag{6.12}$$

so that the envelope function has unit energy, in the sense that $\int_0^\infty e(t; M, r)^2 dt = 1$. Here, $\Gamma(\cdot)$ is the Gamma function, and $T_w = 1/f_a + 0.1R$ is related to the duration of the envelope function. The parameters ε_1 and ε_2 are defined such that the peak of the envelope function occurs at a fraction ε_1 of T_w and the amplitude at time T_w is reduced to a fraction of ε_2 of the maximum amplitude. These parameters are taken to be $\varepsilon_1 = 0.2$ and $\varepsilon_2 = 0.05$ (Boore 1983).

The envelope function $e(t; M, r)$ is shown in Figures 6.3 and Figure 6.4 for different magnitudes and epicentral distances, repectively. From Figure 6.3, it can be seen that increasing the moment magnitude generally increases the duration of the envelope function (Figure 6.3), while from Figure 6.4, the effect of r on the envelope function is not significant.

Figure 6.5 shows the typical ground motions generated at different moment magnitudes and epicentral distances.

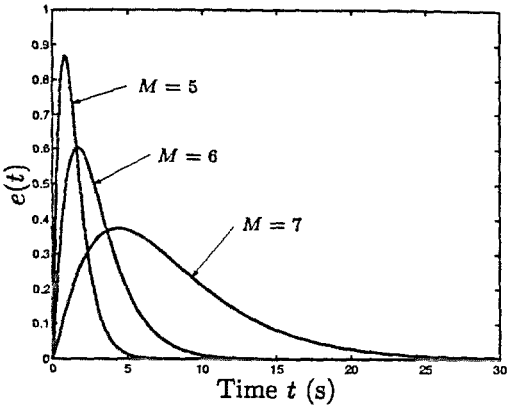

Figure 6.3: Envelope function $e(t; M, r)$ for $r = 20$ km and $M = 5, 6, 7$

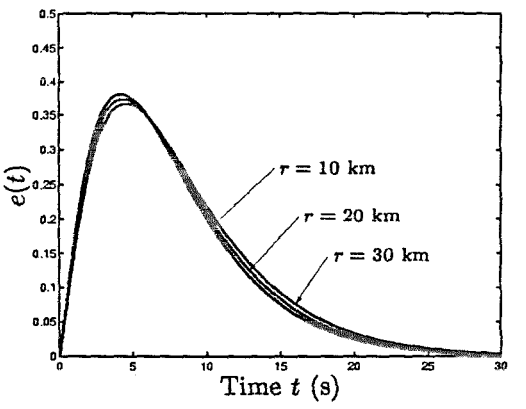

Figure 6.4: Envelope function $e(t; M, r)$ for $M = 7$ and $r = 10, 20, 30$ km

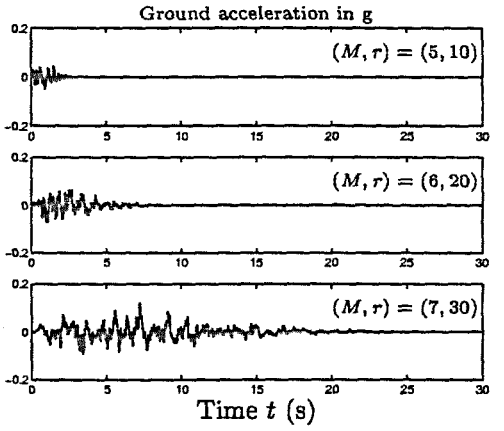

Figure 6.5: Typical ground accelerations generated according to A-S model for different (M, r)

Distribution of stochastic excitation model parameters

Using the A-S model, a synthetic ground acceleration $a(t; \boldsymbol{Z}, M, r)$ for given M and r can be generated, where $\boldsymbol{Z} = [Z_1, \ldots, Z_{n_t}]$ is a standard Normal vector and n_t is the number of time instants. When the seismic hazard aspect is to be addressed, the uncertainty in M and r has to be considered. In this study, the uncertainty in the moment magnitude is modeled by the Gutenberg-Richter relationship, truncated on the interval $[M_{min}, M_{max}]$ (Gutenberg and Richter 1958; Kramer 1996):

$$q(M) = p(M|EQ) = \frac{\beta' \exp(-\beta' M)}{\exp(-\beta' M_{min}) - \exp(-\beta' M_{max})}, \quad M_{\min} \leq M \leq M_{\max} \tag{6.13}$$

where $\beta' = b \log_e(10)$ and b is the coefficient appearing in the annual relative frequency (λ_M) description of the number of earthquakes with magnitude up to M: $\lambda_M = 10^{a - b\,M}$. It is assumed

Table 6.1: Two cases of uncertain situations considered in each example

Case	Uncertain parameters
1	$\boldsymbol{Z}$
2	$\boldsymbol{Z}$, (M,r)

that $M_{min} = 5$, $M_{max} = 8$, $b = 1$.

The earthquakes of magnitude between M_{min} and M_{max} are assumed to occur equally likely in a circular area of radius $r_{max} = 50$ km centered at the site where the structure is situated. This leads to a triangular distribution for the epicentral distance r confined to the interval $[0, r_{max}]$:

$$p(r|EQ) = \begin{cases} 2r/r_{\max}^2 & r \in [0, r_{\max}] \\ 0 & \text{otherwise} \end{cases} \tag{6.14}$$

6.3 Illustrative examples

Three examples are considered to illustrate the application of subset simulation for computing failure probabilities of structures subjected to earthquake risk. Uncertain ground motion is modeled using the A-S stochastic model described in the last section. The sampling time and duration of study are taken to be 0.02 sec. and 30 sec., respectively, for both the simulation of ground motions and dynamic structural analysis. The number of additive excitation parameters involved in the generation of ground motion for a given stochastic model is thus $n_t = 30/0.02 + 1 = 1501$, where the time instants at $t = 0$ and $t = 30$ are also represented.

In each example, two cases corresponding to different uncertain situations as shown in Table 6.1 are considered. In Case 1, only the additive excitation parameters $\boldsymbol{Z} = [Z_1, \ldots, Z_{n_t}]$ for generating the ground motion $a(t; \boldsymbol{Z}, M, r)$ are assumed to be uncertain; the moment magnitude M and epicentral distance r, which are the stochastic model parameters in the problem, are fixed at their nominal values: $M = 7$ and $r = 20$ km. This case corresponds to the classical first excursion problem with a given stochastic model defined by fixed M and r. In Case 2, in addition to the additive excitations, the moment magnitude and epicentral distance are also considered to be uncertain, with probability distributions given by (6.13) and (6.14), respectively. This corresponds to a seismic risk problem where the uncertainty in M and r is addressed.

In the application of subset simulation, the conditional failure regions are chosen such that a conditional failure probability of $p_0 = 0.1$ is attained at all simulation levels. This is done by choosing an approximate threshold adaptively during the simulation, as described in Chapter 5. At each simulation level, $N = 500$ samples are simulated. Failure probabilities ranging from 10^{-3} to 1 will be estimated, or in other words, the response level corresponding to failure probabilities as small

Table 6.2: Choice of proposal PDF for different uncertain parameters

Uncertain parameter	Proposal PDF
Z	1-D symmetric (Metropolis) uniform with maximum step length equal to 1
(M, r)	2-D Kernel sampling density estimated using samples from the last simulation level

as 10^{-3} will be estimated. The total number of samples required to produce the failure probability versus threshold level curve is thus $N_T = 500 + 450 + 450 = 1400$, because 50 failure events from a level are used to start the next level and so only a further 450 samples are required for that level.

The choice of the proposal PDFs used for different uncertain parameters is shown in Table 6.2. For the additive excitation $Z = [Z_1, \ldots, Z_{n_t}]$, each Z_i is grouped as a single component, for which the proposal PDF is chosen as a one-dimensional (chain-adaptive) symmetric uniform distribution with maximum step length $l_i = 1$, that is, $p^*(\xi_i|\theta_i) = 1/2$ if $|\xi_i - \theta_i| \leq 1$ and zero otherwise. For the stochastic model parameters, M and r, a level-adaptive proposal PDF is used, which is constructed as a kernel sampling density using the Markov chain samples from the last simulation level. This choice is used for M and r since it is expected that they control failure. Also, the zero-acceptance phenomenon due to high dimensions is unlikely to happen because the kernel sampling density is constructed as a two-dimensional joint PDF.

6.3.1 Example 1: Linear SDOF oscillator

Consider a single-degree-of-freedom (SDOF) oscillator with natural frequency $f_1 = 1$ Hz and damping ratio $\zeta_1 = 2\%$ subjected to the ground acceleration $a(t; Z, M, r)$:

$$\ddot{Y}(t) + 2\zeta_1(2\pi f_1)\dot{Y}(t) + (2\pi f_1)^2 Y(t) = -a(t; Z, M, r) \tag{6.15}$$

Failure is defined as the exceedence of the displacement response magnitude over the threshold level b within the duration of study $T_d = 30$ sec., that is, the failure event is:

$$F = \{\max_{k=1,\ldots,n_t} |Y(t_k)| > b\} \tag{6.16}$$

where $t_k = (k-1)\Delta t$, $k = 1, \ldots, n_t$ ($n_t = 1501$) are time instants where the response is computed.

Failure probability estimation

Figures 6.6 and 6.7 show the estimates of failure probability for different threshold levels b for Cases 1 and 2, respectively. Note that a total of $N_T = 1400$ samples, i.e., dynamic structural

analyses, are performed to compute the results (solid line) in each figure. The results computed by standard Monte Carlo simulation (MCS) with 10,000 samples (so that the c.o.v. at a failure probability of 10^{-3} is about 30%) is also shown in the figures for comparison. These figures give an idea of how the results computed using subset simulation in a single run approximate the 'exact' failure probabilities (of MCS). To assess quantitatively the statistical properties of the failure probability estimates produced by subset simulation, 50 independent runs of subset simulation (with different seeds used in the random number generator) have been carried out. From the 50 runs, the sample mean and sample c.o.v. of the failure probability estimates are computed. The results for the sample mean for Cases 1 and 2 are shown in Figures 6.8 and 6.9, respectively. These figures show that the sample mean of the failure probability estimates are generally close to the results computed by standard Monte Carlo simulation, except for small failure probabilities near 10^{-3} where the results by MCS are inaccurate due to the number of samples used. It can be concluded from the figures that the failure probability estimates by subset simulation are practically unbiased.

The sample c.o.v. for the failure probability estimates are shown in Figures 6.10 and 6.11. The results are plotted versus different failure probability levels. The average results for the estimates of c.o.v. based on (5.29) and (5.27) are also shown in the figures. Recall that (5.29) assumes the conditional failure probabilities at different simulation levels are independent, while (5.27) assumes they are fully correlated. From Figures 6.10 and 6.11, it can be seen that the trend in the actual c.o.v estimated from the 50 runs is reasonably captured by the estimates based on (5.29) and (5.27), showing that these formulae can be used to assess the c.o.v. of the failure probability estimate in a single run.

The computational efficiency of subset simulation is next compared with that of standard Monte Carlo simulation in terms of the c.o.v. of failure probability estimates computed based on the same number of samples. Note that the number of samples required by subset simulation at the probability levels $P_F = 10^{-1}, 10^{-2}, 10^{-3}$ are $N_T = 500, 950, 1400$, respectively. Using $\delta = \sqrt{(1-P_F)/P_F N_T}$, the c.o.v. of the Monte Carlo estimator using the same number of samples at probability levels $10^{-1}, 10^{-2}$ and 10^{-3} are computed to be 0.13, 0.32 and 0.84, respectively, which are also shown as squares in Figures 6.10 and 6.11. These figures show that as the failure probability decreases, the c.o.v. of the Monte Carlo estimator increases rapidly, while the c.o.v. of subset simulation increases at a much slower rate. This shows that subset simulation can lead to a substantial improvement in efficiency over standard Monte Carlo simulation, especially for estimating small failure probabilities.

Failure analysis using conditional samples

The Markov chain samples at the different failure levels simulated in a single run of subset simulation are next examined for the purpose of failure analysis. Figure 6.12 shows the typical samples of ground acceleration $a(t; \boldsymbol{Z}, M, r)$ that correspond to different levels of failure with failure

probabilities $10^{-1}, 10^{-2}$ and 10^{-3} for Case 1. Note that only the additive excitation parameters $\boldsymbol{Z}$ are uncertain in this case. The response corresponding to these ground excitations are shown in Figure 6.14. Since samples of acceleration time histories are generated for given moment magnitude $M = 7$ and epicentral distance $r = 20$ km, there is not much difference in their duration as well as mean square values. In terms of peak acceleration, they do not differ significantly, either. The major difference among these samples of ground acceleration that leads to different levels of failure lies in the frequency content. Figure 6.16 shows the average spectrum (power spectral density) of the additive excitation parameters $\boldsymbol{Z}$ corresponding to the samples of acceleration time histories at different levels of failure. Here, Level 0 refers to the initial phase of subset simulation where samples are generated from their parameter PDF, i.e., standard Monte Carlo simulation. The spectrum of the additive excitation $\boldsymbol{Z}$ that generate the ground acceleration $a(t; \boldsymbol{Z}, M, r)$ is studied rather than $a(t; \boldsymbol{Z}, M, r)$ itself, because the spectrum of the sequence $\boldsymbol{Z}$ at Level 0 (MCS) is theoretically flat (constant with frequency), which provides an easy reference for comparison. Note that the spectrum of the 500 samples of the additive excitation $\boldsymbol{Z}$ simulated according to its parameter PDF during the first phase of subset simulation (i.e., MCS) are averaged to produce the average spectrum shown in the top plot of Figure 6.16 for Level 0 (MCS). Similarly, the spectrum of the 500 samples of additive excitation corresponding to the 500 Markov chain samples generated at simulation level 1 (conditional on the first failure level) are averaged to produce the average spectrum shown in the middle plot of Figure 6.16 for Level 1.

The spectrum at Level 0 (top plot of Figure 6.16) is almost flat, because there is no conditioning on the samples at this level and therefore the spectrum theoretically corresponds to that of white noise, which is flat up to the Nyquist frequency, being $1/2\Delta t = 25$ Hz. As the simulation level increases, the spectrum develops a peak near 1 Hz, which is the natural frequency of the structure. This illustrates an important statistical feature of the additive excitations that lead to failure in the classical first excursion problem (with fixed structure and stochastic excitation model): *the additive excitation tends to 'tune' itself to the natural frequency of the structure to cause first excursion failure.* In other words, when the stochastic excitation model parameters are fixed, the probable cause of failure for the SDOF structure is due to resonance effects, especially when the threshold level is high. This phenomenon can be explained as follows. The probability of a particular excitation decreases exponentially with the square of its Euclidean norm (energy). When the stochastic excitation model and hence the excitation intensity is fixed, it is not probable that the excitation will have a significantly large energy (e.g., in terms of root mean square value) when failure occurs, since this will mean that the vector of additive excitation parameters $\boldsymbol{Z}$ will have an Euclidean norm in the n_t-dimensional standard Normal space significantly larger than other 'typical' configurations. Rather, a more probable configuration for $\boldsymbol{Z}$ to cause failure is to have its components 'tuned' so that they have a frequency content near the natural frequency of the structure to create a resonance

effect, while the Euclidean norm of the whole vector $\boldsymbol{Z}$ still remains more or less the same.

The situation is different when the stochastic excitation model parameters, i.e., M and r, are uncertain, in addition to the additive excitation parameters $\boldsymbol{Z}$. Figures 6.13 to 6.17 show the conditional samples and the average spectra at different simulation levels for Case 2, where $\boldsymbol{Z}$, M and r are considered uncertain in the problem. Figure 6.13 shows that in this case the excitation intensity and duration of the ground acceleration is significantly different at different simulation levels. The excitation intensity generally increases as the simulation level increases. From Figure 6.17, it can be seen that the spectral peak at 1 Hz for Levels 2 and 3 is not as significant as observed in Case 1 (Figure 6.16). This indicates that the frequency content of the additive excitation $\boldsymbol{Z}$ when failure occurs is not significantly different from its original spectrum (flat), although this does not imply that the frequency content of the ground acceleration will be the same irrespective of whether failure occurs, since the radiation spectrum $A(f; M, r)$ could be different because of the change in the distribution of M and r when failure occurs.

When the moment magnitude M and the epicentral distance r are uncertain, they are the parameters that control failure. Figure 6.18 shows the histograms of M and r at different simulation levels. The histograms are normalized so that they show the fraction of samples (rather than the number of samples) out of the total 500 samples falling in the different bins. The parameter PDF for M and r, given by (6.13) and (6.14), respectively, are shown (with suitable scaling) as a dashed line in each figure for comparison. Note that the samples of M and r at Level 0 are simulated according to their parameter PDF, and so their histograms should compare well with the parameter PDF, as shown in the top plots of Figure 6.18. For Levels 1 and 2, it is noted that the distributions of M and r are quite different from the corresponding parameter PDF. As the level increases, the distribution of M shifts towards the large magnitude regime, while the distribution of r shifts towards the small distance regime. Figure 6.19 shows the scattering of samples of (M, r) at different levels. Since the Markov chain samples are not all distinct, some of the locations shown in the figure contain repeated samples. To show the population of the samples consistently, the dots are shown with area proportional to the number of points situated at the particular location. Figure 6.19 clearly indicates that as the simulation level increases, that is, when failure becomes more severe, the samples of (M, r) shift towards the 'large magnitude, small distance' regime, which agrees with intuition.

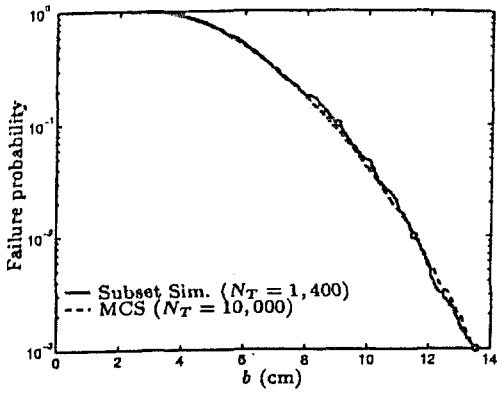

Figure 6.6: Failure probability estimates for Example 1, Case 1

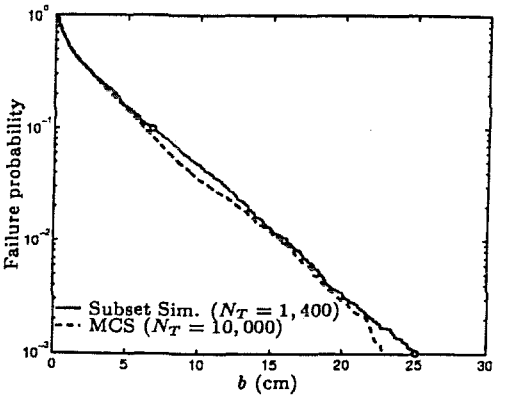

Figure 6.7: Failure probability estimates for Example 1, Case 2

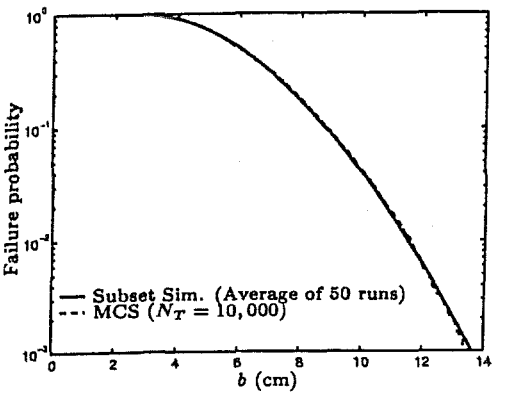

Figure 6.8: Sample mean of failure probability estimates over 50 runs for Example 1, Case 1

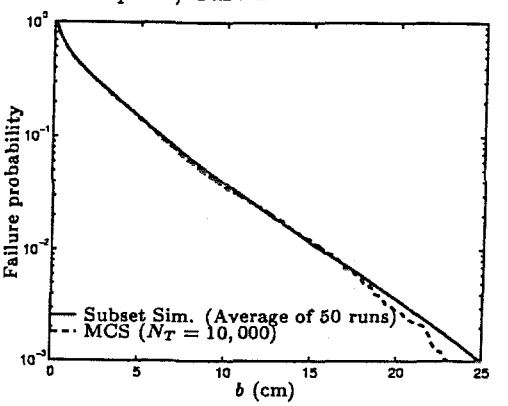

Figure 6.9: Sample mean of failure probability estimates over 50 runs for Example 1, Case 2

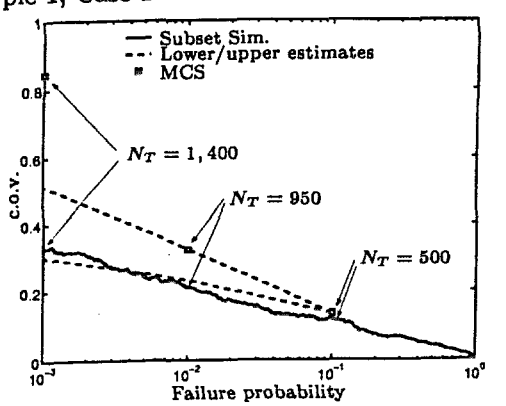

Figure 6.10: Sample c.o.v. of failure probability estimates over 50 runs for Example 1, Case 1

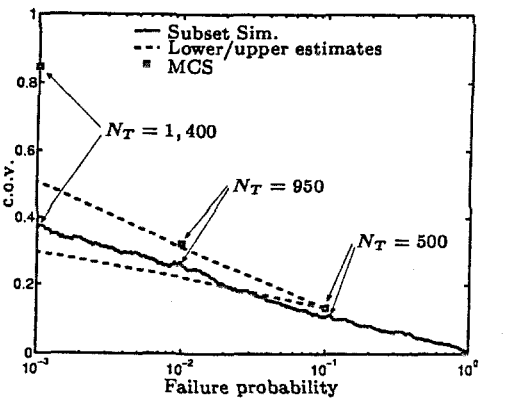

Figure 6.11: Sample c.o.v. of failure probability estimates over 50 runs for Example 1, Case 2

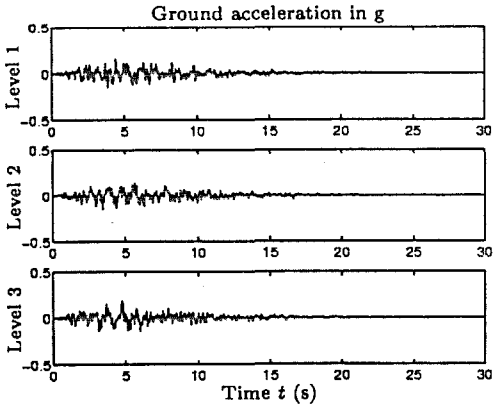

Figure 6.12: Ground motions for Example 1, Case 1, at conditional levels 1, 2, 3

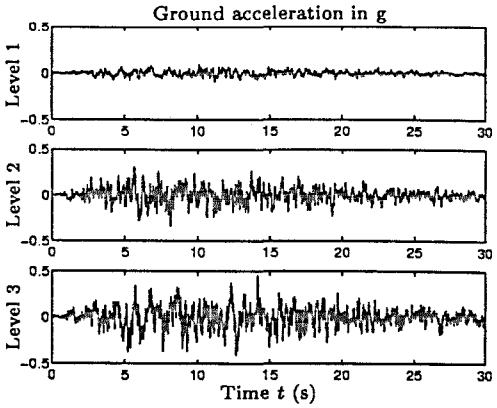

Figure 6.13: Ground motions for Example 1, Case 2, at conditional levels 1, 2, 3

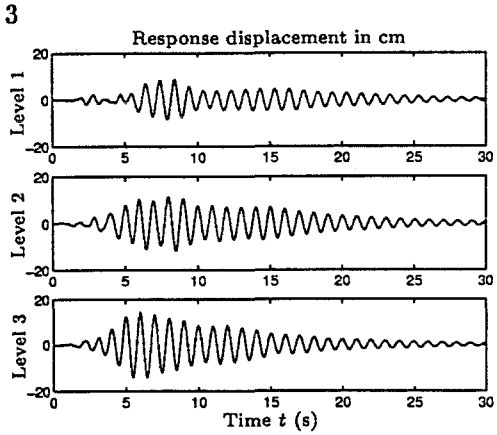

Figure 6.14: Response for Example 1, Case 1, at conditional levels 1, 2, 3

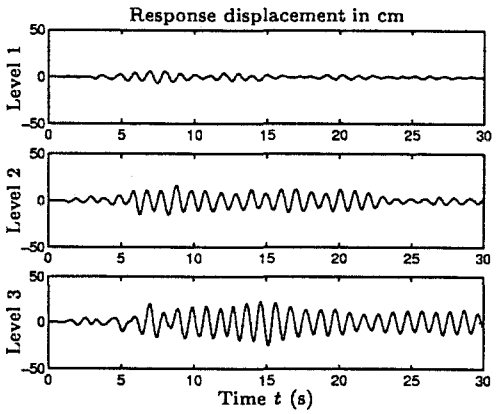

Figure 6.15: Response for Example 1, Case 2, at conditional levels 1, 2, 3

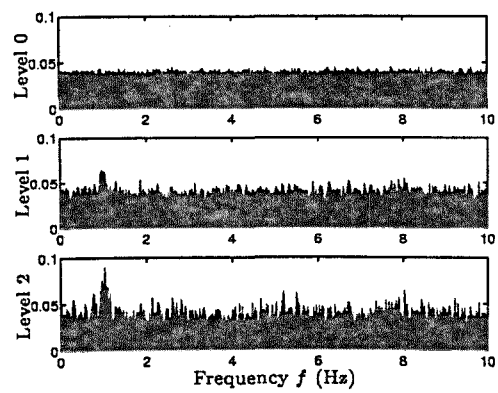

Figure 6.16: Spectra of white noise sequence for Example 1, Case 1, at conditional levels 0, 1, 2

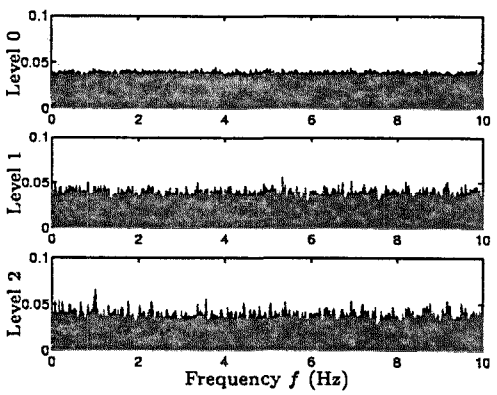

Figure 6.17: Spectra of white noise sequence for Example 1, Case 2, at conditional levels 0, 1, 2

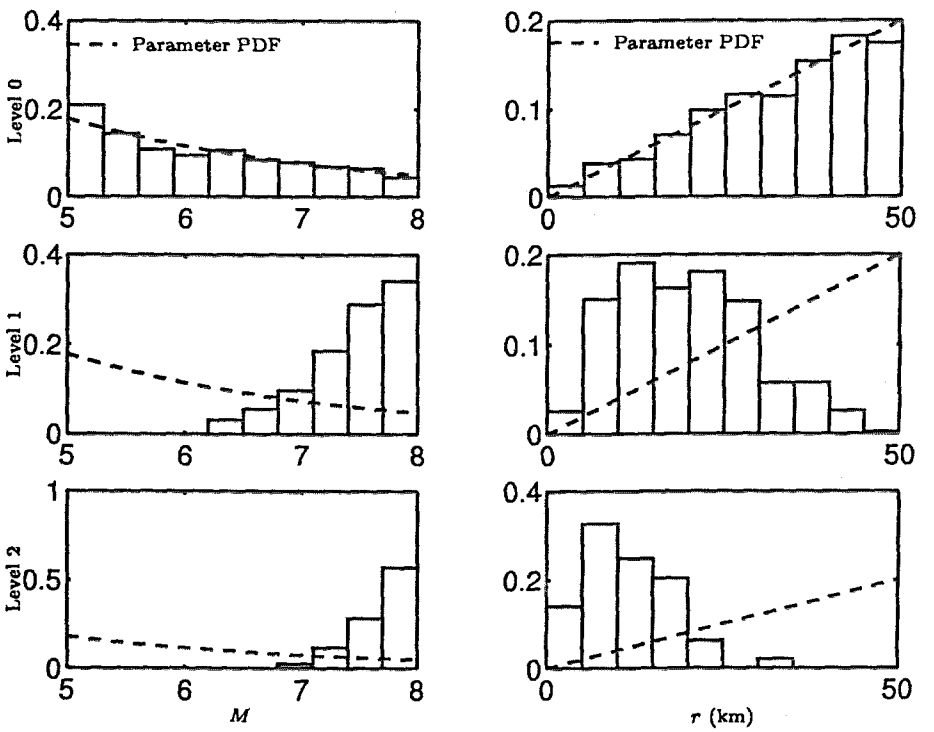

Figure 6.18: Normalized histogram of M and r for Example 1, Case 2, at conditional levels 0, 1, 2

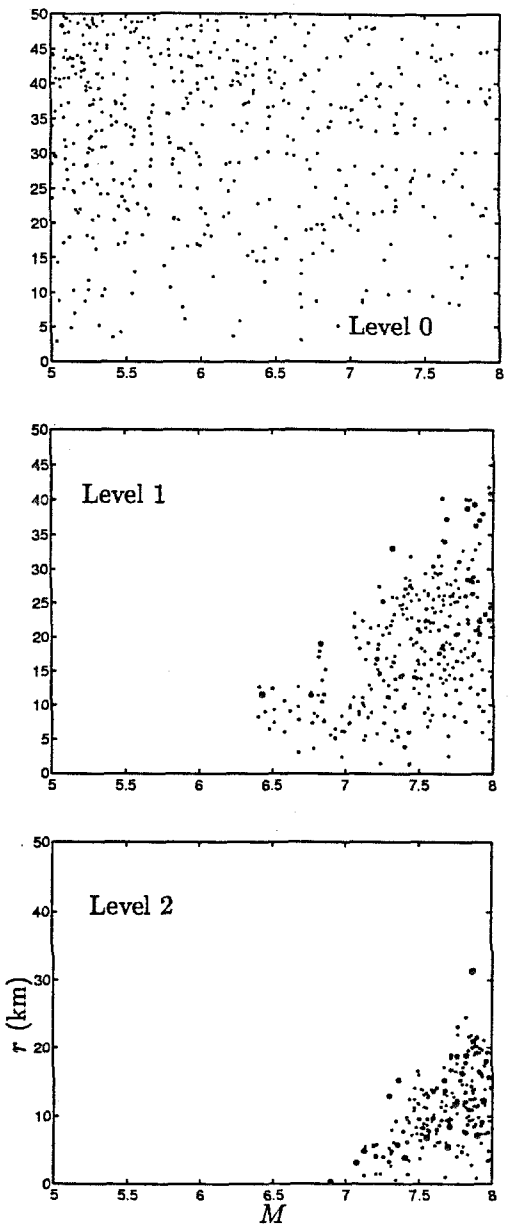

Figure 6.19: Conditional samples of M and r for Example 1, Case 2, at conditional levels 0, 1, 2

6.3.2 Example 2: Linear moment-resisting steel frame

The structure considered in this example is the moment-resisting steel frame considered in Example 2 of Chapter 4, but the stochastic ground motion model is the A-S model described in Section 6.2. As before, failure is defined as the exceedence of interstory drift ratio at any one of the columns within the duration of study.

Failure probability estimation

Figures 6.20 and 6.21 show the estimates of failure probability for different threshold levels b for Cases 1 and 2, respectively (see Table 6.1). The sample mean of failure probability estimates over 50 independent simulation runs for Cases 1 and 2 are shown in Figures 6.22 and 6.23, respectively. These figures show that the failure probability estimates by subset simulation are practically unbiased. The sample c.o.v. for the failure probability estimates computed using 50 independent simulation runs are shown in Figures 6.24 and 6.25. In general, it is observed that the performance of subset simulation in the current example for a multi-degree-of freedom linear structure is similar to Example 1 for a single-degree-of-freedom linear structure, showing that subset simulation is robust to the number of degrees of freedom of the structural model assumed in the analysis.

Failure analysis using conditional samples

Figure 6.26 shows the typical samples of ground acceleration that correspond to different levels of failure with failure probabilities $10^{-1}, 10^{-2}$ and 10^{-3} for Case 1, where only the additive excitations $\boldsymbol{Z}$ are uncertain. The interstory drift ratios of the columns at different floors corresponding to these ground excitations are shown in Figure 6.28. Figure 6.30 shows the average spectrum of the additive excitation $\boldsymbol{Z}$ at different levels of failure in Case 1. Similar to Example 1, as the simulation level increases, the spectrum develops a peak near the natural frequency of the structure (0.56 Hz).

The system behavior for Case 2 of Example 2 is essentially similar to that of Example 1, as shown in Figures 6.27, 6.29, 6.31, 6.32 and 6.33.

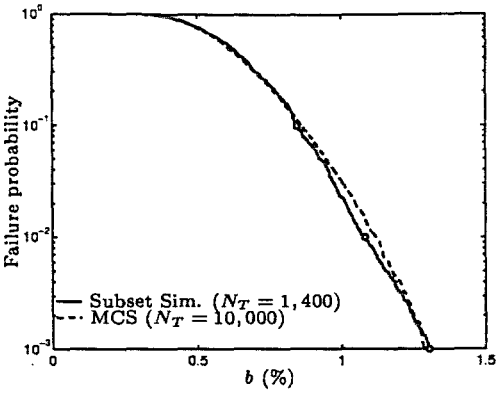

Figure 6.20: Failure probability estimates for Example 2, Case 1

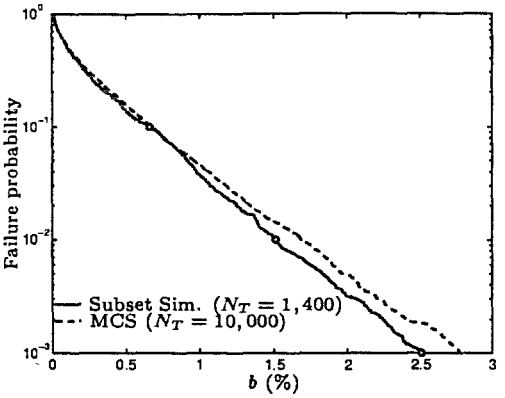

Figure 6.21: Failure probability estimates for Example 2, Case 2

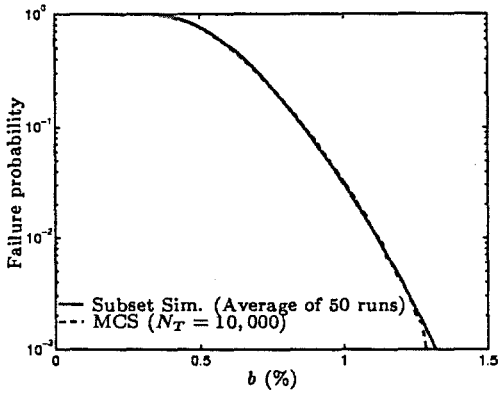

Figure 6.22: Sample mean of failure probability estimates over 50 runs for Example 2, Case 1

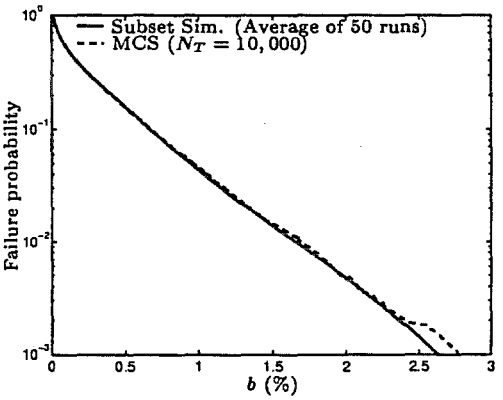

Figure 6.23: Sample mean of failure probability estimates over 50 runs for Example 2, Case 2

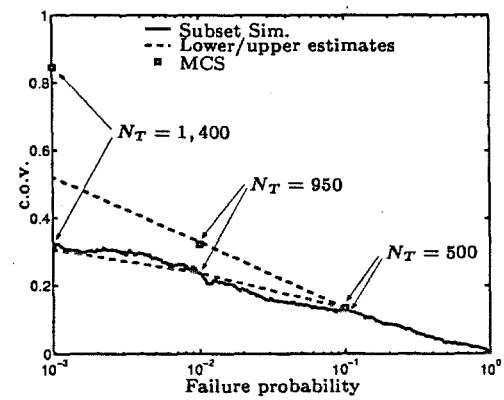

Figure 6.24: Sample c.o.v. of failure probability estimates over 50 runs for Example 2, Case 1

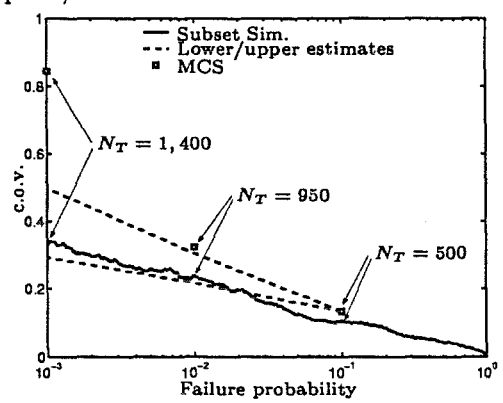

Figure 6.25: Sample c.o.v. of failure probability estimates over 50 runs for Example 2, Case 2

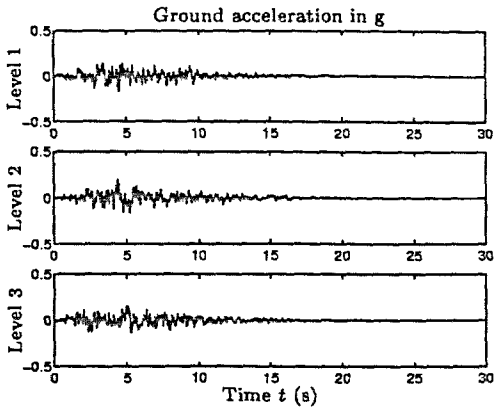

Figure 6.26: Ground motions for Example 2, Case 1, at conditional levels 1, 2, 3

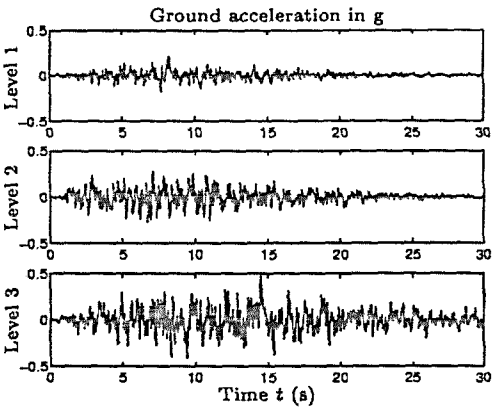

Figure 6.27: Ground motions for Example 2, Case 2, at conditional levels 1, 2, 3

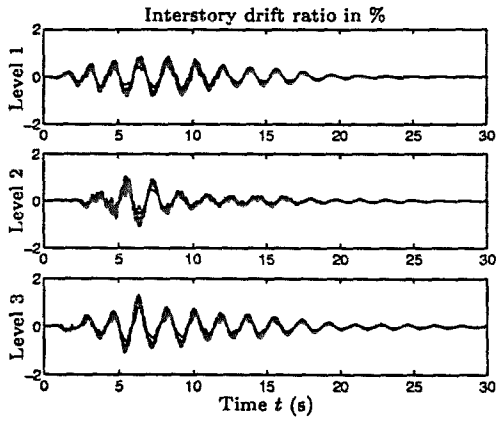

Figure 6.28: Response for Example 2, Case 1, at conditional levels 1, 2, 3

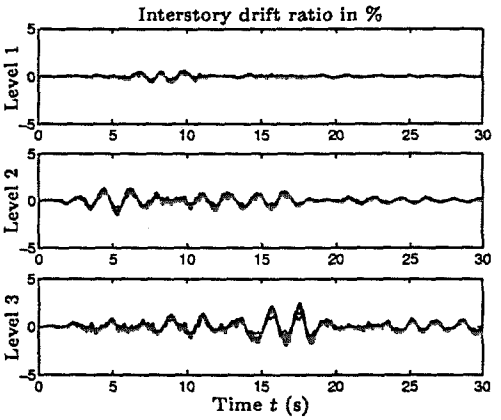

Figure 6.29: Response for Example 2, Case 2, at conditional levels 1, 2, 3

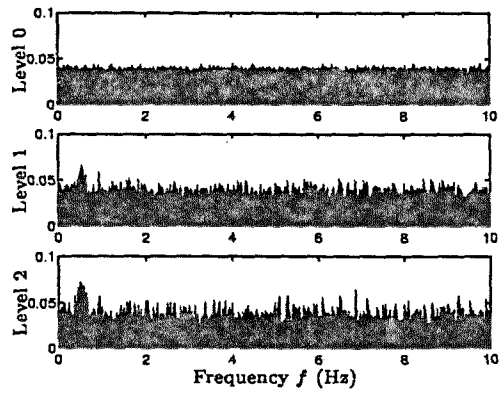

Figure 6.30: Spectra of white noise sequence for Example 2, Case 1, at conditional levels 0, 1, 2

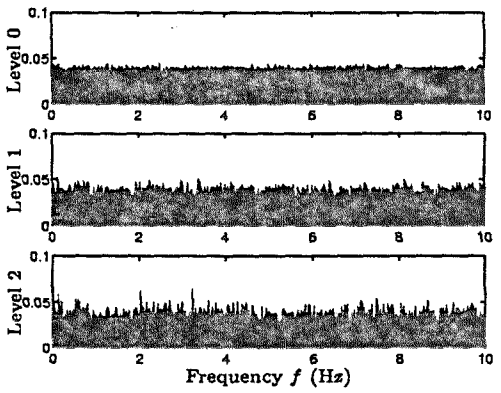

Figure 6.31: Spectra of white noise sequence for Example 2, Case 2, at conditional levels 0, 1, 2

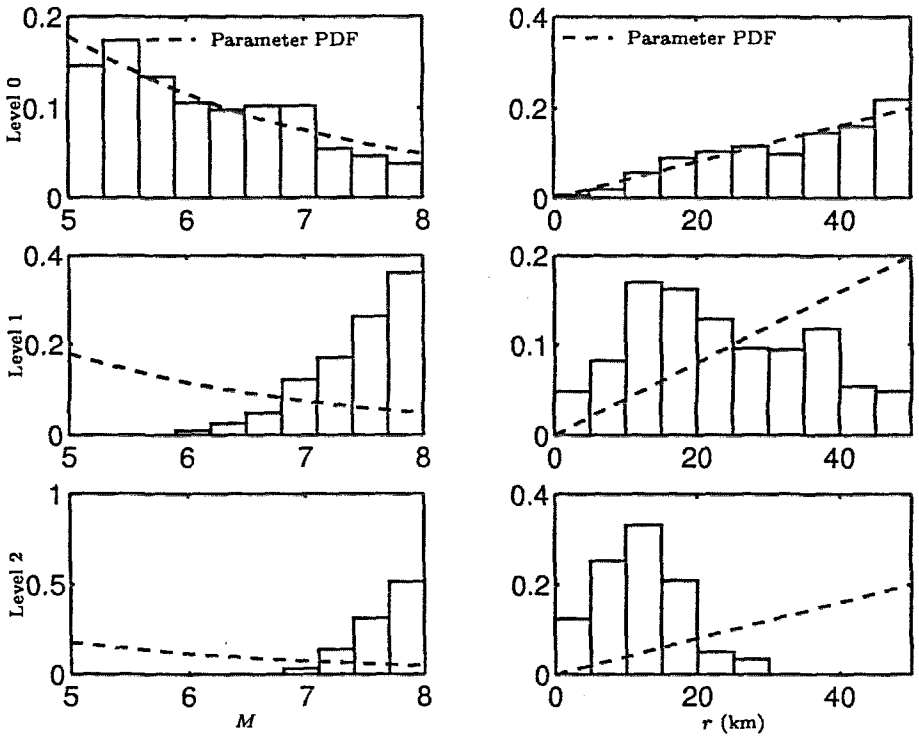

Figure 6.32: Normalized histogram of M and r for Example 2, Case 2, at conditional levels 0, 1, 2

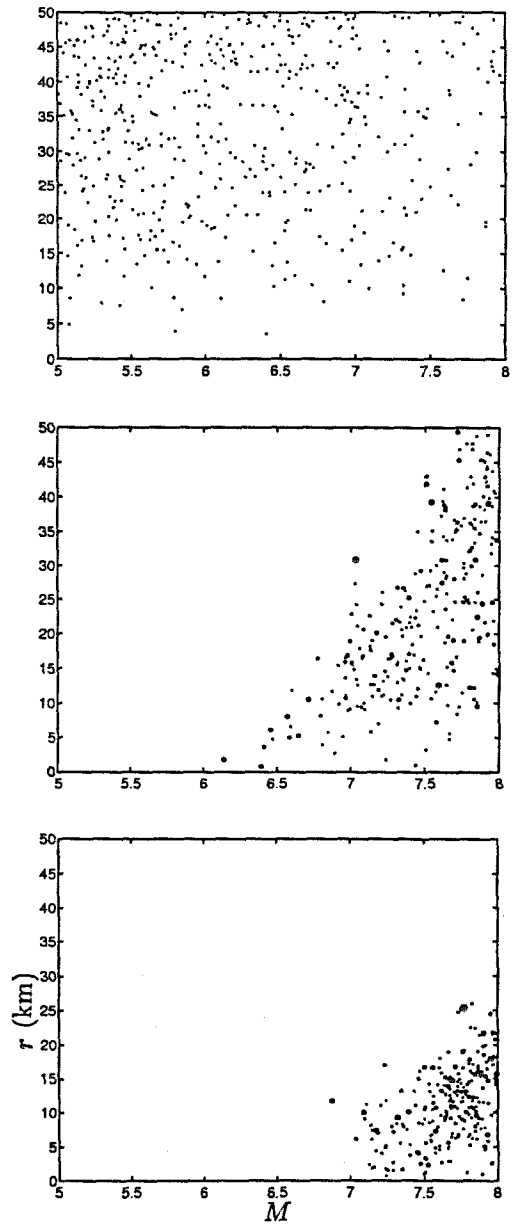

Figure 6.33: Conditional samples of M and r for Example 2, Case 2, at conditional levels 0, 1, 2

6.3.3 Example 3: Nonlinear concrete portal frame

The structural model in this example is a nonlinear concrete portal frame. It corresponds to Example 3 of the illustrative examples for the nonlinear finite element software OpenSees developed under PEER (Pacific Earthquake Engineering Research) Center. The finite element model of the structure and its detailed description can be obtained from the website:

`http://opensees.berkeley.edu/OpenSees/examples.html`

The general properties of the structural model are briefly described here. The frame is 3.66 m high by 9.15 wide. An elastic beam element is used to model the beam connecting the two columns. The reinforced concrete section of the columns are modeled using steel and concrete fibers. The section of each column is 61 cm (24 in) by 38 cm (15 in) wide, with its strong axis perpendicular to the frame, that is, the columns deform in their strong direction during in-plane motion. The section is divided into confined and unconfined concrete regions, for which the fibers are discretized separately. The unconfined concrete region corresponds to a concrete cover of 3.8 cm (1.5 in) thick, with a compressive strength of 34 MPa (5 ksi) at a strain of 0.2% and zero crushing strength at a strain of 0.6%. It is discretized with 10 fibers along the depth of the section. The confined concrete region corresponds to the core of the section, with a compressive strength of 41 MPa (6 ksi) at a strain of 0.4% and a crushing strength of 34 MPa (5 ksi) at a strain of 1.4%. It is discretized with 10 fibers along the depth of the section. The Kent-Scott-Park model (Kent and Park 1971) is used for modeling the concrete material, with degraded linear unloading/reloading according to the work of Karson and Jirsa (1969). Reinforcing steel bars are placed around the interface boundary of the confined and unconfined concrete regions. The reinforcing steel is modeled as a bilinear material with kinematic hardening. The Young's modulus and hardening ratio of steel are assumed to be 207 GPa (30,000 ksi) and 1%, respectively.

The gravity load consists of two point loads of 801 kN (180 kips) at each of the columns, which correspond to approximately 10% of the axial load capacity of the columns. Figure 6.35 shows a pushover curve of the structure. The small-amplitude natural frequency of the structure is 2.6 Hz. Viscous damping is assumed so that the damping ratio for the first mode of vibration at small amplitudes is approximately 0.5%. Additional hysteretic damping develops in the structure during vibration at higher amplitudes.

Failure probability estimation

Figures 6.36 and 6.37 show the estimates of failure probability for different threshold levels b for Cases 1 and 2, respectively (see Table 6.1). The sample mean of failure probability estimates over 50 independent simulation runs for Cases 1 and 2 are shown in Figures 6.38 and 6.39, respectively. These

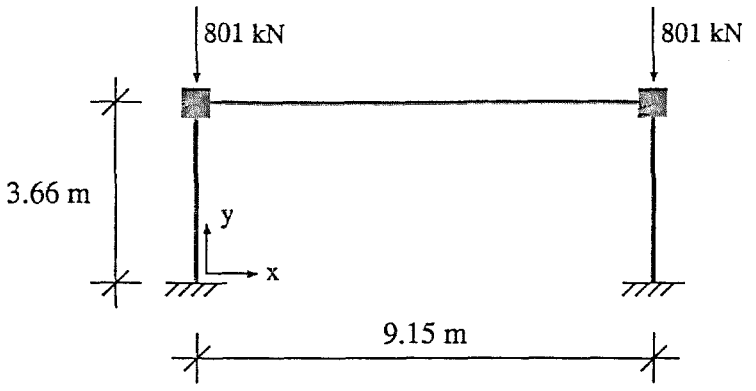

Figure 6.34: Concrete portal frame in Example 3

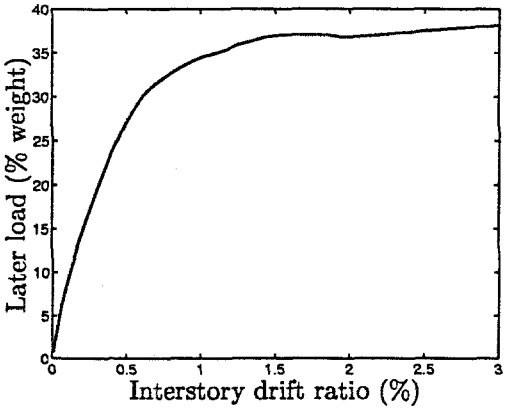

Figure 6.35: Pushover curve for structure in Example 3

figures show that the failure probability estimates by subset simulation are practically unbiased. The sample c.o.v. for the failure probability estimates computed using 50 independent simulation runs are shown in Figures 6.40 and 6.41. In general, it is observed that the performance of subset simulation in the current example for a nonlinear structure is similar to Example 1 for a linear structure, showing that subset simulation is robust to the type of structural model assumed in the analysis.

The trend of the failure probability versus threshold level b shown in Figure 6.39 for Example 3 is qualitatively different from that in Figure 6.9 for Example 1. In particular, in Example 3 (Figure 6.39), the decay rate of failure probability with increasing threshold level b increases at around $b = 0.5\%$. This is due to the hysteretic damping effect that starts to become significant at an interstory drift ratio of 0.5% where significant yielding occurs (see Figure 6.35). The stiffness-softening of the structure in Example 3 starts to become dominant and outweighs the hysteretic damping effect at a drift ratio of around 1%, at which the decay rate decreases. It should be noted that P-Δ effect

has not been accounted for in this example, which means that the interstory drift ratios could have been larger, especially at large drift levels, in addition to the possibility of collapse.

Failure analysis using conditional samples

Figure 6.42 shows the typical samples of ground acceleration that correspond to different levels of failure with failure probabilities $10^{-1}, 10^{-2}$ and 10^{-3} for Case 1, where only the additive excitations $\boldsymbol{Z}$ are uncertain. The interstory drift ratio of the left column (which is essentially the same as that of the right column) corresponding to these ground excitations are shown in Figure 6.44. Figure 6.46 shows the average spectrum of the additive excitation $\boldsymbol{Z}$ at different levels of failure. As the simulation level increases, the spectrum develops a peak near 2 Hz, which is near the natural frequency of the structure (2.6 Hz). These observation are similar to those in Example 1. Nevertheless, the spectral peak in this case is less distinct and does not occur at the small-amplitude natural frequency of the structure. This is possibly due to the softening behavior of the structure at large amplitudes of vibration, which results in an apparently smaller 'resonance frequency' adapted by the Markov chain samples of the additive excitation.

The system behavior for Case 2 of Example 3 is essentially similar to that of Example 1, as shown in Figures 6.43, 6.45, 6.47, 6.48 and 6.49.

6.4 Summary of this chapter

The applicability and efficiency of subset simulation to computing the failure probability of structures with uncertainty in the additive excitation and possibly in the stochastic excitation parameters have been demonstrated with applications to the probabilistic assessment of seismic performance. Failure analysis has been carried out using the samples generated during subset simulation to gain insight into the system behavior when failure occurs. The analysis shows that when only the additive excitation parameters are uncertain, the rare failure scenarios correspond to resonance of the excitation with the structure. On the other hand, when the stochastic excitation parameters are also uncertain, they tend to control failure, due to their multiplicative effects on the response. The conditional distribution of the stochastic excitation model parameters given that failure occurs is significantly different from the parameters PDF originally assumed.

It should be noted that the observations from the system analysis, such as the distribution of the moment magnitudes and epicentral distance when failure occurs, are based on the assumed probability models for the excitation. The results should be interpreted bearing in mind the inherent limitations of the probability models. For example, the distribution of (M, r) in the large magnitude and small distance regime should be viewed bearing in mind that the A-S model is a point-source model which does not directly account for the geometry of the fault and the charac-

teristics of near-source ground motions. In view of this, the failure analysis results either provide channels for calibrating the stochastic excitation models, or otherwise should be interpreted carefully. Nevertheless, on the premise that the quality of stochastic ground motion models will improve, subset simulation provides an efficient tool for estimation of failure probabilities and failure analysis.

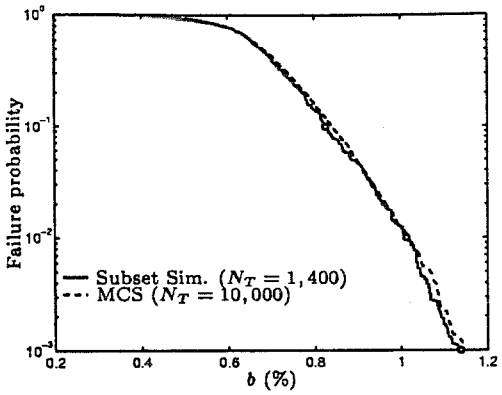

Figure 6.36: Failure probability estimates for Example 3, Case 1

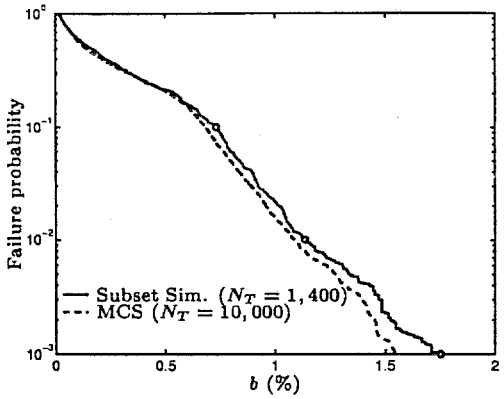

Figure 6.37: Failure probability estimates for Example 3, Case 2

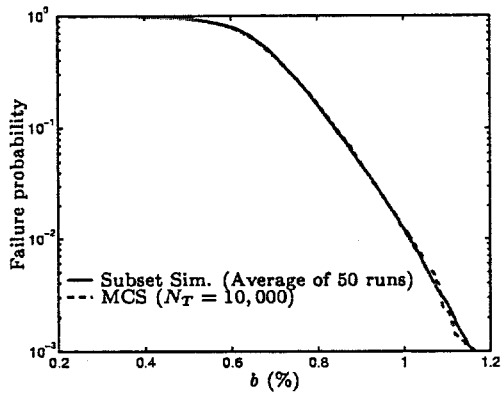

Figure 6.38: Sample mean of failure probability estimates over 50 runs for Example 3, Case 1

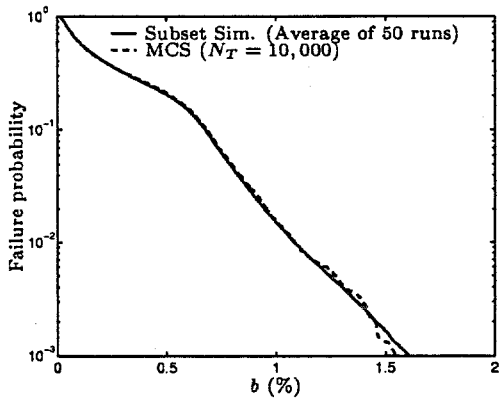

Figure 6.39: Sample mean of failure probability estimates over 50 runs for Example 3, Case 2

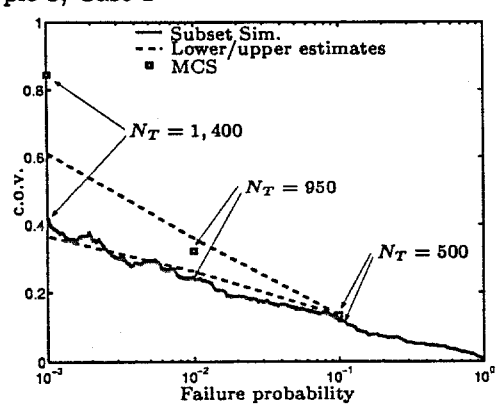

Figure 6.40: Sample c.o.v. of failure probability estimates over 50 runs for Example 3, Case 1

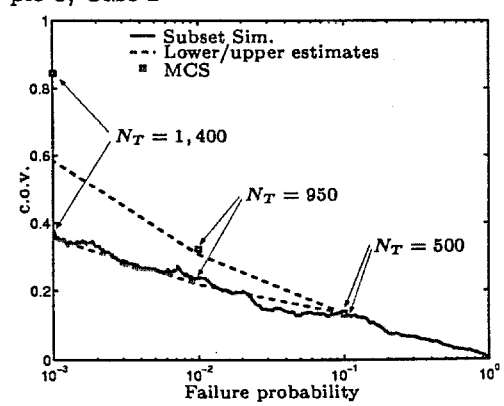

Figure 6.41: Sample c.o.v. of failure probability estimates over 50 runs for Example 3, Case 2

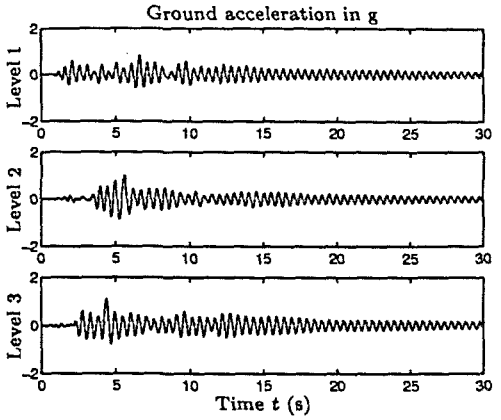

Figure 6.42: Ground motions for Example 3, Case 1, at conditional levels 1, 2, 3

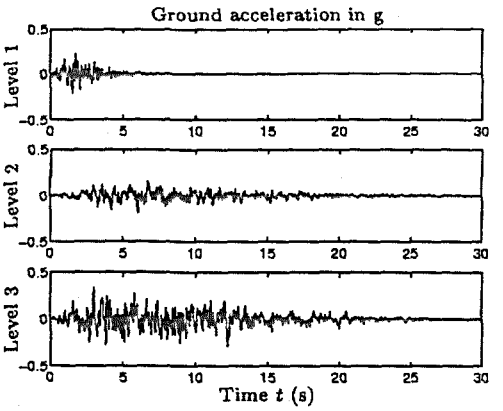

Figure 6.43: Ground motions for Example 3, Case 2, at conditional levels 1, 2, 3

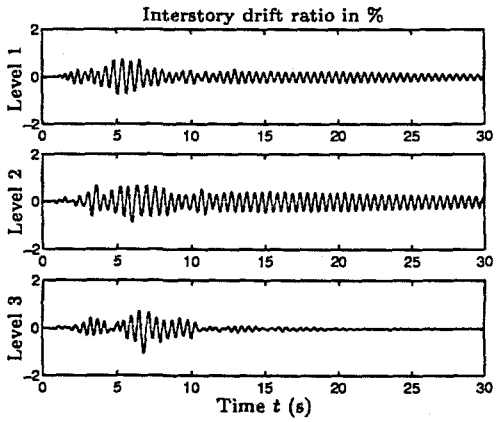

Figure 6.44: Response for Example 3, Case 1, at conditional levels 1, 2, 3

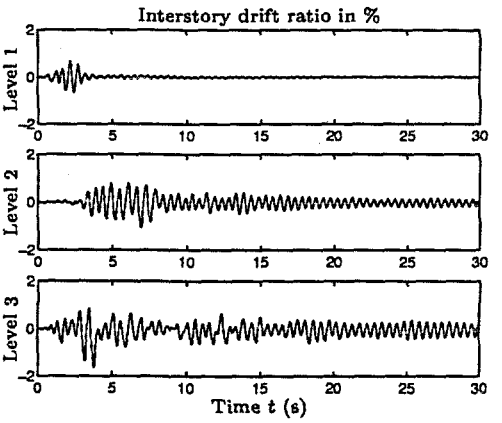

Figure 6.45: Response for Example 3, Case 2, at conditional levels 1, 2, 3

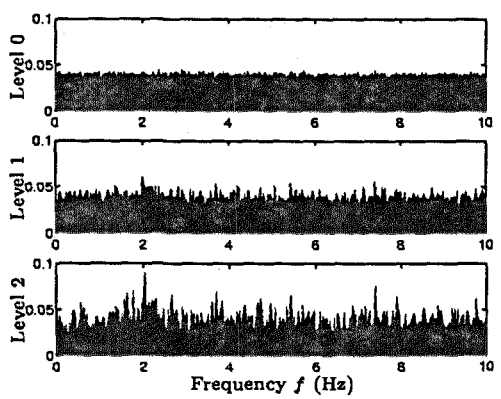

Figure 6.46: Spectra of white noise sequence for Example 3, Case 1, at conditional levels 0, 1, 2

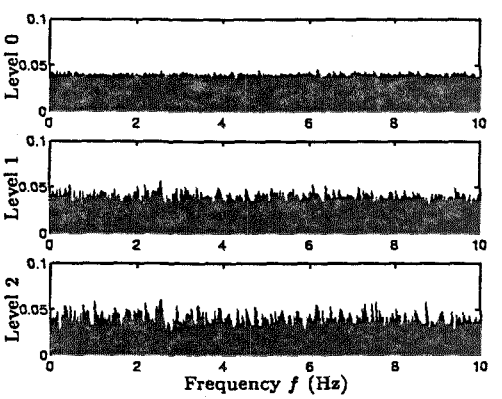

Figure 6.47: Spectra of white noise sequence for Example 3, Case 2, at conditional levels 0, 1, 2

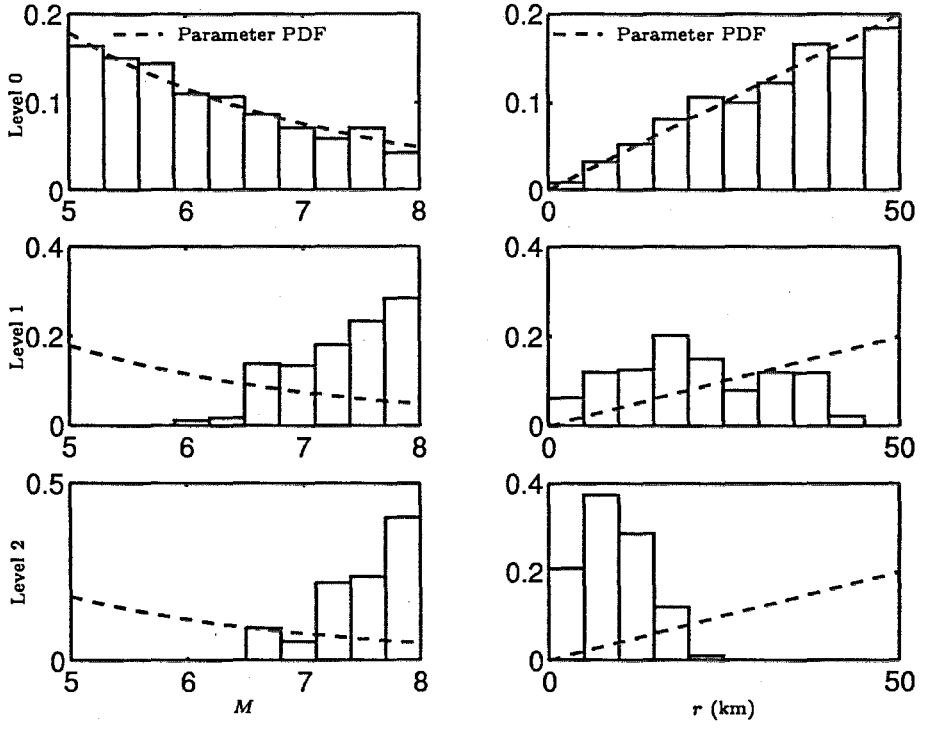

Figure 6.48: Normalized histogram of M and r for Example 3, Case 2, at conditional levels 0, 1, 2

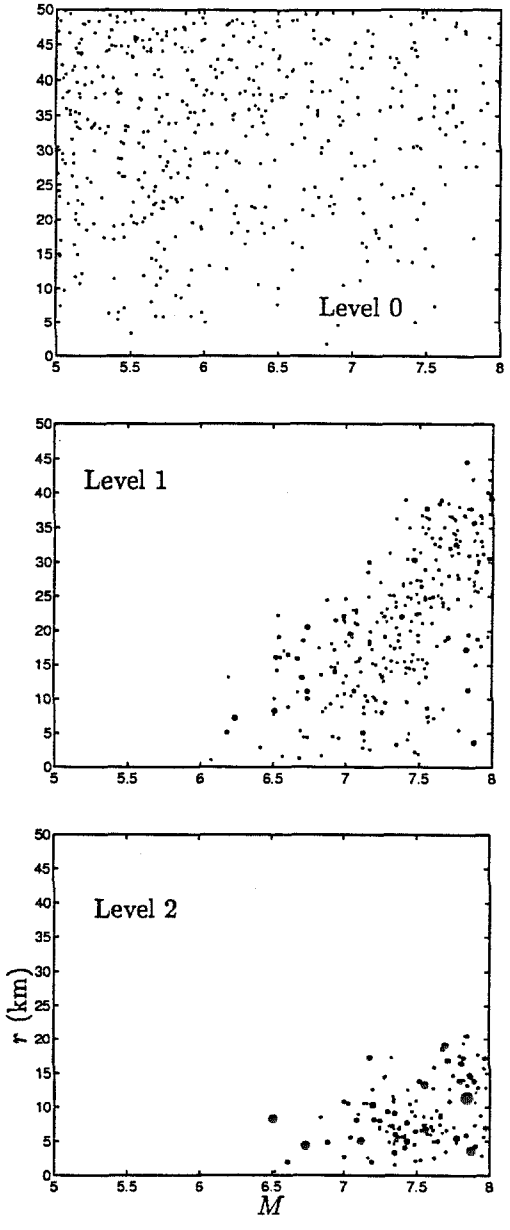

Figure 6.49: Conditional samples of M and r for Example 3, Case 2, at conditional levels 0, 1, 2

Chapter 7 Conclusion

7.1 Conclusions

The use of simulation methods to solve first excursion problems with application to the probabilistic assessment of the seismic performance of structures has been investigated in this dissertation. Two simulation methods have been proposed for solving the first excursion problem with different efficiency and generality.

A pioneering effort has been attempted to address the applicability of importance sampling to problems with a large number of uncertain parameters, which has an important bearing on the potential use of importance sampling for solving first excursion problems as well as reliability problems of structures with a large number of structural model parameters. The results show that importance sampling using some common choices of the importance sampling density is applicable in high dimensions, provided that certain conditions derived in this work are met.

An analytical study of the failure region for the first excursion failure of linear dynamical systems subjected to Gaussian white noise excitation has been carried out. By viewing the failure event as a union of elementary failure events, the analysis shows that each elementary failure event is completely characterized by a design point, which can be computed using impulse response functions of the system. The complexity of the first excursion problem stems from the structure of the union of the elementary failure events. An important consequence of this structure is that, in addition to the global design point, a large number of neighboring design points are important in accounting for the failure probability. Using information from the study of the failure region, an importance sampling density has been proposed as a weighted sum of conditional distributions to account for the contributions from all the elementary failure regions. The proposed importance sampling density is optimal if the elementary failure events are mutually exclusive. Numerical results show that the proposed importance sampling density leads to a very efficient simulation procedure. The efficiency tends to be higher for smaller failure probability or larger damping in the system, which may be explained by the conjecture that in these cases the elementary failure events are closer to being mutually exclusive. Further investigation is needed to substantiate these claims.

The subset simulation method has been developed to solve the first excursion problem for general systems. It is based on expressing a small failure probability as a product of larger conditional failure probabilities, thus turning a simulation problem of rare failure events into several simulation problems of more frequent failure events. The estimation of the conditional failure probabilities is a nontrivial problem, but a modified Markov chain Monte Carlo simulation method is developed

to estimate them efficiently. In addition to estimating failure probabilities, subset simulation also provides an efficient tool for failure analysis, using the Markov chain samples generated during the simulation.

Comparison of the two methods developed in this work, and in general with the methods developed in the literature, reveals that there is a trade-off between efficiency and robustness of a simulation method. The importance sampling method using elementary failure events is very efficient, and only requires about 20 samples for estimating a failure probability with a c.o.v. of 30%, regardless of the failure probability level. It is only applicable to linear systems subjected to Gaussian white noise excitation, however, and therefore it is not robust to the nonlinearity and types of uncertainties in the system. On the other hand, subset simulation can be applied in general, regardless of the type of system and the type of uncertainties, and hence it is quite robust. Numerical results show that on average it requires about 2000 samples to compute a failure probability of 10^{-3} or 10^{-4} with a c.o.v. of 30%, and so it is not as efficient as importance sampling using elementary events for linear systems.

The proposed simulation methods have been applied to compute failure probabilities of structures subjected to uncertain earthquake excitations. Failure analysis has been carried out using the Markov chain samples simulated during subset simulation. The analysis shows that when the stochastic excitation model is fixed, the probable scenario of a rare failure event corresponds to resonance of the excitation with the structure. When the stochastic model parameters are uncertain in the problem, they tend to control failure, and their conditional distributions given that failure occurs are significantly different from their unconditional distributions. The conclusions from the failure analysis should be interpreted bearing in mind the inherent assumptions and limitations of the probability models used.

7.2 Future work

Regarding the development of simulation methods for solving first excursion problems, several directions may be pursued. The idea of importance sampling using elementary events is applicable for any linear system with additive Gaussian uncertainties. This includes excitation uncertainties modeled by Gaussian processes, as well as structural or material uncertainties modeled by random fields. In these cases, important sampling densities similar to the one proposed in this work can be formulated, where the main effort is to derive analytically the design points in terms of Green's functions. For example, an importance sampling density can be formulated for the case when the stochastic excitation is represented in the frequency domain, which will be useful for problems where the excitation is modeled with a target spectrum. Another important task is to investigate the choice of proposal distributions for subset simulation, since they govern the efficiency of the

method. The failure analysis results on the distribution of stochastic excitation model parameters, such as the moment magnitude and epicentral distance of a point-source model, may be used to calibrate stochastic ground motion models as well as the distributions of the model parameters.

From a global perspective, the 'science' of simulation methods, especially for problems with a large number of uncertain parameters, is not well-explored. There are many issues yet to be addressed that have an important bearing on what simulation methods have to offer. For example, is it possible to construct a simulation method that has the same robustness as standard Monte Carlo simulation but that is substantially more efficient? A formal treatment on the limits in robustness and efficiency of simulation methods should give important insights on how we should proceed in developing efficient simulation methods for complex systems with a large number of uncertain parameters. To this end, an information-theoretic approach seems to be a promising direction.

Bibliography

Abraham, F. F. (1986). Computational statistical mechanics: methodology, applications and supercomputing. *Advances in Physics 35*, 1–111.

Aktan, A. E., D. N. Farhey, A. J. Helmicki, D. L. Brown, V. J. Hunt, K. L. Lee, and A. Levi (1997). Structural identification for condition assessment: experimental arts. *Journal of Structural Engineering 123*(12).

Alder, B. J. and T. E. Wainwright (1959). Studies in molecular dynamics. I. General method. *Journal of Chemical Physics 31*, 459–466.

Ang, G. L., A. H.-S. Ang, and W. H. Tang (1992). Optimal importance sampling density estimator. *Journal of Engineering Mechanics, ASCE 118*(6), 1146–1163.

Atkinson, G. M. and W. Silva (2000). Stochastic modeling of California ground motions. *Bulletin of the Seismological Society of America 90*(2), 255–274.

Au, S. K. and J. L. Beck (1999). A new adaptive importance sampling scheme. *Structural Safety 21*, 135–158.

Au, S. K., C. Papadimitriou, and J. L. Beck (1999). Reliability of uncertain dynamical systems with multiple design points. *Structural Safety 21*, 113–133.

Beck, J. L. and S. K. Au (2000). Updating robust reliability using markov chain simulation. In *Proceedings of International Conference on Monte Carlo Simulation*, Monte Carlo, Monaco.

Beck, J. L. and L. S. Katafygiotis (1991). Updating of a model and its uncertainties utilizing dynamic test data. In P. Spanos and C. Brevvia (Eds.), *Proceedings 1st International Conference on Computational Stochastic Mechanics*, Corfu, Greece, pp. 125–136. Computational Mechanics Publications.

Beck, J. L. and L. S. Katafygiotis (1998). Updating models and their uncertainties – Bayesian statistical framework. *Journal of Engineering Mechanics, ASCE 124*(4), 455–461.

Bergman, L. A. and J. C. Heinrich (1981). Petrov-Galerkin finite element solution for the first passage probability and moments of first passage time of the randomly accelerated free particle. *Computer Methods in Applied Mechanics and Engineering 27*, 345–362.

Bertsimas, D. and J. Tsitsiklis (1993). Simulated annealing. *Statistical Science 8*, 10–15.

Besag, J. and P. J. Green (1993). Spatial statistics and Bayesian computation. *Journal of the Royal Statistical Society B. 55*, 25–37.

Bhanot, G. (1988). The Metropolis algorithm. *Report on Progress in Physics 51*, 429–457.

Boore, D. M. (1983). Stochastic simulation of high-frequency ground motions based on seismological models of the radiated spectra. *Bulletin of the Seismological Society of America 73*(6), 1865–1894.

Boore, D. M. and W. B. Joyner (1997). Site amplifications for generic rock sites. *Bulletin of the Seismological Society of America 87*(2), 327–341.

Brune, J. N. (1971a). Correction. *Journal of Geophysical Research 76*, 5002.

Brune, J. N. (1971b). Techonic stress and spectra of seismic shear waves from earthquakes. *Journal of Geophysical Research 75*, 4997–5009.

Bucher, C. G. (1988). Adaptive sampling – an iterative fast Monte Carlo procedure. *Structural Safety 5*, 119–126.

Chib, S. and E. Greenberg (1994). Bayes Inference in regression-models with ARMA(p,q) errors. *Journal of Econometrics 64*(1–2), 183–206.

Chib, S., E. Greenberg, and R. Winkelmann (1998). Posterior simulation and Bayes factors in panel count data models. *Journal of Econometrics 86*(1), 33–54.

Clough, R. and J. Penzien (1975). *Dynamics of Structures*. New York: McGraw-Hill.

Cornell, C. A. (1996). Reliability-based earthquake-resistant design: the future. In *Proceedings of 11th World Conference on Earthquake Engineering*, Acapulco, Mexico.

Cox, R. T. (1961). *The Algebra of Probable Inference*. Baltimore: Johns Hopkins Press.

Crandall, S. H., K. L. Chandirmani, and R. G. Cook (1966). Some first passsage problems in random vibration. *Journal of Applied Mechanics, ASME 33*, 624–639.

Der Kiureghian, A. (2000). The geometry of random vibrations and solutions by FORM and SORM. *Probabilistic Engineering Mechanics 15*, 81–90.

Der Kiureghian, A. and T. Dakessian (1998). Multiple design points in first and second-order reliability. *Structural Safety 20*, 37–49.

Dokainish, M. A. and K. Subbaraj (1989). A survey of direct time-integration methods in computational structural dynamics – I. explicit methods. *Computers and Structures 32*(6), 1371–1386.

Doob, J. L. (1953). *Stochastic Processes*. New York: John Wiley and Sons, Inc.

Drenick, R. F. (1970). Model-free design of aseismic structures. *Journal of Engineering Mechanics, ASCE 96*, 483–493.

Duane, S., A. D. Kennedy, B. J. Pendleton, and D. Roweth (1987). Hybrid Monte Carlo. *Physics Letters B 195*, 216–222.

Engelund, S. and R. Rackwitz (1993). A benchmark study on importance sampling techniques in structural reliability. *Structural Safety 12*, 255–276.

Fishman, G. S. (1996). *Monte Carlo: Concepts, Algorithms, and Applications.* New York: Springer-Verlag.

Freudenthal, A. M. (1947). The safety of structures. *Transactions of ASCE 112*, 125–180.

Freudenthal, A. M. (1956). Safety and the probability of structural failure. *Transactions of ASCE 121*, 1337–1397.

Freudenthal, A. M., J. M. Garrelts, and M. Shinozuka (1966). The analysis of structural safety. *Journal of the Structural Division, Proceedings of ASCE 92*(ST1), 267–325.

Geman, S. and D. Geman (1984). Stochastic relaxation, Gibbs distributions and the Bayesian restoration of images. *IEEE Transactions on Pattern Analysis and Machine Intelligence 6*, 721–741.

Gutenberg, B. and C. Richter (1958). Earthquake magnitude, intensity and acceleration. *Bulletin of the Seismological Society of America 62*(2), 105–145.

Hajek, B. (1988). Cooling schedules for optimal annealing. *Mathematics of Operations Research 13*, 311–329.

Hammersley, J. M. and D. C. Handscomb (1964). *Monte-Carlo Methods.* London: Methuen.

Hanks, T. C. and H. Kanamori (1979). A moment magnitude scale. *Journal of Geophysical Research 84*, 2348–2350.

Hanks, T. C. and R. K. McGuire (1981). The character of high-frequency of strong ground motion. *Bulletin of the Seismological Society of America 71*(6), 2071–2095.

Harbitz, A. (1986). An efficient sampling method for probability of failure calculation. *Structural Safety 3*, 109–115.

Hastings, W. K. (1970). Monte Carlo sampling methods using Markov chains and their applications. *Biometrika 57*, 97–109.

Hohenbichler, M. and R. Rackwitz (1988). Improvement of second-order reliability estimates by importance sampling. *Journal of Engineering Mechanics, ASCE 114*(12), 2195–2198.

Housner, G. W. and P. C. Jennings (1982). *Earthquake Design Criteria.* Engineering Monographs on Earthquake Criteria, Structural Design, and Strong Motion Records. Earthquake Engineering Research Institute.

Hughes, T. (1987). *The finite element method: linear static and dynamic finite element analysis.* Prentice-Hall, Inc.

Jaynes, E. T. (1978). Where do we stand on maximum entropy? In R. D. Levine and M. Tribus (Eds.), *The Maximum Entropy Formalism.* Cambridge, MA: MIT Press.

Jaynes, E. T. (1983). *E. T. Jaynes: Papers on Probability, Statistics, and Statistical Physics.* D. Reidel Publishing Co.

Jumarie, G. (1990). *Relative Information: Theories and Applications.* Springer Series in Synergetics, Vol. 47. New York: Springer-Verlag.

Kanamori, H. (1977). The energy release in great earthquakes. *Journal of Geophysical Research 82,* 2981–2987.

Karamchandani, A., P. Bjerager, and C. A. Cornell (1989). Adaptive importance sampling. In *Proc. 5th ICOSSAR,* San Francisco, pp. 855–862.

Karson, I. D. and J. O. Jirsa (1969). Behavior of concrete under compressive loadings. *Journal of the Structural Division, Proceedings of ASCE 95*(ST12), 2543–2563.

Katafygiotis, L. S. and J. L. Beck (1998). Updating models and their uncertainties – model identifiability. *Journal of Engineering Mechanics, ASCE 124*(4), 463–467.

Kent, D. C. and R. Park (1971). Flexural members with confined concrete. *Journal of the Structural Division, Proceedings of ASCE 97*(ST7), 1969–1990.

Kirkpatrick, S., C. D. Gelatt, and M. P. Vecchi (1983). Optimization by simulated annealing. *Science 220,* 671–680.

Kramer, S. L. (1996). *Geotechnical Earthquake Engineering.* New Jersey: Prentice Hall, Inc.

Kullback, S. (1959). *Information Theory and Statistics.* New York: Wiley.

Langley, R. S. (1988). A 1st passage approximation for Normal stationary random processes. *Journal of Sound and Vibration 122*(2), 261–275.

Lin, Y. K. (1967). *Probabilistic Theory of Structural Dynamics.* McGraw Hill.

Lin, Y. K. and G. Q. Cai (1995). *Probabilistic Structural Dynamics: Advanced Theory and Applications.* New York: McGraw-Hill Book Company.

Liu, P. L. and A. Der Kiureghian (1991). Optimization algorithms for structural reliability. *Structural Safety 9,* 161–178.

Lutes, D. L. and S. Sarkani (1997). *Stochastic Analysis of Structural and Mechanical Vibrations.* New Jersey: Prentice Hall.

Mason, A. B. and W. D. Iwan (1983). An approach to the 1st passage problem in random vibration. *Journal of Applied Mechanics, ASME 50,* 641–646.

Melchers, R. E. (1989). Importance sampling in structural systems. *Structural Safety 6,* 3–10.

Melchers, R. E. (1990). Search-based importance sampling. *Structural Safety 9,* 117–128.

Metropolis, N., A. W. Rosenbluth, M. N. Rosenbluth, and A. H. Teller (1953). Equations of state calculations by fast computing machines. *Journal of Chemical Physics 21*(6), 1087–1092.

Mottershead, J. E. and M. I. Friswell (1993). Model updating in structural dynamics: A survey. *Journal of Sound and Vibration 167*(2), 347–375.

Naess, A. (1990). Approximate first-passage and extremes of narrow-band Gaussian and non-Gaussian random vibrations. *Journal of Sound and Vibration 138*(3), 365–380.

Papadimitriou, C., J. L. Beck, and L. S. Katafygiotis (1997). Asymptotic expansions for reliabilities and moments of uncertain dynamic systems. *Journal of Engineering Mechanics, ASCE 123*(12), 1219–1229.

Papadimitriou, C., J. L. Beck, and L. S. Katafygiotis (2001). Updating robust reliability using structural test data. *Probabilistic Engineering Mechanics 16*(2), 103–113.

Papoulis, A. (1965). *Probability, Random variables, and Stochastic Processes.* McGraw-Hall, Inc.

Pradlwarter, H. J. and G. I. Schuëller (1997a). Exceedance probability of MDOF-systems under stochastic excitation. *Applied Mechanics Review, ASME 50*(11), 168–173.

Pradlwarter, H. J. and G. I. Schuëller (1997b). On advanced Monte Carlo simulation procedures in stochastic structural dynamics. *International Journal of Non-linear Mechanics 32*(4), 735–744.

Pradlwarter, H. J. and G. I. Schuëller (1999). Assessment of low probability events of dynamical systems by controlled Monte Carlo simulation. *Probabilistic Engineering Mechanics 14*, 213–227.

Pradlwarter, H. J., G. I. Schuëller, and P. G. Melnik-Melnikov (1994). Reliability of MDOF-systems. *Probabilistic Engineering Mechanics 9*, 235–243.

Renyi, A. (1970). *Probability Theory.* North-Holland series in applied mathematics and mechanics, Vol. 10. Amsterdam: North-Holland.

Rice, O. C. (1944). Mathematical analysis of random noise. *Bell System Technical Journal 23*, 282–332.

Rice, O. C. (1945). Mathematical analysis of random noise. *Bell System Technical Journal 24*, 46–156.

Roberts, J. B. (1976). First passage probability for nonlinear oscillators. *Journal of Engineering Mechanics, ASCE 102*, 851–866.

Ross, S. M. (1972). *Introduction to probability models.* Probability and mathematical statistics. New York: Academic Press.

Rubinstein, R. Y. (1981). *Simulation and the Monte-Carlo Method.* New York, N.Y.: John Wiley & Sons, Inc.

Rudin, W. (1974). *Real and Complex Analysis*. McGraw–Hill.

Schuëller, G. I., H. J. Pradlwarter, and M. D. Pandey (1993). Methods for reliability assessment of nonlinear systems under stochastic dynamic loading – a review. In *Proceedings of EURODYN'93*, pp. 751–759. Balkema.

Schuëller, G. I. and R. Stix (1987). A critical appraisal of methods to determine failure probabilities. *Structural Safety 4*, 293–309.

SEAOC 1995 (2000). Vision 2000: Performance based seismic engineering of buildings. Technical report, Sacramento, California.

Silverman, B. W. (1986). *Density Estimators*. New York: Chapman and Hall.

Soong, T. T. and M. Grigoriu (1993). *Random Vibration of Mechanical and Structural Systems*. Prentice Hall, Inc.

Spencer, B. F. and L. A. Bergman (1993). On the numerical solution of the Fokker-Planck equation for nonlinear stochastic systems. *Nonlinear Dynamics 4*, 357–372.

Subbaraj, K. and M. A. Dokainish (1989). A survey of direct time-integration methods in computational structural dynamics – II. implicit methods. *Computers and Structures 32*(6), 1387–1401.

Tierney, L. (1994). Markov chains for exploring posterior distributions. *Annals of Statistics 22*, 1701–1762.

Vanmarcke, E. H. (1975). On the distribution of the first-passage time for Normal stationary random processes. *Journal of Applied Mechanics, ASME 42*, 215–220.

Vijalapura, P. K., J. P. Conte, and M. Meghella (2000). Time-variant reliability analysis of hysteretic SDOF systems with uncertain parameters and subjected to stochastic loading. In R. E. Melchers and M. G. Stewart (Eds.), *Applications of Statistics and Probability*, Rotterdam, pp. 827–834. Balkema.

Wen, Y. K. (2000). Reliability and performance based design. In *Proceedings of 8th ASCE Specialty Conference on Probabilitic Mechanics and Structural Reliability*, Notre Dame, Indiana.

Wood, W. W. and F. R. Parker (1957). Monte Carlo equation state of molecules interacting with the Lennad-Jones potential. I. a supercritical isotherm at about twice the critical temperature. *Journal of Chemical Physics 27*(3), 720–733.

Yang, J. N. and M. Shinozuka (1971). On the first excursion probability in stationary narrow-band random vibration. *Journal of Applied Mechanics, ASME 38*, 1017–1022.

Appendix A Some Additional Observations on the Failure Region of SDOF Time-invariant Linear Systems

In this appendix, we present some additional observations on the failure region of SDOF time-invariant linear systems subjected to filtered white noise excitation. The conclusions are expected to hold, however, in more general situations, such as for MDOF systems or filtered white noise excitation, since the essential property underlying these characteristics is the continuity of the unit impulse response function of the system. The discussion is based on continuous-time systems, for the sake of mathematical convenience in analysis, but analogous results hold for discrete-time systems.

We will denote the excitation on the interval $[0,T]$ by $w(t)$, which is assumed to be square-integrable on $[0,T]$, that is, $w \in L^2[0,T]$. The system response corresponding to the excitation w will be denoted by $y(t;w)$:

$$y(t;w) = \int_0^t h(t-\tau)w(\tau)d\tau \tag{A.1}$$

where h is the unit impulse response function. The failure region will then be $F = \{w \in L^2[0,T] : |y(t;w)| > b \text{ for some } t \in [0,T]\}$.

A.1 Neighborhood of points in the failure region

Proposition A.1. *Except for points on the failure boundary, every point w in the failure region has a neighborhood of radius $\rho(w)$ lying entirely inside the failure region where*

$$\rho(w) = \sup_{\tau \in [0,T]} \frac{|y(\tau;w)| - b}{||h||_\tau} \tag{A.2}$$

and

$$||h||_\tau = \sqrt{\int_0^\tau h(s)^2 ds} \tag{A.3}$$

is the Euclidean norm of the unit impulse function h on the interval $[0,\tau]$. In other words, if w is an interior point of F, then $w + \Delta w$ is also an interior point of F for all $\Delta w(t)$ with $||\Delta w||_T < \rho(w)$.

Proof. Let w be an interior point of F. Then $\exists \tau \in [0,T]$ such that $|y(\tau;w)| - b > 0$. At such τ, for

any Δw with $||\Delta w||_T < [|y(\tau;w)| - b]/||h||_\tau$,

$$\begin{aligned}
|y(\tau;\Delta w)| &\le \int_0^\tau |h(\tau-s)\Delta w(s)|ds \\
&\le \sqrt{\int_0^\tau h(\tau-s)^2 ds}\sqrt{\int_0^\tau \Delta w(s)^2 ds} \\
&= ||h||_\tau ||\Delta w||_\tau \\
&\le ||h||_\tau ||\Delta w||_T \\
&< ||h||_\tau \frac{|y(\tau;w)| - b}{||h||_\tau} \\
&= |y(\tau;w)| - b
\end{aligned} \tag{A.4}$$

That is,

$$|y(\tau;w)| - |y(\tau;\Delta w)| > b \tag{A.5}$$

Now,

$$\begin{aligned}
|y(\tau;w+\Delta w)| &= |y(\tau;w) + y(\tau;\Delta w)| \quad \text{by linearity} \\
&\ge |y(\tau;w)| - |y(\tau;\Delta w)| > b
\end{aligned} \tag{A.6}$$

and so $w+\Delta w$ is an interior point of F. In general, choosing τ from $\mathbb{T}(w) = \{\tau \in [0,T] : |y(\tau;w)| > b\}$ to maximize $[|y(\tau;w)| - b]/||h||_\tau$, we conclude for any Δw:

$$||\Delta w||_T < \sup_{\tau \in \mathbb{T}(w)} \frac{|y(\tau;w)| - b}{||h||_\tau} \quad \Rightarrow \quad w + \Delta w \text{ is an interior point of } F \tag{A.7}$$

Finally, since for all $s \in \{[0,T] - \mathbb{T}(w)\}$, $[|y(s;w)| - b]/||h||_s \le 0 < \sup_{\tau \in \mathbb{T}(w)}[|y(\tau;w)| - b]/||h||_\tau$, the value of the supremum in (A.7) is unaffected by taking over all $\tau \in [0,T]$. We thus have

$$||\Delta w||_T < \rho(w) = \sup_{\tau \in [0,T]} \frac{|y(\tau;w)| - b}{||h||_\tau} \quad \Rightarrow \quad w + \Delta w \text{ is an interior point of } F \tag{A.8}$$

and hence the proof. □

A.2 Proximity of neighboring design points

Proposition A.2. *The (Euclidean) distance between neighboring design points corresponding to consecutive up-crossing (down-crossing) failure times separated by sufficiently small Δt is $O(\Delta t)$.*

Proof. Let $\{w_t^*(\tau) : \tau \in [0,T]\}$ be the design point corresponding to the elementary up-crossing

failure event at time t: $F_t^+ = \{y(t) > b\}$. We start by studying the difference $w^*_{t+\Delta t}(\tau) - w^*_t(\tau)$ on $[0,T]$. First note that $w^*_t(\tau) \equiv 0$ for $\tau > t$ and $w^*_{t+\Delta t}(\tau) \equiv 0$ for $\tau > t+\Delta t$. Thus, for $\tau \in (t+\Delta t, T]$,

$$w^*_{t+\Delta t}(\tau) - w^*_t(\tau) \equiv 0 \tag{A.9}$$

and for $\tau \in (t, t+\Delta t)$,

$$w^*_{t+\Delta t}(\tau) - w^*_t(\tau) = w^*_{t+\Delta t}(\tau) \tag{A.10}$$

For $\tau \in (0,t)$, we approximate $w^*_{t+\Delta t}(\tau) - w^*_t(\tau)$ with a first order Taylor expansion with respect to t for small Δt:

$$w^*_{t+\Delta t}(\tau) - w^*_t(\tau) \sim \frac{\partial w^*_t(\tau)}{\partial t}\,\Delta t \tag{A.11}$$

Since $\tau \in (0,t)$, $w^*_t(\tau)$ is given by

$$w^*_t(\tau) = h(t-\tau)\frac{b}{||h||^2_t} \tag{A.12}$$

which gives, upon partial differentiation with respect to t,

$$\frac{\partial w^*_t(\tau)}{\partial t} = b\left[\frac{h'(t-\tau)}{||h||^2_t} - \frac{h(t-\tau)h(t)^2}{||h||^4_t}\right] \tag{A.13}$$

Thus, the square of the Euclidean distance between $w^*_{t+\Delta t}$ and w^*_t is given by

$$\begin{aligned} ||w^*_{t+\Delta t} - w^*_t||^2_T &= \int_0^T |w^*_{t+\Delta t}(\tau) - w^*_t(\tau)|^2\, d\tau \\ &= \int_0^{t+\Delta t} |w^*_{t+\Delta t}(\tau) - w^*_t(\tau)|^2 d\tau \quad \text{by (A.9)} \\ &= \int_0^t |w^*_{t+\Delta t}(\tau) - w^*_t(\tau)|^2\, d\tau + \int_t^{t+\Delta t} |w^*_{t+\Delta t}(\tau)|^2\, d\tau \quad \text{by (A.10)} \end{aligned} \tag{A.14}$$

Using (A.11), the first term on the R.H.S. of (A.14) is approximated by

$$\int_0^t |w^*_{t+\Delta t}(\tau) - w^*_t(\tau)|^2 d\tau \sim \int_0^t \left(\frac{\partial w^*_t(\tau)}{\partial t}\Delta t\right)^2 d\tau = O(\Delta t^2) \tag{A.15}$$

On the other hand, the second term on the R.H.S. of (A.14) is approximated by

$$\int_t^{t+\Delta t} |w^*_{t+\Delta t}(\tau)|^2\, d\tau \sim w^*_{t+\Delta t}(t)^2 \Delta t = \frac{h(t+\Delta t - t)^2}{||h||^4_{t+\Delta t}}\, b^2\, \Delta t = O(\Delta t^3) \tag{A.16}$$

since $h(\Delta t)^2 = O(\Delta t^2)$. So, using (A.14), (A.15) and (A.16), to the leading order of Δt^2,

$$||w^*_{t+\Delta t} - w^*_t||^2_T \sim \int_0^t \left(\frac{\partial w^*_t(\tau)}{\partial t}\right)^2 d\tau\, \Delta t^2 \tag{A.17}$$

Now for $\tau \in (0,t)$, using (A.13),

$$\left(\frac{\partial w^*_t(\tau)}{\partial t}\right)^2 = b^2 \left[\frac{h'(t-\tau)^2}{||h||^4_t} - 2\frac{h'(t-\tau)h(t-\tau)h(t)^2}{||h||^6_t} + \frac{h(t-\tau)^2 h(t)^4}{||h||^8_t}\right] \tag{A.18}$$

Integrating (A.18) with respect to τ from 0 to t, and noting that

$$\int_0^t h'(t-\tau)^2 d\tau = ||h'||^2_t \tag{A.19}$$

$$\int_0^t h'(t-\tau)h(t-\tau)d\tau = \frac{1}{2}h(t)^2 \tag{A.20}$$

$$\int_0^t h(t-\tau)^2\, d\tau = ||h||^2_t \tag{A.21}$$

we have

$$\int_0^t \left(\frac{\partial w^*_t(\tau)}{\partial t}\right)^2 d\tau = b^2\, \frac{||h'||^2_t}{||h||^4_t} \tag{A.22}$$

Finally, using (A.17) and (A.22), we have

$$||w^*_{t+\Delta t} - w^*_t||_T \sim b\Delta t \frac{||h'||_t}{||h||^2_t} = O(\Delta t) \tag{A.23}$$

and hence the proof. □

A.3 Overshooting of design point response

Proposition A.3. *For continuous time systems, the response corresponding to the design point at up-crossing (down-crossing) failure time t will over-shoot the level b after time t. However, the duration of overshoot (over which the response has exceeded the level b) is $O(h(t)^2/||h'||^2_t)$ and the maximum amount of overshoot is $O(h(t)^4/||h||^2_t||h'||^2_t)$, and are thus very small for stable systems at sufficiently large t.*

This proposition is somewhat counter-intuitive. One may expect from intuition that the maximum value of the response $y(\tau; w^*_t)$ corresponding to the excitation w^*_t occurs at time t, since w^*_t is

by definition the excitation with the smallest 'energy' that drives the response to the level b at time t and so should not 'waste' any additional amount of energy to drive the response above b. The proposition says that such a 'waste' of energy is unavoidable, although the amount is very small in common situations when the failure time t is sufficiently large that the unit impulse response has decayed sufficiently compared to $||h||_t$ or $||h'||_t$. Indeed, for discrete-time systems, overshooting may not be apparent, due to discretization error and the fact that the overshoot duration is so small that it may not be captured with the available sampling interval used in numerical integration.

Proof. We first obtain a second order Taylor expansion for the response $y(\tau; w_t^*)$ near time t. For $s > 0$,

$$\begin{aligned} y(t+s; w_t^*) &= \int_0^{t+s} h(t+s-\tau)\frac{h(t-\tau)}{||h||_t^2}U(t-\tau)\, b\, d\tau \\ &= \frac{b}{||h||_t^2}\int_0^t h(t-\tau+s)h(t-\tau)d\tau \quad \text{since } U(t-\tau) \equiv 0 \text{ for } \tau > t \\ &= \frac{b}{||h||_t^2}\int_0^t h(\tau+s)h(\tau)\, d\tau \end{aligned} \tag{A.24}$$

When s is small,

$$h(\tau+s) \sim h(\tau) + h'(\tau)\, s + \frac{1}{2}h''(\tau)\, s^2 \tag{A.25}$$

Substituting (A.25) into (A.24), integrating and simplifying, we have

$$y(t+s; w_t^*) \sim b + \frac{b\, h(t)^2}{2||h||_t^2}\, s + \frac{b}{2||h||_t^2}\left[h'(t)h(t) - ||h'||_t^2\right] s^2 \tag{A.26}$$

Since the first order term with respect to s is always positive, we see that there is always overshooting. However, the time derivative of the response when it crosses b could be very small for stable systems at large failure time t, since then either $h(t) \to 0$ as $t \to \infty$ for strongly stable systems, or $h(t) < \infty$, $||h||_t \to \infty$ as $t \to \infty$ for marginally stable systems.

The duration of overshoot is equal to the time $\hat{t}$ after t when the response crosses the level b again (and goes below b afterwards). It is approximated by solving $y(t+s; w_t^*) = b$ for s, which yields

$$\hat{t} = \frac{h(t)^2}{||h'||_t^2 - h'(t)h(t)} \sim \frac{h(t)^2}{||h'||_t^2} \quad \text{for large } t \tag{A.27}$$

since $h'(t)h(t)$ is small compared to $||h'||_t^2$ for stable systems at large t.

With the quadratic approximation of $y(t+s; w_t^*)$ in (A.26) for small $s > 0$, the time $\hat{s}$ after t at

which the overshoot is maximum is simply given by

$$\hat{s} = \frac{\hat{t}}{2} \tag{A.28}$$

Finally, the maximum amount of overshoot $\delta_{\max}$ is approximated using (A.26) with $s = \hat{s}$ in (A.28):

$$\begin{aligned}
\delta_{\max} &= y(t+\hat{s}; w_t^*) - b \\
&= \frac{b\,h(t)^4}{8||h||_t^2}\left[||h'||_t^2 - h'(t)h(t)\right]^{-1} \\
&\sim \frac{b\,h(t)^4}{8||h||_t^2||h'||_t^2} = O(\frac{h(t)^4}{||h||_t^2||h'||_t^2}) \quad \text{for large } t
\end{aligned} \tag{A.29}$$

□

A.4 A reciprocal relationship of design point responses

The following proposition holds for time-variant systems as well.

Proposition A.4. *For all* $s, t \geq 0$,

$$\sigma_s^2 y(t; w_s^*) = \sigma_t^2 y(s; w_t^*) \tag{A.30}$$

where $\sigma_t^2 = 2\pi S||h||_t^2$ *is the response variance at time* t.

Proof. Result is trivial when $t = s$. Consider $t > s$,

$$\begin{aligned}
\sigma_s^2 y(t; w_s^*) &= \sigma_s^2 \int_0^t h(t,\tau) w_s^*(\tau) d\tau \\
&= 2\pi S \int_0^t h(t,\tau) h(s,\tau) U(s-\tau) d\tau \\
&= 2\pi S \int_0^s h(t,\tau) h(s,\tau) d\tau
\end{aligned} \tag{A.31}$$

since $h(s,\tau) \equiv 0$ for $s < \tau < t$. On the other hand, when $t < s$,

$$\sigma_s^2 y(t; w_s^*) = 2\pi S \int_0^t h(t,\tau) h(s,\tau) d\tau \tag{A.32}$$

Equations (A.31) and (A.32) imply, for all $s, t \geq 0$,

$$\sigma_s^2 y(t; w_s^*) = 2\pi S \int_0^{\min(t,s)} h(t,\tau) h(s,\tau) d\tau \tag{A.33}$$

The proof then follows from the symmetry of the above expression with respect to s and t. □

A.5 Simulation formula for $Z_i^{\perp}$

We show here that the random vector $Z_i^{\perp}$ given by (4.18) is orthogonal to the unit vector $\mathbf{u}_i^*$ and has independent Gaussian components with respect to the basis in the orthogonal complement of $\mathbf{u}_i^*$.

Since $Z_i^{\perp}$ given by (4.18) is a Normal vector, it is sufficient to prove that (1) $Z_i^{\perp}$ is orthogonal to z_i^* and (2) it has uncorrelated components in the $(n-1)$-dimensional orthogonal complement $V_i^{\perp}$ of the one-dimensional subspace spanned by $\mathbf{u}_i^*$.

First,

$$\langle Z_i^{\perp}, \mathbf{u}_i^* \rangle = \langle Z - \langle Z, \mathbf{u}_i^* \rangle \mathbf{u}_i^*, \mathbf{u}_i^* \rangle = \langle Z, \mathbf{u}_i^* \rangle - \langle Z, \mathbf{u}_i^* \rangle \langle \mathbf{u}_i^*, \mathbf{u}_i^* \rangle = 0 \tag{A.34}$$

since $\langle \mathbf{u}_i^*, \mathbf{u}_i^* \rangle = ||\mathbf{u}_i^*||^2 = 1$.

To show the second claim, first note that $Z_i^{\perp}$ has zero mean, since Z does: $\mathsf{E}[Z_i^{\perp}] = \mathsf{E}[Z] - \langle \mathsf{E}[Z], \mathbf{u}_i^*, \mathbf{u} \rangle_i^* = 0$. By the first claim, $Z_i^{\perp}$ is orthogonal to $\mathbf{u}_i^*$ and hence lies in $V_i^{\perp}$, so it has the following Fourier series representation:

$$Z_i^{\perp} = Z - \langle Z, \mathbf{u}_i^* \rangle \mathbf{u}_i^* = \sum_{j=1}^{n-1} A_j v_j \tag{A.35}$$

where $\{v_j : j = 1, \ldots, n-1\}$ is an orthonormal basis in $V_i^{\perp}$ and $\{A_j\}_j$ are the Fourier coefficients given by

$$A_j = \langle Z_i^{\perp}, v_j \rangle = \langle Z, v_j \rangle - \langle Z, \mathbf{u}_i^* \rangle \langle \mathbf{u}_i^*, v_j \rangle = \langle Z, v_j \rangle \tag{A.36}$$

since $\langle \mathbf{u}_i^*, v_j \rangle = 0$ for $v_j \in V_i^{\perp}$. It remains to show that the coefficients $\{A_j\}_j$ are uncorrelated. For $j, k = 1, \ldots, n-1$,

$$\begin{aligned} \mathsf{E}[A_j A_k] &= \mathsf{E}[\langle v_j, Z \rangle \langle Z, v_k \rangle] \\ &= \mathsf{E}[v_j^T Z Z^T v_k] \\ &= v_j^T \mathsf{E}[Z Z^T] v_k \\ &= v_j^T v_k \quad \text{since } \mathsf{E}[Z Z^T] = \text{Identity matrix} \\ &= \delta_{jk} \end{aligned} \tag{A.37}$$

where δ_{jk} is the Kronecker delta: $\delta_{jk} = 1$ if $j = k$ and $\delta_{jk} = 0$ otherwise. Thus $\{A_j\}_j$ are uncorrelated, and the proof is completed.